

*PbD* Thesis

UPC – Program on Environmental Engineering

**Syntrophic acetate oxidation in the anaerobic  
digestion of nitrogen-rich wastes: from  
microbial interactions to process optimization**

Josep Ruiz Sánchez

Supervised by:

Dr. Francesc X. Prenafeta Boldú and Dra. Belén Fernández García

Barcelona, 2018 September





El Dr. Francesc X. Prenafeta Boldí i la Dra. Belén Fernández García de  
GIRO-IRTA

CERTIFIQUEM:

Que en Josep Ruiz Sánchez realitzat sota la nostra direcció el treball titulat:

**“The syntrophic acetate oxidation in anaerobic digestion of  
nitrogen-rich wastes: from microbial interactions to process  
optimization**

presentat en aquesta memòria, i que constitueix la seva Tesi Doctoral per optar  
al Grau de Doctor per la Universitat Politècnica de Catalunya. I perquè es  
tingui coneixement i consti als efectes oportuns, presentem al Programa de  
Doctorat d'Enginyeria Ambiental de l'Institut de Recerca en Ciència i  
Tecnologia de la Sostenibilitat, l'esmentada Tesi Doctoral, signant el present  
certificat a:

Caldes de Montbui, Setembre del 2018

*The failures are also useful, because, well  
analyzed, can lead to success.*  
Alexander Fleming

*Ce sont les microbes qui ont le dernier mot*  
Louis Pasteur



## AGRAÏMENTS

---

Qui m'havia de dir que després d'acabar la carrera de Biotecnologia al 2008 i decidir prendre un “*break*” de ciència i d'estudis em veuria uns anys després redactant una tesis doctoral... Però com diu aquella frase, *la vida dona moltes voltes*, i les voltes em van portar fins al GIRO, on comença i acaba aquesta historia. I entre volta i volta m'he envoltat de gent increïble a la qual he d'agrair immensament el recolzament al llarg d'aquest camí.

En primer lloc, agrair a qui em va donar aquesta oportunitat, els meus supervisors, Francesc X. Prenafeta i Belén Fernandez; pels consells, per la supervisió, per guiar-me en aquest món enrevessat de la ciència i per oferir-me part del seu temps en resoldre els meus dubtes (moltes vegades molt a prop de la crisis). També al Dr. Xavier Flotats i a la Dra. Ivet Ferrer per acceptar la tutoria d'aquesta tesis.

Òbviament, i en aquest racó de la tesis, no puc deixar d'agrair a la Miriam Guivernau el seu enorme recolzament moral en moments crítics, així com el seu talent (que és infinit). Gràcies pels esforços dedicats en aquest treball, i per aquest “*dreamteam*” creat entre gens i microbis; que indiscutiblement també és un “*dreamteam*” de disputes i riures que va més enllà del laboratori. Gràcies també, a una peça clau en la microbiologia d'aquest treball, en Marc Viñas, per ser una font de coneixement i d'idees brillants d'especial importància en aquesta tesis. I al Quim, per tenir sempre la voluntat d'ajudar.

Han sigut quatre anys que m'han donat la oportunitat de conèixer gent meravellosa amb la que compartir moments de treball, però també de compartir riures incansables; Edu, Lluís, Nancy, Lauras, Martina, Carolina, Erica, Nuria, Maycoll... Sense oblidar molts companys del giro que m'han donat suport en aquests anys Victor, Eva, Joan, Miriam, August, Ana S, Ana P, Assumpció,...

Ha sigut un viatge que m'ha portat a molts llocs, entre ells Itàlia. *Sempre sarò grato al Dott Stephano Campanaro. Per la sua gentile e calorosa accoglienza a Padova, e per l'indiscussa e solida formazione nel campo della bioinformatica. È stato un grande piacere imparare da un grande talento.* I parlant d'Italia, no pot faltar la meua companya de fatigues, Jessi. Infinitas

gracias por alegrar mi paso por Padova, por ser mi incondicional en la búsqueda de la Romana, y por seguir ahí, pese la distancia.

Igualment agrair a la meva família i amics pel suport en moments baixos, i celebrar les alegries conjuntes.

I finalment, però òbviament no menys important, a l'Albert. Crec en aquest cas un gràcies no cobriria tot el que ha suposat suportar la tesis. Però gràcies per ficar-me les coses molt fàcils, per ser la estabilitat i la serenitat que a vegades perdo, i per ser el millor company de congressos, de viatges, de riures,... de vida!

A tots, moltes gràcies!!!





# TABLE OF CONTENTS

---

<i>SUMMARY</i> .....	1
<i>RESUMEN</i> .....	3
<i>RESUM</i> .....	5
<i>PREFACE</i> .....	8
<i>PART I</i> .....	0
<i>CHAPTER 1 INTRODUCTION</i> .....	1
<i>1.1 CURRENT STATE</i> .....	2
<i>1.2 ANAEROBIC DIGESTION</i> .....	3
1.2.1 Stages in the anaerobic digestion process.....	4
1.2.2 Process inhibition by nitrogen compounds.....	5
1.2.3 Process inhibition by long chain fatty acids (LCFA).....	7
1.2.4 Process inhibition by sulfate compounds.....	8
1.2.5 Microbiology of anaerobic digestion.....	8
1.2.6 Syntrophic acetate oxidation proces.....	10
<i>1.3 BIOTECHNOLOGICAL STRATEGIES FOR PREVENTING INHIBITION....</i>	<i>13</i>
1.3.1 Pretreatment.....	14
1.3.2 Digester configuration.....	15
1.3.3 Strategies to enhance AD-reactors performance.....	19
<i>1.4 COMPARISON BETWEEN STRATEGIES</i> .....	<i>21</i>
<i>1.5 REFERENCES</i> .....	<i>22</i>
<i>CHAPTER 2 OBJECTIVES</i> .....	<i>32</i>
<i>2.1 OBJECTIVES</i> .....	<i>33</i>
2.1.1 To enrich and identify relevant microorganisms from methanogenic biomass, both in the <i>Bacteria</i> and <i>Archaea</i> domains, that are involved in the syntrophic acetate oxidation (SAO) process.....	34

2.1.2 To assess microbial community structure and dynamics in response to increasing ammonia exposure. ....	34
2.1.3 To characterize the SAO process at the metagenome level in order to pinpoint specific metabolic and physiologic traits that contribute to the stability of the methanogenic activity.....	35
2.1.4 To elucidate the effect of packing materials with different physicochemical properties on the development of methanogenic biomass that functions via the SAO process.....	35
2.1.5 To develop reactor configuration strategies for anaerobic digesters in order to increase the process robustness and stability in front of ammonia inhibition....	36
<b>CHAPTER 3 MATERIALS AND METHODS.....</b>	<b>37</b>
<b>3.1. INTRODUCTION.....</b>	<b>38</b>
<b>3.2. METHANOGENIC ASSAYS: ACTIVITY AND TOXICITY.....</b>	<b>38</b>
<b>3.3. PHYSICOCHEMICAL ANALYTICAL METHODS.....</b>	<b>38</b>
<b>3.4. ALKALINITY.....</b>	<b>38</b>
<b>3.5. TOTAL AND VOLATILE SOLIDS.....</b>	<b>38</b>
<b>3.6. CHEMICAL OXYGEN DEMAND.....</b>	<b>39</b>
<b>3.7. DETERMINATION OF ISOTOPIC CARBON.....</b>	<b>39</b>
<b>3.8. ASSEMBLY AND OPERATION OF CONTINUOUS ANAEROBIC DIGESTERS</b>	<b>40</b>
<hr/>	
3.8.1. Lab-scale digester: general set-up.....	40
3.8.2. Operational conditions.....	40
3.8.3. Stirred reactor.....	41
3.8.4. Hybrid reactor.....	41
3.8.5. Enrichment digester.....	41
<b>3.9. MICROBIOLOGY CHARACTERIZATION.....</b>	<b>42</b>
<hr/>	
3.9.1. Quantitative real-time pcr (qpcr).....	42
3.9.2. Next Generation Sequencing (Illumina Sequencing).....	42
3.9.3. Metagenome sequencing, assembly and binning process.....	43
<b>3.10. REFERENCES.....</b>	<b>44</b>
<hr/>	

<b>PART II.....</b>	<b>46</b>
<b>CHAPTER 4 FUNCTIONAL PLASTICITY OF METHANOGENIC BIOMASS FROM A FULL-SCALE MESOPHILIC ANAEROBIC DIGESTER TREATING NITROGEN-RICH AGRICULTURAL WASTES.....</b>	<b>47</b>
<b>4.1 INTRODUCTION.....</b>	<b>48</b>
<b>4.2 MATERIALS AND METHODS.....</b>	<b>49</b>
<b>4.3 RESULTS AND DISCUSSION.....</b>	<b>51</b>
4.3.1 Methanogenic activity assays .....	51
4.3.2 Isotopic fractionation of biogas .....	51
4.3.3 Microbial community analysis.....	52
4.3.3.1. <i>Quantitative expression profile of selected functional genes</i> .....	52
4.3.3.2. <i>Bacterial community structure and response to ammonia exposure</i> .....	60
4.3.3.3. <i>Archaeal community structure and response to ammonia exposure</i> .....	63
<b>4.4 CONCLUSION.....</b>	<b>66</b>
<b>4.5 REFERENCES.....</b>	<b>67</b>
<b>CHAPTER 5 EFFECT OF AMMONIA ON THE ACTIVE MICROBIOME AND METAGENOME AND FROM STABLE FULL-SCALE DIGESTERS.....</b>	<b>70</b>
<b>5.1 INTRODUCTION.....</b>	<b>71</b>
<b>5.2 MATERIALS AND METHODS.....</b>	<b>73</b>
5.2.1 Biogas plants and sampling procedure .....	73
5.2.2 Analytical methods .....	74
5.2.3 Molecular microbial community characterization.....	74
5.2.3.1 <i>Next generation sequencing of active microbial populations</i> .....	74
5.2.3.2 <i>Metagenome sequencing, assembly and binning process</i> .....	74
5.2.3.3 <i>Biostatistical analysis</i> .....	76
<b>5.3 RESULTS AND DISCUSSION.....</b>	<b>76</b>
5.3.2 Biochemical characterization of the reactors.....	76
5.3.3 Active microbial populations .....	77

5.3.4	Genome reconstruction and phylogenetic assignment .....	81
5.3.5	Functional characterization of methanogenic archaea .....	86
<b>5.4</b>	<b>CONCLUSIONS</b> .....	<b>94</b>
<b>5.5</b>	<b>REFERENCES</b> .....	<b>95</b>
<b>PART III</b>	.....	<b>98</b>
<b>CHAPTER 6 ASSESSMENT OF SAOB-HMA BIOFILMS ACTIVITY, BASED ON ISOTOPIC GAS PROFILING AND MICROBIOLOGICAL CHARACTERIZATION, UNDER A HIGH AMMONIA LEVEL</b> .....		
		<b>99</b>
<b>6.2</b>	<b>INTRODUCTION</b> .....	<b>100</b>
<b>6.3</b>	<b>MATERIALS AND METHODS</b> .....	<b>102</b>
<hr/>		
6.3.1	Experiment .....	102
6.3.2	Confocal scanning laser microscopy (CSLM).....	104
<b>6.4</b>	<b>RESULTS AND DISCUSSION</b> .....	<b>105</b>
<hr/>		
6.4.1	Part 1 – CH <sub>4</sub> production with suspended and attached biomass .....	105
6.4.2	Part 2 – CH <sub>4</sub> production with attached biomass .....	110
6.4.3	Microbial population .....	111
6.4.4	General outcomes .....	122
<b>6.5</b>	<b>CONCLUSIONS</b> .....	<b>122</b>
<b>6.6</b>	<b>REFERENCES</b> .....	<b>123</b>
<b>CHAPTER 7 RESPONSE OF ANAEROBIC METHANOGENIC BIOMASS TO IMMOBILIZED MULTI-WALLED C NANOTUBES EXPOSURE</b> .....		
		<b>127</b>
<b>7.1</b>	<b>INTRODUCTION</b> .....	<b>128</b>
<b>7.2</b>	<b>MATERIALS AND METHODS</b> .....	<b>128</b>
<hr/>		
7.2.1	Multiwall carbon nanotubes immobilization .....	129
7.2.2	Experimental set-up .....	129
7.2.3	Scanning electron microscopy (SEM) .....	130
<b>7.3</b>	<b>RESULTS AND DISCUSSION</b> .....	<b>131</b>
<hr/>		
7.3.1	The feasibility of the immobilisation method.....	131

7.3.2	Methane production and microbial community analysis after CNT exposure .....	132
7.3.2.1	<i>Experiment 1</i> .....	132
7.3.3	Microbial community analysis.....	138
7.3.3.1	<i>Response of methanogenic archaeal communities to MWCNTs and ammonia</i> ...	145
7.3.2	I-CNT dose assessment (Experiment 2) .....	145
<b>7.4</b>	<b>CONCLUSIONS</b> .....	<b>147</b>
<b>7.4</b>	<b>REFERENCES</b> .....	<b>147</b>
<b>CHAPTER 8 IDENTIFICATION OF SYNTROPHIC ACETATE OXIDATION AND ELECTRON TRANSFER MECHANISMS IN METHANOGENIC BIOMASS BY DNA-STABLE ISOTOPE PROBING AND METAGENOMICS</b> .....		
<b>8.1</b>	<b>INTRODUCTION</b> .....	<b>151</b>
<b>8.2</b>	<b>MATERIALS AND METHODS</b> .....	<b>152</b>
<b>8.2.1</b>	<b>EXPERIMENTAL SETUP</b> .....	<b>152</b>
<b>8.2.2</b>	<b>DNA EXTRACTION AND SEPARATION OF <sup>13</sup>C-ENRICHED DNA</b> ....	<b>153</b>
<b>8.2.3</b>	<b>METAGENOME SEQUENCING</b> .....	<b>154</b>
<b>8.3</b>	<b>RESULTS</b> .....	<b>155</b>
<b>8.3.1</b>	<b>EFFECT OF SUPPORT MATERIALS ON METHANOGENIC ACTIVITY</b> ..	<b>155</b>
<b>8.3.2</b>	<b>DNA STABLE-ISOTOPE PROBING OF THE <sup>13</sup>C-ACETATE METABOLISM</b>	<b>156</b>
<b>8.3.3</b>	<b>MICROBIAL COMMUNITY COMPOSITION</b> .....	<b>156</b>
<b>8.3.4</b>	<b>METAGENOME RECONSTRUCTION</b> .....	<b>161</b>
<b>8.4</b>	<b>DISCUSSION</b> .....	<b>166</b>
<b>8.5</b>	<b>CONCLUSION</b> .....	<b>172</b>
<b>8.6</b>	<b>REFERENCES</b> .....	<b>173</b>
<b>PART IV</b>	.....	<b>178</b>
<b>CHAPTER 9 STRATEGIES FOR RECOVERING FROM INHIBITION CAUSED BY AMMONIA AND SULPHATE IN MESOPHILIC BIOGAS FIXED-BED REACTORS</b>		
<b>9.1</b>	<b>INTRODUCTION</b> .....	<b>180</b>

---

<b>9.2</b>	<b><i>MATERIALS AND METHODS</i></b> .....	<b>182</b>
9.2.1	Experimental set-up and operational conditions .....	182
<b>9.3</b>	<b><i>RESULTS AND DISCUSSION</i></b> .....	<b>183</b>
9.3.1	Failure and recovery periods.....	183
9.3.2	Effect of COD/SO <sub>4</sub> <sup>2-</sup> ratio on electron flow and the impact on methanogenic pathway.....	189
9.3.3	Effect of ammonia and sulfate stress on the abundance of methane-producing archaea and sulfate-reducing bacteria .....	191
9.3.3.1	Sulfate reducing bacteria monitorization .....	191
9.3.3.2	Methane-producing archaea monitorization .....	194
<b>9.4</b>	<b><i>CONCLUSIONS</i></b> .....	<b>194</b>
<b>9.5</b>	<b><i>REFERENCES</i></b> .....	<b>195</b>
<b><i>CHAPTER 10 IMPACT OF RECUPERATIVE THICKENING ON SYNTROPHIC MICROBIAL INTERACTIONS AND BIOGAS PRODUCTION IN ANAEROBIC DIGESTION</i></b> .....		<b>199</b>
<b>10.1</b>	<b><i>INTRODUCTION</i></b> .....	<b>200</b>
<b>10.2</b>	<b><i>MATERIALS AND METHODS</i></b> .....	<b>201</b>
10.2.1	Substrate and inoculum origin .....	201
10.2.2	Anaerobic digesters set-up .....	202
10.2.3	Ammonia inhibition test .....	204
10.2.4	Analytical methods .....	204
10.2.5	Microbial community analysis.....	204
<b>10.3</b>	<b><i>RESULTS</i></b> .....	<b>205</b>
10.3.1	Reactors performance .....	205
10.3.2	Ammonium inhibition tests .....	208
10.3.3	Microbial community dynamics .....	208
10.3.3.1	<i>Microbial population in R1-RT</i> .....	208
10.3.3.2	<i>Microbial population in R2-C</i> .....	209

10.3.3.3	<i>Microbial diversity indexes</i> .....	210
10.3.3.4	<i>Quantitative analysis by qPCR</i> .....	210
<b>10.4</b>	<b><i>DISCUSSION</i></b> .....	<b>217</b>
<hr/>		
10.4.1	Impact of recuperative thickening on process performance .....	217
10.4.2	Impact of biomass recuperative thickening on microbial composition ..	218
10.4.2.1	<i>Bacterial community</i> .....	218
10.4.2.2	<i>Archaeal community</i> .....	219
<b>10.5</b>	<b><i>CONCLUSIONS</i></b> .....	<b>220</b>
<b>10.6</b>	<b><i>REFERENCES</i></b> .....	<b>221</b>
<b><i>CHAPTER 11 ASSESMENT OF SUPPORT ASSISTED VS SUPPORT-FREE ANAEROBIC DIGESTION SYSTEM OPERATION UNDER HIGH AMMONIA LEVEL</i></b> .....		
<b>225</b>		
<b>11.1</b>	<b><i>INTRODUCTION</i></b> .....	<b>226</b>
<b>11.2</b>	<b><i>DIGESTERS EXPERIMENTAL SET-UP</i></b> .....	<b>227</b>
<hr/>		
11.2.1	Set-up.....	227
11.2.2	Synthetic medium .....	229
11.2.2	Analytical methods .....	229
11.3.1	Performance.....	230
<b>11.4</b>	<b><i>CONCLUSIONS</i></b> .....	<b>236</b>
<b>11.5</b>	<b><i>REFERENCES</i></b> .....	<b>236</b>
<b><i>PART V</i></b> .....		
<b>242</b>		
<b><i>CHAPTER 12 CONCLUSIONS &amp; FUTURE PERSPECTIVES</i></b> .....		
<b>243</b>		
<b>12.1</b>	<b><i>PART I</i></b> .....	<b>244</b>
<b>12.2</b>	<b><i>PART II</i></b> .....	<b>244</b>
<b>12.3</b>	<b><i>PART III</i></b> .....	<b>245</b>
<b>12.4</b>	<b><i>PART IV</i></b> .....	<b>246</b>
<b><i>ANNEX – CV</i></b> .....		
<b>248</b>		
<hr/>		



## INDEX OF FIGURES

---

- Figure 4.1** Evolution of acetic acid and CH<sub>4</sub>, as well as CH<sub>4</sub> yield, at different TAN concentration: (A) 1 gN-TAN L-1; (B) 3.5 gN-TAN L-1; (C) 6 gN-TAN L-1. Symbols: Asterisks and squares denote acetic acid and CH<sub>4</sub>, both expressed as mg of COD equivalents; discontinu line and circles denote methane yields obtained with the adjusted Gompertz eq. and experimental data, respectively. .... 55
- Figure 4.2** Time-course quantitative PCR results from biomass samples of three independent batches incubated at 1.0, 3.5, and 6.0 gN-TAN L-1 (squares, circles, and triangles). The average (signs) and standard deviation (bars) of the ratio between number of transcripts and gene copies for the bacterial 16S rRNA (A) and the archaeal mcrA (B) has been depicted. Statistical significance in pairwise comparisons (n=3, p<0.05) in relation to the lowest ammonia exposure have been highlighted with an asterisk. .... 59
- Figure 4.3** Relative abundance of bacterial (A) and archaeal (B) ribotypes at the order and genus phylogenetic level, respectively, in terms of 16S rRNA gene and transcript counts. Each bar chart represents the median of two independent duplicates. 1g, 3.5g, 6g TAN ..... 62
- Figure 4.4** Ratio between the relative expression level of bacterial 16S rRNA transcripts obtained in batch at 3.5 gN-TAN L-1 (grey bar) and 6 gN-TAN L-1 (black bar), in relation to that at 1gTAN. Only the species with a RA higher than 0.3% are considered..... 65
- 
- Figure 5.1** Correspondance Analysis biplot on sample scores (circles) and operational taxonomic units (crosses) from the biomass of four anaerobic digesters, concerning the incidence of 16S rRNA transcripts for the Bacteria (left) and Archaea (right) domains..... 87
- Figure 5.2** Hydrogenotrophic methanogenesis and hypothetical acetate assimilation pathways, taken from Richard et al. 2016 and from the reconstructed Methanomicrobiales PGs..... 91
- Figure 5.3** Hypothetic interaction between the WL and GCS metabolic pathways reconstructed from Bacteroidetes, Chloroflexi and Firmicutes genome bins..... 92
- 
- Figure 6.1** Evolution of mean cumulative methane, acetic and VFA, expressed as COD-equivalents. Left top to bottom: control, magnetite, graphite, nylon. Right, top to bottom: steel, zeolite, PTFE, LDPE. Blue-methane part 1 & 2. Green- cetic. Red – total VFA minus a ..... 106

<b>Figure 6.2</b> Taxonomy classification (a) at phylum level of bacteria community and (b) at genera level of archaeal community, based on 16S rRNA (cDNA).....	113
<b>Figure 6.3</b> Chord diagram showing those genus with a relative abundance > 1% in the planktonic biomass samples, using the open software CIRCOS (Krzywinski, M., et al. 2009).....	114
<b>Figure 6.4</b> Chord diagram showing those genus with a relative abundance > 1% in the attached biomass samples, using the open software CIRCOS (Krzywinski, M., et al. 2009).Microbial communities in the biofilms.....	115
<b>Figure 6.5</b> qPCR results of the planktonic and attached biomass samples. Dark grey bars are gene copies and light grey are transcript. Dark grey bars are gene copies and light grey are transcript. A.16SrRNA support B.16SrRNA liquid; C. <i>mcrA</i> support D. <i>mcrA</i> liquid.....	119
<b>Figure 6.6</b> SAOB relative abundance (cDNA), based on 96% of similarity to SAOB literature-described species: (a) attached over the supports or (b) in suspension in the liquid media. Colours: C. ultunense, black; S. schinkii, light grey; T. acetatoydans, .	120
<b>Figure 6.7</b> Confocal laser microscopy images of different support materials. Images: A zeolite; B PTFE; C graphite; D magnetite; E nylon; F LDPE; G steel.....	121

<b>Figure 7.1</b> Time-course methane production in batch incubations. (a) Experiment 1. Symbols: (▼) treatment with I-CNT spheres and 7.0 gN-TAN L <sup>-1</sup> ; (●) control with 3.5 gN-TAN L <sup>-1</sup> ; (○) control with 7.0 gN-TAN L <sup>-1</sup> . (b) Experiment 2. Symbols: (●)3 g I-CNT spheres L <sup>-1</sup> ; (○) 0.5 g I-CNT spheres L <sup>-1</sup> ; (▼) 0.25 g I-CNT spheres L <sup>-1</sup> ; (Δ) 0.02 g I-CNT spheres L <sup>-1</sup> ; (■) without I-CNT spheres.....	134
<b>Figure 7.2</b> SEM images from Experiment 1. (a-b) LDPE pellets without MWCNTs. (c-d) I-CNT spheres. (e-f) I-CNT spheres with attached bacterial after 73 days of incubation. ....	137
<b>Figure 7.3</b> Relative abundance of bacterial (order) (A) and archaeal (genus) (B) ribotypes, in terms of 16S rRNA transcripts counts in methanogenic batch assays, experiment 1.....	143
<b>Figure 7.4</b> Correspondance Analysis biplot on sample scores (circles) and operational taxonomic units (crosses) from the unpacked controls (B-TAN and B+TAN), and batches amended with MWCNTs (Nt Support and NT Media), concerning the abundance of 16S rRNA transcripts bacteria. Only OTUs with a sample relative abundance higher than 3% have been represented. ....	144

**Figure 8.1** Time-course methane production in batch incubations packed with (▲) Nylon, (●) Magnetite and (○) unpacked control..... 156

**Figure 8.2** Relative abundance of bacterial (order) (A) and archaeal (genus) (B) ribotypes, in terms of 16S rRNA gene counts in methanogenic batch assays, for the <sup>13</sup>C (heavy fraction), <sup>12</sup>C (light fraction) and <sup>12</sup>C-Total (total DNA for batches without <sup>13</sup>C-Acetate)..... 157

**Figure 8.3** Relative abundance of bacterial (order) (A) and archaeal (genus) (B) ribotypes, in terms of 16S rRNA gene counts in methanogenic batch assays, for the <sup>13</sup>C (heavy fraction), <sup>12</sup>C (light fraction) and <sup>12</sup>C-Total (total DNA for batches without <sup>13</sup>C-Acetate)..... 158

**Figure 8.4** Correspondance Analysis biplot on sample scores (circles) and operational taxonomic units (triangles) from the unpacked control, and batches amended with magnetite and nylon, concerning the abundance of 16S rRNA gene copies (based on <sup>13</sup>C-DNA) for bacteria (a), archaea (b), and for bacterial metagenomes (c). In a and b only OTUs with a sample relative abundance higher than 3% have been represented; those with a relative abundance higher than 10% have been highlighted in bold..... 159

**Figure 8.5** Abundance of genes involved in the Wood-Ljungdahl pathway based on SEED annotation. c. Control m.Magnetite n. Nylon..... 163

**Figure 8.6** Abundance of genes involved in electron transfer mechanisms based on SEED annotation (cbc cluster, omp, mtrABC, c-type, fdh and pil). c. Control; m.Magnetite; n. Nylon..... 165

**Figure 8.7** GCS system pathway (linked to Wood-Ljungdahl pathway) genes abundance based on SEED annotation..... 169

**Figure 8.8** Conceptual model of syntrophic interaction between acetate oxidizing bacteria and hydrogenotrophic methanogen. Genes directly involved in specific mechanisms have been indicated (cbc, omc, mtrABC, pil).6A Mechanisms involved in unpacked bacthes. 6B Mechanisms involved when conductive materials are introduced in the environment. 6C Electron transfer processes in biofilm formation..... 171

**Figure 9.1** H<sub>2</sub>S concentration before (dark) and after(grey) recovery. b VFA (meq ac) before (dark) and after(grey) recovery. c Evolution of methane content (●) RC (▼) RZ, (Δ) RM and (○) RMZ; d. VFA evolution (●) RC (▼) RZ, (Δ) RM and (○)RMZ and partial alkalinity evolution (◇) RC (□) RZ, (◆) RM and (■) RMZ..... 186

**Figure 9.2** a) VFA (meq ac) before (dark) and after (grey) recovery. b) H<sub>2</sub>S concentration before (dark) and after(grey) recovery..... 187

**Figure 9.3** Main active pathways at different TAN concentrations and ratio COD/SO<sub>4</sub><sup>2-</sup>..... 188

Figure 9.4 Electron flow (%) changes along increment of ratio COD/SO<sub>4</sub><sup>2-</sup>..... 192

**Figure 9.5** Quantitative analysis based on qPCR expressed as *16S* rRNA gene copies/ml, *mcrA* gene copies/ml and *aprA* gene copies/ml..... 193

**Figure 10.1** Evolution of operational and control parameters in digesters R1-RT and R2-C. (a) Free ammonia nitrogen (FAN). (b) Total ammonia nitrogen (TAN). (c) Total volatile fatty acids (VFA). (d) Acetic to propionic acids ratio. (e) Methane yield. (d) Volatile (VS) removal efficiency. Note: vertical dotted lines denote performance periods. Colours: R1-RT, black; R2-C, grey..... 206

**Figure 10. 2** Specific methanogenic activity (SMA), expressed as percentage of the maximum SMA, as a function of the free ammonia (NH<sub>3</sub>; left) o total ammonia (TAN; right) contents in digesters R1-RT and R2-C. (a) Period 1. (b) Period 2. (c) Period 3..... 207

**Figure 10.3** Relative abundance of bacterial (a, c) and archaeal (b, d) populations, obtained by MiSeq analysis based on *16S* rRNA (a, b) and *mcrA* cDNA (c, d), respectively, in digesters R1-RT and R2-C..... 213

**Figure 10.4** Quantification of present and active microorganisms in both digesters R1-RT and R2-C along the performance periods (P1, P2, P3). (a) Bacteria *16S* DNA and *16S* RNA gene transcripts. (b) Archaeal *mcrA* and *mcrA* gene transcripts. Nomenclature: dark grey, *16S* rRNA and *mcrA* transcripts copies in (a) and (b), respectively. .... 215

**Figure 10.5** Canonical correspondence analysis of performance parameters and community in both digesters R1-RT and R2-C along the performance periods (P1, P2, P3). (a) Bacterial-*16S* rRNA (cDNA) reads. (b) Archaeal-*16S* rRNA (cDNA) reads. Note: The selected environmen parameters were the solid retention time (SRT) and the volatile fatty acids (VFA), as well as the total and free ammonia contents (FAN, TAN), were selected for this analysis. Samples scores are denoted by circles and OTUs are denoted by triangles. .... 216

**Figure 11.1** Scheme of lab-scale digesters: (a) R4\_control; (b) R5\_abad; (c) R6\_mix abad. Numbers: 1- Influent. 2- Reactor. 3- Heater. 4- Effluent. 5- Gas flowmeter. 6- Gas counter. 7- Effluent tank. 8- Support material ..... 228

**Figure 11.1** Scheme of lab-scale digesters: (a) R4\_control; (b) R5\_abad; (c) R6\_mix abad. Numbers: 1- Influent. 2- Reactor. 3- Heater. 4- Effluent. 5- Gas flowmeter. 6- Gas counter. 7- Effluent tank. 8- Support material (Continuation from previous page). ..... 229

**Figure 11. 2** Operational parameters of the three continuous systems. (a) OLR. (b) HRT. (c) TAN inside the reactor. (d) Concentration of acetic acid..... 233

**Figure 11. 3** Control parameters of the three continuous systems. (a) COD removal efficiency (%in-COD). (b) Methane productivity ( $\text{Nm}^3\text{CH}_4 \text{ m}^{-3} \text{ d}^{-1}$ ). (c) Methane yield ( $\text{Nm}^3\text{CH}_4/\text{kgCOD}$ ). (d) Alkalinity ratio. (e) Methane content of biogas (%v/v). (f) Propionic to acetic.....234

## INDEX OF TABLES

---

<b>Table 4.1</b> Acetate consumption (rAc) and methane production (rCH <sub>4</sub> ) specific rates, lag phase, methane yield and the apparent fractionation factor ( $\alpha$ C). Depicted values correspond to the average and standard deviation of three independent replicates. ...	53
<b>Table 4.2</b> Estimators of microbial species diversity/richness based on NGS of 16S rRNA genes and transcripts from the Bacteria and Archaea domains, obtained from the initial inoculum and after its incubation during 11 and 17 days under increasing TAN content.....	54
<b>Table 4.3</b> Best match in BLAST searches (GenBank, NCBI, USA) on TAN-responding OTUs (Figure 3). Only OTUs with a relative abundance in the original methanogenic biomass higher than 1% are listed. ....	57
<b>Figure 5.1</b> Correspondance Analysis biplot on sample scores (circles) and operational taxonomic units (crosses) from the biomass of four anaerobic digesters, concerning the incidence of 16S rRNA transcripts for the Bacteria (left) and Archaea (right) domains.....	87
<b>Figure 5.2</b> Hydrogenotrophic methanogenesis and hypothetical acetate assimilation pathways, taken from Richard et al. 2016 and from the reconstructed Methanomicrobiales PGs.....	91
<b>Figure 5.3</b> Hypothetic interaction between the WL and GCS metabolic pathways reconstructed from Bacteroidetes, Chloroflexi and Firmicutes genome bins.....	92
<b>Table 6.1</b> Mineral medium composition.....	103
<b>Table 6.2</b> Main characteristics of the different support media added to each batch analysis.....	104
<b>Table 6. 3</b> Set-up and results of the batch tests with different supports: acetate and TAN concentration at the end of different pulses, methane yield, rate and lag phase, isotopic fractionation ( $\alpha$ c values of each material at exponential phase of second pulse) .....	108
<b>Table 6.4</b> Compilation of data for the support assessment .....	109
<b>Table 7.1</b> Set up results of experiment 1 with differnt TAN concentrations.....	134
<b>Table 7.2</b> Set-up and fitting results of experiment 2 with different I-CNT spheres concentration. Note: * Fresh inoculum at 3.5 gN-TAN L <sup>-1</sup> and without I-CNT spheres. ** Fresh inoculum at 7.0 gN-TAN L <sup>-1</sup> and without I-CNT spheres.....	136

<b>Table 7.3</b> Estimators of microbial species diversity/richness based on NGS of 16S rRNA genes and transcripts from the Bacteria and Archaea domains, obtained from the initial inoculum and after its incubation during 11 and 17 days under increasing TAN content. Predominant assigned genera (abundance > 5%) are also listed.....	140
<b>Table 7.4</b> Best match in BLAST searches (GenBank, NCBI, USA) on TAN-responding OTUs (Figure 3). Only OTUs with a relative abundance in the original methanogenic biomass higher than 1% are listed. ....	141
<b>Table 9.1</b> Physic-chemical and operational parameters before and after recovery strategy application.....	185
<b>Table 10.1</b> Raw materials characterization. Nomenclature: COD, chemical oxygen demand; TS, VS, total and volatile solids; TKN, TAN, total Kjeldhal and ammonia nitrogen; nm, not measured.....	203
<b>Table 10.2</b> Indexes of performance and diversity of Bacteria and Archaea (H' and 1/Simpson). Note: * Mean values of the whole period.....	209
<b>Table 10.3</b> Results of the Canonical Correspondence Analysis from Figure 5a (Bacteria). Note: * Eigen values, weighted correlations between species and environmental axes, cumulative percentage of variance of species data and of species-environment relation, and weighted correlations between environmental and species-canonical axes.....	211
<b>Table 10.4</b> Results of the canonical correspondence analysis of Figure 5b (Archaea). Note: * Eigen values, weighted correlations between species and environmental axes, cumulative percentage of variance of species data and of species-environment relation, and weighted correlations between environmental and species-canonical axes.....	212
<b>Table 11. 1</b> Characterisation of synthetic medium used as inflow in the continuous systems.....	230
<b>Table 11.2</b> Average values of operational and control parameters per continuous system.....	232

## LIST OF ABBREVIATIONS

---

AD	anaerobic digestion
AM	acetotrophic methanogenesis
AMA	acetotrophic methanogenic archaea
BOD	biochemical oxygen demand
C	carbon
CGY	crude glycerine
CI	confidence interval
CH <sub>4</sub>	methane
C/N	carbon nitrogen ratio
CO <sub>2</sub>	carbon dioxide
COD	chemical oxygen demand
CSTR	continuous stirred tank reactor
EPS	extracellular polymers substances
FID	flame ionization detector
FW	food waste
GC	gas chromatograph
H	hydrogen
H <sub>2</sub>	hydrogen gas
HM	hydrogenotrophic methanogenesis
HMA	hydrogenotrophic methanogenic archaea
HRT	hydraulic retention time
IA	intermediary alkalinity
IC <sub>50</sub>	half maximal inhibitory concentration
LCFA	long chain fatty acids
M	mesophilic
MPA	methanogenic population archaea
MP	methane potential
N	nitrogen
NGS	next generation sequencing
NH <sub>4</sub> <sup>+</sup> -N	ammonium nitrogen
O	oxygen
OLR	organic loading rate
P	period
PA	partial alkalinity
P <sub>calCH<sub>4</sub></sub>	heating value of methane
PCR	polymerase chain reaction
PG	population genome
PH <sub>2</sub>	hydrogen partial pressure



qPCR	quantitative polymerase chain reaction
RT-PCR	retrotranscriptase polymerase chain reaction
S	sulphur
SAO	syntrophic acetate oxidation
SAOA	syntrophic acetate oxidation archaea
SAOB	syntrophic acetate oxidation bacteria
SO <sub>4</sub> <sup>-2</sup>	sulphate
SRB	sulphate reducing bacteria
SRT	sludge retention time
t	time
T	temperature
TCD	thermal conductivity detector
TKN	total Kjeldahl nitrogen
TMP	theoretical methane potential
TN	total nitrogen
TS	total solids
T <sub>s</sub>	temperature of the sludge
TSS	total suspended solids
V	volume
VFA	volatile fatty acids
VS	volatile solids
UASB	upflow anaerobic sludge blanket
WAS	waste activated sludge
WW	wastewater
WWTPs	wastewater treatment plants
Y <sub>CH<sub>4</sub></sub>	methane production
ρ:	sludge density
λ:	lag phase
α	coefficient between MP/TMP



## **Summary**

The anaerobic digestion (AD) consists of a cascade of syntrophic interactions between several microbial groups that result in the breakdown of biodegradable organic matter in the absence of oxygen, resulting in the production of biogas, a CH<sub>4</sub> and CO<sub>2</sub>-rich mixture that can be valorised as renewable energy. The anaerobic digestion process has been engineered for a wide range of applications and current technology developments are aimed towards the so-called co-digestion, the treatment of complex mixtures of organic materials (e.g. slaughterhouse wastes) for an increased biogas yield. Nevertheless, the AD process might be hampered by the inhibitory effect of long chain fatty acids, ammonia and sulphate arising from the hydrolysis of proteins.

The main objective of this thesis is to develop innovative techniques and methodologies to degrade protein. As described throughout the following sections, these compounds are potentially inhibitors of AD process, and consequently the production of CH<sub>4</sub> and other value-added compounds. These wastes with high concentration of proteins emit high concentrations of NH<sub>3</sub> when are degraded. It is reported that in this situation, the main population of methanogenic archaea are inhibited. However, the populations with the ability to carry out the hydrogenotrophic methanogenesis are active in this kind of environments. Therefore, increasing acetate oxidising bacteria populations (SAOB) is possible to achieve a syntrophy relation with some hydrogenotrophic archaea (HMA) populations, in this way is possible to avoid the inhibition caused by the NH<sub>3</sub> concentration. Furthermore, sometimes these kind of wastes are associated with rich SO<sub>4</sub><sup>2-</sup> compounds that could be easily reduced to sulphide (H<sub>2</sub>S), molecule that is toxic, corrosive and odorous, producing several problems in the AD process and industrial facilities. The biological reaction that produced these compounds is performed by sulphate-reducing bacteria (SRB). These microbial communities, SRB, have the ability to couple the oxidation of organic matter to the reduction of SO<sub>4</sub><sup>2-</sup> outcompeting directly with methane producing archaea (MPA) and homoacetogenic bacteria for common substrates, and inhibiting the CH<sub>4</sub> production.

In order to carry out this doctoral thesis, two blocks (engineering and microbiological) have been developed that have been integrated as the work progressed. Firstly, different batch-scale studies were carried out in order to monitor the physical-chemical parameters and also the evolution of the microbial communities. In microbiology field, the main objective was to explore the evidence of acetate oxidation via syntrophic interaction between SAOB-HMA. To this end, the abundances of majorities groups were quantified using qPCR analysis based on the 16S rRNA and *mcrA* genes combined with isotopic compounds. Furthermore, the rapid advancement of high-throughput molecular techniques, as shotgun metagenomics sequencing and binning of scaffolds, have been allowed the implementation of genome-centric approaches that generate comprehensive databases from complex environmental samples, which includes complete or nearly-complete microbial genomes.

Secondly, it was necessary that the reactors operated with the appropriate parameters to stablish this syntrophic interaction. As well as, it was also to establish protocols and different parameters concerning the configuration of the reactor based on literature and results obtained from the first set of experiments. Within this block, the hydraulic retention time (HRT), temperature ranges, organic loading rate, reactor configuration was treated. Finally, within this block, the most important point was to found the optimal reactor configuration. As it is known, the structure and the various units that make up a reactor, affect directly the efficiency and optimization of the same. Along this thesis different configurations was tested.

## **Resumen**

La digestión anaerobia (DA) consiste en una cascada de interacciones sintróficas entre diferentes grupos de microorganismos que tiene como principal finalidad la degradación de la materia orgánica con el fin de obtener biogás, una mezcla de  $\text{CH}_4$  y  $\text{CO}_2$  que puede ser de gran valor en el campo de las energías renovables. El proceso de DA ha sido diseñado para una amplia gama de aplicaciones y para obtener un mayor rendimiento de biogás. Sin embargo, el proceso de DA podría verse obstaculizado por el efecto inhibitorio de los ácidos grasos de cadena larga, el amoníaco de la hidrólisis de proteínas o los compuestos sulfurados.

El objetivo principal de esta tesis es desarrollar técnicas y métodos innovadores para degradar las proteínas. Como se describe a lo largo de las siguientes secciones, estos compuestos son potencialmente inhibidores del proceso de DA y, en consecuencia, de la producción de  $\text{CH}_4$ . Este tipo de residuo con alta carga de proteínas emite altas concentraciones de  $\text{NH}_3$  cuando éstas son degradadas. Está reportado que bajo estas condiciones desfavorables el principal grupo de microorganismos productores de  $\text{CH}_4$  (arqueas metanogénicas) se encuentra total o parcialmente inhibido. Sin embargo, dentro de esta gran comunidad de arqueas capaces de producir  $\text{CH}_4$ , existen algunos reductos capaces de mantenerse activas bajo concentraciones de elevado nitrógeno amoniacal mediante la ruta de la metanogénesis hidrogenotrófica. Esta población abre nuevas posibilidades para obtención de biogás de este tipo de residuos. Una de estas opciones consiste en incrementar las poblaciones oxidadoras de acetato para lograr una relación sintrófica estable con estas poblaciones hidrogenotróficas, evitando de este la inhibición causada por  $\text{NH}_3$ . Además, en muchas ocasiones este tipo de residuos con alta carga proteica van asociados a una elevada concentración de compuestos sulfurados, lo que podría conllevar una reducción de éstos a ácido sulfhídrico ( $\text{H}_2\text{S}$ ). Esta molécula es tóxica, corrosiva y olorosa, que provoca varios problemas en DA y en las instalaciones asociadas. La reacción biológica que conlleva a la formación de este compuesto está mediada por el grupo de bacterias conocidas como bacterias sulfato reductoras (SRB). Estas comunidades microbianas, SRB, tienen la capacidad de

acoplar la oxidación de la materia orgánica a la reducción del  $\text{SO}_4^{2-}$  compitiendo directamente por los sustratos comunes con las arqueas productoras de  $\text{CH}_4$  y bacterias homoacetogénicas inhibiendo de este modo, la producción de biogás.

Se han llevado a cabo dos grandes bloques (ingeniería y microbiología) que a medida que se avanzaba con el trabajo han ido integrándose. En primer lugar, se llevaron a cabo diferentes estudios en régimen discontinuo a escala laboratorio, monitorizando los parámetros físicoquímicos y la evolución de las comunidades microbianas. El primer objetivo fue el estudio y análisis de las evidencias de la ruta sintrófica oxidadora de acetato acoplada a una metanogénesis hidrogenotrófica, estudiando las interacciones entre estas dos comunidades. Para ello, se cuantificaron mediante qPCR los dos grupos mayoritarios basándonos en los genes de referencia,  $16\text{S rRNA}$  para la monitorización de las bacterias, y *mcrA* en el caso de las arqueas metanogénicas combinando esta cuantificación con el marcaje de compuestos isotópicos. Además, se ha podido desarrollar estudios centrados en el estudio del genoma gracias a la secuenciación *shotgun* y las herramientas bioinformáticas.

En segundo lugar, uno de los principales era mediante los correctos parámetros de operación de los reactores conseguir la aparición y estabilidad de las sintrofías comentadas anteriormente. Fue fundamental establecer protocolos y marcar los parámetros relacionados con la configuración de los reactores, y para ello se basó el diseño de estos en los resultados obtenidos de los diferentes ensayos discontinuos previos. Siguiendo en esta línea, se analizaron meticulosamente parámetros como tiempo de retención hidráulico, velocidad de carga orgánica, rangos de temperatura y configuración del reactor. Finalmente, uno de los puntos críticos fue la elección y diseño de los reactores. Es bien sabido, que el diseño y operación del digestor es crucial para un desarrollo óptimo del proceso, por ello se probaron diferentes configuraciones.

## Resum

La digestió anaeròbia (DA) consisteix en una cascada d'interaccions sintròfiques entre diferents grups de microorganismes que tenen com a principal finalitat la degradació de la matèria orgànica per obtenir biogàs, una barreja de  $\text{CH}_4$  i  $\text{CO}_2$  pot ser de gran valor en el camp de les energies renovables. El procés de la DA ha sigut dissenyat per una ampli espectre de residus, (per exemple, restes d'escorxadors) per obtenir un major rendiment de biogàs. No obstant, el procés de la DA es podria veure obstaculitzat per l'efecte inhibitori dels àcids grassos de cadena llarga, la hidròlisi de les proteïnes o els compostos sulfurats.

L'objectiu principal d'aquesta tesis es desenvolupar tècniques i mètodes innovadors per la degradació de les proteïnes, principalment. Com es descriu al llarg de les pròximes seccions, aquests compostos son potencialment inhibidores del procés de la DAa, i en conseqüències, de la producció de  $\text{CH}_4$ . Està descrit a la literatura que sota aquestes condicions desfavorables el principal grup de microorganismes productors de  $\text{CH}_4$  (arquees metanogèniques) es troba total o parcialment inhibit. No obstant, dins d'aquesta gran comunitat de microorganismes existeixen reductes que son capaços de mantenir la activitat metanogènica tot i trobar-se sota aquestes condicions d'inhibició, mitjançant la ruta metanogènica hidrogenotròfica. Aquesta població doncs, ha obert noves possibles vies per la obtenció de biogàs partint d'aquests productes altament inhibitoris. Una d'aquestes opcions, consisteix en incrementar aquelles poblacions que son capaces d'oxidar l'acetat per aconseguir establir una sintròfia amb les poblacions hidrogenotrofiques, evitant així, la inhibició causada per  $\text{NH}_3$ . A més, en moltes ocasions aquest tipus de residus porten associats altes càrregues de compostos sulfurats, el que podria portar posteriorment a una reducció d'aquests compostos a la formació d'àcid sulfhídric ( $\text{H}_2\text{S}$ ). Aquesta molècula, és tòxica, corrosiva i olorosa, que a més provoca problemes dins del propi procés i és altament perjudicial per les instal·lacions. Aquesta molècula es forma principalment de manera biològica, portada a terme pels bacteris coneguts com sulfato reductors (SRB). Aquestes comunitats, SRB, tenen la capacitat d'acoblar l'oxidació de la matèria

orgànica amb la reducció dels compostos sulfurats, competint directament pels substrats comuns amb els arquees hidrogenotrofs i els bacteris homoacetogenics, inhibint així la producció de CH<sub>4</sub>.

Amb la finalitat de desenvolupar aquesta tesis doctoral, s'han portat a terme dos grans blocs experimentals (enginyeria i microbiologia) que a mesura que el treball avançava s'han integrat progressivament l'un amb l'altre. Dins del bloc de la microbiologia, el primer objectiu va ser l'estudi i l'anàlisi de les evidències de la ruta sintròfica oxidadora d'acetat acoblada a la metanogènesi hidrogenotrofica, estudiant les interaccions entre aquestes dues grans comunitats. Es van quantificar mitjançant anàlisis de qPCR els dos grups majoritaris bastant-nos en els gens de referència, 16SrRNA per bacteris i *mcrA* per arquees metanogèniques combinat amb un estudi de marcatge isotòpic. Complementàriament, el ràpid avenç de les tecnologies moleculars d'alt impacte com la seqüenciació *shotgun* i les eines bioinformàtiques, han permès desenvolupar estudis centrats en el genoma i poder generar bases de dades més accessibles i àmplies relacionades amb la complexitat del microbioma ambiental. Per aquest motiu, aprofitant aquestes grans noves tecnologies s'ha pogut ampliar i profunditzar en el coneixement de les interaccions entre les comunitats microbianes i de part dels gens involucrats en la digestió d'aquest tipus de residus.

En segon lloc, un dels principals objectius del segon bloc era mitjançant els correctes paràmetres d'operació dels reactors aconseguir l'aparició i estabilitat de les sintròfies comentades anteriorment. Va ser fonamental també, establir protocols i marcar els paràmetres relacionals amb la configuració dels reactors, per aquest motiu, es va basar el disseny d'aquests digestors en els resultats obtinguts dels experiments discontinus previs. Seguint en aquesta línia, es van analitzar minuciosament paràmetres com el temps de retenció hidràulic, velocitat de càrrega orgànica, rangs de temperatura i configuració del reactor.

Finalment, un dels punts crítics pel bon funcionament del projecte va ser l'elecció i disseny dels reactors. Es coneix, que el disseny i l'operació dels digestors es de vital importància per un desenvolupament òptim dels processos, per això es van provar diferents configuracions.



*Resum*

## Preface

This thesis has been developed within the research GIRO program (Spanish acronym of *Integral Management of Organic Waste*) of IRTA (Catalá acronym of *Institute for Agri-Food Research and Technology*), under the supervision of Dr. Francesc X. Prenafeta Boldú and Dra. Belén Fernández García, as a part of the Environmental engineering PhD program of the Politechnic University of Catalonia (UPC, Spain). The activities encompass in this thesis were financially supported by INIA (Spanish acronym of *National Institute of Agricultural and Food Research and Technology*, Spanish Ministry of Economy and Competitiveness), and carried out within the framework of the projects INIA-RTA2012-00098-00-00 (PROGRAMO) and INIA-2017-0023 (PIONER). Josep Ruiz has the FPI-INIA-RTA2012-00098-00-00 fellowship, which included abroad stage at Università di Padova, under Dr. Stefano Campanaro supervision.

This thesis focuses on linking the operation of lab-scale anaerobic digesters, under different hydraulic configurations, and the microbial interactions in ammonia/sulfate rich environments under a multidisciplinary point of view. The metabolic syntrophic interactions, based on bacteria-archaea hydrogen transfer, is widespread in natural anaerobic regions of our planet, from forest soils to deep sea sediments, because it is a well-known strategy to survive in such extreme environments. However, there is a lack of knowledge about syntrophic relation and how are they established under more concentrated nitrogen environments, such anaerobic digesters. Thereby, this is the main topic that this thesis wants to elucidate.

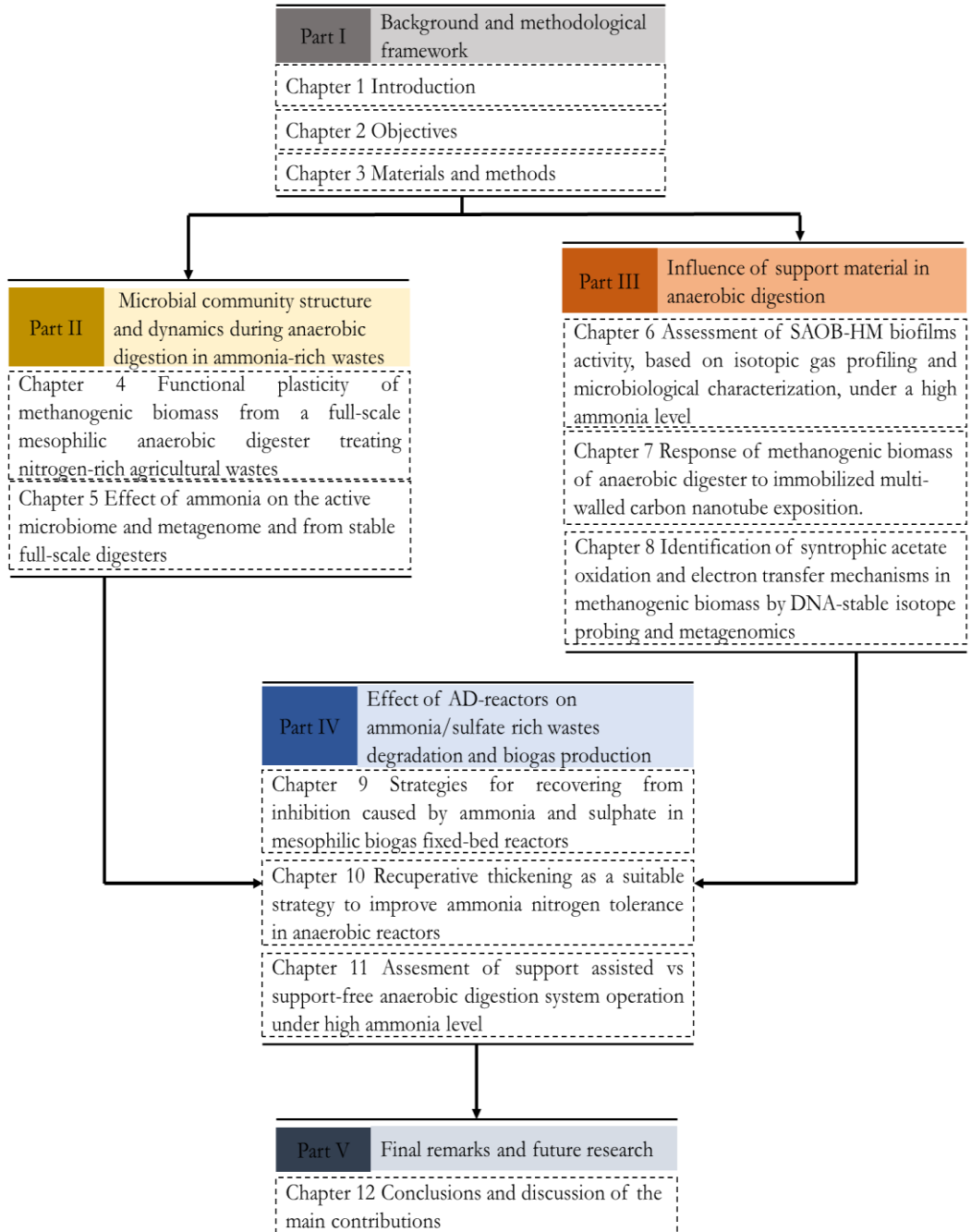
The present document is divided into 4 parts and 12 chapters represented schematically in this section (below). **Part I** comprises a general introduction (**Chapter 1**), the motivation and objectives (**Chapter 2**) and the main methodologies and procedures (**Chapter 3**). **Part II** comprises two chapters focused on the study of microbial populations and their interactions when subjected to high concentrations of ammonium. In **Chapter 4**, a better understanding of active microbial communities subjected to increasing high concentration of ammonia-N from both applied and

fundamental perspectives. Complementary in **Chapter 5** an assessment based on shotgun metagenomics sequencing combined with binning of scaffolds of population genomes was done for better understanding of the microbial community in industrial AD reactors operated at different ammonia levels

**Part III** comprises three chapters intend to delve into the microbial communities, genomes, metabolic pathways, proteins and genes that surround anaerobic nitrogen-rich environments influenced by the introduction of support material. For that, In **Chapter 6**, different support materials were assessed for biofilm formation of ammonia N tolerant microorganisms under anaerobic conditions. In **Chapter 7**, a specific case of support material with bioelectrochemical properties as an enhancer of syntrophic interactions of anaerobic microorganismos was evaluated. To finalize this part, in **Chapter 8**, advanced bioinformatic techniques were combined with the isotopic labeling of DNA, in order to elucidate those genes really involved in the assimilation of acetate and those genes implicated in the different interactions with different kind of supports.

**Part IV** comprises three chapters dedicated to mesophilic lab-scale digesters. In **Chapter 9**, four identical anaerobic digesters, with different support materials (zeolite and magnetite), were operated to improve the methanogenic archaea resilience towards inhibitors (ammonia and sulphate) after implementing a recovery strategy. In **Chapter 10**, recuperative thickening, applied to stirred tank anaerobic digesters submitted to high ammonia N levels, enhanced the activity of syntrophic acetate oxidizers and hydrogenotrophic archaeal members. In **Chapter 11**, three lab-scale mesophilic reactors, amended with different support materials (magnetite, nylon, and zeolite), were operated and evaluated under two configurations: continuous stirred tank and assisted basket reactors.

**Part V** is the last part of this document and comprised one chapter (**Chapter 12**) that summarizes the knowledge generated in this research, the general conclusions and the upcoming challenges in the field of anaerobic digestion focused on inhibitory compounds and microbioma.



General overview



# Part I

---

Background and methodological  
framework

# Chapter 1 Introduction

---

This chapter introduces the general fundamentals of anaerobic digestion and the importance of treating anaerobically nitrogen, sulphate and fatty acids rich compounds to avoid environmental contamination, meanwhile are obtaining renewable energies. Special attention was given to the microbial communities and process aspects that involve anaerobic digestion.

## **1.1. Current state**

Organic wastes arising from farming have traditionally been used in agriculture as fertilizers in order to close the nutrient cycle and prompt a sustainable management in the food production sector. However, the intensification and industrialization of livestock production and transformation has resulted in several changes and challenges concerning the management of farms and crops. The interrelations between the animal and plant production sectors has been altered in many places because of the exponential increase of livestock with respect to agriculture. This uncoupling between both sectors has resulted in a number of environmental impacts that are briefly discussed herein.

According to the Spanish National Association of Meat Industries (Anice 2015), the meat production is the 4th Spanish industrial sector, and is composed of about 3,000 SME (slaughterhouses, meat processing, etc.). It occupies by far the first place of the entire food industry, with over of 21,164 M€ of turnover (more than 20% of the food sector and 2% of the total Spanish GDP), and represents more than 20% of the total employment in the food industry.

On the other hand, it is estimated that about 2,000,000 tons per year of animal waste are generated in Spain. This data includes 380,000 tons for the animals that die on the farm itself and whose collection and treatment costs annually 150 M€ (MAGRAMA 2010). Yet, animal dejections are the most abundant source of organic waste from the livestock sector, being its application as a fertilizer according to the European Directive 91/676/EEC, the main management strategy. The agronomical application of manure in areas of high farming density is limited according to the level of nutrients extraction from the crops, and by the degree of nitrate pollution of the underlying aquifers. In such vulnerable areas, it is necessary to implement systems for the processing of manure that facilitate the recovery and export of the nitrogen surplus nitrogen or, as the last instance, its elimination.

Currently it is stimulating the activity around the development of schemes that are applied to different scales to manage with environmental and health guarantees, both of the dead animals and the waste of the meat industry, as the livestock excrement. One of the major technological strategies proposals to tackle this problem is founded on the process of anaerobic digestion (AD). The economic viability of AD depends, among other factors, on the specific production of methane per unit of treated residue, and on the cost/benefit relationship from the management of the generated nutrients. In this context, the current trend to increase the technical and economic viability of AD plants consist on its operation in a regime known as co-anaerobic



digestion (co-AD). That is, to combine by-products, usually from the food industry, which contain a high energy potential (e.g., wastes rich in fats and proteins) with other wastes, usually partly biodegraded, which provide specific benefits like the presence of oligoelements and buffer capacity (e.g. animal dejections, sewage sludge, etc.). The co-AD takes advantage of complementarity in the composition of the different substrates to increase the specific production of methane and unify the management of different wastes.

However, there are still major challenges to the process that currently remain to be fully resolved at the technological level. On the one hand, the AD of waste with a high nitrogen content (e.g., manure, slaughterhouse waste, food waste, etc.) can lead to the inhibition of the methanogenic acetotrophic archaea, which are particularly sensitive to the accumulation of the  $\text{NH}_4$  and volatile fatty acids (VFA Zhang et al. 2014). This limitation can be overcome through the enrichment syntrophic acetate oxidizing bacteria (SAOB) in conjunction with certain groups of hydrogenotrophic archaea (HMA), because both populations are more resistant to ammonia and fatty acids (Hao et al. 2011, 2015; Lu et al. 2013; Westerholm et al. 2012). The SAOB are characterized by their low rate of cell growth and by their ability to develop as litotrophic, producing acetate from  $\text{H}_2$  and  $\text{CO}_2$  or perform the reverse process in with the hydrogenotrophic archaea, depending on the partial pressure of hydrogen (Schnurer et al. 2008). That metabolic pathway is used also in the reverse sense as main mechanism for energy conservation and for synthesis of acetyl-CoA and cell carbon from CO, known as Wood-Ljungdahl (W-L) pathway.

## **1.2. Anaerobic digestion**

AD naturally occurs in environments where molecular oxygen and other electron acceptors are lacking, such as in waterlogged soils, lake and oceanic basin sediments, and in the gut of humans and other animals, especially ruminants. AD might also be an unwanted anthropogenic process because of the methane generated in landfills, rice paddies, intensive livestock production, etc. which contributes to the global greenhouse effect (Salminen and Rintala 2002). Yet, AD can be turned into a helpful biotechnological process when applied to the treatment of bulk organic materials such as agricultural, livestock, industrial, or municipal wastes. In fact, AD is a widely common technology to treat animal dejections in farms, which are generally characterized by a wide range in the content of solids (5-40%) that is equivalent to the 25-35% BOD of such waste (Hansen, Angelidaki et al. 1998). The AD process is generally divided into four basic steps which are explained in section 1.2.1.

Therefore, AD reactors must be designed for enhancing the activity of the methanogenic biomass, as the economic feasibility of the technology often relies in an optimized biogas production for waste to energy conversion. It is therefore necessary to understand the process-limiting factors, which in many cases are ultimately related to the microbial interactions that take place inside the reactor (Hansen, Angelidaki et al. 1998).

### **1.2.1 Stages in the anaerobic digestion process**

The AD of organic matter is a complex process that encompasses several biochemical reactions, catalysed by different microbial groups that interact in a syntrophic consortium. These reactions occur simultaneously in cascade, and are grouped in four major stages: hydrolysis, acidogenesis, acetogenesis, and methanogenesis (Ahring et al., 1992).

The polymeric organic substrates cannot be used directly by microorganisms unless they are hydrolyzed into soluble compounds, which can pass through the cell wall. Hence, hydrolysis is the necessary first step in the anaerobic degradation of complex organic matter. The action extracellular hydrolytic enzymes produced by microorganisms carry out the breakdown of these complex molecules (Morgenroth et al., 2002). The hydrolytic stage can be the limiting process overall speed of the process, especially when treating wastes with high solids content. Furthermore, the hydrolysis depends on the process temperature, hydraulic retention time, the biochemical composition of substrate (percentage of lignin, carbohydrates, proteins and fats), particle size, pH levels, the concentration of hydrolysis products, and of inhibitors (Veeken et al., 2000).

Complex substrates comprise three basic types of macromolecules: carbohydrates, proteins and lipids. Protein is an important substrate in the process of anaerobic digestion because besides being a source of carbon and energy, amino acids derived from its hydrolysis have a high nutritional value (Mata-Alvarez et al., 2000). Proteins are hydrolyzed into peptides and amino acids by the action of proteolytic enzymes called proteases. Some of these amino acids are used directly in the synthesis of new cell material and the rest are degraded to volatile fatty acids (VFA), CO<sub>2</sub>, H<sub>2</sub>S and NH<sub>3</sub> in subsequent stages. The degradation of lipids in anaerobic environments begins with the breakdown of fats by the action of hydrolytic enzymes called lipases producing long chain fatty acids and glycerol (Angelidaki and Ahring, 1992).

During the acidogenic stage the fermentation of hydrolyzed soluble molecules results in compounds that can be used directly by the methanogenic bacteria (acetic and formic acids, H<sub>2</sub>), and smaller organic compounds (mainly propionic, butyric, valeric,

and lactic acids, and ethanol) that are subsequently oxidized by the acetogenic bacteria (Vandevivere et al., 2003). During this step a wide range of substrates can be fermented, such as, glycerol, fatty acids, aminoacids, monosaccharides, etc (Donoso-Bravo et al., 2009). Nevertheless, the most abundant sources are monosaccharides and aminoacids. The metabolic pathways to ferment these compounds are completely different because the capability to utilise both compounds is widespread (Ganidi et al., 2009).

In acetogenic step is when the different intermediary molecules are used to acetate synthesis, which included the formation of acetate from CO<sub>2</sub> reduction, as well as, from the degradation of organic acids. In this step is necessary to keep low the hydrogen partial pressure in order to preserve favourable thermodynamic conditions for the optimum conversion of VFAs to acetate (Lee and Zinder, 1988). However, it is always not possible, to draw a clear distinction between acetogenic and acidogenic reactions. Since Acetate and H<sub>2</sub> are produced during acidification and acetogenic reactions and both of them are substrates for subsequent methanogenic microbes (Donoso-Bravo et al., 2009).

The final methanogenic stage is driven by strict anaerobic archaea. Here, methanogens use the intermediate products of the preceding stages and convert them into CO<sub>2</sub>, CH<sub>4</sub> and H<sub>2</sub>O (Daniels et al., 1984; Thauer et al., 1993). These components make up the majority of the biogas emitted from the system. Methanogenesis is sensitive to both high and low pHs and occurs between pH 6.5 and pH 8. The remaining, indigestible material the microbes cannot use and any dead bacterial remains constitute the digestate (Zeikus et al., 1975).

### **1.2.2 Process inhibition by nitrogen compounds**

Another important component involved in anaerobic digestion of organic waste is ammonia, generated after the digestion of proteins. It is widely accept that high concentration of ammonia is toxic for anaerobic biomass (Hunik et al., 1990). The TAN values is a combination of FAN (NH<sub>3</sub>), and ionized ammonium nitrogen (NH<sub>4</sub><sup>+</sup>) (Kayhanian, 1994) whose concentration are directly related to pH and temperature. NH<sub>3</sub> is known as the active component that causes the ammonia inhibition since its capability to permeabilise on the cellular membrane (Siles et al., 2010). In addition, it can cause a disturbance in pH that affects cells and some reactions because the inhibition of some specific enzymes (Hansen, Angelidaki et al. 1998). However, ammonia has an important role, because low concentration of this compound, less than 0.5 gN·L<sup>-1</sup> can cause a decrease in CH<sub>4</sub> production because of loss of biomass, and loss of acetotrophic methanogenic activity (PoggiVaraldo,

RodriguezVazquez et al. 1997). This is because there is a deficiency of nitrogen as nutrient in the medium, and because the loss of buffer activity that this compound provides.

Like the negative impact of nitrogen deficiency for microbial development occurring at low concentrations, a high concentration of  $\text{NH}_3$  may cause a severe disturbance in the anaerobic process. Such as, a decrement of microbial activity and consequently a decrement in  $\text{CH}_4$  production. Primary inhibition because of accumulation of ammonia in the reactor might also result in the buildup of intermediate digestion products like VFA, which might contribute further to microbial inhibition and reactor failure (Calli, Mertoglu et al. 2005). The wide range of the reported inhibiting total ammonia concentrations might be due to differences in the system, such as in the microbial community structure of the methanogenic biomass, nature of substrate, operational conditions of the reactor, temperature and pH affecting ammonia dissociation, and the acclimation period. Some studies reported that when TAN exceeds  $3.0 \text{ gN}\cdot\text{L}^{-1}$ , the inhibition of the AD process occurs independently of the pH, while others studies claim that it is possible to observe a partial inhibition at  $2.5 \text{ gN}\cdot\text{L}^{-1}$  of TAN (Koster and Lettinga 1984).

As it previously described, the  $\text{NH}_3$  inhibition is mainly caused by FAN, which is the easily permeable nitrogen compound. This way of nitrogen is depending on three parameters (temperature, pH and TAN) (Hansen, Angelidaki et al. 1998). Several studies report different concentrations of AD inhibition, at different concentrations of FAN. In the digestion of swine manure in a continuous reactor, inhibition by FAN was noticed at  $1.6 - 2.6 \text{ gN}\cdot\text{L}^{-1}$  FAN, within a range of temperature between  $55 - 60$  °C and pH of  $7.9 - 8.1$ . Other studies revealed that when the temperature is lower, the inhibitory FAN concentration is also lower. At  $37$  °C, the concentration required to stop the anaerobic process is  $0.75 \text{ gN}\cdot\text{L}^{-1}$  FAN, value that is two times lower than that at  $55$  °C (Salminen and Rintala 2002).

$\text{NH}_3$  levels, together with temperature, reactor configuration and operation have been identified as the very important factors that determine the microbial community composition in full-scale anaerobic digesters (Hunik et al., 1990). Furthermore, the inhibitory effects of ammonia on methanogenic microbial consortia are also considered to have a relevant impact in the last biodegradation stages, concerning the activity of HMA, which consume  $\text{H}_2$  and formate, and of acetotrophic methanogens that feed on acetate (Calli et al., 2005; Sung and Liu, 2003). The later methanogens are considered to be most sensitive to ammonia. Due to biogas production through anaerobic process of organic matter needs complex microbial communities and

interaction, the reduced methanogenic activity subsequently influences reaction pathways higher up in the degradation chain (Wang et al., 2015).

### **1.2.3 Process inhibition by long chain fatty acids (LCFA)**

The hydrolysis of lipids is generally regarded as a fast process, while the overall conversion rate is limited either by further long chain fatty acids (LCFA) metabolic conversion rates or by physical processes, like dissolution and adsorption of these fatty acids (Cirne et al., 2007). The inhibitory effect affects both syntrophic acetogens and methanogens (Rinzema et al., 1994; Hwu et al., 1998), but LCFA inhibition is regarded as reversible and, after a lag phase, those microorganisms are able to efficiently convert the accumulated LCFA (Pereira et al., 2004; Palatsi et al., 2009; 2010a). It has been reported that LCFA inhibit anaerobic microorganisms at very low concentrations (Alves et al., 2001; Hwu et al., 1996; Pereira et al., 2005; Shin et al., 2003). Methanogens were reported to be more susceptible to LCFA inhibition compared to acidogens (Pereira et al., 2003; Broughton, Thiele et al. 1998). LCFA are known to hinder the AD process by means of four main two factors:

- Adsorption of LCFA onto the microbial surface has been proposed as the main mechanism of microbial inhibition, in that it affects the transport of nutrients through the cell membranes (Pereira et al., 2005; Palatsi et al., 2010a).
- The detrimental effect of LCFA adsorption on biomass is also due to the resulting sludge flotation and washout (Koster and Cramer 1987).
- Specific enzymes can be inhibited by LCFA as well, which results in the generation of toxic peroxidation and autooxidation products (Cammarota, Teixeira et al. 2001).
- Finally, the biodegradation of LCFA might limit the overall AD process because of the slow growth of LCFA-consuming bacteria (Angelidaki and Ahring 1995) and because the breakdown of LCFA requires a low H<sub>2</sub> partial pressure.

Hence, LCFA inhibition is dependent on the specific surface area of the sludge, the adaptation/acclimation of key microorganisms and the microbial community structure and functionality, and on the carbon chain length and the saturation degree, parameters that affect the hydrophobicity and metabolism of these molecules (Hwu et al., 1996).

### 1.2.4 Process inhibition by sulfate compounds

Several industrial wastewaters (e.g. paper mills, chemical industries and pharmaceutical companies) are rich in COD, TAN and sulphate ( $\text{SO}_4^{2-}$ ). Wastewater containing sulphur compounds are usually treated using biological and physicochemical methodologies. Even though physicochemical methods are effective, their limitations restrict their usage (Zhao et al., 2016). These limitations include the need for separation and appropriate disposal of the solid phase that increases energy demand and economic costs. Such limitations can be overcome by biological treatments such as the AD process (Sarti and Zaiat, 2011).

During the treatment of these wastewaters, sulphur compounds are reduced to sulphide ( $\text{H}_2\text{S}$ ), a gaseous molecule that is toxic, corrosive and malodorous, thus producing several problems in the process efficiency and on the maintenance of industrial facilities (Karunakaran et al., 2016). Sulfate-reducing bacteria (SRB) perform biological reactions that yield this compound. These microorganisms have the ability to couple the oxidation of organic matter to the reduction of  $\text{SO}_4^{2-}$  and, therefore, they depend on hydrolytic and fermentative bacteria that degrade complex organic matter (Ali Shah et al., 2014). Hence,  $\text{H}_2\text{S}$  is generated from the proliferation of SRB in anaerobic bioreactors, where they compete with MPA and homoacetogenic bacteria for common substrates (Muyzer and Stams, 2008). Furthermore,  $\text{H}_2\text{S}$  readily permeates cell membranes and denatures native proteins inside the cytoplasm producing sulphide cross-links between polypeptide chains (Annachatre and Suktrakoolvait, 2015). Sulphides are also involved in the precipitation of non-alkali metals in digesters, as a consequence reduce their availability for methanogenic archaea (Isa et al., 1986).

### 1.2.5 Microbiology of anaerobic digestion

The microbial populations involved in the methanogenic anaerobic degradation of organic matter are composed of a complex community of strict anaerobic facultative members of the *Bacteria* and *Archaea* domains, both with a prokaryotic cell organization type. Bacteria compose the predominant community and are involved in all metabolic processes previously described, except in methanogenesis, which is exclusive of archaea (Conrad, 1999). The latter domain, though present at much lower levels, play a key role as the sole responsible for methane production. The microorganisms in domain *Eukarya* (fungi, yeasts, etc), play a minor role in anaerobic digesters and are usually not considered in most of the AD applications. According to Griffin et al. (2004), eukaryotes constituted only a 0.8% of the microbiota involved

in the anaerobic co-digestion of municipal solid waste and biosolids. However, it should be borne in mind that many yeasts have an anaerobic fermentative metabolism and might therefore contribute to the AD process.

The main representatives of the Bacteria domain in anaerobic digesters are framed in the phyla *Bacteroidetes*, *Chloroflexi*, *Firmicutes*, *Actinobacteria* and *Proteobacteria* (St-Pierre and Wright, 2014). In the case of the archaeas, all representatives methanogens belong to two classes of phylum Euryarchaeota and Crenarchaeota. Additionally, the bacteria are in the majority not only in regard to quantity with respect to the archaea but also in regard to their biodiversity, which is logical considering the specialized role of the archaeal methanogens, and the high number of metabolic functions that support the bacteria in these environments (Jabłoński et al., 2015).

During the first steps of AD, before to methanogenesis, different groups of microorganisms that have a specific role develop each step. The first stage, hydrolysis, is formed by those bacteria with high hydrolytic capabilities, known as hydrolytic-fermentative bacteria (Ali Shah et al., 2014). During this stage, the microbes enrolled have the function to hydrolyze the particulate substrate, carbohydrates, proteins and lipids to organic monomers.

Secondly, the carbonic products of these reactions are either acetate, propionate and butyrate, produced by acidogenic microbes and subsequently converted to acetate and hydrogen by acetogenic bacteria (Müller, 2003). In this step, that group of microbes convert the end-products of the hydrolytic/fermentative bacteria into the key substrates for the methanogenesis (Shumkov and Terehova, 1995). It is not worth to mention, that in this step there are a relevant group of microbes known as SAO that can oxidize acetate to  $H_2$  and  $CO_2$  when their products are directly used by  $H_2$ -scavenging methanogens (that group is extensively described in section 1.2.6) (Schnürer et al., 1999).

Finally, the process is completed with the group composed by methanogenic archaea, which consume the products produced by acetogenic/acidogenic microbes and convert them into  $CH_4$  and  $CO_2$  (Liu and Whitman, 2008). For that reason, methanogenic archaea have a key position in the methanisation.  $CH_4$  can be produced by two different communities acetogenic and HMA depending the environmental conditions (pH, temperature, HRT, substrate, etc). There another minor group belonging to methanogens, that are able to produce  $CH_4$  from methylated C1 compounds (methanol, methylamines, methylmercaptopropionate, etc) (Conrad, 1999).

From these different methanogenic paths, AM is the most important source of CH<sub>4</sub> production since 70% of the total global CH<sub>4</sub> production comes from acetate source, while the 30% provides from H<sub>2</sub>, CO<sub>2</sub> and formate (Conrad et al., 2009). All AMA belongs to *Methanosarcinales* order, being *Methanosarcinacea* family where members are acetoclastic obligated, while members belonging to *Methanosarcinacea* family are being able to produce CH<sub>4</sub> from others sources as CO<sub>2</sub>, CO and methylated C<sub>1</sub> compounds (Stams, 1994). Instead, HM is more widespread because the ability to utilize H<sub>2</sub> as an electron donor for CO<sub>2</sub> reduction is a common mechanism. Members of *Methanomicrobiales*, *Methanococcales*, *Methanocellales*, *Methanobacteriales* and *Methanopyrales* could perform that path. Stams and Plugge (2009) described that this methanogenic path represent one of the main inertspecies electron transfer process in anaerobic environments that is established between H<sub>2</sub>-forming acetogenic bacteria and H<sub>2</sub>-consuming archaea. While, methylotrophic pathway is the most limited path, exclusively of *Methanosarcinales* order and *Methanosphaera* sp (Shima and Thauer, 2005).

### 1.2.6 Syntrophic acetate oxidation proces

Syntrophy can be defined as any type of crossfeeding of molecules between microbial species, but a restricted definition is applied for anaerobic syntrophic metabolism. In that case, syntrophy is a close mutualistic interaction in a very specific nutritional situation where the level of exchanged intermediates must be kept low for an efficient cooperation, so that syntrophic partners combine their metabolic capabilities to catabolise a substrate that neither one of them can process alone (McInerney et al., 2009; Morris et al., 2013).

It has been shown that due to this relationship of sintrophy, different populations of bacteria and archaeas are capable of achieving the degradation of different substrates producing CH<sub>4</sub> as final product even in environments with high concentrations of inhibitory compounds, such as NH<sub>3</sub>, SO<sub>4</sub><sup>2-</sup>, LCFA, etc. One of these inhibitory compounds that can be remedied by stimulating a relationship of sintrophy is the excess of NH<sub>3</sub> that produces the protein metabolism (Barua and Dhar, 2017; Mosbæk et al., 2016). As it extensively described, methanogens can utilize simple organic substrate, as formate, methanol, CO<sub>2</sub>/H<sub>2</sub> and acetate for their subsequently utilization in CH<sub>4</sub> production (Demirel and Scherer, 2008). Therefore, methanogenic archaea need to build syntrophic relations with other microbial communities for that CH<sub>4</sub> production from macromolecules originated from biodegradation of complex organic compounds (Fotidis et al., 2014). In many anaerobic environments, H<sub>2</sub> and formate have been identified as electron shuttle between methanogenic and fermentative communities, and during many years, it was thought as the most suitable mechanism for this interaction between these communities (Schink et al., 2017).



A relevant syntrophic interaction that could be beneficial in the context of a high  $\text{NH}_3$  content is that composed SAOB and HMA. This syntrophy allows the degradation of acetate, for its later transformation into  $\text{CH}_4$ , without the intervention AMA (Westerholm et al., 2011). A number of studies have shown that the SAO process contribute with a relatively high level to the conversion of acetate into  $\text{CH}_4$  in AD reactors set and operated under diverse conditions (Westerholm et al., 2012; Schnurer & Nordberg; Schnurer et al., 1999).

During the SAO process, both SAOB and HMA populations are mutually dependent on each other for performing their metabolic activities, because acetate oxidation can only proceed if the syntrophic methanogenic partner keeps the  $\text{H}_2$ /formate level low enough, but still suitable for the HMA (Coates et al., 1996). Under standard conditions, the oxidation of acetate to  $\text{CO}_2$  and  $\text{H}_2$  is a thermodynamically unfavourable reaction that can only proceed when HMA consume  $\text{H}_2$  (Hattori, 2008; Stams, 1994).

It has been suggested that the mechanism for converting acetate syntrophically occurs by an oxidative Wood–Ljungdahl (W–L) pathway, as used by certain  $\text{SO}_4^{2-}$ -reducers and AMA (Schuchmann K and Müller V, 2014). The W–L pathway is used by SAOB in a reductive way when growing heterotrophically, and can be viewed as a series of reactions resulting in the reduction of two molecules of  $\text{CO}_2$  to a bound methyl and carbonyl group, which finally form the acetyl moiety of acetyl-CoA (Ragsdale, 2008). It is currently unknown whether there are any differences between the pathways operating in one direction (forming acetate) and the other (consuming acetate). The W–L pathway has been reported to occur in anaerobic environments such as lake sediments, oil reservoirs and nutrient-enriched soils (Muller, Sun et al. 2011; Strous, Heijnen et al. 1998; Schnurer and Nordberg 2008). Furthermore, the obtained electrons from this cascade reactions must be removed in order to achieve a redox balance and regenerate the oxidized acceptor.

SAO process could be also carried out by a putative previous step known as glycine cleavage system pathway resported recently by Nobu et al., (2015). However, this alternative pathway to acetate degradation still needs further research, as well as, it is needed to explore deeper insight other pathway with direct influence on SAO metabolism. In fact, until now most of the studies aimed to study the microbial community structure in AD systems were based on high throughput amplicon sequencing of the 16S rRNA. Therefore, at this level of profoundness only allows an approximate description of the microbial communities composition. For this reason, it is necessary the application of more powerful approaches based on the analysis of shotgun short reads performed to decipher the metabolic network.

Consequently, until now there are few bacteria described to be able to perform the SAO process in association with different HMA primarily belonging to the genera *Methanothermobacter* (Kato et al., 2014), *Methanosarcina* and *Methanoculleus* (Mosbæk et al., 2016). Some examples of known SAOB are the strain AOR (Lee and Zinder, 1988), and the thermophilic species *Thermacetogenium phaeum* (Hattori et al., 2000) and *Thermotoga lettingae* (Balk et al., 2002), and the mesophilic *Clostridium ultunense* (Schnurer et al., 1996), *Syntrophaceticus schinkii* (Westerholm et al., 2010) and *Tepidanaerobacter acetatoxydans* (Westerholm et al., 2011). For that, the application of the shotgun analyses will allow the exploration of genome sequences involved in SAO process, which remain poorly characterized. To complete this gap, it would be useful to study the specific microbiome that confer N-rich AD systems and unravel the genomes of the species directly involved in this extreme conditions.

In the other hand, since it is demonstrated that this syntrophy is robustness in front of NH<sub>3</sub>-stressed environments, the use of those SAO-HM consortia could provide a new solution to alleviate the NH<sub>3</sub> inhibitory effect in AD process. However, these microorganisms are slow growers (HMA) compared with their main competitors, the AMA, *Methanosarcina* and *Methanosaeta*, because some of them have duplication time until 70 days (Westerholm et al., 2012). For this reason, they need residence times within the reactor very high to overcome this inhibition. Several studies have considered strategies for improving process operations with protein materials to retain and increase the presence of this NH<sub>3</sub> tolerant consortium, e.g., pretreatment applications, use of additives, change of operational parameters, different reactor configurations or also the introduction of materials that favoured biomass retention, as well as, enhance the interspecies electron transfer.

Actually, recent studies highlighted that some bacterial communities could transfer electron to methanogenic archaea without shuttle molecules, phenomenon known as direct interspecies electron transfer (DIET) (Zhao et al., 2016). Several investigations have shown that facilitate DIET process by adding conductive materials enhance the methanogenic parameters and it has beneficial effect to alleviate inhibitory compounds effect (Cuetos et al., 2017; Liu et al., 2014; Zhuang et al., 2015). This electron exchange could be performed by cell-to-cell contact, allowing biodegradation and CH<sub>4</sub> production in a metabolically more efficient manner. This evidence was initially supported by the electron transfer characteristics found on *Geobacter metallireducens* and *Geobacter sulfurreducens* with *Methanosaeta* spp. in a methanogenic digester (Rotaru et al., 2014). Furthermore, it has also been proven that the addition of non-biological conductive materials, such as hematite, magnetite, biochar, carbon nanotubes, etc. stimulates the methanogenic activity (Cruz Viggí et al., 2014; Li et al., 2015). Syntrophic communities can growth attached onto the surface of these

materials and use its conductive traits for electron transfer. These materials can enhance the metabolic energy investment since they reduce the necessity of conductive pilis used in DIET phenomena (Walker et al., 2016).

### **1.3. Biotechnological strategies for preventing inhibition**

There are different strategies to mitigate the effects of biological inhibition due to inhibitory compounds in AD systems (Weiland 2010) that are focused to modulate the different operational parameter and the concentration of the toxic compound that bacteria are exposed. However, different methods are being developed to enrich and/or acclimate certain bacterial populations to optimize their growth in more extreme conditions (Chen et al., 2008; Yenigün and Demirel, 2013).

One strategy could be the applications of pre-treatments, in order to modulate the release of the inhibitory compounds and because in most cases increase the biodegradation and/or hydrolysis (Carrère et al., 2010). Complementary, biomass acclimation is usually quoted as explanation for such wide range of inhibitory levels and types of N-rich wastes and to improve microbial resilience under high TAN concentrations (Niu et al., 2015). This is also a good option to estimate a population shift from AMA to the more N-resilient SAOB-HMA (Ho et al., 2013).

That microbial shift is also affected by operational parameters, such as temperature, reactor configuration, OLR, HRT, SRT, etc (Westerholm et al., 2012). In fact, SRT is a key parameter to avoid the wash-out effect of the SAOB-HMA tandem. As it is described previously in section 1.2.6, the doubling time of SAOB-HMA is higher than AMA members. Consequently, an increment of SRT can enhance N-rich wastes AD performance. It is possible to achieve this prolonged the SRT by increasing the HRT, the use of high density bacterial granular as in Upflow anaerobic sludge blanket digestion (UASB) reactors or estimate the microbial biofilm attached to carriers in packed-bed reactors. These configurations prevent bacterial washout and provide a larger surface area for faster biofilm development and improved methanogenesis (Qureshi et al., 2005). The biofilm formation on carrier materials improves the conversion rates by reducing its sensitivity toward inhibitory compounds or conditions. Barana et al., (2013) evidenced that the efficiency of removing organic matter in fixed-bed reactors is directly related to the characteristics of the support material used for immobilization of anaerobes.

Numerous strategies have been explored in order to prevent or control NH<sub>3</sub> inhibition, but extra investigation is needed to develop and establish a fully functional operational procedure. Nevertheless, one of the most promising strategy to overcome

NH<sub>3</sub> inhibition is stimulating the SAOB-HMA consortia in continuous digesters by adjusting the operational configuration and the surrounding parameters.

### **1.3.1 Pretreatment**

As said previously, one of the main limiting factors of the AD process is the disintegration and the hydrolysis of the solid organic substrates. For this reason, the application of physico-chemical pretreatment is regarded as a suitable strategy to improve the process efficiency (Agbor et al., 2011). In addition, the current legislation that applies to treatment and use of certain wastes, depending on the category and type of waste, requires the implementation of pre-treatments in order to comply with biosafety issues (López Torres and Espinosa Llorens, 2008)

The waste pre-treatments may be physical (mechanical grinding, milling or shearing, ultrasounds, irradiation, application of high temperatures and/or pressures), chemical (ozonization, application of acidic and alkaline solutions), and biological (use of enzymes, inoculation of fungi, composting) (Elliott and Mahmood, 2007; Mata-Alvarez et al., 2000; Zheng et al., 2014). These individual process can be combined into, for example, thermo-chemical treatments. The pre-treatments that have most commonly been applied to the meat industry are:

- Enzymatic pretreatment. Literature reports that the pretreatment of rich in oil and grease substrates can minimize the problems that cause such compounds, because it is known that lipids hydrolysis is considered a limiting step in biogas generation and organic matter removal in anaerobic digestion process (Pei, Hu et al. 2010). This pretreatment is made with lipases, enzymes that can catalyse the hydrolysis of triacylglycerol to fatty acids and others small molecules. These enzymes could be a successful alternative for minimize the problems that present the degradation of rich-lipids wastewaters, and indirectly is a good option to decrease the organic matter concentration and suspended solids (Sangave and Pandit 2006; Gomes, Papa et al. 2011).
- Thermal pretreatment. In thermal pretreatment, the substrate is heated (typically 70-190°C) under pressure for up to 20-60 minutes. In the laboratory, this can be carried out with pressure cookers, autoclaves or microwave heaters. Dry substrates need additional water before thermal treatment. Some researchers concluded that the optimum conditions of thermal pre-treatments are temperatures between 160-180 °C and treatment times between 30-60 minutes Some proposed the application of temperature only for 60 seconds (Dohanyos et al, 2004) while another proposed the application of the pre-treatment at low temperature (70 °C) but for several days (Gavala et al., 2003; Ferrer et al., 2008).

- Ultrasound treatment. Ultrasound treatment can be used as pretreatment for sludge or to treat the liquid effluent from anaerobic digesters, for example to aid solid-liquid separation. Ultrasound frequencies (over 20 kHz) cause cavities to form and then implode, producing shockwaves in a process called cavitation. These forces cause the disruption of microbial cell walls in the liquid. In general, this technology is used for treatment of sewage sludge (Pilli et al., 2011). One of the limiting factors in the anaerobic digestion is the disintegration and the hydrolysis of the solid organic substrates, such as the waste meat, livestock waste, etc. For this reason, one of the strategies that it can favor the digestion of these is the physico-chemical pretreatment of wastes. In addition, the current legislation that applies to these wastes uses and treatments requires, depending on the category and type of waste, to carry out pretreatments as a step to apply the allowed recovery processes, such as anaerobic digestion.

### **1.3.2 Digester configuration**

AD is a complex process that consist of a cascade of microbial reactions catalysed by microbial communities' consortia. This dependence between microbes is a key factor in biogas production. However, the microbes involved in the different stages during AD process have different optimal growth conditions, a different physiology, kinetics, nutrient requirements and sensitivity levels to environmental changes (Pohland & Ghosh, 1971). For that reason, the imbalance between the different microbial groups is one of the most important reason for digester failure and instability. Furthermore, the AD systems are also significantly governed by operation conditons by the influent strength, temperature, pH, HRT or organic loading rate (Yuan and Zhu, 2016).

Although most of the high rate systems have demonstrated their applicability for different kind of wastewater over OLR and rich in different pollutants, there exist certain differences in the preference of AD reactor configuration

In conventional CSTR digesters, the HRT is rather similar to SRT. Therefore, in order to prevent the washout of microorganisms and untreated matter, acidogenesis requires sufficient time for biodegradation by HRT adjustment. Effective HRT for acidogenesis varies from 0.25 to 2 days, owing to different composition and concentration of the substrate or to different reactor configuration (Myint et al., 2007).

The successful and cost-effective application of AD in waste treatment can be attributed to an efficient uncoupling of the SRT from the HRT, due to the slow

growth rate of methanogens. This is usually accomplished by a long-term retention system (biofilms, granules) or by means of partial digestate recirculation. Hybrid reactors with different support media such as bentonite or polyurethane foam have been successfully used for hog and cattle slaughterhouse wastewater (Rajakumar et al, 2011; Borja et al, 1998).

The technological challenge lies in enhancing the bacterial activity together with good mixing to ensure a high rate of contact between cells and their substrate. Anaerobic baffled reactors were designed primarily for soluble waste, but they can be modified in order to increase the ability of entrapping microbe-rich small particles (Faisal&Unno, 2001) or to reduce entrance velocities on the incoming flow.

- *Upflow anaerobic sludge blanket reactor.* The upflow anaerobic sludge blanket reactor (UASB) is a single tank process in anaerobic co-digestion treatment that achieves high removal of organic pollutants. In this reactor, wastes enter the reactor from the bottom and flows upward. A suspended sludge blanket filters and treats the sludge flow through it bacteria that are living in the sludge break doing anaerobic digestion. The upflow regime and the motion of gas bubbles allow mixing without mechanical assistance. With this type of reactor is possible to introduce the feed in various types to regulate the concentration of fats are introduced. In this way it is possible to introduce waste at different times and get that biomass acclimate and can withstand higher concentrations of fat, and another pollutants (Lettinga 1995).

Furthermore, this type of reactor can be joined to other chain, allowing contaminants have been treated at different times in this way it is possible to reduce exposure of biomass to high concentrations of toxic. Thus, acetogenic bacteria degrade part of the waste in a first reactor, and then are treated by methanogenic bacteria production to produce methane in the second reactor (Schmidt and Ahring 1996). Two-phase separation system is to enhance anaerobic digestion by providing more optimal environments for each major group of microorganisms and their associated biological reactions.

The two-phase anaerobic system was demonstrated to be effective in treating synthetic dairy wastewater, in terms of lipid and double-bond removal efficiencies. It has reported that using a two stage UASB system for treatment of oil wastes; it is possible to achieve a 90% reduction of COD with previous dissolved air flotation system (Haugen, Bakke et al. 2015).

- *Hybrid upflow anaerobic sludge blanket (HUASB) reactor.* It is an alternative interesting technology for the treatment of various types of wastewater. Since

it combines the advantages of both upflow anaerobic sludge blanket (UASB) and upflow anaerobic filter (UAF) reactors for solid retention, gas–solid–liquid (GLS) separation, biomass attachment, growth enhancement of methanogenic bacteria and non-clogging (Zhang, Jing et al. 2011). The lower part of the HUASB reactor consists of UASB portion where flocculent and granular sludge were developed, whereas the upper part of the HUASB reactor serves as a fixed film reactor (Haugen, Bakke et al. 2015).

Hybrid UASB reactors with different support media such as bentonite and polyurethane foam have been successfully used for hog and cattle slaughterhouse wastewaters. The characteristics of substrate used in these studies were different compared to each other. In general, flow and characteristics of each slaughterhouse wastewater vary depends on size and type of animals slaughtered (Rajakumar, Meenambal et al. 2012).

- *Sequencing batch reactor (SBR)*. It has been shown to be a highly efficient, simply operated process for the treatment of municipal, industrial and agricultural wastewater. In this kind of reactor biomass technology procedure, consist in batch steps instead of others reactors that work continuously and these steps can be summarised as follows: Feed, react, settle and decant.

Sequencing batch, permit more flexible process, because the changeable cyclic phasing that contributes an efficient nutrient removal and improve effluent quality. The quality depends on sludge settlability and efficient decanting facility (Arora, Barth et al. 1985).

Then, because of changes we can make in the phases of this reactor, and changes in the different steps, it is possible to regulate the concentrations of toxic compounds for anaerobic population bacteria, such as lipids and nitrogen compounds to allow acclimatization of the digestion bacteria. In a same way, modifications of cycles and phase times create a flexible process and hazardous wastes in each batch can be tested before decanting. Potential disadvantages may include poor clarification and turbid effluent as well as increased complexity when using multiple reaction vessels (Lawrence K, et al 2009).

Batch reactor allow also, to attach these reactors with other techniques such as membranes, or filters, in order to control the amount of compounds that are in contact with the biomass, or to retain and extract from effluent. But also can be used a single reactor, and the concentration of nitrogen, fats, and

the rest of compound are introduced in the concentration is determined by the concentration which is in the influent (Arora, Barth et al. 1985).

(Hendrik schalk, 2014) Report in his article a successful treatment that he was achieved with 97% BOD reduction, 96% nitrogen (N) reduction and 80% phosphorous (P)reduction. Membrane treatment assured a soluble, solids-free effluent treated winery wastewater with a sequencing batch biofilm reactor and achieved COD reduction efficiency of between 86 and 99% at a loading rate of ca.  $8.8 \text{ kgCOD} \cdot \text{m}^{-3} \cdot \text{d}^{-1}$ .

- *Upflow anaerobic sludge-fixed film bioreactor (UASFF)*. It is one of the granular sludge bioreactors that are used for the rapid biotransformation of organic matter to methane with the help of granulated microbial aggregates. The UASFF reactor is a hybrid reactor with an upflow fixed film (UFF) part over an upflow anaerobic sludge blanket (UASB) section. (Ahmed, Yaakob et al. 2015) UASFF bioreactor with tubular flow behaviour was developed in order to shorten the start-up period at low hydraulic retention time (HRT). The reactor was operated at 38 °C and HRT of 1.5 and 3 days. The organic loading was gradually increased from 2.63 to 23.15  $\text{g COD} \cdot \text{g}^{-1} \cdot \text{d}^{-1}$ . Granular sludge was rapidly developed within 20 days. The size of granules increased from an initial pinpoint size to reach 2 mm. Methane yield of 0.346  $\text{l CH}_4 \cdot \text{g}^{-1} \text{COD removed}$  at the highest organic loading rate (OLR) was obtained (Najafpour, Zinatizadeh et al. 2006; Zinatizadeh, Younesi et al. 2009). The use of an internal upflow anaerobic fixed film section caused the flocculated biomass to precipitate over the sludge blanket. The precipitated biomass served as suitable and natural hydrophobic core to form a spatial arrangement of microbial species in the process of mature bio-granulation (Najafpour, Zinatizadeh et al. 2006).
- *Submerged anaerobic membrane bioreactor (SAMBR)*. For efficient stabilization of the acidogenic effluent, the feasibility of using SAMBR was tested for the methanogenesis process to determine the best operational condition for coupling. The process performance was evaluated by decreasing the HRT from 20 days. A SAMBR with a working volume of 0.6 L was operated semi-continuously under mesophilic (35 °C) conditions. A U-shaped membrane module was placed in the middle of the reactor. The module consisted of a hollow fiber microfiltration membrane. The fiber, made of polypropylene, had a nominal pore size of 0.45  $\mu\text{m}$ . The effective membrane filtration area was 0.003  $\text{m}^2$  and the total flux (measured as the permeation rate) from each reactor was controlled using a peristaltic pump (Gao et al., 2011; Kim et al.,



2011) .The SAMBR for methanogenesis showed a CH<sub>4</sub> yield increment by decreasing HRT. It is also observed in this mechanism the formation of a gel layer by colloidal particles, which acts as a secondary membrane, this cake layer could be formed in short time especially since low HRTs can lead a greater formation of microbial products.

### **1.3.3 Strategies to enhance AD-reactors performance**

As it has been described up to this point, there are several procedures and methodologies to mitigate partially the inhibitory effect of NH<sub>3</sub> in AD processes. However, not all the technologies and protocols described to date have been able to obtain performance or production at optimal levels. For this reason, it is necessary to continue investigating for new methodologies or to improve the existing ones in order to reach optimal levels of production. As discussed so far, there are different methods such as pretreatments or different configurations of reactors that have shown positive results. However, different studies suggest that modifying existing configurations with biomass attachment (biofilm formation) or recuperative thickening strategies (RT) it will be possible to improve AD performance.

A suitable approach to mitigate NH<sub>3</sub> inhibition in AD process is the addition of biofilm carriers to the reactor. Methanogenic biomass (bacteria and archaea) involved in CH<sub>4</sub> production has the capability to growth attached to biofilm carrier and stimulate the biofilm formation. These structures are assemblages of microbes, attached to a surface and envolved in an extracellular polymeric substance matrix that confer high resistance in front to external perturbances. The biofilm development has distinct steps, from single cells adhesion by van del Waals forces or polar interactions of H<sub>2</sub>-bond type, to the extension of microbial colonization. Any of these steps depends on properties of carriers (roughness, hydrophobicity, surface charge) and cell walls of microbial strains (composition, hydrophobicity) (Li and Liu, 2017; Dang and Lovell, 2016).

Biofilm growth presents several advantages over a planktonic mode of existence, such increased resistance or adaptation to environmental stresses, as shock loadings, pH, temperature changes, or to mitigate the effect of toxics and inhibitors (Li and Liu, 2017; Garrett et al., 2008). Consequently, biofilms contribute to a more efficient AD performances (increment of efficient degradation, CH<sub>4</sub> yield ...) because with this structure increment the available biomass due to the higher density of cells in biofilms.

The potential of this option can now be enhanced in order to take advantage of important advances in the fields of microbial ecology, molecular biology, immobilization techniques and advanced bioreactor design (Pepper, J Gentry, et al 2002). For this reason, advanced bioreactor design can take advantage of compartmentalisation and the use of different structures to include those support material, to confine the key microorganisms in the process to a bioreactor (Ahhammad et al., 2013; Zheng et al., 2015). However, it is also known that effective operation of biological treatment systems relies on highly active microorganisms carrying out the process, and therefore on the ratio of resistant microorganisms to the contaminant being treated.

Although there are a vast number of studies reporting different materials to promote biofilm formation. Such as, methanogenic consortia on clays, alumina-based ceramics, polymeric materials (nylon, polyehetiene-glycol, polytetrafluoroethylene, etc.), metal carriers (iron oxide, magnetite, etc.) or stainless steel (Muñoz et al., 1997; Lalov et al., 2001; Zhao et al., 2007; Sheng et al., 2008; Li and Logan, 2004; Hellman et al., 2010; Ahhammad et al., 2013; Fuchslocher Hellemann et al., 2013; Ojha et al., 2017). Or studies reporting the beneficial effect of electrically conductive materials such as magnetite or activated carbon that promote DIET. There is a lack of studies specially focused on packing material for SAOB - HMA retention. For this reason, it is considered necessary to continue investigating the properties of the materials that make them susceptible to be colonized by specific microbial communities. As well as, it find suitable configurations to contain this type of materials.

As it is pointed out before in this section, there are others suitable strategy to increase SRT (without increment HRT) and consequently enhance AD performance. RT is a relatively low cost technique, and is a simpler option for digesters that allows an increment of the treatment capacity with minor additional space or capital investment (Yang et al., 2017). With this operation, a proportion of the sludge is recovered and reintroduced in the digester.

RT increases the microbial population concentration, the retention of micronutrients (Lin et al., 2013; Zhang et al., 2013) and improves the C/N ratio by removing the soluble TAN from the liquid phase (Nagao et al., 2012). It is reported that with this operation is possible to increase 25% the capacity of digester volume without any expansion of the digester. In comparison to other AD technologies, RT is more effective than the feed pre-treatment method focused on the increment of treatment capacity but without extra energy input. This is a great advantage to operate under thermophilic conditions, and lead to more stable operation in mesophilic range (Labatut et al., 2014).

Furthermore, as it is focus in previous works, one of the strategies to NH<sub>3</sub> microbial acclimation is focused on choosing adequate biomass retention time and, in this sense, SRT is a crucial parameter for SAO communities. In addition, recent studies report that the short-term that methanogenic biomass is exposed to aerobic conditions has no significant damage on the methanogenic activity (Batstone et al., 2015). For that reason, it is interesting to consider the applicability and the impact of RT on the enhancement of AD performance through the biomass acclimation to ammonia, as well as, the influence that this operation could have on methanogenic biomass evolution.

#### 1.4 Comparison between strategies

Different items as described in the literature describe different strategies to be able to solve the problem involving the inhibitory compounds, however the problem is still present when these waste reach high concentrations. The following section present some hypothesis and strategies examining the impact of digesters configurations and parameters as hydraulic/solid retention time on syntrophic communities, as SAO.

At the level of pre-treatment, there are different strategies to minimize the toxic effects of intermediary metabolites. Nevertheless, are not sufficient for an optimum degradation. For this reason, throughout this work the pre-treatment only will be used for the disinfection of the waste, as it is mandatory by law.

Based on the literature, it has been chosen to work with different reactor configurations, and observe the behavior of them regard the conventional configurations. In this way proving if the modifications carried out represent an increase in the degradation of this type of waste. As it previously described, to avoid the wash out of the syntrophic communities is necessary to increase the microbial retention time over the microbial doubling time. That time in SAO consortia could be more than 28 days (Schnürer et al., 1994). In all the reactors described in section 1.3.2 it is possible to increased HRT as a prevention of ammonia inhibition, but results reported in the literature are very widespread to establish a standard time. Since some studies described that a well-known SAO bacteria as *C. ultunense*, *T. acetatoydans* and *P. lettingae* have been detected at HRT between 24–64, 24–101 and 40–60 days respectively (Solli et al., 2014; Fotidis et al., 2013; Westerholm et al., 2012, 2011). Past works on acclimatization over ammonia focused also on choosing an adequate control of operational parameters such as temperature or OLR or co-digestion to optimize the C/N ratio (Niu et al., 2015; Rajagopal et al., 2013; Romero-Güiza et al., 2014). However, these approaches are sometimes not feasible or not cost-effective enough to be applied at full-scale.

Another feasible strategy to overcome ammonia inhibition is the formation of granular sludge or the introduction of support material in the reactor, as described (Habouzit et al., 2014; Poirier et al., 2017; Zhao et al., 2015). That material could serve as support to promote the biofilm formation or but also since the distance between the bacteria and hydrogenotrophic archaeal members is reduced, which facilitates interspecies electron transfer process explained above (Baek et al., 2017; Li et al., 2017; Zhao et al., 2016). It is reported that the presence of certain materials encourages the emergence of syntrophy relations capable of withstanding high concentrations of toxic compounds and increases the hydrocarbon degrading capacity of the colonies.

## 1.5 References

Anice website <https://www.anice.es>

- Agbor, V.B., Cicek, N., Sparling, R., Berlin, A., Levin, D.B., 2011. Biomass pretreatment: Fundamentals toward application. *Biotechnol. Adv.* 6:675-686
- Ahammad, S.Z., Davenport, R.J., Read, L.F., Gomes, J., Sreekrishnan, T.R., Dolfing, J., 2013. Rational immobilization of methanogens in high cell density bioreactors. *RSC Adv.* 3, 774–781.
- Ahring, B.K., Angelidaki, I., Johansen, K., 1992. Anaerobic treatment of manure together with industrial waste. *Water Sci. Technol.* 7:311-381
- Ahring, B.K., Sandberg, M., Angelidaki, I., 1995. Volatile fatty acids as indicators of process imbalance in anaerobic digestors. *Appl. Microbiol. Biotechnol.* 43, 559–565.
- Ali Shah, F., Mahmood, Q., Maroof Shah, M., Pervez, A., Ahmad Asad, S., 2014. Microbial ecology of anaerobic digesters: The key players of anaerobiosis. *Sci. World J.* vol 2014
- Alves, M.M., Mota Vieira, J.A., Alvares Pereira, R.M., Pereira, M.A., Mota, M., 2001. Effect of lipids and oleic acid on biomass development in anaerobic fixed-bed reactors. Part I: Biofilm growth and activity. *Water Res.* 1:264-270
- Angelidaki, I., Ahring, B.K., 1992. Effects of free long-chain fatty acids on thermophilic anaerobic digestion. *Appl. Microbiol. Biotechnol.* 37, 808–812.
- Annachhatre, A.P., Suktrakoolvatt, S., 2015. Biological Sulfate Reduction Using Molasses as a Carbon Source. *Water Environ. Res.* 73, 118–126.
- Arora, M.L., Barth, E.F., Umphres, M.B., 1985. Technology Evaluation of Sequencing Batch Reactors. *Source J. (Water Pollut. Control Fed.)* 8:867-865
- Baek, G., Jung, H., Kim, J., Lee, C., 2017. A long-term study on the effect of magnetite supplementation in continuous anaerobic digestion of dairy effluent – Magnetic separation and recycling of magnetite. *Bioresour. Technol.* 241, 830–840.
- Balk, M., Weijma, J., Stams, A.J.M., 2002. *Thermotoga lettingae* sp. nov., a novel thermophilic, methanol-degrading bacterium isolated from a thermophilic anaerobic reactor. *Int. J.* 4:1361-1368

- Barana, A.C., Lopes, D.D., Martins, T.H., Pozzi, E., Damianovic, M.H.R.Z., Del Nery, V., Foresti, E., 2013. Nitrogen and organic matter removal in an intermittently aerated fixed-bed reactor for post-treatment of anaerobic effluent from a slaughterhouse wastewater treatment plant. *J. Environ. Chem. Eng.* 1, 453–459.
- Barua, S., Dhar, B.R., 2017. Advances towards understanding and engineering direct interspecies electron transfer in anaerobic digestion. *Bioresour. Technol.* 244:698-707
- Batstone, D.J., Lu, Y., Jensen, P.D., 2015. Impact of dewatering technologies on specific methanogenic activity. *Water Res.* 1:78-85
- Borja, Rafael, Banks, Charles J., Wang, Zhengjian and Mancha, Angela (1998) Anaerobic digestion of slaughterhouse wastewater using a combination sludge blanket and filter arrangement in a single reactor. *Bioresource Technology*, 65 (1-2), 125-133.
- Broughton, M.J., Thiele, J.H., Birch, E.J., Cohen, A., 1998. Anaerobic batch digestion of sheep tallow. *Water Res.* 5:1423-1428
- Calli, B., Mertoglu, B., Inanc, B., Yenigun, O., 2005. Effects of high free ammonia concentrations on the performances of anaerobic bioreactors. *Process Biochem.* <https://doi.org/10.1016/j.procbio.2004.05.008>
- Cammarota, M.C., Teixeira, G.A., Freire, D.M.G., 2001. Enzymatic pre-hydrolysis and anaerobic degradation of wastewaters with high fat contents. *Biotechnol. Lett.* <https://doi.org/10.1023/A:1011973428489>
- Carrère, H., Dumas, C., Battimelli, A., Batstone, D.J., Delgenès, J.P., Steyer, J.P., Ferrer, I., 2010. Pretreatment methods to improve sludge anaerobic degradability: A review. *J. Hazard. Mater.* <https://doi.org/10.1016/j.jhazmat.2010.06.129>
- Chen, Y., Cheng, J.J., Creamer, K.S., 2008. Inhibition of anaerobic digestion process: A review. *Bioresour. Technol.* 99, 4044–4064. <https://doi.org/10.1016/j.biortech.2007.01.057>
- Cirne, D.G., Paloumet, X., Björnsson, L., Alves, M.M., Mattiasson, B., 2007. Anaerobic digestion of lipid-rich waste-Effects of lipid concentration. *Renew. Energy.* <https://doi.org/10.1016/j.renene.2006.04.003>
- Coates, J.D., Coughlan, M.F., Colleran, E., 1996. Simple method for the measurement of the hydrogenotrophic methanogenic activity of anaerobic sludges. *J. Microbiol. Methods.* [https://doi.org/10.1016/0167-7012\(96\)00915-3](https://doi.org/10.1016/0167-7012(96)00915-3)
- Conrad, R., 1999. Contribution of hydrogen to methane production and control of hydrogen concentrations in methanogenic soils and sediments. *FEMS Microbiol. Ecol.* [https://doi.org/10.1016/S0168-6496\(98\)00086-5](https://doi.org/10.1016/S0168-6496(98)00086-5)
- Conrad, R., Claus, P., Casper, P., 2009. Characterization of stable isotope fractionation during methane production in the sediment of a eutrophic lake, Lake Dagow, Germany. *Limnol. Oceanogr.* 54, 457–471. <https://doi.org/10.4319/lo.2009.54.2.0457>
- Cruz Viggì, C., Rossetti, S., Fazi, S., Paiano, P., Majone, M., Aulenta, F., 2014. Magnetite particles triggering a faster and more robust syntrophic pathway of methanogenic propionate degradation. *Environ. Sci. Technol.* 48, 7536–7543. <https://doi.org/10.1021/es5016789>
- Cuetos, M.J., Martinez, E.J., Moreno, R., Gonzalez, R., Otero, M., Gomez, X., 2017. Enhancing anaerobic digestion of poultry blood using activated carbon. *J. Adv. Res.* 8, 297–307. <https://doi.org/10.1016/j.jare.2016.12.004>

- Dang, H., Lovell, C.R., 2016. Microbial Surface Colonization and Biofilm Development in Marine Environments. *Microbiol. Mol. Biol. Rev.* 80, 91–138. <https://doi.org/10.1128/MMBR.00037-15>
- Daniels, L., Sparling, R., Sprott, G.D., 1984. The bioenergetics of methanogenesis. *BBA Rev. Bioenerg.* [https://doi.org/10.1016/0304-4173\(84\)90002-8](https://doi.org/10.1016/0304-4173(84)90002-8)
- Demirel, B., Scherer, P., 2008. The roles of acetotrophic and hydrogenotrophic methanogens during anaerobic conversion of biomass to methane: A review. *Rev. Environ. Sci. Biotechnol.* 7, 173–190. <https://doi.org/10.1007/s11157-008-9131-1>
- Donoso-Bravo, A., Retamal, C., Carballa, M., Ruiz-Filippi, G., Chamy, R., 2009. Influence of temperature on the hydrolysis, acidogenesis and methanogenesis in mesophilic anaerobic digestion: Parameter identification and modeling application. *Water Sci. Technol.* <https://doi.org/10.2166/wst.2009.316>
- Elliott, A., Mahmood, T., 2007. Pretreatment technologies for advancing anaerobic digestion of pulp and paper biotreatment residues. *Water Res.* <https://doi.org/10.1016/j.watres.2007.06.017>
- Fotidis, I.A., Karakashev, D., Kotsopoulos, T.A., Martzopoulos, G.G., Angelidaki, I., 2013. Effect of ammonium and acetate on methanogenic pathway and methanogenic community composition. *FEMS Microbiol. Ecol.* 83, 38–48. <https://doi.org/10.1111/j.1574-6941.2012.01456.x>
- Fotidis, I.A., Wang, H., Fiedel, N.R., Luo, G., Karakashev, D.B., Angelidaki, I., 2014. Bioaugmentation as a solution to increase methane production from an ammonia-rich substrate. *Environ. Sci. Technol.* 48, 7669–7676. <https://doi.org/10.1021/es5017075>
- Ganidi, N., Tyrrel, S., Cartmell, E., 2009. Anaerobic digestion foaming causes - A review. *Bioresour. Technol.* 100, 5546–5554. <https://doi.org/10.1016/j.biortech.2009.06.024>
- Gao, W.J., Lin, H.J., Leung, K.T., Schraft, H., Liao, B.Q., 2011. Structure of cake layer in a submerged anaerobic membrane bioreactor. *J. Memb. Sci.* <https://doi.org/10.1016/j.memsci.2011.03.019>
- Garrett, T.R., Bhakoo, M., Zhang, Z., 2008. Bacterial adhesion and biofilms on surfaces. *Prog. Nat. Sci.* 18, 1049–1056. <https://doi.org/10.1016/j.pnsc.2008.04.001>
- Griffin, M.E., McMahon, K.D., Mackie, R.I., Raskin, L., 1998. Methanogenic population dynamics during start-up of anaerobic digesters treating municipal solid waste and biosolids. *Biotechnol. Bioeng.* [https://doi.org/10.1002/\(SICI\)1097](https://doi.org/10.1002/(SICI)1097)
- Habouzit, F., Gévaudan, G., Hamelin, J., Steyer, J.P., Bernet, N., 2011. Influence of support material properties on the potential selection of Archaea during initial adhesion of a methanogenic consortium. *Bioresour. Technol.* 102, 4054–4060. <https://doi.org/10.1016/j.biortech.2010.12.023>
- Hansen, K.H., Angelidaki, I., Ahring, B.K., 1998. Anaerobic Digestion of Swine Manure: Inhibition By Ammonia. *Water Res.* 32, 5–12. [https://doi.org/10.1016/S0043-1354\(97\)00201-7](https://doi.org/10.1016/S0043-1354(97)00201-7)
- Hao, L., Lü, F., Mazéas, L., Desmond-Le Quéméner, E., Madigou, C., Guenne, A., Shao, L., Bouchez, T., He, P., 2015. Stable isotope probing of acetate fed anaerobic batch incubations shows a partial resistance of acetoclastic methanogenesis catalyzed by

- Methanosarcina to sudden increase of ammonia level. *Water Res.* 69, 90–99. <https://doi.org/10.1016/j.watres.2014.11.010>
- Hao, L.P., Lü, F., He, P.J., Li, L., Shao, L.M., 2011. Predominant contribution of syntrophic acetate oxidation to thermophilic methane formation at high acetate concentrations. *Environ. Sci. Technol.* 45, 508–513. <https://doi.org/10.1021/es102228v>
- Hattori, S., Galushko, A.S., Kamagata, Y., Schink, B., 2005. Operation of the CO dehydrogenase/acetyl coenzyme A pathway in both acetate oxidation and acetate formation by the syntrophically acetate-oxidizing bacterium *Thermacetogenium phaeum*. *J. Bacteriol.* 187, 3471–3476. <https://doi.org/10.1128/JB.187.10.3471-3476.2005>
- Hattori, S., Kamagata, Y., Hanada, S., Shoun, H., 2000. *Thermacetogenium phaeum* gen. nov., sp. nov., a strictly anaerobic, thermophilic, syntrophic acetate-oxidizing bacterium. *Int. J. Syst. Evol. Microbiol.* 50, 1601–1609. <https://doi.org/10.1099/00207713-50-4-1601>
- Hellman J., Ek A., Sundberg C., Johansson M., 2010. Mechanisms of increased methane production through re-circulation of magnetic biomass carriers in an experimental continuously stirred tank reactor. IWA Publishing, 12th World Congress on Anaerobic Digestion (AD12)
- Ho, D.P., Jensen, P.D., Batstone, D.J., 2013. Methanosarcinaceae and acetate-oxidizing pathways dominate in high-rate thermophilic anaerobic digestion of waste-activated sludge. *Appl. Environ. Microbiol.* <https://doi.org/10.1128/AEM.01730-13>
- Hunik, J.H., Hamelers, H.V.M., Koster, I.W., 1990. Growth-rate inhibition of acetoclastic methanogens by ammonia and pH in poultry manure digestion. *Biol. Wastes* 32, 285–297. [https://doi.org/10.1016/0269-7483\(90\)90060-6](https://doi.org/10.1016/0269-7483(90)90060-6)
- Isa, Z., Grusenmeyer, S., Vestraete, W., 1986. Sulfate reduction relative to methane production in high-rate anaerobic digestion: Technical aspects. *Appl. Environ. Microbiol.*
- Jabłoński, S., Rodowicz, P., Łukaszewicz, M., 2015. Methanogenic archaea database containing physiological and biochemical characteristics. *Int. J. Syst. Evol. Microbiol.* 65, 1360–1368. <https://doi.org/10.1099/ijss.0.000065>
- Jing, Z., Hu, Y., Niu, Q., Liu, Y., Li, Y.Y., Wang, X.C., 2013. UASB performance and electron competition between methane-producing archaea and sulfate-reducing bacteria in treating sulfate-rich wastewater containing ethanol and acetate. *Bioresour. Technol.* 137, 349–357. <https://doi.org/10.1016/j.biortech.2013.03.137>
- Kangle, K.M., Kore, S. V, Kore, V.S., Kulkarni, G.S., 2012. Recent Trends in Anaerobic Codigestion : A Review. *Univers. J. Environ. Res. Technol.*
- Karunakaran, E., Vernon, D., Biggs, C.A., Saul, A., Crawford, D., Jensen, H., 2016. Enumeration of sulphate-reducing bacteria for assessing potential for hydrogen sulphide production in urban drainage systems. *Water Sci. Technol.* 73, 3087–3094. <https://doi.org/10.2166/wst.2016.026>
- Kato, S., Yoshida, R., Yamaguchi, T., Sato, T., Yumoto, I., Kamagata, Y., 2014. The effects of elevated CO<sub>2</sub> concentration on competitive interaction between aceticlastic and syntrophic methanogenesis in a model microbial consortium. *Front. Microbiol.* <https://doi.org/10.3389/fmicb.2014.00575>

- Kayhanian, M., 1994. Performance of a high-solids anaerobic digestion process under various ammonia concentrations. *J. Chem. Technol. Biotechnol.* 59, 349–352. <https://doi.org/10.1002/jctb.280590406>
- Kim, J., Kim, K., Ye, H., Lee, E., Shin, C., McCarty, P.L., Bae, J., 2011. Anaerobic fluidized bed membrane bioreactor for wastewater treatment. *Environ. Sci. Technol.* <https://doi.org/10.1021/es1027103>
- Koster, I.W., Cramer, A., 1987. Inhibition of methanogenesis from acetate in granular sludge by long-chain fatty acids. *Appl. Environ. Microbiol.* <https://doi.org/10.1016/j.tibtech.2011.11.003>
- Labatut, R. a, Angenent, L.T., Scott, N.R., 2014. Conventional mesophilic vs. thermophilic anaerobic digestion: a trade-off between performance and stability. *Water Res.* <https://doi.org/10.1016/j.watres.2014.01.035>
- Lalov, I.G., Krysteva, M.A., Phelouzat, J.L., 2001. Improvement of biogas production from vinasse via covalently immobilized methanogens. *Bioresour. Technol.* [https://doi.org/10.1016/S0960-8524\(01\)00045-1](https://doi.org/10.1016/S0960-8524(01)00045-1)
- Lee, M.J., Zinder, S.H., 1988. Hydrogen partial pressures in a thermophilic acetate-oxidizing methanogenic coculture. *Appl. Environ. Microbiol.* 54, 1457–61. <https://doi.org/10.1002/cphc.200900055>
- Lettinga, G., 1995. Anaerobic digestion and wastewater treatment systems. *Antonie Van Leeuwenhoek.* <https://doi.org/10.1007/BF00872193>
- Li, L.-L., Tong, Z.-H., Fang, C.-Y., Chu, J., Yu, H.-Q., 2015. Response of anaerobic granular sludge to single-wall carbon nanotube exposure. *Water Res.* 70, 1–8. <https://doi.org/10.1016/j.watres.2014.11.042>
- Li, Y., Zhang, Y., Yang, Y., Quan, X., Zhao, Z., 2017. Potentially direct interspecies electron transfer of methanogenesis for syntrophic metabolism under sulfate reducing conditions with stainless steel. *Bioresour. Technol.* 234, 303–309. <https://doi.org/10.1016/j.biortech.2017.03.054>
- Lin, L., Wan, C., Liu, X., Lei, Z., Lee, D.J., Zhang, Y., Tay, J.H., Zhang, Z., 2013. Anaerobic digestion of swine manure under natural zeolite addition: VFA evolution, cation variation, and related microbial diversity. *Appl. Microbiol. Biotechnol.* 97, 10575–10583. <https://doi.org/10.1007/s00253-013-5313-z>
- Liu, F., Rotaru, A.-E., Shrestha, P.M., Malvankar, N.S., Nevin, K.P., Lovley, D.R., 2014. Magnetite compensates for the lack of a pilin-associated c-type cytochrome in extracellular electron exchange. *Environ. Microbiol.* 17, 648–55. <https://doi.org/10.1111/1462-2920.12485>
- Liu, Y., Whitman, W.B., 2008. Metabolic, phylogenetic, and ecological diversity of the methanogenic archaea, in: *Annals of the New York Academy of Sciences.* <https://doi.org/10.1196/annals.1419.019>
- Liu, Y., Yang, S.F., Li, Y., Xu, H., Qin, L., Tay, J.H., 2004. The influence of cell and substratum surface hydrophobicities on microbial attachment. *J. Biotechnol.* 110, 251–256. <https://doi.org/10.1016/j.jbiotec.2004.02.012>



- López Torres, M., Espinosa Llorens, M. d C., 2008. Effect of alkaline pretreatment on anaerobic digestion of solid wastes. *Waste Manag.* <https://doi.org/10.1016/j.wasman.2007.10.006>
- Lü, F., Hao, L., Guan, D., Qi, Y., Shao, L., He, P., 2013. Synergetic stress of acids and ammonium on the shift in the methanogenic pathways during thermophilic anaerobic digestion of organics. *Water Res.* 47, 2297–2306. <https://doi.org/10.1016/j.watres.2013.01.049>
- Mata-Alvarez, J., Macé, S., Llabrés, P., 2000. Anaerobic digestion of organic solid wastes. An overview of research achievements and perspectives. *Bioresour. Technol.* 74, 3–16. [https://doi.org/10.1016/S0960-8524\(00\)00023-7](https://doi.org/10.1016/S0960-8524(00)00023-7)
- McInerney, M.J., Sieber, J.R., Gunsalus, R.P., 2009. Syntrophy in anaerobic global carbon cycles. *Curr. Opin. Biotechnol.* <https://doi.org/10.1016/j.copbio.2009.10.001>
- Min, D., Cheng, L., Zhang, F., Huang, X.N., Li, D.B., Liu, D.F., Lau, T.C., Mu, Y., Yu, H.Q., 2017. Enhancing Extracellular Electron Transfer of *Shewanella oneidensis* MR-1 through Coupling Improved Flavin Synthesis and Metal-Reducing Conduit for Pollutant Degradation. *Environ. Sci. Technol.* 51, 5082–5089. <https://doi.org/10.1021/acs.est.6b04640>
- Morgenroth, E., Kommedal, R., Harremoës, P., 2002. Processes and modelling of hydrolysis of particulate organic matter in aerobic wastewater treatment - a review. *Water Sci. Technol.*
- Morris, B.E.L., Henneberger, R., Huber, H., Moissl-Eichinger, C., 2013. Microbial syntrophy: Interaction for the common good. *FEMS Microbiol. Rev.* <https://doi.org/10.1111/1574-6976.12019>
- Mosbæk, F., Kjeldal, H., Mulat, D.G., Albertsen, M., Ward, A.J., Feilberg, A., Nielsen, J.L., 2016. Identification of syntrophic acetate-oxidizing bacteria in anaerobic digesters. *ISME J.* 2, 1–14. <https://doi.org/10.1038/ismej.2016.39>
- Müller, V., 2003. Energy Conservation in Acetogenic Bacteria. *Appl. Environ. Microbiol.* <https://doi.org/10.1128/AEM.69.11.6345-6353.2003>
- Muñoz M., Sanchez J., Rodríguez-Maroto J., Borrego J., Moriñigo M., 1997. Methane production in anaerobic sludges supplemented with two support materials and different levels of acetate and sulphate. *Water Res* 5:1236-1242
- Muyzer, G., Stams, A.J.M., 2008. The ecology and biotechnology of sulphate-reducing bacteria. *Nat. Rev. Microbiol.* <https://doi.org/10.1038/nrmicro1892>
- Myint, M., Nirmalakhandan, N., Speece, R.E., 2007. Anaerobic fermentation of cattle manure: Modeling of hydrolysis and acidogenesis. *Water Res.* <https://doi.org/10.1016/j.watres.2006.10.026>
- Nagao, N., Tajima, N., Kawai, M., Niwa, C., Kurosawa, N., Matsuyama, T., Yusoff, F.M., Toda, T., 2012. Maximum organic loading rate for the single-stage wet anaerobic digestion of food waste. *Bioresour. Technol.* <https://doi.org/10.1016/j.biortech.2012.05.045>
- Najafpour, G.D., Zinatizadeh, A.A.L., Mohamed, A.R., Hasnain Isa, M., Nasrollahzadeh, H., 2006. High-rate anaerobic digestion of palm oil mill effluent in an upflow anaerobic sludge-fixed film bioreactor. *Process Biochem.* <https://doi.org/10.1016/j.procbio.2005.06.031>

- Niu, Q., Takemura, Y., Kubota, K., Li, Y.-Y., 2015. Comparing mesophilic and thermophilic anaerobic digestion of chicken manure: Microbial community dynamics and process resilience. *Waste Manag.* <https://doi.org/10.1016/j.wasman.2015.05.012>
- Nobu, M.K., Narihiro, T., Rinke, C., Kamagata, Y., Tringe, S.G., Woyke, T., Liu, W.-T., 2015. Microbial dark matter ecogenomics reveals complex synergistic networks in a methanogenic bioreactor. *ISME J.* 9, 1710–1722. <https://doi.org/10.1038/ismej.2014.256>
- Palatsi, J., Illa, J., Prenafeta-Boldú, F.X., Laureni, M., Fernandez, B., Angelidaki, I., Flotats, X., 2010. Long-chain fatty acids inhibition and adaptation process in anaerobic thermophilic digestion: Batch tests, microbial community structure and mathematical modelling. *Bioresour. Technol.* <https://doi.org/10.1016/j.biortech.2009.11.069>
- Palatsi, J., Laureni, M., Andrés, M. V., Flotats, X., Nielsen, H.B., Angelidaki, I., 2009. Strategies for recovering inhibition caused by long chain fatty acids on anaerobic thermophilic biogas reactors. *Bioresour. Technol.* <https://doi.org/10.1016/j.biortech.2009.04.046>
- Palatsi, J., Viñas, M., Guivernau, M., Fernandez, B., Flotats, X., 2011. Anaerobic digestion of slaughterhouse waste: Main process limitations and microbial community interactions. *Bioresour. Technol.* 102, 2219–2227. <https://doi.org/10.1016/j.biortech.2010.09.121>
- Pereira, M.A., Cavaleiro, A.J., Mota, M., Alves, M.M., 2003. Accumulation of long chain fatty acids onto anaerobic sludge under steady state and shock loading conditions: Effect on acetogenic and methanogenic activity, in: *Water Science and Technology*.
- Pereira, M.A., Pires, O.C., Mota, M., Alves, M.M., 2005. Anaerobic biodegradation of oleic and palmitic acids: Evidence of mass transfer limitations caused by long chain fatty acid accumulation onto the anaerobic sludge. *Biotechnol. Bioeng.* <https://doi.org/10.1002/bit.20548>
- Pilli, S., Bhunia, P., Yan, S., LeBlanc, R.J., Tyagi, R.D., Surampalli, R.Y., 2011. Ultrasonic pretreatment of sludge: A review. *Ultrason. Sonochem.* <https://doi.org/10.1016/j.ultsonch.2010.02.014>
- Poggi-Varaldo, H.M., Rodríguez-Vázquez, R., Fernández-Villagómez, G., Esparza-García, F., 1997. Inhibition of mesophilic solid-substrate anaerobic digestion by ammonia nitrogen. *Appl. Microbiol. Biotechnol.* 47, 284–291. <https://doi.org/10.1007/s002530050928>
- Pohland, F.G., Ghosh, S., 1971. Developments in anaerobic stabilization of organic wastes - the two-phase concept. *Environ. Lett.* <https://doi.org/10.1080/00139307109434990>
- Poirier, S., Madigou, C., Bouchez, T., Chapleur, O., 2017. Improving anaerobic digestion with support media: Mitigation of ammonia inhibition and effect on microbial communities. *Bioresour. Technol.* 235, 229–239. <https://doi.org/10.1016/j.biortech.2017.03.099>
- Qureshi, N., Annous, B.A., Ezeji, T.C., Karcher, P., Maddox, I.S., 2005. Biofilm reactors for industrial bioconversion process: Employing potential of enhanced reaction rates. *Microb. Cell Fact.* <https://doi.org/10.1186/1475-2859-4-24>
- Ragsdale, S.W., 2008. Enzymology of the Wood-Ljungdahl pathway of acetogenesis, in: *Annals of the New York Academy of Sciences.* pp. 129–136. <https://doi.org/10.1196/annals.1419.015>

- Rajagopal, R., Mass, D.I., Singh, G., 2013. A critical review on inhibition of anaerobic digestion process by excess ammonia. *Bioresour. Technol.* <https://doi.org/10.1016/j.biortech.2013.06.030>
- Rajakumar, R., Meenambal, T., Saravanan, P.M., Ananthanarayanan, P., 2012. Treatment of poultry slaughterhouse wastewater in hybrid upflow anaerobic sludge blanket reactor packed with pleated poly vinyl chloride rings. *Bioresour. Technol.* <https://doi.org/10.1016/j.biortech.2011.10.030>
- Romero-Güiza, M.S., Astals, S., Chimenos, J.M., Martínez, M., Mata-Alvarez, J., 2014. Improving anaerobic digestion of pig manure by adding in the same reactor a stabilizing agent formulated with low-grade magnesium oxide. *Biomass and Bioenergy.* <https://doi.org/10.1016/j.biombioe.2014.04.034>
- Rotaru, A.E., Shrestha, P.M., Liu, F., Markovaite, B., Chen, S., Nevin, K.P., Lovley, D.R., 2014. Direct interspecies electron transfer between *Geobacter metallireducens* and *Methanosarcina barkeri*. *Appl. Environ. Microbiol.* 80, 4599–4605. <https://doi.org/10.1128/AEM.00895-14>
- Salminen, E., Rintala, J., 2002. Anaerobic digestion of organic solid poultry slaughterhouse waste—a review. *Bioresour. Technol.* [https://doi.org/10.1016/S0960-8524\(01\)00199-7](https://doi.org/10.1016/S0960-8524(01)00199-7)
- Sarti, A., Zaiat, M., 2011. Anaerobic treatment of sulfate-rich wastewater in an anaerobic sequential batch reactor (AnSBR) using butanol as the carbon source. *J. Environ. Manage.* 92, 1537–1541. <https://doi.org/10.1016/j.jenvman.2011.01.009>
- Schmidt, J.E., Ahring, B.K., 1996. Granular sludge formation in upflow anaerobic sludge blanket (UASB) reactors. *Biotechnol. Bioeng.* [https://doi.org/10.1002/\(SICI\)1097](https://doi.org/10.1002/(SICI)1097)
- Schnürer, A., Houwen, F.P., Svensson, B.H., 1994. Mesophilic syntrophic acetate oxidation during methane formation by a triculture at high ammonium concentration. *Arch. Microbiol.* 162, 70–74. <https://doi.org/10.1007/s002030050103>
- Schnürer, A., Nordberg, A., 2008. Ammonia, a selective agent for methane production by syntrophic acetate oxidation at mesophilic temperature. *Water Sci. Technol.* 57, 735–740. <https://doi.org/10.2166/wst.2008.097>
- Schnürer, A., Zellner, G., Svensson, B.H., 1999. Mesophilic syntrophic acetate oxidation during methane formation in biogas reactors. *FEMS Microbiol. Ecol.* 29, 249–261. [https://doi.org/10.1016/S0168-6496\(99\)00016-1](https://doi.org/10.1016/S0168-6496(99)00016-1)
- Shima, S., Thauer, R.K., 2005. Methyl-coenzyme M reductase and the anaerobic oxidation of methane in methanotrophic Archaea. *Curr. Opin. Microbiol.* 8, 643–648. <https://doi.org/10.1016/j.mib.2005.10.002>
- Shin, H., Kim, S.H., Le, C.Y., Nam, S.Y., 2003. Inhibitory effects of long-chain fatty acids on VFA degradation and beta-oxidation. *Water Sci. Technol.*
- Shumkov, S., Terehova, S., 1995. Biological treatment of coals for their conversion to methane. *Coal Sci. Technol.* [https://doi.org/10.1016/S0167-9449\(06\)80155-2](https://doi.org/10.1016/S0167-9449(06)80155-2)
- Siles, J.A., Brekelmans, J., Martín, M.A., Chica, A.F., Martín, A., 2010. Impact of ammonia and sulphate concentration on thermophilic anaerobic digestion. *Bioresour. Technol.* 101, 9040–9048. <https://doi.org/10.1016/j.biortech.2010.06.163>

- Solli, L., Håvelsrud, O.E., Horn, S.J., Rike, A.G., 2014. A metagenomic study of the microbial communities in four parallel biogas reactors. *Biotechnol. Biofuels*. <https://doi.org/10.1186/s13068-014-0146-2>
- St-Pierre, B., Wright, A.D.G., 2014. Comparative metagenomic analysis of bacterial populations in three full-scale mesophilic anaerobic manure digesters. *Appl. Microbiol. Biotechnol.* 98, 2709–2717. <https://doi.org/10.1007/s00253-013-5220-3>
- Stams, a. J.M., 1994. Metabolic interactions between anaerobic bacteria in methanogenic environments. *Antonie van Leeuwenhoek, Int. J. Gen. Mol. Microbiol.* 66, 271–294. <https://doi.org/10.1007/BF00871644>
- Sung, S., Liu, T., 2003. Ammonia inhibition on thermophilic anaerobic digestion. *Chemosphere*. [https://doi.org/10.1016/S0045-6535\(03\)00434-X](https://doi.org/10.1016/S0045-6535(03)00434-X)
- Thauer, R.K., Hedderich, R., Fischer, R., 1993. Reactions and Enzymes Involved in Methanogenesis from CO<sub>2</sub> and H<sub>2</sub>, in: *Methanogenesis*. [https://doi.org/10.1007/978-1-4615-2391-8\\_5](https://doi.org/10.1007/978-1-4615-2391-8_5)
- Vandevivere, P., Baere, L. De, Verstraete, W., 2003. Types of anaerobic digesters for solid wastes. *Biomethanization of OFMSW*.
- Veeken, A., Kalyuzhnyi, S., Scharff, H., Hamelers, B., 2000. Effect of pH and VFA on Hydrolysis of Organic Solid Waste. *J. Environ. Eng.* [https://doi.org/10.1061/\(ASCE\)0733-9372\(2000\)126:12\(1076\)](https://doi.org/10.1061/(ASCE)0733-9372(2000)126:12(1076))
- Walker, D.J.F., Dang, Y., Holmes, D.E., Lovley, D.R., 2016. The electrically conductive pili of *Geobacter* species are a recently evolved feature for extracellular electron transfer. *Microb. Genomics* 2. <https://doi.org/10.1099/mgen.0.000072>
- Wang, H., Fotidis, I.A., Angelidaki, I., 2015. Ammonia effect on hydrogenotrophic methanogens and syntrophic acetate-oxidizing bacteria. *FEMS Microbiol. Ecol.* 91. <https://doi.org/10.1093/femsec/fiv130>
- Weiland, P., 2010. Biogas production: Current state and perspectives. *Appl. Microbiol. Biotechnol.* <https://doi.org/10.1007/s00253-009-2246-7>
- Westerholm, M., Dolfing, J., Sherry, A., Gray, N.D., Head, I.M., Schnürer, A., 2011a. Quantification of syntrophic acetate-oxidizing microbial communities in biogas processes. *Environ. Microbiol. Rep.* 3, 500–505. <https://doi.org/10.1111/j.1758-2229.2011.00249.x>
- Westerholm, M., Levén, L., Schnürer, A., 2012. Bioaugmentation of syntrophic acetate-oxidizing culture in biogas reactors exposed to increasing levels of ammonia. *Appl. Environ. Microbiol.* 78, 7619–7625. <https://doi.org/10.1128/AEM.01637-12>
- Westerholm, M., Roos, S., Schnürer, A., 2011b. *Tepidanaerobacter acetatoxydans* sp. nov., an anaerobic, syntrophic acetate-oxidizing bacterium isolated from two ammonium-enriched mesophilic methanogenic processes. *Syst. Appl. Microbiol.* 34, 260–266. <https://doi.org/10.1016/j.syapm.2010.11.018>
- Westerholm, M., Roos, S., Schnürer, A., 2010. *Syntrophaceticus schinkügen* nov., sp. nov., an anaerobic, syntrophic acetate-oxidizing bacterium isolated from a mesophilic anaerobic filter. *FEMS Microbiol. Lett.* 309, 100–104. <https://doi.org/10.1111/j.1574-6968.2010.02023.x>
- Yenigün, O., Demirel, B., 2013. Ammonia inhibition in anaerobic digestion: A review. *Process Biochem.* 48, 901–911. <https://doi.org/10.1016/j.procbio.2013.04.012>

- Yuan, H., Zhu, N., 2016. Progress in inhibition mechanisms and process control of intermediates and by-products in sewage sludge anaerobic digestion. *Renew. Sustain. Energy Rev.* <https://doi.org/10.1016/j.rser.2015.12.261>
- Zeikus, J.G., Weimer, P.J., Nelson, D.R., Daniels, L., 1975. Bacterial methanogenesis: Acetate as a methane precursor in pure culture. *Arch. Microbiol.* <https://doi.org/10.1007/BF00447312>
- Zhang, F., Zhang, Y., Ding, J., Dai, K., Van Loosdrecht, M.C.M., Zeng, R.J., 2014. Stable acetate production in extreme-thermophilic (70°C) mixed culture fermentation by selective enrichment of hydrogenotrophic methanogens. *Sci. Rep.* <https://doi.org/10.1038/srep05268>
- Zhang, L., Ouyang, W., Lia, A., 2012. Essential Role of Trace Elements in Continuous Anaerobic Digestion of Food Waste. *Procedia Environ. Sci.* <https://doi.org/10.1016/j.proenv.2012.10.014>
- Zhao Q., Wang C., Liu Y., Wang S. 2007. Bacterial adhesion on metal-polymer composite coatings. *International Journal of Adhesion & Adhesives* 27(2), 85-91.
- Zhao, Z., Zhang, Y., Holmes, D.E., Dang, Y., Woodard, T.L., Nevin, K.P., Lovley, D.R., 2016. Potential enhancement of direct interspecies electron transfer for syntrophic metabolism of propionate and butyrate with biochar in up-flow anaerobic sludge blanket reactors. *Bioresour. Technol.* 209, 148–156. <https://doi.org/10.1016/j.biortech.2016.03.005>
- Zhao, Z., Zhang, Y., Woodard, T.L., Nevin, K.P., Lovley, D.R., 2015. Enhancing syntrophic metabolism in up-flow anaerobic sludge blanket reactors with conductive carbon materials. *Bioresour. Technol.* 191, 140–145. <https://doi.org/10.1016/j.biortech.2015.05.007>
- Zheng, H., Li, D., Stanislaus, M.S., Zhang, N., Zhu, Q., Hu, X., Yang, Y., 2015. Development of a bio-zeolite fixed-bed bioreactor for mitigating ammonia inhibition of anaerobic digestion with extremely high ammonium concentration livestock waste. *Chem. Eng. J.* 280, 106–114. <https://doi.org/10.1016/j.cej.2015.06.024>
- Zheng, Y., Zhao, J., Xu, F., Li, Y., 2014. Pretreatment of lignocellulosic biomass for enhanced biogas production. *Prog. Energy Combust. Sci.* <https://doi.org/10.1016/j.pecs.2014.01.001>
- Zhuang, L., Tang, J., Wang, Y., Hu, M., Zhou, S., 2015. Conductive iron oxide minerals accelerate syntrophic cooperation in methanogenic benzoate degradation. *J. Hazard. Mater.* 293, 37–45. <https://doi.org/10.1016/j.jhazmat.2015.03.039>
- Zinatizadeh, A.A.L., Younesi, H., Bonakdari, H., Pirsaeheb, M., Pazouki, M., Najafpour, G.D., Hasnain Isa, M., 2009. Effects of process factors on biological activity of granular sludge grown in an UASFF bioreactor. *Renew. Energy.* <https://doi.org/10.1016/j.renene.2008.10.013>

# Chapter 2 Objectives

---

The objectives of the thesis, the research chronology and the thesis outline are presented.

## 2.1. Objectives

The general purpose of this thesis is to gain a deeper insight into the biodiversity, ecophysiology, genomics, and interactions of methanogenic microbial populations that are characteristic from environments with inhibitory concentrations of ammonia. Especial attention has been given to the syntrophic acetate oxidation, and on how this process contributes to the stabilization of anaerobic digesters treating organic wastes that produce such inhibitors. Innovative reactor configuration and design aspects for an optimized treatment of nitrogen-rich wastes have also been investigated.

The general aim of this dissertation has been unfolded into a number specific research objectives, which are developed further in the subsequent sections:

- To enrich and identify relevant microorganisms from methanogenic biomass, both in the *Bacteria* and *Archaea* domains, that are involved in the syntrophic acetate oxidation (SAO) process.
- To assess microbial community structure and dynamics in response to increasing ammonia exposure.
- To characterize the SAO process at the metagenome level in order to pinpoint specific metabolic and physiologic traits that contribute to the stability of the methanogenic activity.
- To elucidate the effect of packing materials with different physicochemical properties on the development of methanogenic biomass that functions via the SAO process.
- To development reactor configuration strategies for anaerobic digesters in order to increase the process robustness and stability in front of ammonia inhibition.

### **2.1.1 To enrich and identify relevant microorganisms from methanogenic biomass, both in the *Bacteria* and *Archaea* domains, that are involved in the syntrophic acetate oxidation (SAO) process.**

The selection of a suitable methanogenic biomass for the inoculation of full-scale digesters is often a critical bottleneck during the start-up period. The adaptation of such inoculum to the reactor operational conditions and feed composition is a fundamental aspect for a subsequent optimal performance. The selection of adapted biomass is particularly relevant when digesters are subjected to relatively high levels of ammonia, conditions in which the SAO process appears to be a key feature. Therefore, an in-depth characterization of the microbial community structure of different sources of methanogenic biomass more-or-less adapted to ammonia was the first step of this work (Part II). Conventional methanogenic activity assays are not sufficiently specific to elucidate the interactions between bacteria and archaea during the SAO process. Hence, to overcome these experimental limitations, an innovative approach that integrated isotopic fractionation of biogas components, in order to distinguish between acetotrophic and hydrogenotrophic methanogenesis, along with culture independent molecular tools, was implemented on different sources of methanogenic biomass. The methodologies implemented in the current work have been described in detail in Chapter 3.

### **2.1.2 To assess microbial community structure and dynamics in response to increasing ammonia exposure.**

The efficiency and stability of AD process is completely dependent upon the syntrophic activity of microbes belonging to different functional guilds performing hydrolysis, fermentation, acetogenesis and methanogenesis. However, the majority of microorganisms in these systems have not yet been cultivated. For this reason, if limited to culture-dependent methodologies, the knowledge of microbial ecology related to AD subjected to high ammonia would remain incomplete. For that, in order to fully understand the structure and dynamics of microbial community interdisciplinary studies are needed. Therefore, to decipher microbial community and their syntrophic interaction in these conditions it will combine batch methanogenic activity with in-depth characterization of microbial populations by next-generation sequencing (at DNA and RNA levels) and through the quantification of the expression level of relevant genes and transcripts. These approaches are extensively described during part II and III.



**2.1.3 To characterize the SAO process at the metagenome level in order to pinpoint specific metabolic and physiologic traits that contribute to the stability of the methanogenic activity.**

Until now, few species have been described as SAOB. However, it is known that this process is carried out satisfactorily without the need to find the species described in the literature as SAOB. For this reason within this objective, it is intended to obtain a better understanding of the microbial community interactions at the genome level in AD reactors when exposed to different ammonia levels. For this purpose, an interdisciplinary strategy combining isotopic profiling of biogas samples with whole metagenomics shotgun sequencing and binning of scaffolds into population genomes (PG) has been developed (these strategies are described in chapter 5 and 8). It is pretended that this novel approach facilitated the functional analysis of genes in relation to ammonia exposure, the reconstruction of probable metabolic pathways for methanogenesis and acetate assimilation, and the identification of novel species that might be involved in the SAO process.

**2.1.4 To elucidate the effect of packing materials with different physicochemical properties on the development of methanogenic biomass that functions via the SAO process.**

As it was previously described on chapter 1, it is known that microbial communities tend to grow in biofilm, and this provides them favorable conditions for their growth and confer them resistance to environmental disturbances. Certain support materials favour the adherence of microorganisms and, consequently, increase the amount of retained biomass inside bioreactors, thus resulting in higher substrate conversion yields. These packed systems usually are more stable with respect to high organic loadings, shock loadings or changes in pH and temperature. However, not all microorganisms behave the same in the same material, because the nature of different support materials strongly influenced the microbial communities through biofilm formation and/or the alternative electron transfer mechanisms. Therefore, to cover the lack of knowledge about the SAO biofilm, an extensive study is planned to test materials with different natures and characteristics, based on combination of batch assay, next generation sequencing at DNA and RNA level and metagenomics approach. The different activities and assays focused to cover this gap on SAO knowledge are mainly concentrated on the part II of this dissertation.

**2.1.5 To develop reactor configuration strategies for anaerobic digesters in order to increase the process robustness and stability in front of ammonia inhibition.**

In this block, which is mainly treated on part IV, it will run continuous anaerobic digesters with clear predominance of the SAO process. During this part, it is intended to operate different configurations of reactors, but with similar operational parameters. In all of them, it wants to monitor the degradation of N-rich waste, and in some of them, the degradation of N-rich and  $\text{SO}_4^{2-}$  wastes.

The first configuration was the RT in continuous stirred reactors and the second strategy was the addition of support materials, that boost biofilm formation or electron transfer between species, becoming the stirred reactor in a hybrid one and thus, introducing the assisted basket reactor.

In all of them the microbial dynamics based on (diversity, abundance, density) indexes were studied to evaluate the effect of solid retention time on ammonia resilience and resistance, linking them to conventional AD performance parameters and inhibition assessment (toxicity assays).

# **Chapter 3 Materials and methods**

---

This chapter details the experimental setups used for the experiments carry out in this thesis. The adopted multidisciplinary methodological approach for the analysis of the experimental data is also described. This was based such on the analytical and bioreactors performance combined with microbial communities and process characterization by means of molecular biology approaches and bioinformatics procedures.

### 3.1. Introduction

To conduct the study, and to achieve the objectives, a rigorous methodology based on pertinent quality standards of the group. Then describes the steps and the necessary details within each analytical.

### 3.2. Methanogenic assays: activity and toxicity

The method consists in the anaerobic fermentation of organic samples, with a known quantity of inoculum and nutrient supplementation, in discontinuous. The extent of the activity is carried out through the analysis of the head of the reactor, together with the analysis of COD removed and the evolution of the fatty acids.

### 3.3. Physicochemical analytical methods

Total Kjeldhal nitrogen (TKN), total ammonia nitrogen (TAN) and pH were determined according to the Standard Methods (APHA). Biogas composition (CH<sub>4</sub> and CO<sub>2</sub>) and the concentration of individual volatile fatty acids (VFA) in the liquid media, including acetic (Ac), propionic, butyric, valeric and caproic acids, were measured on a Varian CP-3800 gas chromatograph equipped with a Varian Hayesep-Q 80-100 mesh capillary column and a TCD detector, or a TRB-FFAP capillary column and a FID detector for the analysis of biogas or VFA, respectively.

### 3.4. Alkalinity

Total alkalinity (TA) was determined according to standard methods (APHA, 2005) through titration to pH 4.3 with H<sub>2</sub>SO<sub>4</sub> 0.5 N. Partial alkalinity (PA, titration from the original pH sample to pH 5.75, an alkalinity which corresponds roughly to bicarbonate alkalinity) was determined to obtain intermediate alkalinity (IA, titration from 5.75 to 4.3, approximately the VFA alkalinity). Alkalinity is expressed in calcium carbonate units according to the following equations:

### 3.5. Total and volatile solids

Total (TS) and volatile solids (VS) were determined according to standard methods (APHA, 2005). TS were obtained drying a well homogenised sample in a stove at 105 °C for 24h to constant weight, and are calculated with the following equation:

$$TS(\%) = 100 - \frac{W_W - W_D}{W_W - T} \cdot 100$$

Next, the sample is calcined at 550 °C in the muffle during 3.5 hours and weighed. The weight difference between the TS and the obtained ashes is the VS content.

$$VS(\%) = 100 - \frac{W_w - W_a}{W_w - T} \cdot 100$$

where  $W_w$ ,  $W_d$ ,  $W_a$  and  $T$  are the weight (g) of the wet sample, the dry sample, the ashes and the capsule, respectively.

### 3.6. Chemical oxygen demand

Chemical oxygen demand (COD) was analysed according to an optimised standard method (Noguerol et al., 2012). The sample was oxidised with 1.5 mL of digestion reagent (potassium dichromate, 0.5 N, mercury sulphate and sulphuric acid 95-97%) and 1.5 mL of catalyst (silver sulphate 1%, and sulphuric acid 95-97%) and digested at 150 °C for 2 h in a digester (Hach Lange LT 200). Dichromate concentration was measured colorimetrically (spectrophotometer Hach Lange DR 2800). For soluble COD measurement the samples were previously filtered through a 0.45 µm pore diameter Nylon syringe filter (Scharlau, S.L.).

### 3.7. Determination of isotopic carbon

Isotopic fractionation analyses were carried out by gas chromatography combustion–isotope ratio mass spectrometry (GC–IRMS). An Agilent 6890 gas chromatograph was fitted with a split/splitless injector and coupled to an isotope ratio mass spectrometer (Delta Plus Finnigan MAT) via a combustion interface (850°C), consisting of a 60 cm quartz tube (0.65 mm ID) filled with copper oxide. A liquid nitrogen cold trap was used to remove water. Separation was achieved on a Cpsil5CB (Chrompack) fused silica capillary column (60 m×0.32 mm; 0.12 µm film thickness) using He as carrier gas. The oven temperature was held at 40°C for 1 min, and increased to 320°C at a rate of 10°C min<sup>-1</sup>. This final temperature was maintained for 25 minutes. Squalene was used as internal standard. Each sample was run in triplicate to ensure reproducibility within ±0.2‰ (1σ), relative to the Vienna Pee Dee Belemnite (VPDB) standard. All carbon isotopic ratios were expressed as ‰ relative to the VPDB standard, and the apparent fractionation factor (αC) was determined according to Conrad et al., (2009). A αC with the range of 1.040 – 1.055 was assigned to a predominantly acetotrophic AD process, while that of 1.055 – 1.080 was mainly hydrogenotrophic (Conrad, 2005; Penning and Conrad, 2007).

### **3.8. Assembly and operation of continuous anaerobic digesters**

#### **3.8.1. Lab-scale digester: general set-up**

The reactor is the principal element where take place the process of anaerobic digestion. It is a hermetic and Pyrex glass container with a cover made of either glass or steel. It has sampling points located in cover of the digester (for liquid effluent or biogas sample collection), and connections points (to locate sensors as temperature probe). The reactor is connected to the different circuits: feed and effluent tanks, stirrer, pumping system, biogas counting system, and cooling/ heating system. Metal clamps metal used to make all connections.

The feed circuit includes: influent reservoir, which characteristics are related to the nature of the material to be storage (viscosity or solid content of the substrate, capability to be degrade, storage temperature, etc.); pumping equipment to regulate precisely the quantity of influent, allowing to dose and control the flow inside of reactor; and finally connection devices and pipes, usually made of plastics or silicon, easily to disassemble/ assemble in order to maintain the whole circuit clean.

The deposit or balloon effluent is the element responsible for collecting the effluent of the reactor together with biogas. This tank separates the liquid biogas and the latter measuring equipment production. Among the reactor effluent tank, there are manual valves that allow isolating the reactor and prevent the entry of oxygen at the time of collection or emptying effluent, as well as one sampling point to extract the gas phase sample through a septum. Regarding pipes of this element, they should be of a material impermeable to gases.

At lab-scale digesters, the biogas flow is measured by means of the liquid (water, oil) displacement based meters. This is the case of the commercial counter Ritter and the own-made counter with communicating vessels, also called Mariotte device.

The stirring systems (influent, digester) are time-controlled and the temperature inside the digester is kept constant by means of the temperature probe that control thermostatic bath, pumping system and the closed water bath.

#### **3.8.2. Operational conditions**

The selection of the digesters is based on the cellular retention time (SRT) is big enough to be SAOB and SAOA remain in the digester. In continuous systems, the time required to double the amount of microorganisms (dependent therefore, the growth rate of each population) is related to the retention time. In systems without

recirculation, the hydraulic retention time (HRT) and cell are equal. In recirculating systems or with biomass immobilized in brackets, the HRT and the SRT are different.

### **3.8.3. Stirred reactor**

This is a conventional continuous reactor, which has the power input and dual output; one for the effluent and another outlet for gas accumulation. It has mechanical agitation. The gas produced is counted by means of a Ritter counter. This reactor is launched with synthetic feed (composed by gelatine and glycerine) to activate the inoculum in the starting stage of operation, and then the feed is replaced by a real waste mixture with the aim of progressively increasing TAN concentration. In order to study the effect of different values of biomass retention, two similar stirred reactors are performed but with and without partial recirculation of the effluent.

### **3.8.4. Hybrid reactor**

This hybrid reactor is a kind of granular sludge bioreactor that is used for degradation of organic matter and converts it to methane with microbial film formation. The reactor has an immobilized basket that contains the inert support particles available for biofilm attachment. The selection of this support material is previously done by means of batch tests.

Due to the expected retention of biomass over the support material, the HRT is less than the previous reactor because biomass retention is achieved with biofilm. Regarding to agitation, it is done with gas recirculation that forms gas bubbles and shake the content of the reactor. Another way to agitate the reactor is doing with the feed entrance that goes from down to up the reactor.

### **3.8.5. Enrichment digester**

This reactor presents a configuration similar to the first one, which has the power input and dual output; one for the effluent and another outlet for gas accumulation. It has mechanical agitation. The gas produced is counted by means of a Ritter counter. It is operating in a temperature range mesophil 37 °C, with a constant agitation, and presents a HRT of 50 days. This nourishing with gelatine and glycerol, which gives you a carbon source but at the same time introduces TAN concentration of 4g/L.

### 3.9. Microbiology characterization

#### 3.9.1. Quantitative real-time pcr (qpcr)

Total genomic DNA and RNA from all previously centrifuged biomass samples (pellets) were simultaneously extracted by an adapted protocol of the PowerMicrobiome™ RNA Isolation kit (Qiagen). The RNA extracts were treated during 10 min at 25 °C with 10 units of DNase I to remove any contamination of genomic DNA, and directly subjected to a 16S rRNA-based PCR amplification to verify their purity (Prenafeta-Boldú et al., 2014). RNA extracts were subsequently transcribed to cDNA by means of PrimeScript™ RT reagent Kit (Perfect Real Time, Takara) following the manufacturer's instructions. cDNA and DNA extracts were kept frozen at –80 °C until further analysis.

Total and active bacterial populations and methanogenic archaea were quantified by means of qPCR amplification of 16S rRNA and *mcrA* genes, respectively (Sotres et al., 2014). Reactions were carried out using the Brilliant II SYBR Green qPCR Master Mix (Stratagene, La Jolla, CA, USA) on a Real-Time PCR System Mx3000P (Stratagene). The specificity of the qPCR amplifications was determined by observations of the corresponding melting curves and gel electrophoresis profiles. To prepare the corresponding standard curves two duplex DNA were synthesized (Metabion GmbH). Ten-fold serial dilutions of both standard genes were subjected to qPCR assays in duplicate showing a linear response between 101 and 108 gene copy numbers. The qPCR standards for both genes fitted quality standards with amplification efficiencies between 90 and 110% and R2 above 0.985. All results were processed by the MxPro™ QPCR software (Stratagene, La Jolla, CA).

#### 3.9.2. Next Generation Sequencing (Illumina Sequencing)

Massive bar-coded 16S rRNA gene libraries targeting V1–V3 and V3–V4 hypervariable regions from bacterial and archaeal populations, respectively, were sequenced by means of Illumina MiSeq System Platform in Molecular Research DNA LP (Shallowater, USA). Downstream MiSeq data analysis was carried out by using QIIME software version 1.8.0. Trimming of the 16S rRNA barcoded sequences into libraries was carried out using QIIME software version 1.8.0. ([www.qiime.org](http://www.qiime.org)). Quality filtering of the reads was performed at Q25, prior to the grouping into Operational Taxonomic Units (OTUs) at a 97% sequence homology cutoff and taxonomic assignment according to the Greengenes database.

The alpha biodiversity parameters of every sample (number of observed OTUs, the inverted Simpson index, Shannon index, Goods coverage, and Chao1 richness



estimator) were calculated using the Mothur software v.1.35.9 (<http://www.mothur.org>). The number of contigs were rarefacted to the lowest number among the different samples. Correspondence analysis (CA) of bacterial MiSeq data (relative OTU distribution matrix) was performed by means of XLSTAT 2014 software (Addinsoft, Paris, France).

### 3.9.3. Metagenome sequencing, assembly and binning process

Genomic DNA extracts from each sample were prepared for sequencing using Nextera DNA Library Preparation Kit (Illumina, San Diego, CA, USA). All the samples were paired-end sequenced ( $2 \times 150$  bp) using Illumina HiSeq 2500 (Molecular Research DNA, Shallowater, TX, USA). Paired-end sequences were quality-filtered and adaptors were removed with the Trimmomatic software (v0.33) using the following parameters: Illumina clip (NexteraPE-PE:2:30:10), leading (10), trailing (10), sliding window (4:20, minlen (65). Assembly was performed using metaSPAdes (3.9.0) with kmers 55, 77, 99 and a minimum scaffold length of 500 bp. Quality of the assembly was checked using QUAST. Gene finding was performed with Prodigal (v2.6.2) ran in metagenomic mode. Protein-encoding genes were annotated using the reverse-position specific BLAST algorithm with the COG RPSBLAST database (Galperin et al., 2015); only results with e-value lower than  $10^{-5}$  were retained. Genes were also annotated according to KEGG using GhostKOALA. Scaffolds were binned into population genomes (PGs) using two strategies: the MetaBAT (v0.25.4) (parameters --specific, -m 1500) (Kang et al., 2015), and the hierarchical clustering followed by canopy profile selection (Campanaro et al., 2016). Completeness and contamination of PGs were estimated using the Lineage\_wf workflow of CheckM (Parks et al., 2015) and the PGs obtained from the two approaches were compared using the “bin-compare” module of the same software (Parks et al., 2015). PGs were considered as univocally identified by one binning strategy when they had less than 20% of the bases in common with those extracted by the other software (54 PGs). Conversely, all the remaining PGs (83 with overlap higher than 50% and 44 with overlap included between 20% and 50%) were compared as follows: completeness and contamination of each PG obtained with the two binning strategies were combined using the formula  $[\text{completeness} - (\text{contamination} * 3)]$  and each PG was selected from the strategy where it displayed the higher value. After selection, scaffolds assigned to more than one PG were removed, and completeness and contamination was determined again for the PGs included in the final selection. The bioinformatic functional analysis was limited to those that satisfied strict requirements (completeness  $> 50\%$ , contamination lower than  $20\%$ ). Functional analysis of the PGs was based on KEGG annotation determined for all PGs and, additionally, gene

function was also determined by Rapid Annotation using Subsystem Technology (RAST) server (Overbeek et al., 2014).

Taxonomical assignment of the obtained PGs was performed using PhyloPhlan (v0.99). Those having incomplete confidence were checked using the PhyloPythiaS web server (Patil et al., 2012) and assigned to a clade only when more than 50% of the genome sequence displayed coherent results. The presence of genomes belonging to the same species in the NCBI microbial genome database and in PGs recovered in previous assemblies was determined using the Average Nucleotide Identity calculation as previously described (Treu et al., 2016). Abundance of genes and PGs in the different reactors was considered as directly related to scaffold coverage. This parameter was determined aligning reads on the assembly using the Bowtie 2 software (v2.2.4) and converting the result in the corresponding coverage value using the BEDTools package (v2.17.0). Results were normalized considering the sample with the lower number of reads as a reference. Coverage values were visualized with MeV in order to identify the behaviour of PGs in different samples.

### 3.10. References

- 90/667/EEC. 2002. Regulation (EC) No 1774/2002 of the European Parliament and of the Council, 3 October 2002, laying down health rules concerning animal by-products not intended for human consumption. Official Journal of the European Community.
- Campanaro, S., Treu, L., Kougias, P.G., De Francisci, D., Valle, G., Angelidaki, I., 2016. Metagenomic analysis and functional characterization of the biogas microbiome using high throughput shotgun sequencing and a novel binning strategy. *Biotechnol. Biofuels* 9, 26.
- Galperin, M.Y., Makarova, K.S., Wolf, Y.I., Koonin, E. V., 2015. Expanded Microbial genome coverage and improved protein family annotation in the COG database. *Nucleic Acids Res.* 43, D261–D269.
- Kang, D.D., Froula, J., Egan, R., Wang, Z., 2015. MetaBAT, an efficient tool for accurately reconstructing single genomes from complex microbial communities. *PeerJ* 3, e1165.
- Nogueroles, J., Rodríguez-Abalde, A., Romero, E., Flotats, X., 2012. Determination of Chemical Oxygen Demand in Heterogeneous Solid or Semisolid Samples Using a Novel Method Combining Solid Dilutions as a Preparation Step Followed by Optimized Closed Reflux and Colorimetric Measurement. *Analytical Chemistry*. 84, 5548–5555.
- Overbeek, R., Olson, R., Pusch, G.D., Olsen, G.J., Davis, J.J., Disz, T., Edwards, R.A., Gerdes, S., Parrello, B., Shukla, M., Vonstein, V., Wattam, A.R., Xia, F., Stevens, R., 2014. The SEED and the Rapid Annotation of microbial genomes using Subsystems Technology (RAST). *Nucleic Acids Res.* 42.
- Parks, D.H., Imelfort, M., Skennerton, C.T., Hugenholtz, P., Tyson, G.W., 2015. CheckM: assessing the quality of microbial genomes recovered from isolates, single cells, and metagenomes. *Genome Res.* 25, 1043–55.
- Patil, K.R., Roune, L., McHardy, A.C., 2012. The phyloPythiaS web server for taxonomic assignment of metagenome sequences. *PLoS One* 7.

Treu, L., Kougias, P.G., Campanaro, S., Bassani, I., Angelidaki, I., 2016. Deeper insight into the structure of the anaerobic digestion microbial community; The biogas microbiome database is expanded with 157 new genomes. *Bioresour. Technol.* 216, 260–266.

# Part II

---

Microbial community structure and dynamics during anaerobic digestion in ammonia-rich wastes

# Chapter 4 Functional plasticity of methanogenic biomass from a full-scale mesophilic anaerobic digester treating nitrogen-rich agricultural wastes

---

To unravel the effects of increasing ammonium concentrations on methanogenic activity and the associated metabolically active microbiome, sludge from a full-scale anaerobic digester treating nitrogen-rich wastes was characterized in methanogenic batch activity assays at different total ammonia concentrations (1, 3.5 and 6 gN-TAN L<sup>-1</sup>). Predominance of syntrophic acetate oxidation (SAO) linked to strictly hydrogenotrophic methanogenic activity was demonstrated at total ammonia nitrogen concentrations of 3.5 gN-TAN L<sup>-1</sup> and above by compound specific isotopic analysis of biogas components (CO<sub>2</sub> and CH<sub>4</sub>).

*Part of this chapter was presented as an oral communication in AD14 conference.*

*This chapter was published as: Ruiz-Sánchez J, Vila J, Guivernau M, Vinas M, Riau V, Fernández B, Prenafeta-Boldu FX. Functional plasticity of methanogenic biomass from a full-scale mesophilic anaerobic digester treating nitrogen-rich agricultural wastes. Science of The Total Environment, 2019. 649,760-769,*

## 4.1 Introduction

The anaerobic digestion (AD) of organic materials is a well-consolidated technology for the treatment and revalorization of organic waste into renewable energy (methane from biogas), and contributes significantly to the sustainability of several industrial processes (Lettinga, 2010). However, a significant proportion of the organic waste generated by the agrifood sector contains relatively large amounts of nitrogenated compounds (i.e. animal dejections, slaughterhouse by-products, and other protein-rich food-processing wastes), which are decomposed into ammonia under anaerobic conditions. Free ammonia is a well-known inhibitor of methanogenic activity because of its interference to the cell-membrane ion-transport mechanism (Yenigün and Demirel, 2013). Such inhibitory effects might affect all microbial communities involved in the AD syntrophy, but the methanogenic archaea appear to be particularly sensitive to ammonia stress (Demirel and Scherer, 2008). Yet, not all methanogens are affected equally; acetoclastic methanogenic archaea (AMA), which under normal conditions are responsible for most of the generated methane, have been described to be particularly vulnerable to relatively high total ammonia nitrogen concentrations ( $\text{TAN} > 3.5 \text{ gN-TAN L}^{-1}$ ) (Banks et al., 2012; Schnürer and Nordberg, 2008). Conversely, the less sensitive hydrogenotrophic methanogenic archaea (HMA) are able to remain active at those concentrations, with a reported TAN inhibition threshold up to  $5 \text{ gN-TAN L}^{-1}$  (Wang et al., 2015). Furthermore, AMA inhibition by ammonia might result in the accumulation of acetate up to inhibitory levels, thus contributing further to a negative feedback mechanism that eventually leads to complete reactor failure (Wang et al., 2015).

Under such high concentrations of ammonia and/or acetate, the so-called syntrophic acetate oxidizing bacteria (SAOB) are able to reverse the homoacetogenic pathway and convert acetate to carbon dioxide and hydrogen (Schnürer et al., 1999). This process is thermodynamically favourable through the concomitant consumption of hydrogen by HMA and, therefore, the syntrophic association between SAOB and HMA prevents the inhibition of methanogenesis during the AD of nitrogen-rich substrates (Petersen and Ahring, 1991). The fundamental role of SAOB in the AD process under high ammonia conditions was already recognized in the late nineties but, so far, relatively little is known about the diversity, physiology and biochemistry of these microorganisms (Hattori, 2008). An increasing number of SAOB strains have been isolated in the recent years and their physiology and genetics have been characterized quite thoroughly, but information on the diversity, occurrence and role of SAOB in full-scale anaerobic digesters is still limited. Recent studies based on the isotopic profiling of biogas components from industrial anaerobic digesters fed with  $^{13}\text{C}$ -labelled acetate have indicated the predominance of the HMA methanogenic

pathway under relatively high ammonia exposure, which might be conducive to the enrichment of SAOB (Hao et al., 2015).

The present study aims to gain a deeper insight into the microbial interactions, both of metabolically active bacterial and archaeal populations involved in the SAO process, occurring in methanogenic biomass from an industrial anaerobic digester treating nitrogen-rich agricultural wastes with no previous records of process inhibition. A diversified research approach has been adopted for this purpose, which combined batch methanogenic activity assays with Compound-Specific Isotope Analysis (CSIA) of  $^{13}\text{C}/^{12}\text{C}$  natural isotopic fractionation of methane and carbon dioxide in the generated biogas with the in-depth characterization of present and metabolically active microbial populations by 16S-Illumina sequencing. Time course expression of relevant genes from the total active bacteria and methanogenic archaea was quantified by qPCR assessment of 16S rRNA and *mcrA* genes and transcripts.

## 4.2 Materials and methods

The methanogenic biomass was collected from a 1,500 m<sup>3</sup> full-scale stirred tank reactor for anaerobic co-digestion of pig slurry and protein-rich agricultural wastes (Vila-sana, Lleida, Spain), operated under mesophilic temperature and with a hydraulic retention time of 65 days. The inoculum was characterised in terms of its content of TAN (5.2 gN-TAN L<sup>-1</sup>), chemical oxygen demand (101.2 gO<sub>2</sub> L<sup>-1</sup>), volatile suspended solid (VSS; 61.2 gVSS L<sup>-1</sup>), pH (8.3) and acetic acid (0.0 gAc L<sup>-1</sup>). A detailed description of methodologies is shown in Chapter 3.

Experiments were conducted in triplicate batch cultures (120 mL total volume, 60 mL working volume, inoculated with 12.7 gVSS L<sup>-1</sup>), containing 1.0, 3.5 or 6.0 gN-TAN L<sup>-1</sup>, added as NH<sub>4</sub>Cl, and 2.35 gAc L<sup>-1</sup> as sodium acetate. Anaerobic conditions were generated by flushing N<sub>2</sub> during 10 min. Cultures were incubated at 37<sup>0</sup>C under rotatory shaking and a bicarbonate buffer solution was added to maintain a constant pH (8) throughout the experiment. Control vials with nor acetate neither ammonia were included to assess the endogenous CH<sub>4</sub> production of the inoculum.

Samples from the headspace of each culture were taken periodically for the characterization of the biogas composition during the experiment. Samples of the biogas accumulated at the end of the incubation were collected for analysing the natural  $^{13}\text{C}/^{12}\text{C}$  isotopic fractionation of CH<sub>4</sub> and CO<sub>2</sub> (see Chapter 3). Specific rates of acetate consumption and CH<sub>4</sub> production were determined and expressed as gCOD gVSS<sup>-1</sup> d<sup>-1</sup> (conversion factors: 2.857 gCOD mLCH<sub>4</sub><sup>-1</sup>; 1.067 gCOD gAc<sup>-1</sup>).

CH<sub>4</sub> yield (mLCH<sub>4</sub> gCOD<sup>-1</sup>), lag phase and specific CH<sub>4</sub> production rate (rCH<sub>4</sub>; mgCOD gVSS<sup>-1</sup> d<sup>-1</sup>) were calculated after fitting the experimental data to the modified Gompertz equation.

Samples from each batch replicate (1 mL) were collected after 0, 7, 11 and 17 days of incubation (labelled as t<sub>0</sub>, t<sub>2</sub>, t<sub>4</sub> and t<sub>5</sub>), and directly centrifuged (4°C, 20,000 g, 5 minutes). The clarified fractions (supernatant) were used for determination of the concentration of individual volatile fatty acids (VFA) including acetic (Ac), propionic, butyric, valeric and caproic acids, were monitored in each vial. All pellets were kept at -80°C until further processing via molecular biology tools. Total genomic DNA and RNA from all previously centrifuged biomass samples (pellets) were simultaneously extracted, as well as total and active bacterial populations and methanogenic archaea were quantified by means of qPCR amplification of 16S rRNA and *mcrA* genes, respectively (see Chapter 3).

The time course evolution of methanogenic activity and expression of 16S rRNA and *mcrA* genes determined the sampling periods for high throughput sequencing. The microbial community structure was characterized by 16S-Illumina sequencing analysis after 11 and 17 days, respectively for batches exposed to 1.0 and 3.5 gN-TAN L<sup>-1</sup> and 6.0 gN-TAN L<sup>-1</sup>, when the maximum CH<sub>4</sub> production rates and gene expression level was recorded (Figures 4.1 and 4.2).

The alpha biodiversity parameters of every sample (number of observed OTUs, the inverted Simpson index, Shannon index, Goods coverage, and Chao1 richness estimator). The number of contigs were rarefacted to the lowest number among the different samples. Correspondence analysis (CA) of bacterial MiSeq data (relative OTU distribution matrix) was performed. The sequence data from the MiSeq NGS assessment were submitted to the Sequence Read Archive (SRA) of the National Center for Biotechnology Information (NCBI) under the study accession number PRJNA385091.

The Shapiro-Wilk test was performed to determine whether data were normally distributed. Considering the paired structure and normal distribution of the data, an analysis of variance (ANOVA) was performed. The combination of factors were the sampling period (t<sub>0</sub>, t<sub>7</sub>, t<sub>11</sub> and t<sub>17</sub> days) and the experiments (1.0, 3.5 and 6.0 gN-TAN·L<sup>-1</sup>) for each ratio. Subsequently, pairwise comparisons Fisher's least significant difference (LSD) were applied to test differences between batches by sampling periods. The significance threshold was established at 0.05 type I error. All statistical analysis were performed by means of XLSTAT 2018 software (Addinsoft, Paris, France).



## 4.3 Results and discussion

### 4.3.1 Methanogenic activity assays

The specific acetate uptake rate ( $r_{Ac}$ ) in freshly collected methanogenic biomass from the studied agricultural anaerobic digester was rather similar, regardless of the concentration of supplemented ammonia up to 3.5 gN-TAN L<sup>-1</sup>, but the  $r_{Ac}$  decreased by 46% at 6.0 gN-TAN L<sup>-1</sup> (Table 4.1). Despite the fact that all tested batches reached a similar CH<sub>4</sub> yield, the CH<sub>4</sub> production rate ( $r_{CH_4}$ ) decreased by 26% and 31% upon ammonia exposure at 3.5 and 6.0 gN-TAN L<sup>-1</sup>, with respect to the  $r_{CH_4}$  at 1 gN-TAN L<sup>-1</sup> (Figure 4.1, Table 4.1). This apparent higher vulnerability of acetate-utilizing microorganisms might be the result of the well-known susceptibility of AMA to ammonia (Hunik et al., 1990). Under such conditions, acetate might also be consumed by the SAOB but this metabolic process has been associated to relatively low conversion rates (Sun et al., 2014). Along with a high ammonia content, those digesters were often characterized by a prolonged biomass retention time and thermophilic temperature, parameters that have been identified as crucial for the enrichment of the rather slow-growing SAO microbial communities (Sun et al., 2014).

### 4.3.2 Isotopic fractionation of biogas

Compound-Specific Isotope Analysis (CSIA) of <sup>13</sup>C/<sup>12</sup>C natural isotopic fractionation of biogas components from the batch activity assays provided a deeper insight on the predominance of acetotrophic or hydrogenotrophic methanogenic pathways, in relation to the content of ammonia. Most of the previous studies on the application of isotopic analysis of biogas for the characterization of anaerobic digesters subjected to high ammonia levels were based on using radioactive (Karakashev et al., 2006; Sun et al., 2014) or stable (Mulat et al., 2014) isotope-labelling at the C<sub>2</sub> position (methyl group) of acetate. The sole recovery of the labelling in the generated CH<sub>4</sub>, instead of the CO<sub>2</sub>, would then be the result of exclusive acetotrophic methanogenesis, and a ratio of biogas label recovery <sup>14</sup>C-CO<sub>2</sub>/<sup>14</sup>C-CH<sub>4</sub> higher than 1 was considered as a prove for hydrogenotrophy. The approach implemented here was based on the fractionation of naturally occurring carbon isotopes by using unlabelled acetate in the experiments (Conrad et al., 2009), which has the advantage of its cost effectiveness and avoids the handling of often expensive, and sometimes dangerous, labelled substrates. The apparent fractionation factor ( $\alpha_C$ ) as defined by Whiticar and Faber (1986) from the measured CO<sub>2</sub> and CH<sub>4</sub>, and later reviewed by (Conrad et al., 2009) was used. This factor indicates that environments with a  $\alpha_C < 1.055$  are dominated by AMA, while those with a  $\alpha_C > 1.065$  (up to 1.085) point to the predominance of HMA. From the  $\alpha_C$  values calculated in the present study, it can be concluded that increasing

the ammonia content prompted a metabolic shift in methanogenesis from AMA at 1.0 gN-TAN L<sup>-1</sup> to a HMA activity that was predominant at 3.5 gN-TAN L<sup>-1</sup>, and even exclusive at 6.0 gN-TAN L<sup>-1</sup> (Table 4.1). Concurrent predominance of the hydrogenotrophic pathway with the consumption of acetate (added as the sole VFA and electron source in the present study), strongly supports the hypothesis that biomass from the studied anaerobic digester contained SAO species that are active under relatively high ammonia content.

### 4.3.3 Microbial community analysis

#### 4.3.3.1. Quantitative expression profile of selected functional genes

The effect of ammonia on the expression ratio (qPCR quantification of transcripts versus gene copies) of specific functional genes from bacteria (16S rRNA) and methanogenic archaea (*mcrA*) was consistent with the previously observed profiles of acetate consumption and CH<sub>4</sub> generation (Figure 4.1). The bacterial 16S rRNA expression ratio increased in time, reaching a maximum value at around day 11 that was maintained until the end of incubations at day 17 (Figure 4.2a). This maximum expression ratio was a 30% and a 70% lower at 3.5 gN-TAN L<sup>-1</sup> and 6.0 gN-TAN L<sup>-1</sup>, in relation that of 1.0 gN-TAN L<sup>-1</sup>. Despite the fact that the expression of ribosomal genes must be regarded as a global metabolic indicator for all bacteria, and so it cannot univocally be associated to the acetotrophic activity, it might partly explain the reduction in rAc that occurred at high ammonia concentrations (Table 4.1).

For the archaea, instead, a much more specific gene directly related to methanogenesis was targeted. The expression ratio of *mcrA* genes at low and intermediate ammonia concentrations (1.0 – 3.5 gN-TAN L<sup>-1</sup>) was very similar (Figure 4.2b). The observed values were rather low during the first 5 days of incubation but they sharply peaked at around day 11, to decrease again at day 17. Such unimodal profile fits the observed lag-phase in CH<sub>4</sub> production of approximately 6 days (Table 4.1) and the exponential phase in CH<sub>4</sub> accumulation that followed, before the declining phase that started shortly after day 11 (Figure 4.1). Incubations with the highest ammonia concentration (6.0 gN-TAN L<sup>-1</sup>) resulted in expression ratio that was lower than those at low and intermediate ammonia exposure (Figure 4.2b). As discussed previously, these batches showed the longest lag-phases and lowest rCH<sub>4</sub> production, but similar CH<sub>4</sub> yields were eventually achieved (Table 4.1).

**Table 4. 1** Acetate consumption ( $r_{Ac}$ ) and methane production ( $r_{CH_4}$ ) specific rates, lag phase, methane yield and the apparent fractionation factor ( $\alpha_C$ ). Depicted values correspond to the average and standard deviation of three independent replicates.

TAN (gN L <sup>-1</sup> )	$r_{Ac}$ (mgCOD gVSS <sup>-1</sup> d <sup>-1</sup> )	$r_{CH_4}^a$ (mgCOD gVSS <sup>-1</sup> d <sup>-1</sup> )	Lag phase (d) <sup>a</sup>	Methane yield (mLCH <sub>4</sub> gCOD <sup>-1</sup> )	$\alpha_C$	Predominant methanogenic pathway <sup>b</sup>
1	16.80±0.42	13.61±0.25	6.37±0.15	238.41±9.76	1.054±0.017	Acetotrophic
3.5	16.93±0.35	12.71±0.26	6.28±0.13	245.63±13.54	1.077±0.001	Hydrogenotrophic
6	9.10±0.35	9.86±0.02	10.17±0.10	251.15±2.21	1.080±0.000	Exclusively hydrogenotrophic

**Table 4. 2** Estimators of microbial species diversity/richness based on NGS of 16S rRNA genes and transcripts from the Bacteria and Archaea domains, obtained from the initial inoculum and after its incubation during 11 and 17 days under increasing TAN content.

Parameter	Microbial group	Inoculum	1.0 g N-TAN L <sup>-1</sup>	
			Genes	Transcripts
No. of reads	Bacteria	217,432	85,745	53,318
	Archaea	193,179	54,798	134,018
No. of OTU <sup>a</sup>	Bacteria	4,720	3,241	2,032
	Archaea	373	282	183
Coverage <sup>b</sup> (%)	Bacteria	99.42	99.90	99.87
	Archaea	99.97	99.89	99.96
Shannon (diversity)	Bacteria	4.05	3.89	4.30
	Archaea	2.72	2.39	1.48
Simpson (diversity)	Bacteria	8.76	7.66	24.03
	Archaea	8.02	6.73	2.80
Chao1 (richness) <sup>c</sup>	Bacteria	5,592 (64)	5,047 (127)	3,364 (116)
	Archaea	414 (14)	362 (25)	258 (28)
Predominant genera (% relative abundance)	Bacteria	<i>Longilinea</i> (36) <i>Clostridium</i> (10) <i>Bacteroides</i> (9) <i>Leptolinea</i> (7)	<i>Longilinea</i> (39) <i>Leptolinea</i> (11) <i>Clostridium</i> (9) <i>Bacteroides</i> (6)	<i>Alkaliphilus</i> (13) <i>Sphingobacterium</i> (11) <i>Leptolinea</i> (9) <i>Levilinea</i> (6)
	Archaea	<i>Methanoculleus</i> (31) <i>Methanobrevibacter</i> (26) <i>Methanosarcina</i> (17) <i>Methanosaeta</i> (9)	<i>Methanoculleus</i> (40) <i>Methanosarcina</i> (17) <i>Methanosaeta</i> (15) <i>Methanomassiliococcus</i> (9)	<i>Methanosaeta</i> (53) <i>Methanoculleus</i> (33) <i>Methanomassiliococcus</i> (8)

**Table 4.1** Estimators of microbial species diversity/richness based on NGS of 16S rRNA genes and transcripts from the Bacteria and Archaea domains, obtained from the initial inoculum and after its incubation during 11 and 17 days under increasing TAN content.( Continuation from previous page)

Parameter	Microbial group	3.5 g N-TAN L <sup>-1</sup>		6.0 g N-TAN L <sup>-1</sup>	
		Genes	Transcripts	Genes	Transcripts
No. of reads	Bacteria	68,355	112,479	69,224	58,836
	Archaea	68,513	141,590	84,996	168,908
No. of OTU <sup>a</sup>	Bacteria	3,110	3,514	3,105	2538
	Archaea	325	185	211	201
Coverage <sup>b</sup> (%)	Bacteria	99.85	99.92	99.88	99.85
	Archaea	99.92	99.96	99.92	99.97
Shannon (diversity)	Bacteria	4.02	4.64	3.92	4.62
	Archaea	2.37	1.52	2.13	1.70
Simpson (diversity)	Bacteria	8.21	24.37	7.31	26.68
	Archaea	5.71	3.11	4.93	3.34
Chao1 (richness) <sup>c</sup>	Bacteria	4,927 (126)	4,516 (77)	4,974 (130)	3,760 (99)
	Archaea	383 (17)	272 (33)	338 (44)	243 (16)
mgCOD Predominant genera (% relative abundance)	Bacteria	<i>Longilinea</i> (38) <i>Clostridium</i> (9) <i>Bacteroides</i> (8) <i>Leptolinea</i> (6)	<i>Alkaliphilus</i> (17) <i>Sphingobacterium</i> (11) <i>Leptolinea</i> (6) <i>Pseudomonas</i> (6) <i>Mariniphaga</i> (5)	<i>Longilinea</i> (40) <i>Bacteroides</i> (10) <i>Clostridium</i> (9) <i>Synergistes</i> (5)	<i>Alkaliphilus</i> (17) <i>Leptolinea</i> (8) <i>Pseudomonas</i> (7) <i>Symbiobacterium</i> (6) <i>Levilineaca</i> (5) <i>Mariniphaga</i> (5)
	Archaea	<i>Methanocullens</i> (38) <i>Methanomassiliococcus</i> (22) <i>Methanosarcina</i> (13) <i>Methanosaeata</i> (10)	<i>Methanosaeata</i> (44) <i>Methanocullens</i> (42) <i>Methanomassiliococcus</i> (9)	<i>Methanocullens</i> (41) <i>Methanomassiliococcus</i> ( 28) <i>Methanosarcina</i> (14) <i>Methanobrevibacter</i> (8)	<i>Methanocullens</i> (61) <i>Methanomassiliococcus</i> (24) <i>Methanosaeata</i> (7)

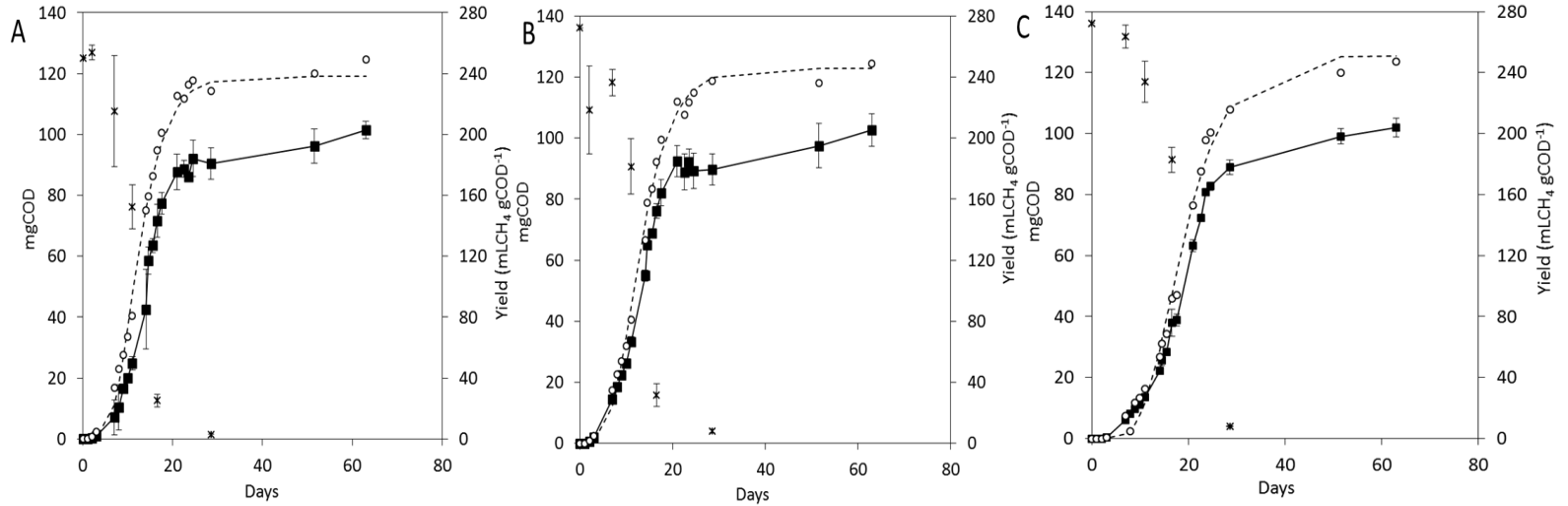


**Figure 4.1** Evolution of acetic acid and CH<sub>4</sub>, as well as CH<sub>4</sub> yield, at different TAN concentration: (A) 1 gN-TAN L<sup>-1</sup>; (B) 3.5 gN-TAN L<sup>-1</sup>; (C) 6 gN-TAN L<sup>-1</sup>. Symbols: Asterisks and squares denote acetic acid and CH<sub>4</sub>, both expressed as mg of COD equivalents; discontinu line and circles denote methane yields obtained with the adjusted Gompertz eq. and experimental data, respectively.

**Table 4. 3** Best match in BLAST searches (GenBank, NCBI, USA) on TAN-responding OTUs (Figure 3). Only OTUs with a relative abundance in the original methanogenic biomass higher than 1% are listed.

OTU	Identification <sup>a</sup>	Abundance (%)	Accession nr	H (%)	Source
1	<i>Longilinea</i>	30.31	JQ155218	99	Undefined full-scale anaerobic digester
2	<i>Leptolinea</i>	7.97	JQ104843	95	Undefined full-scale anaerobic digester
3	<i>Bacteroides</i>	7.67	GQ134121	99	Mesophilic anaerobic SBR treating swine waste (4.9 g N-TAN L <sup>-1</sup> )
6	<i>Levilinea saccharolytica</i>	1.15	EU407212	99	Household anaerobic digester
7	<i>Clostridium</i>	3.31	GQ995170	96	Mesophilic lab-scale anaerobic digester treating food industrial waste
12	<i>Acetovibrio</i>	1.45	GQ995163	99	Mesophilic lab-scale reactor treating food industrial waste
16	<i>Clostridium</i>	1.71	LN849648	99	Mesophilic lab-scale anaerobic digester reactor treating poultry manure
17	<i>Acholeplasma</i>	1.00	JN998160	99	Ammonium-stressed lab scale anaerobic digester
18	<i>Synergistes</i>	2.03	GQ134214	92	Mesophilic anaerobic SBR treating swine waste (1.0 g N-TAN L <sup>-1</sup> )

**Table 4.3** Best match in BLAST searches (GenBank, NCBI, USA) on TAN-responding OTUs (Figure 3). Only OTUs with a relative abundance in the original methanogenic biomass higher than 1% are listed. (Continuation from previous page)

OTU	Identification <sup>a</sup>	Abundance (%)	Accession nr	H (%)	Source
22	<i>Sterolibacterium denitrificans</i>	2.06	HM149064	92	Microbial fuel cell treating dairy wastewater
23	<i>Longilinea</i>	1.18	JQ104456	99	Undefined full-scale anaerobic digester
31	<i>Clostridium</i>	1.14	GQ136858	99	Mesophilic anaerobic SBR treating swine waste (5.2 g N-TAN L <sup>-1</sup> )
36	<i>Bacillus</i>	1.62	HQ183753	99	Undefined leachate sediment
2873	<i>Longilinea</i>	1.63	CU922827	98	Mesophilic anaerobic digester treating municipal wastewater sludge

<sup>a</sup> According to the GreenGenes database.



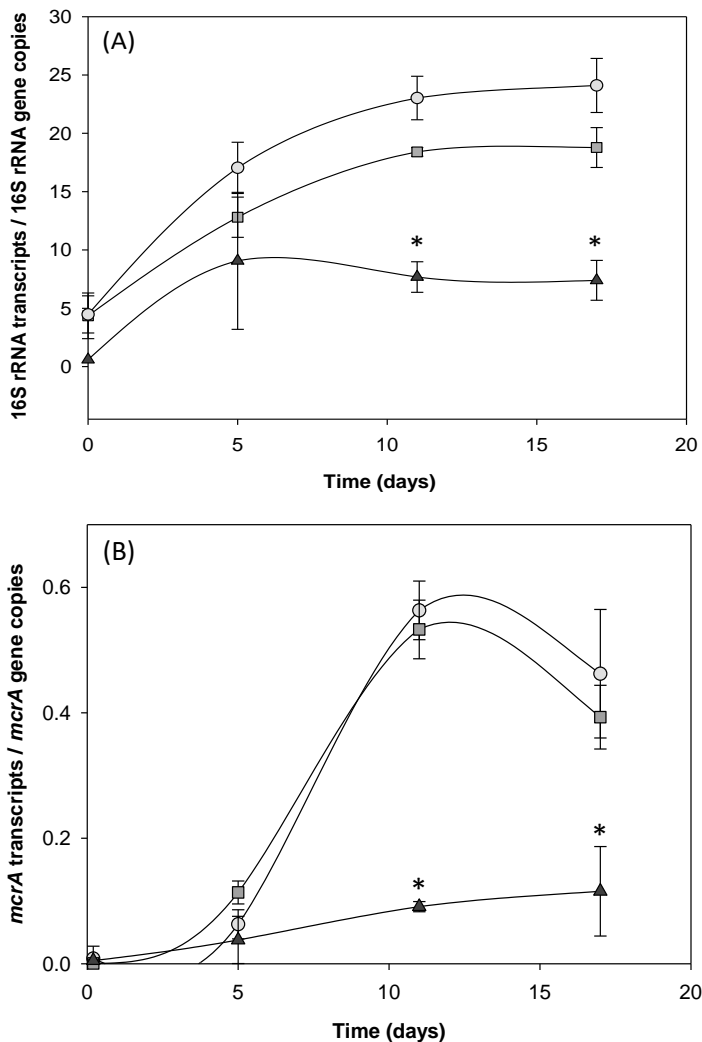


**Figure 4. 2** Time-course quantitative PCR results from biomass samples of three independent batches incubated at 1.0, 3.5, and 6.0 gN-TAN L-1 (squares, circles, and triangles). The average (signs) and standard deviation (bars) of the ratio between number of transcripts and gene copies for the bacterial 16S rRNA (A) and the archaeal *mcrA* (B) has been depicted. Statistical significance in pairwise comparisons ( $n=3$ ,  $p<0.05$ ) in relation to the lowest ammonia exposure have been highlighted with an asterisk.

#### 4.3.2.2. Bacterial community structure and response to ammonia exposure

The microbial community structure from the most active period during the batch activity assays was assessed by high throughput DNA sequencing. A total reads of 440,756 and 224,133 high quality 16S rRNA ribosomal genes and transcripts (cDNA) were obtained for the Bacteria. These reads were grouped into operational taxonomic units (OTU, defined at 97% sequence homology cut-off) and confidently assigned to specific taxa (Table 5.2). The Good's coverage estimator on the percentage of the total species (as OTU) represented at any given sample was above 99%, indicating that the observed bacterial species encompassed most of the samples' populations. Species biodiversity (Shannon and inverted Simpson indexes) and richness (Chao1) were rather similar among samples, with an estimated number of species in the original inoculum of 5,592. Species richness in active bacterial populations (cDNA ribotype libraries) was always lower than that corresponding to the present species (DNA ribotype libraries), but the biodiversity of the active population increased upon ammonia exposure. This indicates that most, yet not all, species from the inoculum were metabolically active under the tested conditions, but ammonia triggered the response of a more complex bacterial community

The bacterial community structure, based on 16S rRNA gene counts, remained relatively stable during all assays regardless of the TAN concentration (Figure 4.3). Representatives of the order Anaerolineales were predominant, with a relative abundance (RA) of more than 40% in all assays. Other important groups included members of the orders *Clostridiales* (16%) and *Bacteroidales* (9–12%), the former being particularly relevant as it encompasses most of the recently described SAOB. A previous metagenomic study (Ruiz-Sánchez et al., 2018) suggested that members of phyla *Bacteroidetes*, along with *Chloroflexi*, might encompass yet undescribed SAOB. In contrast with this rather stable microbial community structure, significant differences were observed in the active community when exposed to increasing ammonia concentrations. Members of the *Clostridiales* (22–26% RA) and *Anaerolineales* (14–20% RA) were among the most metabolically active communities (in terms of ribosomal transcripts). Other relevant active groups were *Bacteroidales* (9–12% RA), *Burkholderiales* (5–8% RA), *Pseudomonadales* (5–7% RA) and *Planctomycetales* (3% RA). In contrast to these groups, which displayed little sensitivity to ammonia, Sphingobacteriales showed a clear negative correlation with the concentration of ammonia, so that their relative expression level decreased from 15% to 1% upon an ammonia supplementation from 1.0 to 6.0 gN-TAN L<sup>-1</sup>.

The highest expression shift along with increasing TAN concentrations was observed for a number of OTUs related to the genera *Thioalkalispira*, *Clostridium*, *Bellilinea*, *Longilinea*, *Bacteroides* and *Acetovibrio*; while representatives of the genera *Natronoanaerobium*, *Sphingobacterium*, and *Synergistes* appeared to be inhibited at 6.0 gN-TAN L<sup>-1</sup> (Figure 4.4). Individual BLAST searches from the sequences of the “ammonia-philic” OTUs yielded uncultured bacteria from a variety of anaerobic digesters that might have been exposed to relatively high ammonia levels (Table 4.3). Of particular interest is OTU 1, which appears to be somewhat related to the genus *Longilinea* (94% sequence homology) and was by far the most abundant ammonia-responding OTU (30% in RA of expressed ribosomal transcripts). The second most active species (OTU 2, 8% in RA), also belonged to the class *Anaerolineae* (*Chloroflexi*), and displayed its highest similarity to a member of the genus *Leptolinea* (88% sequence homology). Four additional OTUs affiliated within the same class (genera *Levilinea* and *Bellilinea*) also increased their relative activity in the presence of ammonia, but their abundance was significantly lower. The class *Anaerolineae* was described in order to accommodate four new isolates originating from mesophilic UASB reactors (*Levilinea saccharolytica* and *Leptolinea tardivitalis*) (Yamada et al., 2006), a rice paddy soil (*Longilinea arvoryzae*), and a thermophilic digester (*Bellilinea caldifistulae*) (Yamada et al., 2007). They have relatively prolonged doubling times (45 – 92 h) and differ in their optimal temperature for growth, which could explain the low occurrence of the thermophilic *Bellilinea* in the mesophilic reactor. Interestingly, *Longilinea* and *Bellilinea* share the fact that growth is enhanced in co-cultivation with hydrogenotrophic methanogens. Nevertheless, neither H<sub>2</sub>/CO<sub>2</sub> nor acetate served as sole carbon sources for growth in pure cultures, so that their potential role as SAOB might be put into question.

A ribotype distantly related to *Bacteroides* (OTU 3) could also have played a relevant role in the anaerobic digestion of nitrogen-rich substrates, given its relatively high expression level (8% RA of ribosomal transcripts). Despite poor phylogenetic definition, OTU 3 exhibits a relatively high sequence similarity to several uncultured bacteria from anaerobic digesters, including an anaerobic SBR treating swine waste at 4.9 g N-TAN L<sup>-1</sup> (Angenent et al., 2002). A number of unidentified clostridia (OTUs 7, 16, and 31) with a significant presence in the methanogenic biomass (>1%) increased their relative expression under high TAN concentrations, and revealed high sequence similarity with ribotypes previously reported in other ammonia-rich anaerobic digesters. It could thus well be that some of the above mentioned OTUs correspond to yet undescribed SAOB.

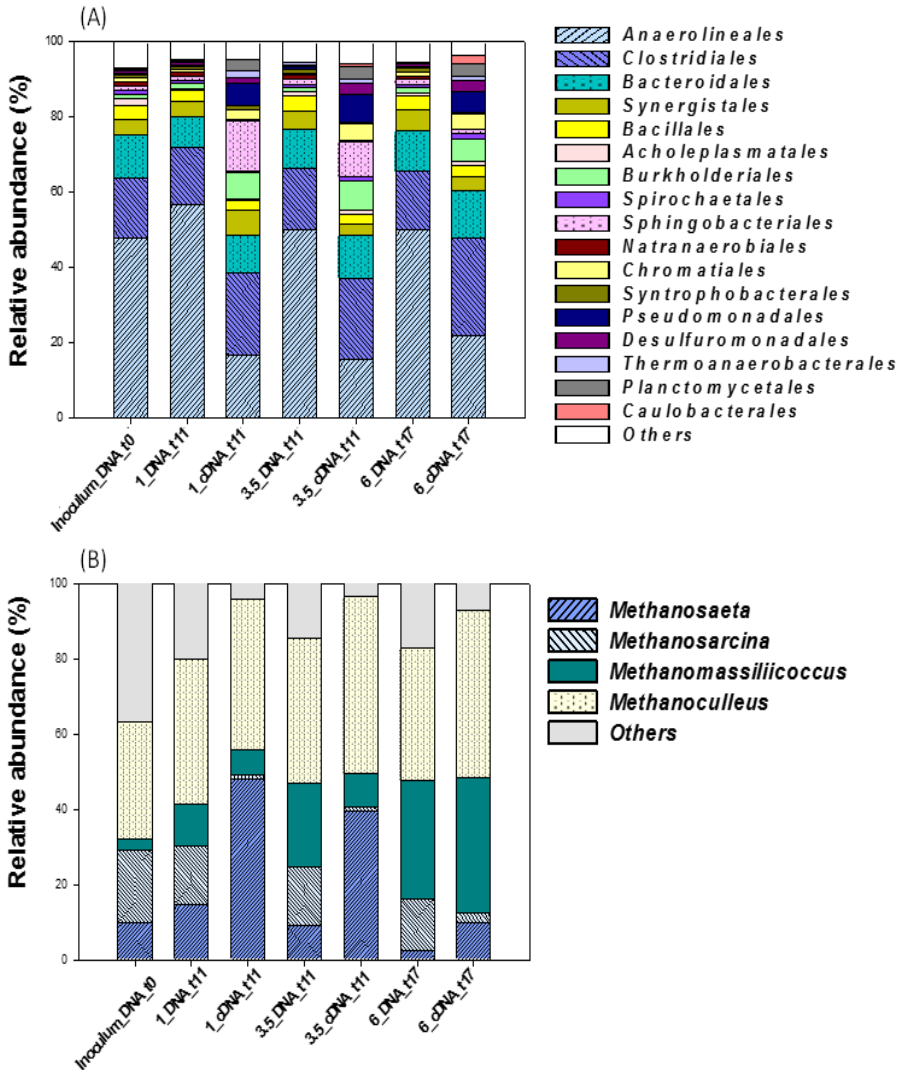


**Figure 4.3** Relative abundance of bacterial (A) and archaeal (B) ribotypes at the order and genus phylogenetic level, respectively, in terms of 16S rRNA gene and transcript counts. Each bar chart represents the median of two independent duplicates. 1g, 3.5g, 6g TAN

The high throughput sequencing data from this study was mined for the presence of well-known SAOB (Fotidis et al., 2013). OTUs homologous to the thermotolerant/thermophilic *Tepidanaerobacter acetatoxydans* and *Thermacetogenium phaeum* were detected, but in very low abundance and only in certain samples. Therefore, these particular thermophilic species played a minor role in the studied mesophilic reactor. Nevertheless, the proven hydrogenotrophy at relatively high TAN levels and the absence of acetate accumulation, suggested that other non-described mesophilic SAO microbial communities must be active in the biomass.

#### 4.3.2.3. Archaeal community structure and response to ammonia exposure

High throughput DNA sequencing of the Archaea yielded 401,486 genes and 444,516 transcript reads. As with the bacteria, the Good's coverage estimator for the archaea was above 99%, but the Chao1 estimator was one order of magnitude lower, with a predicted 414 archaeal species in the original inoculum. Both the biodiversity and number of active archaea were always lower than those corresponding to the present species (DNA ribotype libraries) so that, contrary to the bacteria, an increasing ammonia exposure generated a less diversified response of the archaeal community.

A significant community shift in response to increasing ammonia concentrations (Table 4.2, Figure 4.3). The trend observed here for the methanogenic archaea, with a shift from AMA to HMA, is consistent with that reported for other anaerobic digesters under increasing TAN/FAN concentrations (Wang et al., 2015). The original methanogenic biomass (inoculum) was primarily composed by strict hydrogenotrophic orders, such as *Methanomicrobiales* (32% RA) and *Methanobacteriales* (26% RA), but also the metabolically versatile *Methanosarcinales* (29% RA), which encompasses both hydrogenotrophic and acetotrophic species. The novel methanoarchaeal order *Methanomassiliicoccales* was also present at a lower, yet relevant, abundance (<6%). This order has commonly been found in the gut of animals (Söllinger et al., 2016) but is also widely distributed in landfills, rice fields, marine thermal vents and in fresh water (Li et al. 2016). The order *Methanomassiliicoccales* encompasses the former, recently reclassified, order *Thermoplasmatales* (Adam et al., 2017; Borrel et al., 2014).

The microbial community profiles of active archaea were rather similar at 1.0 and 3.5 gN-TAN L<sup>-1</sup>, with representatives of the *Methanosarcinales* and *Methanomicrobiales* orders as the most active species (Figure 5.3). In particular, species in *Methanosaeta*, an obligate acetoclastic methanogenic genus, were the most active (>40% RA of ribosomal transcripts) at 1.0 and 3.5 gN-TAN L<sup>-1</sup>. At

6.0 gN-TAN L<sup>-1</sup>, though, representatives of the *Methanomicrobiales*, primarily in the genus *Methanoculleus*, were more active than those from the *Methanosarcinales* (61% versus 11% RA of ribosomal transcripts), indicating that hydrogenotrophy had become the predominant methanogenic process. This finding is in agreement with the direct relationship between hydrogenotrophy and ammonia content, observed previously from the isotopic fractionation profiles (Table 4.1). *Methanoculleus* spp. might have become the main hydrogenotrophic syntrophic SAOB partner because of its H<sub>2</sub> high affinity, but also because the related amino acid auxotrophies that govern interspecies interactions in syntrophic communities (Embree et al., 2015).

Interestingly, a comparatively high expression level was observed at the highest ammonia content for the *Methanomassiliicoccales* (36% RA) in detriment of *Methanosarcinales*, which includes both *Methanosarcina* spp. and *Methanosaeta* spp. (Figure 4.3). Species from the *Methanomassiliicoccales* have recently been found in various anaerobic environments and have become a research subject due to their scarcely known biology (Ziganshin et al., 2016). This order is characterized by the presence of quaternary ammonium efflux pumps (Borrel et al., 2014), which might explain its higher expression level under high ammonia concentrations. Yet, there might be other metabolic specificities that could play a relevant role as well. Species in the *Methanomassiliicoccales* lack the methyl-branch of the archaeal type Wood–Ljungdahl pathway and the coenzyme M methyltransferase (MTR) complex and, therefore, are methyl-dependent hydrogenotrophic methanogens in which the energy conservation process is not fully understood (Adam et al., 2017). It seems, though, that methanogenesis is performed by methyltransferases that contain the rare amino acid pyrrolisine, allowing the transfer of methyl-groups from methanol, methylated-amines, and dimethyl sulfide to Coenzim M (H-S-CoM) (Nordgård, 2017). In a recent genomic analysis (Lang et al., 2015), it has been proposed that *Methanomassiliicoccales* are capable of heterotrophic growth on acetate and of synthesizing acetyl-CoA from this substrate, but also from formate and CO<sub>2</sub>. These findings would agree with the previous identification of a new uncultured archaeon belonging to this order from a metagenomic characterization of an anaerobic digester, which harboured genes of the acetyl-CoA pathway (Campanaro et al., 2016). This archaeon also possessed the *fhdA* gene encoding a glutathione-dependent formaldehyde dehydrogenase to formate. It also lacks the archaeal-type CO dehydrogenase cluster (CODH) encoded by *cdhA* but has a (near-) complete bacterial-type CODH encoded by *cooS* (Adam et al., 2018), which is used by aerobic and anaerobic carboxyotrophs to oxidize CO to CO<sub>2</sub> and generate electrons (Brady et al., 2015).

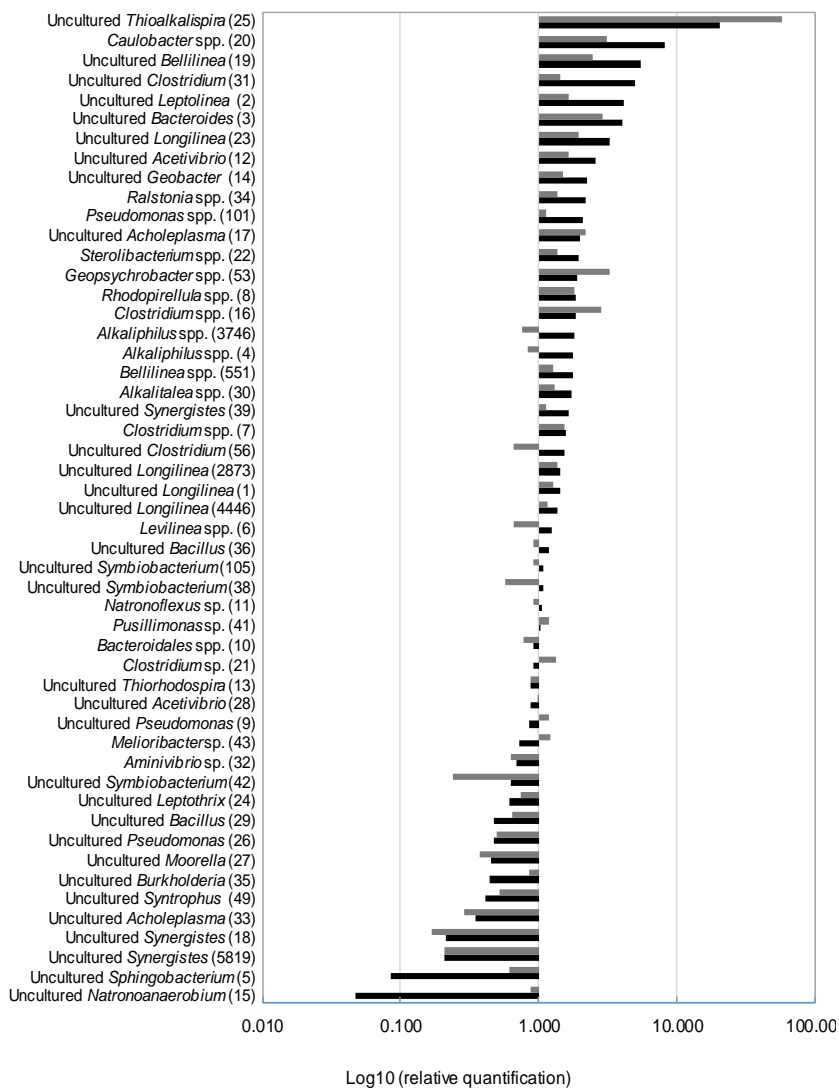


**Figure 4.4** Ratio between the relative expression level of bacterial 16S rRNA transcripts obtained in batch at 3.5 gN-TAN L<sup>-1</sup> (grey bar) and 6 gN-TAN L<sup>-1</sup> (black bar), in relation to that at 1gTAN. Only the species with a RA higher than 0.3% are considered.

This phenomenon was probably the result of a horizontal gene transfer event that may have had an important impact on the evolution of this archaeal lineage (Spang et al., 2017). For the *Methanomicrobiales* and the *Methanomassiliococcales*, these enzymes are only able to function in the oxidative direction due to their inability of carbon fixation

Hence, considering the relevance of the predominant OTUs affiliated to *Methanomassiliococcales* from the present study, an in silico assessment with different databases (RDP, GreenGenes and BLAST) in relation to other 16S rRNA sequences related to *Methanomassiliococcales*. As a result, the affiliation of OTU4 to the *Methanomassiliococcales* and, more specifically, to the genus *Methanomassiliococcus* was confirmed.

#### 4.4 Conclusion

An interdisciplinary approach was applied to better understand the functional aspects of methanogenic microbial communities in relation to an increasing ammonia exposure. Biomass from a full-scale anaerobic digester adapted to relatively high ammonia concentrations displayed a swift change from acetotrophic to hydrogenotrophic methanogenesis upon increasing ammonia levels, as revealed by biogas isotopic fractionation profiles and by molecular analysis of active microbial species in laboratory batch assays. The biological activity was negatively affected by ammonia, both in terms of methane production and acetate consumption rates. Such tendency was also verified in relation to a decreasing expression level of relevant functional genes for the Bacteria and the Archaea, but a similar methane yield was eventually achieved with all tested nitrogen conditions.

In contrast to the microbial community structure, which remained relatively stable during the experiments, significant changes in the active bacterial and archaeal populations were observed in relation to ammonia exposure. Despite the evidences for the occurrence of the SAO process observed under high ammonia concentrations (hydrogenotrophy and lack of acetate accumulation), none of the SAOB that are currently known from the literature, which primarily belong to the order *Clostridiales*, played a significant role in the studied biomass. In an earlier study with this reactor based on a metagenomics characterization of its biomass, we already suggested that new yet undescribed SAOB belonging to the *Chloroflexi* and *Bacteroidales* might be in play (Ruiz-Sánchez et al., 2018). Here we have found a variety of bacterial species (often uncultured) related to these taxa that were



stimulated upon ammonia exposure and, therefore, must be considered as potential SAOB.

While strict acetotrophic methanogens from the genus *Methanosaeta* (*Methanosarcinales*) were the most active under low ammonia concentrations, representatives of the predominantly hydrogenotrophic genus *Methanoculleus* (*Methanomicrobiales*) were the most active under high ammonia exposure. Species in this genus have recurrently been described as syntrophic partners for the SAOB (Frank et al., 2016; Ruiz-Sánchez et al., 2018). Such HMA-SAOB association could be explained by the fact that *Methanoculleus* are particularly competitive at relatively low hydrogen availability and, therefore, might be better adapted when bacterial metabolic rates are limited by the presence of ammonia (Neubeck et al., 2016). We have also highlighted the importance of species from the *Methanomassiliicoccales* order as syntrophic methanogenic partners

In summary, our results indicate that methanogenic biomass adapted to a relatively high ammonia content can rather easily change its metabolic routes in response to the concentration of ammonia. Such functional plasticity is determined by the activation of specific populations from a biodiverse microbial community.

## 4.5 References

- American Public Health Association (APHA) (2005) Standard method for examination of water and wastewater, 21st edn. APHA, AWWA, WPCF, Washington
- Adam PS, Borrel G, Brochier-Armanet C, Gribaldo S. 2017. The growing tree of Archaea: New perspectives on their diversity, evolution and ecology. ISME J.
- Adam PS, Borrel G, Gribaldo S. 2018. Evolutionary history of carbon monoxide dehydrogenase/acetyl-CoA synthase, one of the oldest enzymatic complexes. Proc. Natl. Acad. Sci.:201716667.
- Angenent LT, Sung S, Raskin L. 2002. Methanogenic population dynamics during startup of a full-scale anaerobic sequencing batch reactor treating swine waste. Water Res. 36:4648–4654.
- Banks CJ, Zhang Y, Jiang Y, Heaven S. 2012. Trace element requirements for stable food waste digestion at elevated ammonia concentrations. Bioresour. Technol. 104:127–135.
- Borrel G, Parisot N, Harris HMB, Peyretailade E, Gaci N, Tottey W, Bardot O, Raymann K, Gribaldo S, Peyret P, O’Toole PW, Bruge`re JF. 2014. Comparative genomics highlights the unique biology of *Methanomassiliicoccales*, a Thermoplasmatales-related seventh order of methanogenic archaea that encodes pyrrolysine. BMC Genomics 15.
- Brady AL, Sharp CE, Grasby SE, Dunfield PF. 2015. Anaerobic carboxydrotrophic bacteria in geothermal springs identified using stable isotope probing. Front. Microbiol. 6.

- Campanaro S, Treu L, Kougias PG, De Francisci D, Valle G, Angelidaki I. 2016. Metagenomic analysis and functional characterization of the biogas microbiome using high throughput shotgun sequencing and a novel binning strategy. *Biotechnol. Biofuels* 9:26.
- Conrad R. 2005. Quantification of methanogenic pathways using stable carbon isotopic signatures: A review and a proposal. *Org. Geochem.* 36:739–752.
- Conrad R, Claus P, Casper P. 2009. Characterization of stable isotope fractionation during methane production in the sediment of a eutrophic lake, Lake Dagow, Germany. *Limnol. Oceanogr.* 54:457–471.
- Demirel B, Scherer P. 2008. The roles of acetotrophic and hydrogenotrophic methanogens during anaerobic conversion of biomass to methane: A review. *Rev. Environ. Sci. Biotechnol.* 7:173–190.
- Embree M, Liu JK, Al-Bassam MM, Zengler K. 2015. Networks of energetic and metabolic interactions define dynamics in microbial communities. *Proc. Natl. Acad. Sci.* 112:15450–15455.
- Fotidis IA, Karakashev D, Angelidaki I. 2013. Bioaugmentation with an acetate-oxidising consortium as a tool to tackle ammonia inhibition of anaerobic digestion. *Bioresour. Technol.* 146:57–62.
- Frank JA, Arntzen MØ, Sun L, Hagen LH, McHardy AC, Horn SJ, Eijsink VGH, Schnürer A, Pope PB. 2016. Novel Syntrophic Populations Dominate an Ammonia-Tolerant Methanogenic Microbiome. *mSystems* 1:e00092-16.
- Hao L, Lü F, Mazéas L, Desmond-Le Quéméner E, Madigou C, Guenne A, Shao L, Bouchez T, He P. 2015. Stable isotope probing of acetate fed anaerobic batch incubations shows a partial resistance of acetoclastic methanogenesis catalyzed by Methanosarcina to sudden increase of ammonia level. *Water Res.* 69:90–99.
- Hattori S. 2008. Syntrophic acetate-oxidizing microbes in methanogenic environments. *Microbes Environ.* 23:118–127.
- Hunik JH, Hamelers HVM, Koster IW. 1990. Growth-rate inhibition of acetoclastic methanogens by ammonia and pH in poultry manure digestion. *Biol. Wastes* 32:285–297.
- Karakashev D, Batstone DJ, Trably E, Angelidaki I. 2006. Acetate oxidation is the dominant methanogenic pathway from acetate in the absence of Methanoacetaceae. *Appl. Environ. Microbiol.* 72:5138–5141.
- Lang K, Schuldes J, Klingl A, Poehlein A, Daniel R, Brune A. 2015. New mode of energy metabolism in the seventh order of methanogens as revealed by comparative genome analysis of “*Candidatus Methanoplasma termitum*.” *Appl. Environ. Microbiol.* 81:1338–1352.
- Lettinga G. 2010. Challenges of a feasible route towards sustainability in environmental protection. *Front. Environ. Sci. Eng. China* 4:123–134.
- Mulat DG, Ward AJ, Adamsen APS, Voigt NV, Nielsen JL, Feilberg A. 2014. Quantifying contribution of syntrophic acetate oxidation to methane production in thermophilic anaerobic reactors by membrane inlet mass spectrometry. *Environ. Sci. Technol.* 48:2505–2511.
- Neubeck A, Sjöberg S, Price A, Callac N, Schnürer A. 2016. Effect of nickel levels on hydrogen partial pressure and methane production in methanogens. *PLoS One* 11.
- Pelissari C, Guivernau M, Viñas M, de Souza SS, García J, Sezerino PH, Ávila C. 2017. Unraveling the active microbial populations involved in nitrogen utilization in a vertical subsurface flow constructed wetland treating urban wastewater. *Sci. Total Environ.* 584–585:642–650.

- Penning H, Conrad R. 2007. Quantification of carbon flow from stable isotope fractionation in rice field soils with different organic matter content. *Org. Geochem.* 38:2058–2069.
- Petersen SP, Ahring BK. 1991. Acetate Oxidation in A Thermophilic Anaerobic Sewage-Sludge Digester - the Importance of Non-Aceticlastic Methanogenesis from Acetate. *Fems Microbiol. Ecol.* 86:149–157.
- Prenafeta-Boldú FX, Rojo N, Gallastegui G, Guivernau M, Viñas M, Elías A. 2014. Role of Thiobacillus thioparus in the biodegradation of carbon disulfide in a biofilter packed with a recycled organic pelletized material. *Biodegradation* 25:557–568.
- Ruiz-Sánchez J, Campanaro S, Guivernau M, Fernández B, Prenafeta-Boldú FX. 2018. Effect of ammonia on the active microbiome and metagenome from stable full-scale digesters. *Bioresour. Technol.* 250:513–522.
- Schnürer A, Nordberg A. 2008. Ammonia, a selective agent for methane production by syntrophic acetate oxidation at mesophilic temperature. *Water Sci. Technol.* 57:735–740.
- Schnürer A, Zellner G, Svensson BH. 1999. Mesophilic syntrophic acetate oxidation during methane formation in biogas reactors. *FEMS Microbiol. Ecol.* 29:249–261.
- Söllinger A, Schwab C, Weinmaier T, Loy A, Tveit AT, Schleper C, Urich T. 2016. Phylogenetic and genomic analysis of Methanomassiliococcales in wetlands and animal intestinal tracts reveals clade-specific habitat preferences. *FEMS Microbiol. Ecol.* 92.
- Sotres A, Díaz-Marcos J, Guivernau M, Illa J, Magrí A, Prenafeta-Boldú FX, Bonmatí A, Viñas M. 2014. Microbial community dynamics in two-chambered microbial fuel cells: Effect of different ion exchange membranes. *J. Chem. Technol. Biotechnol.* n/a-n/a.
- Spang A, Caceres EF, Ettema TJG. 2017. Genomic exploration of the diversity, ecology, and evolution of the archaeal domain of life. *Science* (80-).
- Sun L, Müller B, Westerholm M, Schnürer A. 2014. Syntrophic acetate oxidation in industrial CSTR biogas digesters. *J. Biotechnol.* 171:39–44.
- Wang H, Fotidis IA, Angelidaki I. 2015. Ammonia effect on hydrogenotrophic methanogens and syntrophic acetate-oxidizing bacteria. *FEMS Microbiol. Ecol.* 91.
- Whiticar MJ, Faber E. 1986. Methane oxidation in sediment and water column environments-Isotope evidence. *Org. Geochem.* 10:759–768.
- Yamada T, Imachi H, Ohashi A, Harada H, Hanada S, Kamagata Y, Sekiguchi Y. 2007. *Bellilinea caldifistulae* gen. nov., sp. nov and *Longilinea arvoryzae* gen. nov., sp. nov., strictly anaerobic, filamentous bacteria of the phylum Chloroflexi isolated from methanogenic propionate-degrading consortia. *Int. J. Syst. Evol. Microbiol.* 57:2299–2306.
- Yamada T, Sekiguchi Y, Hanada S, Imachi H, Ohashi A, Harada H, Kamagata Y. 2006. *Anaerolinea thermolimosa* sp. nov., *Levilinea saccharolytica* gen. nov., sp. nov. and *Leptolinea tardivitalis* gen. nov., sp. nov., novel filamentous anaerobes, and description of the new classes *Anaerolineae* classis nov. and *Caldilineae* classis nov. in the . *Int. J. Syst. Evol. Microbiol.* 56:1331–1340.
- Yenigün O, Demirel B. 2013. Ammonia inhibition in anaerobic digestion: A review. *Process Biochem.* 48:901–911.
- Ziganshin AM, Ziganshina EE, Kleinstuber S, Nikolausz M. 2016. Comparative analysis of methanogenic communities in different laboratory-scale anaerobic digesters. *Archaea* 2016.

## Chapter 5 Effect of ammonia on the active microbiome and metagenome and from stable full-scale digesters

---

Metagenomic analysis and characterization of the ribosomal transcriptome were performed on the biomass of four full scale biogas reactors (two operated at a high ammonia concentration, in relation to other two that had a relatively low concentration). About 13 Gbp of metagenomics sequence data were obtained through Illumina HiSeq sequencing. More than half a million of protein-encoding genes and 73 population genomes (PG) were extracted by applying a combination of two binning processes. The obtained results evidenced the lack of knowledge about the core biogas microbiome and metabolic pathways regarding syntrophic acetate oxidation process, since the vast majority of 73 PG have not been identified previously as microbial species playing a significant role in ammonia-rich bioreactors. Furthermore, a functional genetic analysis provided a global overview of the metabolic aspects, and revealed the expression of key genes related with acetate metabolism and nitrogen stress.

*Part of this chapter was presented as a poster communication in AD15 Beijing conference.*

*This chapter was published as: Ruiz-Sánchez J, Campanaro S, Guivernau M, Fernández B, Prenafeta-Boldú FX. Effect of ammonia on the active microbiome and metagenome from stable full-scale digesters. *Bioresour Technol.* 2018 Feb;250 513-522. doi:10.1016/j.biortech.2017.11.068.*

## 5.1 Introduction

The anaerobic digestion (AD) of organic materials is a well-consolidated process for the treatment and revalorization of organic waste into biogas, a renewable energy source, and digestate that can be used as biofertilizer. This technology contributes significantly to the sustainability of industrial processes (Watson-Craik and Stams, 1995) but it also has some limitations that might hinder its full applicability. A high nitrogen content in organic wastes poses one of the major drawbacks to the AD process (Braun et al., 1981) as nitrogen contained in biopolymers (i.e. proteins, nucleic acids, etc.) will largely be converted into ammonia during the anaerobic digestion process. It is well known that in the ammonium/ammonia chemical equilibrium, the second species has a significant negative effect on microorganisms due to its easy membrane crossing (Hansen et al., 1998). Once in the cytoplasm, it causes pH shifts that result in the inhibition of enzymes involved in fundamental biochemical reactions (Fotidis et al., 2014). This negative effect is particularly marked for the acetotrophic methanogenic archaea (AMA) (Fotidis et al., 2013b). Hence, feeding the digester with nitrogen-rich organic materials, such as animal dejections, slaughterhouse wastes, and residues from the food industry, often results in unstable reactor performance and operational failure in full-scale anaerobic digesters.

Several strategies to overcome the problem of ammonia inhibition in AD have been reported and reviewed in the literature (Yenigün and Demirel, 2013). Most of the proposed solutions are based on modified reactor configurations to control the concentration of ammonia (Kayhanian, 1994). However, alternative methods have also been developed, such as the enrichment of the methanogenic biomass with ammonia-resistant microbes (Fotidis et al., 2013a). The adaptation of microbial populations to nitrogen concentrations that are generally regarded as toxic (e.g. >3g TAN/L) has been reported under different conditions: (i) discontinuous or pulse ammonia exposure (Demirel and Scherer, 2008), (ii) supplementation with micronutrients (Cruz Viggli et al., 2014), (iii) addition of adsorbents like biofibers and zeolite (Wang et al., 2011) and (iv) nitrogen dilution by co-digestion (Borowski and Kubacki, 2015). However, most of these strategies are expensive, time consuming, and the final outcome is not always satisfactory.

The development of alternative more feasible methodologies to improve biogas production from nitrogen-rich wastes requires a more detailed comprehension of the mechanisms conferring ammonia tolerance to the involved microbial populations. AMA inhibition by ammonia results in the accumulation of acetate, which can prompt further inhibition. Alternatively, the acetate excess can be metabolized to hydrogen and carbon dioxide via the so-called syntrophic acetate oxidation pathway (SAO) (Hattori, 2008;

Schnürer et al., 1994). Some bacteria that are adapted to high ammonia concentrations efficiently use the SAO pathway for energy yield. Such bacteria (SAOB) become relevant for the AD process when its abundance and activity reach a certain threshold, so that the generated H<sub>2</sub> and CO<sub>2</sub> are reduced to methane by concurrent hydrogenotrophic archaea (HMA) (Angelidaki and Ahring, 1993). In the SAO process both SAOB and HMA are mutually dependent in a syntrophic association determined by the low levels of hydrogen/formate due to the HMA metabolism, so that acetate oxidation becomes thermodynamically favourable for the SAOB (Luo et al., 2002). It has been suggested that the mechanism for the SAO process occurs by the reversion of the Wood Ljungdahl (WL) pathway, which is rather widespread in several bacterial and archaeal species (e.g. certain sulphate reducers and acetotrophic methanogens) (Mosbæk et al., 2016; Müller et al., 2013).

The relevance of specific biochemical pathways in a well-adapted AD microbiome is related to the abundance and activity of certain species harbouring these pathways. Until now, most of the studies aimed to investigate the microbial community structure in AD biomass were based on the high throughput amplicon sequencing of the 16S rRNA gene. This approach targets only one or two hypervariable regions of ribosomal genes for phylogenetic affiliation and, therefore, inference of functional traits is limited to those species that have previously been described. Hence, this approach only allows an approximate description of the microbiome function based on the known ecophysiology of the identified species. More powerful approaches for the study of the AD microbiome are emerging, which are based on the analysis of shotgun short reads performed without previous assembly. In these studies, species identification is based on the comparison of sequences with those available from public databases. Unfortunately, these studies performed using unassembled short reads show some limitations because these sequences are error prone and contain only minimal signal for homology searches. Hence, it is convenient to elaborate a genome-centric approach and generate an appropriate database that includes complete or nearly-complete microbial genomes obtained from diverse samples that are representative of the biogas microbiome under different conditions. This collection of genomes allows then correlation studies between species abundance, taxonomic composition, process performance and functional/metabolic properties of the microbiome. For this reason, one of the most rapid and convenient methods to recover genome sequences of single microbes from the assembled reads is the binning process, resulting in the classification of scaffolds into single biological entities named Population Genomes (PGs). Although de novo assembly of shotgun sequence in microbial community is challenging, the data obtained after the binning process can improve the reliability of gene finding and annotation and allows the discovery of novel microbial species and genomic elements (De Francisci et al., 2015).

Recently, the binning approach has been applied to the AD microbial community with the general aim of unravelling the biogas microbiome (Campanaro et al., 2016; Treu et al., 2016), in order to obtain a genomic database that includes the most abundant PGs and to measure their transcriptional activity. However, the genome sequences of the microbiome involved in the SAO process are still poorly characterized. To bridge the gap, it would be important to examine the peculiar microbial composition of reactors digesting N-rich wastes and to investigate the genomes of the species proliferating under such rather extreme condition.

The present study is aimed at obtaining a better understanding of the microbial community interactions at the genome level in AD reactors when exposed to different ammonia levels. For this purpose, an interdisciplinary strategy combining isotopic profiling of biogas samples with whole metagenomics shotgun sequencing (WMS) and binning of scaffolds into population genomes (PG) has been developed. This novel approach facilitated the functional analysis of genes in relation to ammonia exposure, the reconstruction of probable metabolic pathways for methanogenesis and acetate assimilation, and the identification of novel species that might be involved in the SAO process.

## **5.2 Materials and methods**

### **5.2.1 Biogas plants and sampling procedure**

The present study was performed on four full-scale anaerobic digesters designed as continuous stirred tank reactors (CSTR) and operated under mesophilic conditions (Table 9.1). The influent substrate of the reactors was pig manure codigested with different organic wastes from the food industry varying in nitrogen content (R1, R2 and R3), and primary and secondary sludge from an urban wastewater treatment plant (R4). Digestate samples (5 L) were collected from the reactors' effluent, filtered for removing coarse fibrous particles, and thoroughly homogenized prior to its further processing. A 3 mL subsample was then taken and preserved into 6 mL of LifeGuard™ Soil Preservation solution (Qiagen). Total DNA/RNA was extracted in triplicate from biomass pellets obtained from the previous solution by centrifugation (1.5 mL, 4,000 g, 30', 4°C) by an adapted protocol of PowerMicrobiome® RNA Isolation Kit (MoBio Laboratories Inc., Carlsbad, CA, USA). RNA purification and reverse transcription (RT) to cDNA was performed as previously reported in (Pelissari et al., 2017). DNA and cDNA extracts from the three sample replicates were pooled together prior to sequencing. The remaining original sample volume was characterized in physicochemical terms.

## 5.2.2 Analytical methods

Volatile fatty acids (VFA) and total ammonia nitrogen (TAN) were determined according to the Standard Methods for Wastewater from the American Public Health Association, the American Water Works Association, and the Water Pollution Control Federation (APHA, AWA, WEF, 2005). Biogas components (CH<sub>4</sub> and CO<sub>2</sub>) were elucidated with a Varian CP-3800 gas chromatograph (GC; Varian, Walnut Creek, CA, USA) fitted with Hayesep Q 80/100 Mesh (2m× 1/800 × 2.0 mSS) packed column (Varian) and thermal conductivity detector. Isotopic fractionation of <sup>13</sup>C/<sup>12</sup>C from methane and carbon dioxide in biogas samples was measured with an Agilent 6890 GC (Agilent Technologies Palo Alto, CA, USA) coupled with a Delta Plus Finnigan MAT isotope ratio mass spectrometer (IRMS; ThermoFinnigan MAT, Bremen, Germany) (Lv et al., 2014). Samples were run in triplicate and the δCH<sub>4</sub> and δCO<sub>2</sub> values were expressed as a ‰ relative to the Vienna Pee Dee Belemnite (VPDB) standard. The apparent fractionation factor (αC) was determined according to (Conrad et al., 2009), who established that a αC in the range of 1.040 – 1.055 corresponded to a predominantly acetotrophic methanogenesis, while that of 1.055 – 1.080 was mainly hydrogenotrophic.

## 5.2.3 Molecular microbial community characterization

### 5.2.3.1 Next generation sequencing of active microbial populations

Massive bar-coded 16S rRNA gene libraries targeting V1–V3 and V3–V4 hypervariable regions from bacterial and archaeal populations, respectively, were sequenced by means of Illumina MiSeq System Platform in Molecular Research DNA LP (Shallowater, USA) by following the protocol described in (Pelissari et al., 2017). Downstream MiSeq data analysis was carried out by using QIIME software version 1.8.0. Trimming of the 16S rRNA barcoded sequences into libraries was carried out using QIIME software version 1.8.0. ([www.qiime.org](http://www.qiime.org)). Quality filtering of the reads was performed at Q25, prior to the grouping into Operational Taxonomic Units (OTUs) at a 97% sequence homology cutoff and taxonomic assignment according to the Greengenes database. Data from the MiSeq NGS analysis was submitted to the Sequence Read Archive (SRA) of the National Center for Biotechnology Information (NCBI) under the accession number PRJNA356200.

### 5.2.3.2 Metagenome sequencing, assembly and binning process

Genomic DNA extracts from each sample were prepared for sequencing using Nextera DNA Library Preparation Kit (Illumina, San Diego, CA, USA). All the samples were paired-end sequenced (2 × 150 bp) using Illumina HiSeq 2500 (Molecular Research DNA, Shallowater, TX, USA). Paired-end sequences were quality-filtered and adaptors



were removed with the Trimmomatic software (v0.33) using the following parameters: Illumina clip (NexteraPE-PE:2:30:10), leading (10), trailing (10), sliding window (4:20, minlen (65) (Bolger et al, 2014). Assembly was performed using metaSPAdes (3.9.0) with kmers 55, 77, 99 and a minimum scaffold length of 500 bp. Quality of the assembly was checked using QUAST. Gene finding was performed with Prodigal (v2.6.2) ran in metagenomic mode. Protein-encoding genes were annotated using the reverse-position specific BLAST algorithm with the COG RPSBLAST database (Galperin et al., 2015); only results with e-value lower than 10<sup>-5</sup> were retained. Genes were also annotated according to KEGG using GhostKOALA. Scaffolds were binned into population genomes (PGs) using two strategies: the MetaBAT (v0.25.4) (parameters --specific, -m 1500) (Kang et al., 2015), and the hierarchical clustering followed by canopy profile selection (Campanaro et al., 2016). Completeness and contamination of PGs were estimated using the Lineage\_wf workflow of CheckM (Parks et al., 2015) and the PGs obtained from the two approaches were compared using the “bin-compare” module of the same software (Parks et al., 2015). PGs were considered as univocally identified by one binning strategy when they had less than 20% of the bases in common with those extracted by the other software (54 PGs). Conversely, all the remaining PGs (83 with overlap higher than 50% and 44 with overlap included between 20% and 50%) were compared as follows: completeness and contamination of each PG obtained with the two binning strategies were combined using the formula [completeness-(contamination\*3)] and each PG was selected from the strategy where it displayed the higher value. After selection, scaffolds assigned to more than one PG were removed, and completeness and contamination was determined again for the PGs included in the final selection. The bioinformatic functional analysis was limited to those that satisfied strict requirements (completeness > 50%, contamination lower than 20%). Functional analysis of the PGs was based on KEGG annotation determined for all PGs and, additionally, gene function was also determined by Rapid Annotation using Subsystem Technology (RAST) server (Overbeek et al., 2014).

Taxonomical assignment of the obtained PGs was performed using PhyloPhlan (v0.99). Those having incomplete confidence were checked using the PhyloPythiaS web server (Patil et al., 2012) and assigned to a clade only when more than 50% of the genome sequence displayed coherent results. The presence of genomes belonging to the same species in the NCBI microbial genome database and in PGs recovered in previous assemblies was determined using the Average Nucleotide Identity calculation as previously described (Treu et al., 2016). Abundance of genes and PGs in the different reactors was considered as directly related to scaffold coverage. This parameter was determined aligning reads on the assembly using the Bowtie 2 software (v2.2.4) and converting the result in the corresponding coverage value using the BEDTools package

(v2.17.0). Results were normalized considering the sample with the lower number of reads as a reference. Coverage values were visualized with MeV in order to identify the behaviour of PGs in different samples.

### 5.2.3.3 Biostatistical analysis

The microbial community structure of the different reactors was assessed and compared via multivariate Canonical Analysis (CA) using the CANOCO5 software (Microcomputer Power, Ithaca, NY, USA). The incidence matrix of OTUs based on 16S rRNA transcripts for both Bacteria and Archaea was used as the input data and the obtained samples and OTUs-species scores were depicted in 2D-plots. Estimators on microbial biodiversity (Shannon) and species richness (Chao1) were obtained using the Mothur software (v1.35.1).

## 5.3 Results and discussion

### 5.3.2 Biochemical characterization of the reactors

Four full-scale CSTR anaerobic digesters treating agricultural and urban organic wastes were collected and characterized in biochemical terms (Table 5.1). The measured TAN ranged from  $<3$  gTAN L<sup>-1</sup> in R3 and R4, considered henceforth as operated under a relatively low ammonia content, up to  $>6$  gTAN L<sup>-1</sup> in R1 and R2, which were subjected to an ammonia exposure within the inhibitory range (Braun et al., 1981;Yenigün and Demirel, 2013). Measurable VFA were mostly composed of acetate and the concentration was well below the levels that are commonly associated to process instability (Ahring et al., 1995). The pH remained within the slightly alkaline range in all cases as well. Interestingly, methane richness in the biogas was positively correlated with TAN, ranging from 66% and 74% in R1 and R2, to 50% and 49% in R3 and R4.

Further confirmation on the predominant methanogenic pathway was explored by the profiling of the <sup>13</sup>C/<sup>12</sup>C isotopic ratio in CH<sub>4</sub> and CO<sub>2</sub> from biogas (Table 9.1). The apparent fractionation factor ( $\alpha_C$ ) demonstrated that the biomass of the digesters operated at high ammonia content (R1 and R2) was exclusively hydrogenotrophic, while that of the reactors with a low ammonia content (R3 and R4) was a rather, yet not exclusively, acetotrophic. The combination of stable operation under high TAN exposure, along with hydrogenotrophic methanogenesis, made R1 and R2 good candidates for the occurrence of the SAO process. The isotopic profiling of biogas has

previously been proposed as a technique for monitoring process stability in full-scale anaerobic digesters (Lv et al., 2014). However, the costly and cumbersome GC-IMRS equipment needed for this purpose currently poses serious limitations to a practical routine application. With this respect, the in situ monitoring of biogas methane richness as an indicator of hydrogenotrophy could be a more feasible alternative, but further research is needed for confirming this trend.

### **5.3.3 Active microbial populations**

The microbial community structure of the active species in the four studied anaerobic digesters was characterized by NGS of 16S rRNA transcripts. Two gene libraries of 408,194 and 218,359 reads were obtained for the Bacteria and Archaea domains, which were grouped respectively into 4,059 and 351 different OTUs, respectively. The Good's coverage estimator on the percentage of the total active species (as OTUs) represented in any given sample was above 99%, indicating that a very significant proportion of the entire sample population had been observed. The number of expected OTUs (Chao 1) for the Bacteria was about one order of magnitude higher than that for the Archaea in all reactors. Interestingly, the Chao1 species richness estimate was significantly higher in reactors R1 and R2 operated at relatively high TAN than in R3 and R4 that were ran at low TAN values, which indicates that ammonia exposure is conducive to a more complex community structure of active microorganisms.

**Table 5. 1** Operational and physicochemical parameters in four industrial anaerobic digesters treating different organic wastes containing variable amounts of ammonia, and apparent fractionation.

Operational and physico-chemical parameters										
Reactor	Influent	Location	Volume (m <sup>3</sup> )	HRT (d)	pH	Acetic (mg·L <sup>-1</sup> )	Propionic (mg·L <sup>-1</sup> )	Butyric (mg·L <sup>-1</sup> )	TAN (g·L <sup>-1</sup> )	CH <sub>4</sub> (%)
R1	Pig manure and food waste	Vilasana (Lleida)	1,500	65	8.05	176	0	0	6	66
R2	Pig manure and silage	Torregrossa (Lleida)	1,300	30	7.59	308	0	0	7	74
R3	Pig manure	Gimenells (Lleida)	2,500	20	7.84	292	41	8	2	49
R4	Primary (30%) and secondary sludge (70%) from urban wastewater	La Llagosta (Barcelona)	1,400	>40	7.80	357	16	0	1.9	50

**Table 5. 1** Operational and physicochemical parameters in four industrial anaerobic digesters treating different organic wastes containing variable amounts of ammonia, and apparent fractionation. (Continuation from previous page).

Reactor	Influent	Location	Biogas isotopic fractionation parameters			
			$d^{13}CO_2$	$d^{13}CH_4$	$\alpha_C$	Methanogenic pathway
R1	Pig manure and food waste	Vilasana (Lleida)	17.41	-58.19	1.080	HMA
R2	Pig manure and silage	Torregrossa (Lleida)	29.07	-54.40	1.088	HMA
R3	Pig manure	Gimenells (Lleida)	5.29	-47.66	1.056	AMA/HMA
R4	Primary (30%) and secondary sludge (70%) from urban wastewater	La Llagosta (Barcelona)	-6.78	-61.63	1.058	AMA/HMA

Multivariate Correspondence Analysis (CA) showed very similar sample scores distribution patterns for both the Bacteria and the Archaea domains and encompassed more than 80% of the samples variance (Figure 5.1). The digesters R1 and R2 were characterized by rather similar microbial populations, which would be the results of the selective pressure of high ammonia exposure. The most active bacteria, in terms of a sample's relative abundance of expressed ribosomal transcripts higher than 10%, were associated to representatives of the strictly anaerobic genera *Longilinea* (fam. *Chloroflexi*) and *Alloprevotella* (fam. *Bacteroidetes*). The later genus has recently been established in order to accommodate a number of novel species closely related to the genus *Prevotella* that are linked to the fermentative metabolism of carbohydrates to certain volatile fatty acids (Moore et al., 1994). The former genus has been proposed for the new species *Longilinea arvoryzae*, which was isolated from rice paddy soil soaked with water. This species has been described to grow on certain sugars and polysaccharides. Growth was enhanced in co-cultivation with hydrogenotrophic methanogens but it was not able to assimilate acetate under laboratory conditions. The digesters R3 and R4, operated at a relatively low TAN, presented a rather distinct and specific active microbiota. The predominant bacterium in R3 (32% of ribosomal transcripts) was related to the genus *Sporocytobaga*, which has been described as an efficient cellulose-degrading taxon (Du et al., 2011), while R4 was dominated by *Nitratalea* (14% of ribosomal transcripts), an alkaliphilic taxon that ferments simple sugars to acids but that is not able to grow on acetate (Anil Kumar et al., 2010). Such differences between the two digesters could be explained by the very different feeding composition: pig manure in R3 and primary and secondary sludge from urban wastewater in R4.

Concerning the archaeal active populations, methanogenesis under high ammonia exposure was carried out by hydrogenotrophic archaea, primarily from the genera *Methanococcus* (39% and 27% in relative abundance in R1 and R2) and *Methanomassiliicoccus* (30% and 52% in R1 and R2), while at low ammonia content there was a more significant involvement of OTUs associated to the obligate acetotrophic genus *Methanosaeta* (59% and 27% in R3 and R4), formerly *Methanobrix*. These findings are in agreement with the observed isotopic profiles of biogas components concerning the ammonia concentration inside the digesters (Table 9.1). However, despite clear hydrogenotrophy in R1 and R2, none of the observed active bacterial OTUs was associated to the know SAOB counterpart species that have so far been described in the literature: the thermophilic *Thermaetogenium phaeum* and *Pseudothermotoga lettingae*, the thermotolerant *Tepidanaerobacter acetatoxydans*, and the mesophilic *Clostridium ultunense* and *Syntrophaceticus schinkii*. It is clear that the biodiversity of SAOB is likely to be wider than those currently known microorganism and that this metabolic function in the hydrogenotrophic digesters R1 and R2 might very well be carried out by other, currently unknown, SAOB species.

### 5.3.4 Genome reconstruction and phylogenetic assignment

Methanogenic biomass samples collected from the above-described digesters were processed by Illumina shotgun sequencing. Between 5.1 and 7.4 million of reads depending on the sample were obtained, accounting after quality filtering for ~13 Gbp of metagenomic sequence. The assembly resulted in 289,272 scaffolds, after removing those shorter than 500 bp. The gene-finding and annotation process resulted in the identification of 535,434 protein-encoding genes. In total, 73 non-redundant population genomes (PG) were extracted, taxonomically assigned, and their abundance in every sample determined (Table 9.2).

Recent metagenomics studies were aimed at unravelling the unknown biodiversity by using different binning strategies, but only part of the recovered PGs have been deposited in public databases (Treu et al., 2016). In order to overcome this limitation, the taxonomic classification performed using PhyloPhlan was complemented by the verification of the PGs presence in the NCBI microbial genome database, by using the ANI calculation (Campanaro et al., 2017). Yet, only 2 PGs could reliably be identified as known species, the bacterium *Coprothermobacter proteolyticus*, and the archaeon *Methanosaeta concillii*, and 3 PGs were assigned at the genus level, with a predominance of *Clostridium*, *Alkaliphilus* and *Treponema*. The remaining 68 PGs could only be associated to higher taxonomic categories in the Bacteria (64 PGs) and the Archaea (4 PGs). These results are not unexpected considering the lack of available genomes from the AD microbiome, particularly under the less common conditions such as the SAO process (Treu et al., 2016). Some of the unknown PGs obtained in this study have previously been found in metagenomic studies on laboratory-scale reactors fed with cattle manure at thermophilic and mesophilic conditions: *Bacteroidales* sp. IRTA0001, *Bacteroidales* sp. IRTA0005, *Prevotellaceae* sp. IRTA0006, *Spirochaeta* sp. IRTA0072 (Tsapekos et al., 2017)(Treu et al., 2016); *Methanosaeta concillii* IRTA0015 was only found in reactors fed with cattle manure and alpha-cellulose (Tsapekos et al., 2017). In terms of the relative abundance of the observed PGs (see detail information in supplementary material), 3 PGs were predominant in the high TAN digesters R1 and R2: *Bacteroidales* sp. IRTA0007 (11.3%), *Bacteroidales* sp. IRTA0025 (12.8%) and *Chloroflexi* sp. IRTA0011 (24.5%). This pattern is coherent with the previously observed in active microbiome (Figure 5.1), where a representative of *Alloprevotella* (phylum *Bacteroidetes*) and *Longilinea* (phylum *Chloroflexi*) were the most abundant. No common genomes were found in the digesters R3 and R4, considering a relative abundance >1%, which is in agreement with the significant population differences between this two reactors in terms of active microorganisms.

**Table 5. 2** Taxonomic assignment and completeness of the PGs assembled from biomass samples from the studied full-scale digesters

	Genome	Completeness	Abbreviation	Genome	Completeness
Ah_IRTA0024	Acholeplasmataceae_IRTA0024	78,10%	Cl_IRTA0030	Clostridiales sp.IRTA0030	45,70%
Ac_IRTA0016	Acidobacteria sp.IRTA0016	99,10%	Co_IRTA0018	Coprothermobacter_proteolyticus_IRTA0018	77,10%
Ac_IRTA0035	Acidobacteria sp.IRTA0035	66,00%	De_IRTA0047	Deltaproteobacteria sp.IRTA0047	45,70%
Ac_IRTA0044	Acidobacteria sp.IRTA0044	74,50%	De_IRTA0071	Deltaproteobacteria sp.IRTA0071	98,10%
Ac_IRTA0048	Acidobacteria sp.IRTA0048	33,00%	En_IRTA0049	Enterococcus sp.IRTA0049	93,30%
Ac_IRTA0070	Acidobacteria sp.IRTA0070	21,70%	Me_IRTA0013	Methanomicrobiales sp.IRTA0013	64,70%
Ac_IRTA0065	Actinobacteria sp.IRTA0065	81,00%	Me_IRTA0014	Methanomicrobiales sp.IRTA0014	97,10%
Ac_IRTA0069	Actinobacteria sp.IRTA0069	16,20%	Me_IRTA0028	Methanomicrobiales sp.IRTA0028	91,20%
Al_IRTA0041	Alkaliphilus sp.IRTA0041	87,60%	Me_IRTA0038	Methanomicrobiales sp.IRTA0038	100,00%
Ba_IRTA0001	Bacteroidales sp.IRTA0001	93,30%	Mc_IRTA0015	Methanosaeta_concillii_IRTA0015	72,70%
Ba_IRTA0002	Bacteroidales sp.IRTA0002	44,80%	Mi_IRTA0058	Microbacteriaceae sp.IRTA0058	36,20%
Ba_IRTA0003	Bacteroidales sp.IRTA0003	68,60%	Pe_IRTA0006	Prevotellaceae sp.IRTA0006	99,00%
Ba_IRTA0004	Bacteroidales sp.IRTA0004	27,60%	Pr_IRTA0061	Proteobacteria sp.IRTA0061	47,60%
Ba_IRTA0005	Bacteroidales sp.IRTA0005	73,30%	Pr_IRTA0066	Proteobacteria sp.IRTA0066	67,60%
Ba_IRTA0007	Bacteroidales sp.IRTA0007	79,00%	Sp_IRTA0072	Spirochaeta sp.IRTA0072	94,20%
Ba_IRTA0008	Bacteroidales sp.IRTA0008	91,40%	Sy_IRTA0073	Synergistaceae sp.IRTA0073	95,20%
Ba_IRTA0009	Bacteroidales sp.IRTA0009	50,50%	Sy_IRTA0031	Syntrophomonadaceae sp .IRTA0031	66,70%
Ba_IRTA0025	Bacteroidales sp.IRTA0025	99,00%	Sy_IRTA0034	Syntrophomonadaceae sp .IRTA0034	69,50%
Ba_IRTA0025	Bacteroidales sp.IRTA0025	99,00%	Sy_IRTA0034	Syntrophomonadaceae sp .IRTA0034	69,50%



**Table 5.2** Taxonomic assignment and completeness of the PGs assembled from biomass samples from the studied full-scale digesters. (Continuation from previous page)

Abbreviation	Genome	Completeness	Abbreviation	Genome	Completeness
Ba_IRTA0037	Bacteroidales sp.IRTA0037	95,20%	Th_IRTA0074	Thermotogaceae sp.IRTA0074	47,10%
Ba_IRTA0057	Bacteroidales sp.IRTA0057	76,20%	Tr_IRTA0033	Treponema sp.IRTA0033	99,00%
Ba_IRTA0059	Bacteroidales sp.IRTA0059	48,60%	Un_IRTA021	Unclassified sp.IRTA021	65,70%
Ba_IRTA0060	Bacteroidales sp.IRTA0060	86,70%	Un_IRTA026	Unclassified sp.IRTA026	96,20%
Ch_IRTA0010	Chloroflexi sp.IRTA0010	94,20%	Un_IRTA027	Unclassified sp.IRTA027	60,00%
Ch_IRTA0011	Chloroflexi sp.IRTA0011	99,00%	Un_IRTA040	Unclassified sp.IRTA040	82,90%
Ch_IRTA0012	Chloroflexi sp.IRTA0012	92,20%	Un_IRTA042	Unclassified sp.IRTA042	65,70%
Ch_IRTA0039	Chloroflexi sp.IRTA0039	73,80%	Un_IRTA045	Unclassified sp.IRTA045	64,80%
Ch_IRTA0043	Chloroflexi sp.IRTA0043	65,00%	Un_IRTA050	Unclassified sp.IRTA050	81,90%
Cl_IRTA0022	Clostridia sp.IRTA0022	58,10%	Un_IRTA051	Unclassified sp.IRTA051	92,40%
Cl_IRTA0023	Clostridia sp.IRTA0023	46,70%	Un_IRTA052	Unclassified sp.IRTA052	24,80%
Cl_IRTA0032	Clostridia sp.IRTA0032	96,20%	Un_IRTA053	Unclassified sp.IRTA053	27,60%
Cl_IRTA0062	Clostridia sp.IRTA0062	67,60%	Un_IRTA054	Unclassified sp.IRTA054	14,30%
Cl_IRTA0019	Clostridiaceae sp.IRTA0019	48,60%	Un_IRTA055	Unclassified sp.IRTA055	42,90%
Cl_IRTA0036	Clostridiales. IRTA0036	86,70%	Un_IRTA056	Unclassified sp.IRTA056	10,50%
Cl_IRTA0046	Clostridiales. IRTA0046	78,10%	Un_IRTA063	Unclassified sp.IRTA063	60,00%
Cl_IRTA0017	Clostridiales sp.IRTA0017	12,40%	Un_IRTA064	Unclassified sp.IRTA064	23,80%
Cl_IRTA0020	Clostridiales sp.IRTA0020	93,30%	Un_IRTA067	Unclassified sp.IRTA067	25,70%
Cl_IRTA0029	Clostridiales sp.IRTA0029	28,60%	Un_IRTA068	Unclassified sp.IRTA068	41,00%

**Table 5. 3** Counts on relevant genes from PGs encoding for enzymes that are directly involved in the in the SAO process

	Enzyme name	Gene	Gene counts			
			R1	R2	R3	R4
<b>Wood-Ljungdahl pathway</b>	formyltetrahydrofolate synthetase	Ftfhs	1558	1840	764	911
	methenyltetrahydrofolate cyclohydrolase	FolD	994	856	249	58
	methylenetetrahydrofolate dehydrogenase	FolD	864	1734	485	668
	methylenetetrahydrofolate reductase	Met	1498	1812	712	902
	CO-methylating acetyl-CoA synthase	CdhC	93	570	73	22
<b>Glycine cleavage system pathway</b>	formyltetrahydrofolate synthetase;	Ftfhs	1558	1840	764	911
	methenyltetrahydrofolate cyclohydrolase	FolD	994	856	249	58
	methylenetetrahydrofolate dehydrogenase	FolD	864	1734	485	668
	Glycine cleavage system complex	Gcs	3027	3477	1747	2044
	pyruvate formate-lyase	PflA	3281	3793	2449	1820
	L-serine ammonia-lyase	SdaA	0	115	48	271
	pyruvate dehydrogenase	PdhA	2	216	20	210

**Table 5.3** Counts on relevant genes from PGs encoding for enzymes that are directly involved in the in the SAO process. (Continuation from previous page)

	Enzyme code	Enzyme name	Gene	Gene counts			
				R1	R2	R3	R4
<b>Hydrogenotrophic methanogenesis</b>	EC 1.2.99.5	formylmethanofuran dehydrogenase	Fwd	3767	3417	642	217
	EC 2.3.1.101	formylmethanofuran-tetrahydromethanopterin	Ftr	197	316	47	3
	EC 3.5.4.27	methenyltetrahydrofolate cyclohydrolase	Mch	108	685	72	208
	EC 1.5.98.2	5,10-methylenetetrahydromethanopterin	Mer	290	330	47	8
	EC 2.1.1.86	tetrahydromethanopterin methyltransferase	Mtr	817	720	85	3
<b>Acetotrophic methanogenesis</b>	EC 2.3.3.-	CO dehydrogenase/acetyl-CoA synthase	Cdh	93	570	73	22
	EC 6.2.2.1	Acetyl CoA synthase	Acs	40	264	6	115
	EC 2.3.1.8	Phosphate acetyltransferase	Pta	455	786	658	991
	EC 2.7.2.1	Acetokinase	Ack	564	438	563	501
<b>Complementary genes</b>	EC 6.2.1.1	acetyl-CoA synthetase	Acs	1769	1923	979	289

Archaeal PGs were represented only by 4 PGs that belonged to the order of strict hydrogenotrophic methanogens *Methanomicrobiales* and by 1 PG that could be assigned to the strict acetotrophic species *Methanosaeta concilii*. Interestingly, the *Methanomicrobiales*-associated PGs were the most abundant in the high TAN digesters R1 (IRTA0013, IRTA0014 and IRTA0028) and R2 (IRTA0038), while *M. concilii* (IRTA0015) was the predominant methanogen in R3 and R4. The analysis of the partial 16S rDNA gene sequence of PGs IRTA0014 and IRTA0028 revealed their similarity to *Methanoculleus bourgensis* (97%) and *Methanoculleus sediminis* (97%), respectively, which also corresponds with the profile of predominant 16S rRNA transcripts (Figure 1).

### 5.3.5 Functional characterization of methanogenic archaea

In order to gain a deeper insight in the SAO process in the studied digesters, the obtained metagenomes were searched for genes encoding for the methanogenic hydrogenotrophic and acetotrophic pathways, as well as the Wood-Ljungdahl pathway (WL) present in homoacetogenic bacteria, which is suspected to be reversed during the SAO process (Table 5.3). Concerning the archaeal genomes, several encoding genes related to acetotrophic methanogenesis enzymes could be assembled and were found in all reactors at a similar abundance, but with a slight increase in R4. It is noteworthy to mention that the gene encoding for acetyl-CoA synthase (ACS; EC 6.2.1.1), a key enzyme of the acetate activation to acetyl-CoA, was assembled in the genome of *Methanoculleus*. This finding supports the studies of (Barret et al., 2015) claiming that some *Methanoculleus* species from swine storage tanks could assimilate acetate as carbon source for growth. In relation to this, an hypothetical acetotrophic pathway has been described for *Methanococcus maripaludis*, a well-known hydrogenotrophic methanogen, where acetate acts as a carbon source but cannot replace CO<sub>2</sub>/H<sub>2</sub> as energy source (Richards et al., 2016). In the present study, it was possible to reconstruct this hypothetical pathway (Figure 5.2) for the genome bins within *Methanomicrobiales* that are related to *Methanoculleus*.

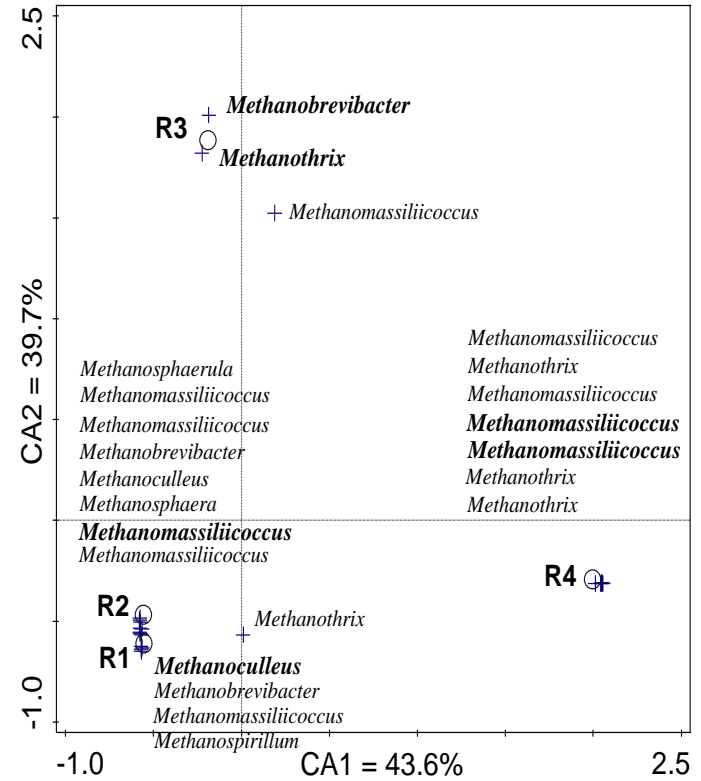
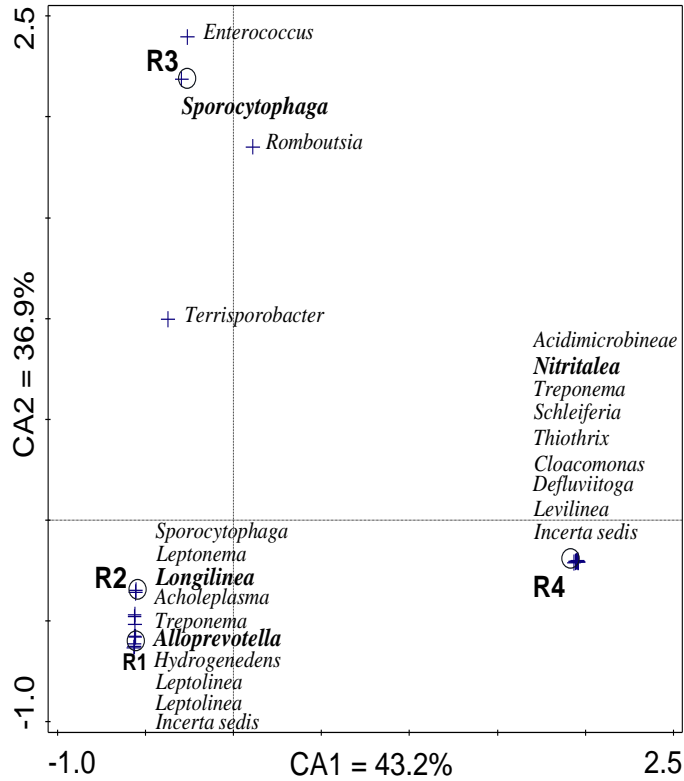


**Figure 5. 1** Correspondance Analysis biplot on sample scores (circles) and operational taxonomic units (crosses) from the biomass of four anaerobic digesters, concerning the incidence of 16S rRNA transcripts for the Bacteria (left) and Archaea (right) domains.

All required enzymes were found except that encoding for the CO dehydrogenase (CODH: EC 1.2.99.2), probably because of incomplete genome sequence. Nonetheless, this enzyme was previously assembled in the *Methanoculleus bourgensis* MS2T complete genome GCA\_000304355.2 (Maus et al., 2012) and, therefore, it has been considered in Figure 5.2. In support of the hypothesis on the dual hydrogenotrophic and acetotrophic metabolic capacity of *Methanoculleus* spp., representatives of this genus have been found in acetate-rich environments.

Regarding the hydrogenotrophic methanogenic pathway, all related encoding genes were assembled successfully. These genes were also found at a higher abundance in R1 and R2 (Table 5.3), which is in accordance to both the observed populations of active archaea and the isotopic profile of the biogas in these reactors. From an energetic point of view, and concerning the electron-transport properties, methanogenic pathways require an electrochemical Na<sup>+</sup> and H<sup>+</sup> gradient during growth, as well as the presence of ferredoxins (Fd). Fd are required for different substrate reductions, such as that of CO<sub>2</sub> to CH<sub>4</sub>, where heterodisulfide (CoM-SS-CoB) is formed in the last step of methanogenesis. This reaction is exergonic and H<sub>2</sub>-dependent and, therefore, in methanogenic archaea without cytochromes (i.e. certain species in *Methanomicrobiales*), is energetically coupled to the cytoplasmic enzyme complex MvhADG/HdrABC that mediates the flavin-based electron bifurcation (Thauer et al., 2008), and to a F420-dependent formate dehydrogenase (FDH), so that formate is used as an electron donor. The genes encoding for the protein FdhD, which is essential for the FDH activity, and the different subunits of heterodisulfide reductase (HdrABC), were assembled successfully. However, the [NiFe] hydrogenase MvhADG could not be found (Figure 5.2).

Membrane bound electron transport systems are connected to energy conservation by Na<sup>+</sup> or H<sup>+</sup> translocating enzymes. Interestingly, the encoding gene RnfD from the membrane bound Rnf complex was detected within the *Methanomicrobiales* PGs (*Methanoculleus*). This enzymatic complex was recently shown to conserve energy by the reversible translocation of H<sup>+</sup>/Na<sup>+</sup> from Fd oxidation with NAD<sup>+</sup>, and was found overexpressed under acetotrophic growth conditions (Li et al., 2006). Thus, further research to detect the expression of this complex in *Methanoculleus* spp. is necessary to reinforce the hypothetical acetate assimilation pathway mentioned before (Figure 5.2).

Most of *Methanosarcinales* contains the energy-converting [NiFe] hydrogenase (Ech), that has a similar function to that of the Rnf complex (Buckel and Thauer, 2013), but performs the Na<sup>+</sup> or H<sup>+</sup> translocation by Fd oxidation with H<sub>2</sub> production. Furthermore, it has been described that Ech is absolutely required for the reduction of CO<sub>2</sub> to formylmethanofuran by H<sub>2</sub> (Hedderich, 2004). For the methanogens without

cytochromes (i.e. *Methanomicrobiales*), it has been proposed that the Eha and/or Ehb hydrogenase complex is the energy-converting hydrogenase required for CO<sub>2</sub> reduction, but this enzyme complex could not be assembled in the present study. Likewise, Ech and Eha/Ehb are phylogenetically related to complex I of the respiration chain (Thauer et al., 2008). Genes related to different subunits of the NADH:ubiquinone oxidoreductase (Nuo) from complex I were assembled in *Methanoculleus* PGs, such as NuoB, NuoC, NuoI and NuoL, which are homologous to subunits of the membrane-bound [NiFe] hydrogenases.

Moreover, encoding genes for the NfnAB complex, which performs the reduction of Fd with NADPH to the reduction of NAD<sup>+</sup>, were found. The NfnAB complex is a heterodimeric enzyme composed of the subunits NfnA and NfnB, and has binding sites for NAD(P)<sup>+</sup>, FAD and one [2Fe–2S] cluster (Buckel and Thauer, 2013). These energetic complexes were not previously described for the *Methanoculleus* genus, so the present study could bring new insights into the capacity of *Methanomicrobiales* PGs to generate redox potential, phenomenon that is essential for acetate assimilation/dissimilation pathways. All these enzymes and their potential roles, as well as their putative interactions, have been depicted in Figure 5.2.

On the other hand, the predominance of *Methanoculleus* species in R1 and R2 could be explained by their extremely efficient H<sub>2</sub> consumption. It has been found that *M. bourgensis* could grow at a pH<sub>2</sub> as low as 0,15Pa (Neubeck et al., 2016), thus being more competitive than other hydrogenotrophic methanogenic archaea (HMA). Furthermore, the hydrogenotrophic pathway dominates in nitrogen-rich methanogenic environments, because HMA are less sensitive to ammonia inhibition and prompt syntrophic interactions with the SAOB, mainly with homoacetogens from the *Clostridia* class (phylum *Firmicutes*) (Hattori, 2008). In R1 and R2, the *Firmicutes* phylum was represented by 12% in relative abundance of the total active bacterial population. Moreover, a similar abundance profile identified by Mev Cluster software showed a possible association between *Methanoculleus* and homoacetogenic *Firmicutes*: *Clostridia* sp. IRTA0023 and *Methanomicrobiales* sp. IRTA0038. Nonetheless, another putative syntrophic association was observed between *Chloroflexi*\_IRTA10&11, *Bacteroidales*\_IRTA3&4 and *Methanomicrobiales* sp. IRTA13&28.

The WL acetyl-CoA pathway has been studied as an important metabolic route for biosynthesis of acetate by homoacetogenic bacteria, but it also plays a fundamental role in the SAO process when reversed. The swift consumption of H<sub>2</sub> by the methanogenic counterparts keeps the pH<sub>2</sub> low enough to make the reaction sufficiently exergonic ( $\Delta$ GSAO-HM = -36 kJ; Müller et al., 2013). Here, genes encoding for the WL Acetyl-CoA pathway have been found in higher abundance in R1 and R2 (Table 5.3, Figure

5.3). However, no genes were found for the enzymes EC 1.2.1.43 and EC 2.1.1.258 in any of the studied samples, which might be due to incomplete sequencing. Based on the genome bins within *Bacteroidetes*, *Chloroflexi* and *Firmicutes* it was possible to reconstruct the WL Acetyl-CoA pathway for every phylum, enabling a detailed metabolic reconstruction and identification of the essential genes involved in the homoacetogenic and reverse WL pathways (Figure 5.3).

So far, all known SAOB are encompassed within the phylum *Firmicutes* and the enzyme formyltetrahydrofolate synthetase (FTHFS, EC 6.3.4.3) has been described as crucial for the SAO process (Sun et al., 2014). Despite that many primers have been designed to target the FTHFS gene, the involvement of this enzyme in other pathways hinders its potential use as a specific SAOB biomarker. In contrast, the acetyl-CoA synthase (EC 6.2.1.1; ACS) is exclusive to the acetyl-CoA pathway and, therefore, it might be a more accurate target for detecting acetogenic bacteria. Interestingly, this gene was very abundant in the PGs within *Bacteroidetes* and *Chloroflexi*. Based on this information, the results obtained in the present study suggest that unknown representatives in the phyla *Bacteroidetes* and *Chloroflexi* could be involved in the SAO process due to their potential capability for acetate assimilation/dissimilation. This hypothesis would agree with previous studies that evidenced the possible association of novel acetogens within these phyla (Barret et al., 2015). Furthermore, it has recently been proposed that some species from the *Thermotogae* phylum have the ability to syntrophically degrade acetate despite the fact that their WL pathway appears to be truncated (Nobu et al., 2015). This phenomenon would be possible thanks to the mediation of the glycine cleavage system (GCS), which was also detected in the transcriptome of the well-known SAOB *Syntrophaceticus schinkii* (Zhuang et al., 2015). Interestingly, genes encoding for the enzymes involved in the GCS pathway were found in the studied samples (Table 5.3). From the coverage values it was evident that this pathway was prevalent in R1 and R2 (Table 9.3) and could be reconstructed in PGs from *Chloroflexi* and *Bacteroidetes* (Figure 5.3).



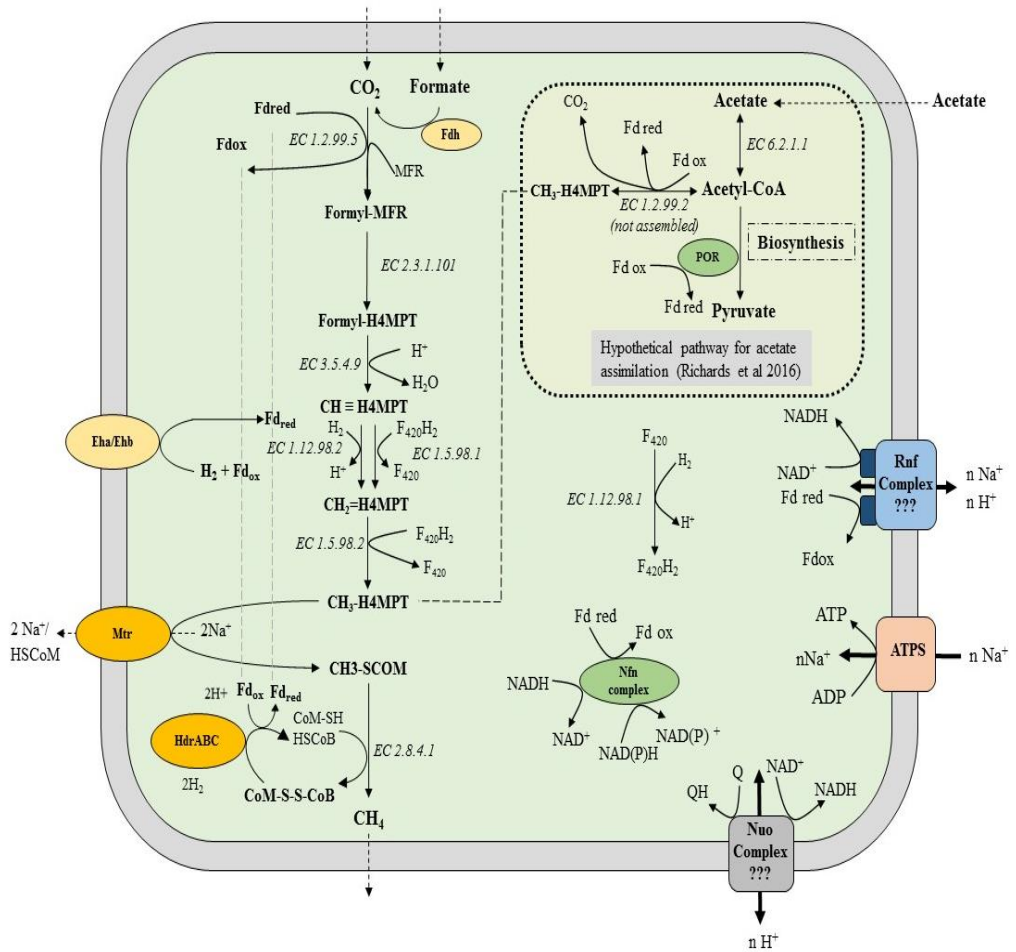


**Figure 5. 2** Hydrogentrophic methanogenesis and hypothetic acetate assimilation pathways, taken from Richard et al. 2016 and from the reconstructed Methanomicrobiales PGs.

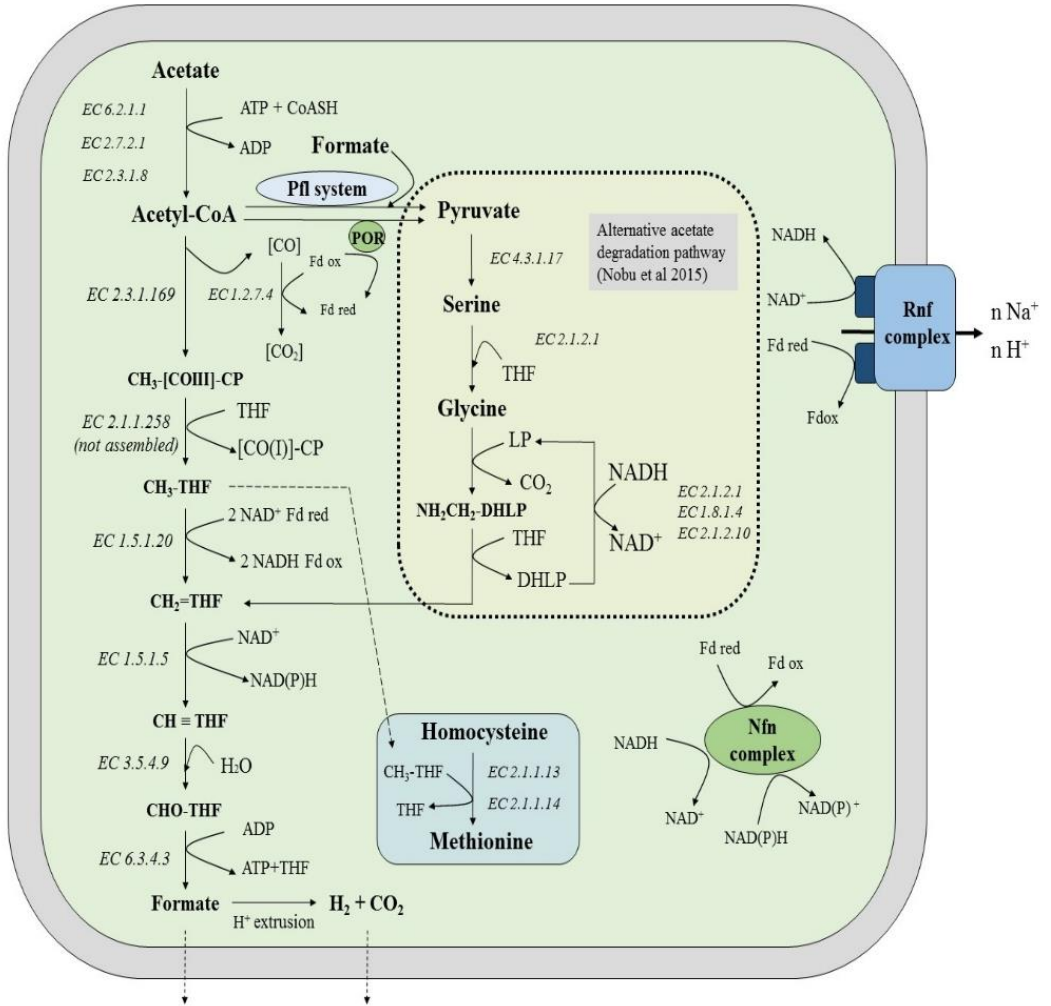


**Figure 5. 3** Hypothetic interaction between the WL and GCS metabolic pathways reconstructed from Bacteroidetes, Chloroflexi and Firmicutes genome bins.

It was also remarkable that PGs from both *Chloroflexi* and *Bacteroidetes* also presented a high abundance of the gene encoding for the pyruvate:flavodoxin oxidoreductase (POR, EC 1.2.7.1), which mediates the conversion of acetyl-CoA to pyruvate (Figure 5.3). This enzyme is involved in the generation of low-potential reductants, such as Fd or flavodoxin (Fv), and can be utilized in several processes, including hydrogen metabolism and nitrogen fixation. Furthermore, the obtained electrons must be removed in order to achieve a redox balance and regenerate the oxidized acceptor. That process could be carried out by a putative previous step to GCS pathway. Interestingly, genes encoding for enzyme mediators of the methionine metabolism from homocysteine were also clearly dominant in R1 and R2, and could be related with the GCS pathway concerning the pyruvate-formate lyase system (pfl) that is S-adenosylmethionine dependent. At the same time, this process is a constant source of folate molecules (THF), indispensable in the GCS pathway.

From the energetic point of view of acetogenesis, the WL and GCS pathways have been described to be equivalent in terms of ATP yield (Nobu et al., 2015). Alternatively, homoacetogens require the redox potential generated by bifurcating hydrogenases (Hattori et al., 2005). To achieve that potential, the Rnf and nfnAB genes complexes have been identified as proton-translocating ferredoxin:NAD<sup>+</sup> oxidoreductases. They contribute to the ATP synthesis by H<sup>+</sup>-translocating ATPases under both autotrophic and heterotrophic growth conditions and are required in the syntrophic degradation pathways (Frank et al., 2016; Nobu et al., 2015). Rnf encoding genes were identified mainly in *Bacteroidetes* PGs, but were also detected in some PGs from *Chloroflexi* and *Firmicutes*. These genes are involved in the energy-conservation system, as previously determined for known acetogens such as *C. kluyveri*, *A. woodii* and *C. ljungdablii* (Buckel and Thauer, 2013). On other hand, the Nfn cluster was also found in some *Chloroflexi* PGs and in the vast majority of *Bacteroidetes* PGs. This cluster is a paramount enzymatic complex for the acetogenic metabolism that catalyses the reversible transfer of electrons from reduced Fd and NADH to 2 NADP<sup>+</sup> (Mock et al., 2015). However, only the subunit B of the Nfn encoding gene (nfnB) could be sequenced in this study. The Nfn cluster has been found previously in *Thermotogae* and *Chloroflexi* and was involved in different syntrophic strategies (Nobu et al., 2015). Additionally, the fdhE (extra-cytoplasmic formate dehydrogenases) gene from *Firmicutes* and *Bacteroidetes* PGs was also assembled. This gene was described as specific in syntrophic bacteria (Worm et al., 2014). This latter work focused on butyrate and propionate degraders, but the present findings suggest a similar relationship in acetate degradation process.

In summary, the phyla *Chloroflexi* and *Bacteroidales* might harbour novel syntrophic partners of *Methanoculleus* spp. that would carry out the SAO process. In a recent review (Schink et al., 2017), the role of H<sub>2</sub> and formate as key players in methanogenic

degradation was discussed, since methanogens consume H<sub>2</sub> and/or formate at low concentrations in syntrophy with bacteria. Specific H<sub>2</sub> thresholds upon species could explain why growth on formate seems to be restricted to methanogens without cytochromes, such as in *Methanoculleus* spp. Moreover, formate can act as an interspecies electron and H<sub>2</sub> transfer, where both might be used alternatively or simultaneously as electron carriers, and pools are equilibrated by formate hydrogen lyase (FHL) where FDH is involved (Schink et al., 2017). The presence of *fdhD* and *E*, and the formate regulon *fhfA* as a decisive gene of the FHL complex in *Bacteroidales* and *Chloroflexi* genomic bins, supports a possible syntrophy with *Methanoculleus*, due the capacity to excrete formate. This hypothesis is supported by a recent study on the anaerobic degradation of long-chain n-alkanes (Liang et al 2016), in which species belonging to the *Anaerolineaceae* family (*Chloroflexi*) could act as formate producing acetogenic/SAOB, and formate would subsequently be employed by *Methanoculleus* in hydrogenotrophic methanogenesis.

Altogether, we hypothesize that, besides the well-known homoacetogens from the Firmicutes phylum, other bacterial species that are important for the SAO process are encompassed in the phyla *Bacteroidetes* and *Chloroflexi*. However, the possible metabolic pathway for the syntrophic oxidation of acetate remains unclear because both phyla contain the genes for WL and GCS metabolic routes. It seems highly probable that representatives of *Bacteroidetes* and *Chloroflexi* play a key role in biogas reactors subjected to high ammonia levels. Yet, despite the significant sequencing and metagenome reconstruction efforts of the present study, there are still uncertainties concerning the SAO process which deserve further research.

## 5.4 Conclusions

The current study demonstrates that the stable operation of common full-scale anaerobic digesters fed with high nitrogen loads can be achieved thanks to the selective enrichment of specific SAOB and HMA. An interdisciplinary approach was applied for this purpose based on the combination of isotopic-biogas profiles, the description of the active microbiome, and the functional characterization of the metagenome. Some novel aspects were identified thanks to the comparison between digesters subjected to high and low ammonia content. From the 73 PGs assembled successfully in this study only 7 could be assigned at the species level, evidencing the lack of knowledge on the microbial biodiversity in AD systems. Representatives of the phyla *Bacteroidetes* and *Chloroflexi* might harbour potential SAOB and an alternative syntrophic acetate degradation pathway via glycine cleavage system (GCS) is proposed. *Methanoculleus* was the main HMA partner and the hydrogenotrophic pathway was assembled.

Interestingly, a hypothetical route for the assimilation of acetate was also reconstructed for this archaeon.

## 5.5 References

- Ahring, B.K., Sandberg, M., Angelidaki, I., 1995. Volatile fatty acids as indicators of process imbalance in anaerobic digesters. *Appl. Microbiol. Biotechnol.* 43, 559–565.
- Angelidaki, I., Ahring, B.K., 1993. Thermophilic anaerobic digestion of livestock waste: the effect of ammonia. *Appl. Microbiol. Biotechnol.* 38, 560–564.
- Anil Kumar, P., Srinivas, T.N.R., Pavan Kumar, P., Madhu, S., Shivaji, S., 2010. *Nitritalea halalkaliphila* gen. nov., sp. nov., an alkaliphilic bacterium of the family “Cyclobacteriaceae”, phylum Bacteroidetes. *Int. J. Syst. Evol. Microbiol.* 60, 2320–2325.
- Barret, M., Gagnon, N., Morissette, B., Kalmokoff, M.L., Topp, E., Brooks, S.P.J., Matias, F., Neufeld, J.D., Talbot, G., 2015. Phylogenetic identification of methanogens assimilating acetate-derived carbon in dairy and swine manures. *Syst. Appl. Microbiol.* 38, 56–66.
- Borowski, S., Kubacki, P., 2015. Co-digestion of pig slaughterhouse waste with sewage sludge. *Waste Manag.* 40, 119–126.
- Braun, R., Huber, P., Meyrath, J., 1981. Ammonia toxicity in liquid piggery manure digestion. *Biotechnol. Lett.* 3, 159–164.
- Buckel, W., Thauer, R.K., 2013. Energy conservation via electron bifurcating ferredoxin reduction and proton/Na<sup>+</sup> translocating ferredoxin oxidation. *Biochim. Biophys. Acta.*
- Campanaro, S., Treu, L., Cattani, M., Kougias, P.G., Vendramin, V., Schiavon, S., Tagliapietra, F., Giacomini, A., Corich, V., 2017. In vitro fermentation of key dietary compounds with rumen fluid: A genome-centric perspective. *Sci. Total Environ.* 584–585, 683–691.
- Campanaro, S., Treu, L., Kougias, P.G., De Francisci, D., Valle, G., Angelidaki, I., 2016. Metagenomic analysis and functional characterization of the biogas microbiome using high throughput shotgun sequencing and a novel binning strategy. *Biotechnol. Biofuels* 9, 26.
- Conrad, R., Claus, P., Casper, P., 2009. Characterization of stable isotope fractionation during methane production in the sediment of a eutrophic lake, Lake Dagow, Germany. *Limnol. Oceanogr.* 54, 457–471.
- Cruz Vigg, C., Rossetti, S., Fazi, S., Paiano, P., Majone, M., Aulenta, F., 2014. Magnetite particles triggering a faster and more robust syntrophic pathway of methanogenic propionate degradation. *Environ. Sci. Technol.* 48, 7536–7543.
- De Francisci, D., Kougias, P.G., Treu, L., Campanaro, S., Angelidaki, I., 2015. Microbial diversity and dynamicity of biogas reactors due to radical changes of feedstock composition. *Bioresour. Technol.* 176, 56–64.
- Demirel, B., Scherer, P., 2008. The roles of acetotrophic and hydrogenotrophic methanogens during anaerobic conversion of biomass to methane: A review. *Rev. Environ. Sci. Biotechnol.* 7, 173–190.
- Du, Z., Zhang, Z., Miao, T., Wu, J., Lü, G., Yu, J., Xiao, J., Chen, G., 2011. Draft genome sequence of the novel agar-digesting marine bacterium HQM9. *J. Bacteriol.*
- Fotidis, I.A., Karakashev, D., Angelidaki, I., 2014. The dominant acetate degradation pathway/methanogenic composition in full-scale anaerobic digesters operating under different ammonia levels. *Int. J. Environ. Sci. Technol.* 11, 2087–2094.
- Fotidis, I.A., Karakashev, D., Angelidaki, I., 2013a. Bioaugmentation with an acetate-oxidising consortium as a tool to tackle ammonia inhibition of anaerobic digestion. *Bioresour. Technol.* 146, 57–62.

- Fotidis, I.A., Karakashev, D., Kotsopoulos, T.A., Martzopoulos, G.G., Angelidaki, I., 2013b. Effect of ammonium and acetate on methanogenic pathway and methanogenic community composition. *FEMS Microbiol. Ecol.* 83, 38–48.
- Frank, J.A., Arntzen, M.Ø., Sun, L., Hagen, L.H., McHardy, A.C., Horn, S.J., Eijsink, V.G.H., Schnürer, A., Pope, P.B., 2016. Novel Syntrophic Populations Dominate an Ammonia-Tolerant Methanogenic Microbiome. *mSystems* 1, e00092-16.
- Galperin, M.Y., Makarova, K.S., Wolf, Y.I., Koonin, E. V., 2015. Expanded Microbial genome coverage and improved protein family annotation in the COG database. *Nucleic Acids Res.* 43, D261–D269.
- Hansen, K.H., Angelidaki, I., Ahring, B.K., 1998. Anaerobic Digestion of Swine Manure: Inhibition By Ammonia. *Water Res.* 32, 5–12.
- Hattori, S., 2008. Syntrophic acetate-oxidizing microbes in methanogenic environments. *Microbes Environ.* 23, 118–127.
- Hattori, S., Galushko, A.S., Kamagata, Y., Schink, B., 2005. Operation of the CO dehydrogenase/acetyl coenzyme A pathway in both acetate oxidation and acetate formation by the syntrophically acetate-oxidizing bacterium *Thermacetogenium phaeum*. *J. Bacteriol.* 187, 3471–3476.
- Hedderich, R., 2004. Energy-Converting [NiFe] Hydrogenases from Archaea and Extremophiles: Ancestors of Complex I. *J. Bioenerg. Biomembr.* 36, 65–75.
- Kang, D.D., Froula, J., Egan, R., Wang, Z., 2015. MetaBAT, an efficient tool for accurately reconstructing single genomes from complex microbial communities. *PeerJ* 3, e1165.
- Kayhanian, M., 1994. Performance of a high-solids anaerobic digestion process under various ammonia concentrations. *J. Chem. Technol. Biotechnol.* 59, 349–352.
- Langille, M., Zaneveld, J., Caporaso, J.G., McDonald, D., Knights, D., Reyes, J., Clemente, J., Burkepile, D., Vega Thurber, R., Knight, R., Beiko, R., Huttenhower, C., 2013. Predictive functional profiling of microbial communities using 16S rRNA marker gene sequences. *Nat. Biotechnol.* 31, 814–21.
- Li, Q., Li, L., Rejtar, T., Lessner, D.J., Karger, B.L., Ferry, J.G., 2006. Electron transport in the pathway of acetate conversion to methane in the marine archaeon *Methanosarcina acetivorans*. *J. Bacteriol.* 188, 702–710. doi:10.1128/JB.188.2.702-710.2006
- Luo, H.W., Zhang, H., Suzuki, T., Hattori, S., Kamagata, Y., 2002. Differential expression of methanogenesis genes of *Methanothermobacter thermoautotrophicus* (formerly *Methanobacterium thermoautotrophicum*) in pure culture and in cocultures with fatty acid-oxidizing syntrophs. *Appl. Environ. Microbiol.* 68, 1173–1179.
- Lv, Z., Hu, M., Harms, H., Richnow, H.H., Liebetrau, J., Nikolauz, M., 2014. Stable isotope composition of biogas allows early warning of complete process failure as a result of ammonia inhibition in anaerobic digesters. *Bioresour. Technol.* 167, 251–259.
- Maus, I., Wibberg, D., Stantscheff, R., Eikmeyer, F.G., Seffner, A., Boelter, J., Szczepanowski, R., Blom, J., Jaenicke, S., König, H., Pühler, A., Schlüter, A., 2012. Complete genome sequence of the hydrogenotrophic, methanogenic archaeon *Methanoculleus bourgensis* strain MS2T, isolated from a sewage sludge digester. *J. Bacteriol.*
- Moore, L. V., Johnson, J.L., Moore, W.E., 1994. Descriptions of *Prevotella tanneri* sp. nov. and *Prevotella enoca* sp. nov. from the human gingival crevice and emendation of the description of *Prevotella zoogloformans*. *Int. J. Syst. Bacteriol.* 44, 599–602.
- Mosbæk, F., Kjeldal, H., Mulat, D.G., Albertsen, M., Ward, A.J., Feilberg, A., Nielsen, J.L., 2016. Identification of syntrophic acetate-oxidizing bacteria in anaerobic digesters. *ISME J.* 2, 1–14.
- Müller, B., Sun, L., Schnürer, A., 2013. First insights into the syntrophic acetate-oxidizing bacteria—a genetic study. *Microbiologyopen* 2, 35–53.

- Neubeck, A., Sjöberg, S., Price, A., Callac, N., Schnürer, A., 2016. Effect of nickel levels on hydrogen partial pressure and methane production in methanogens. *PLoS One* 11.
- Nobu, M.K., Narihiro, T., Rinke, C., Kamagata, Y., Tringe, S.G., Woyke, T., Liu, W.-T., 2015. Microbial dark matter ecogenomics reveals complex synergistic networks in a methanogenic bioreactor. *ISME J.* 9, 1710–1722.
- Overbeek, R., Olson, R., Pusch, G.D., Olsen, G.J., Davis, J.J., Disz, T., Edwards, R.A., Gerdes, S., Parrello, B., Shukla, M., Vonstein, V., Wattam, A.R., Xia, F., Stevens, R., 2014. The SEED and the Rapid Annotation of microbial genomes using Subsystems Technology (RAST). *Nucleic Acids Res.* 42.
- Parks, D.H., Imelfort, M., Skennerton, C.T., Hugenholtz, P., Tyson, G.W., 2015. CheckM: assessing the quality of microbial genomes recovered from isolates, single cells, and metagenomes. *Genome Res.* 25, 1043–55.
- Patil, K.R., Roune, L., McHardy, A.C., 2012. The phyloPythiaS web server for taxonomic assignment of metagenome sequences. *PLoS One* 7.
- Pelissari, C., Guivernau, M., Viñas, M., de Souza, S.S., García, J., Sezerino, P.H., Ávila, C., 2017. Unraveling the active microbial populations involved in nitrogen utilization in a vertical subsurface flow constructed wetland treating urban wastewater. *Sci. Total Environ.* 584–585, 642–650.
- Richards, M.A., Lie, T.J., Zhang, J., Ragsdale, S.W., Leigh, J.A., Price, N.D., 2016. Exploring hydrogenotrophic methanogenesis: A genome scale metabolic reconstruction of *Methanococcus maripaludis*. *J. Bacteriol.* 198, 3379–3390.
- Schink, B., Montag, D., Keller, A., Müller, N., 2017. Hydrogen or formate: Alternative key players in methanogenic degradation. *Environ. Microbiol.*
- Schnürer, A., Houwen, F.P., Svensson, B.H., 1994. Mesophilic syntrophic acetate oxidation during methane formation by a triculture at high ammonium concentration. *Arch. Microbiol.* 162, 70–74.
- Sun, L., Müller, B., Westerholm, M., Schnürer, A., 2014. Syntrophic acetate oxidation in industrial CSTR biogas digesters. *J. Biotechnol.* 171, 39–44.
- Thauer, R.K., Kaster, A.-K., Seedorf, H., Buckel, W., Hedderich, R., 2008. Methanogenic archaea: ecologically relevant differences in energy conservation. *Nat. Rev. Microbiol.* 6, 579–91.
- Treu, L., Kougias, P.G., Campanaro, S., Bassani, I., Angelidaki, I., 2016. Deeper insight into the structure of the anaerobic digestion microbial community; The biogas microbiome database is expanded with 157 new genomes. *Bioresour. Technol.* 216, 260–266.
- Wang, Q., Yang, Y., Yu, C., Huang, H., Kim, M., Feng, C., Zhang, Z., 2011. Study on a fixed zeolite bioreactor for anaerobic digestion of ammonium-rich swine wastes. *Bioresour. Technol.* 102, 7064–7068.
- Watson-Craik, I. a, Stams, a J., 1995. Anaerobic digestion. *Antonie Van Leeuwenhoek* 67, 1–2.
- Worm, P., Koehorst, J.J., Visser, M., Sedano-Nuñez, V.T., Schaap, P.J., Plugge, C.M., Sousa, D.Z., Stams, A.J.M., 2014. A genomic view on syntrophic versus non-syntrophic lifestyle in anaerobic fatty acid degrading communities. *Biochim. Biophys. Acta.* 1837, 2004–2016.
- Yenigün, O., Demirel, B., 2013. Ammonia inhibition in anaerobic digestion: A review. *Process Biochem.* 48, 901–911.
- Zhuang, L., Tang, J., Wang, Y., Hu, M., Zhou, S., 2015. Conductive iron oxide minerals accelerate syntrophic cooperation in methanogenic benzoate degradation. *J. Hazard. Mater.* 293, 37–45

# **Part III**

---

Influence of support material in anaerobic digestion



## **Chapter 6 Assessment of SAOB-HMA biofilms activity, based on isotopic gas profiling and microbiological characterization, under a high ammonia level**

---

In this chapter, seven biofilm carriers (zeolite, magnetite, nylon, steel, low-density polyethylene, graphite and polytetrafluoroethylene) were assessed to enhance the activity SAOB and HMA under 3.5 gN L<sup>-1</sup>, as ammonia. In the on-going study, the SAOB-HMA biofilm formation was successfully attained. The results suggest that magnetite and nylon could enhance the proliferation of SAOB and HMA, while zeolite avoided the presence of HMA, due to its capacity to retain ammonia and thus decreasing the stress induced by ammonia. The enrichment in SAOB was observed in those biofilms supported by magnetite, steel and graphite, satisfying the direct electron transfer process between these materials and syntrophic bacteria.

*Part of this chapter was presented as a poster in DAAL XII Peru conference.*

## 6.2 Introduction

Anaerobic systems comprise a complex community of hydrolytic, fermentative, syntrophic, homoacetogenic and methanogenic microorganisms. Fatty acids and H<sub>2</sub>, as main intermediates, might inhibit these systems and require syntrophic consumption to avoid unstable performance or biological dysfunction of anaerobic digesters (AD) (Chauhan et al., 2005). In fact, acetate accumulation is being commonly used as indicator of methanogenesis unbalance (Nguyen et al., 2015), specially in those AD where AMA are responsible for near 70% of methane production under no inhibitory conditions. HMA were responsible of the remaining 30% (Angelidaki and Ahring, 1993).

The HMA, with higher ammonia and acetate tolerance (Wang et al 2015), have gain interest because their relation with syntrophic SAOB, a homoacetogenic bacteria. AD communities with a clear enrichment or population shift towards SAOB – HMA tandem have been recently reported, when submitted to high total ammonia nitrogen (TAN) levels (> 3-7 gTAN L<sup>-1</sup>) (Fotidis et al., 2014; Westerholm et al., 2012), although the low growth rate of SAOB (70 days of duplication time (Westerholm et al., 2012) in contrast with 12 days of duplication for AMA (Mori et al., 2012)). Little is known about the biodiversity of SAOB, though it appears that there are a number of clearly distinct clusters of mesophilic and thermophilic species in AD submitted to ammonia inhibition (Yenigün and Demirel, 2013). Identified SAOB reported in literature are *Clostridium ultunense* strain BST (Schnürer et al., 1996); *Syntrophacetivus schinkii* (Westerholm et al., 2010); *Tepidanaerobacter acetatoxydans* (Westerholm et al. 2011); AOB (Lee and Zinder, 1988); *Thermacetogenium phaeum* strain PB (Hattori et al., 2000) or *Thermotoga lettingae* (Balk et al., 2002).

The immobilization of syntrophic consortia, as biofilms or granules, improves the transfer of intermediates, due to the reduction of the interspecies distance and local H<sub>2</sub> and/or acetate threshold limits (Chauhan et al., 2005). Biofilms consist of a hydrated mix of bacterial cells and their extracellular polymeric substances plus cations and particulate matter. The use of carriers is known as enhancement strategy of the methane production and the substrate conversion yields in AD (Henze and Harremoes, 1983). They present several advantages to the bacteria over a planktonic mode of existence, such increased resistance or adaptation to environmental stresses, as shock loadings, pH, temperature changes, or to mitigate the effect of toxics and inhibitors (Li and Liu, 2017; Karadag et al., 2015).

The biofilm development has distinct steps, from single cells adhesion by van del Waals forces or polar interactions of H-bond type (Renner and Weibel, 2011), to the extension of microbial colonization. Any of these steps depends on properties of carriers

(roughness, hydrophobicity, surface charge) and cell walls (composition, hydrophobicity) (Li and Liu, 2017; Renner and Weibel, 2011) of microbial strains.

Good adhesion of methanogenic consortia on clays, alumina-based ceramics, polymeric materials (nylon, polyethylene-glycol, polytetrafluoroethylene, etc.), metal carriers (iron oxide, magnetite, etc.) and stainless steel has been reported (Chauhan et al., 2005; Zhao et al., 2007; Sheng et al., 2008; Li and Logan, 2004; Hellman et al., 2010; Ahammad et al., 2013; Fuchslocher Helleman et al., 2013). The use of zeolites and active carbon under TAN inhibitory levels has been reported (Cuetos et al., 2017): authors reported that zeolites, presenting a high local conductivity, caused an increase in the apparent kinetic constant of the process resulting in values twice those observed in control reactors (Montalvo et al., 2012).

Activity is also favoured by electrically conductive materials, such as magnetite or activated carbon that promote direct interspecies electron transfer (DIET), a more effective mechanism for interspecies electron exchange than indirect transfer via the production of reduced molecules such as H<sub>2</sub> and formate (Cruz Viggli et al., 2014; Ramm et al., 2014).

Therefore, the colonization of support materials might enhance syntrophic associations in aggregates and thus, the methanogenic activity (Sanchez et al., 1994), but studies on packing for SAOB - HMA is still very preliminary.

The aim of this work was to evaluate seven support materials to assess the activity of SAOB – HMA, in a rich TAN and mesophilic environment. In this study, moreover the identification of known methanogens and the already identified SAOB, the quantification of the expression level of support-attached and planktonic species was assessed by means RT-qPCR. To gain a deeper insight on the microbial community structure, the high throughput sequencing of 16S rRNA-based cDNA libraries was also implemented. A direct biofilm observation by confocal scanning laser microscopy (CSLM), together with indexes as methanogenic activity and isotopic labelling fractionation of the biogas, was done.

## 6.3 Materials and methods

### 6.3.1 Experiment

The inoculum for this experiment was collected in a mesophilic full-scale stirred reactor (Lleida, Spain), running at stationary state with a average hydraulic retention time of 65 days and organic loading rate of 2 kgCOD m<sup>-3</sup> d<sup>-1</sup>. The influent contained pig manure and food waste cosubstrates, that produced a mean TAN content of 3.2-4.5 gN-TAN L<sup>-1</sup> in the effluent. The inoculum was characterised by a total VFA concentration of 5.3 gAcetate-eq L<sup>-1</sup>, being the acetate the main VFA (66% total VFA), volatile suspended solids (VSS) of 25.8 gVSS L<sup>-1</sup> and 2.1 gTAN L<sup>-1</sup>.

Methanogenic batch assays on acetate at 35°C were performed in triplicate using glass vials of nominal volume of 120 mL. Each vial was fulfilled with 60 mL of inoculum and 18 mL of support material, flushed with N<sub>2</sub> gas and hermetically closed. A control without any support material (inoculum alone) was prepared in parallel. Seven support material were used (Table 7.1): zeolite, magnetite, nylon, polytetrafluoroethylene (PTFE), steel, graphite and low density polyethylene (LDPE). Each material took up the 30% of the inoculum volume per vial, accounting different quantities due to the diverse density of these materials: 18 g for zeolite and graphite, 20 g for nylon and PTFE, 79 g for magnetite, 18 g for LDPE, 7 g for steel.

The TAN inhibitory level of this experiment was set-up in 3.5 g TAN L<sup>-1</sup> based on (Kayhanian, 1994), which reported TAN inhibitory values >2.5 gTAN L<sup>-1</sup>, and moreover when this is a common concentration in industrial reactors treating animal manure, food wastes or slaughter waste house (Ruiz-Sánchez et al., 2018). There is a wide range of free ammonia nitrogen (1.7-14 gTAN L<sup>-1</sup>) reported as AD inhibitor in literature (Chen et al., 2008) and even studies that have been reported TAN concentrations extremely high, from 19 to 25 g TAN L<sup>-1</sup> (Poirier et al., 2017).

The experiment was divided into two parts. In the first part (days 0 to 79), the enhancement of activity and the biofilm formation, even under TAN inhibitory conditions, were the objective. A minimum quantity (1.5 mL per vial) of a buffered (a solution at pH 8 with sodium bicarbonate 1 g L<sup>-1</sup>) concentrated solution of NH<sub>4</sub>Cl and sodium acetate was added at day 0 (pulse 1a) to adjust the initial acetate in 3.5 gAcetate L<sup>-1</sup> in each vial. A second acetate pulse was done at day 43 of part 1 (pulse 1b), to attain again the initial acetate value of 3.5 gAcetate L<sup>-1</sup> (Table 7.2). Only in this second pulse labelled acetate (Sigma Aldrich, Spain), that accounted the 10% of total initial acetate, was added in order to measure the isotopic fractionation of the biogas once the CH<sub>4</sub> production stopped (day 69).

In the second part (days 70 to 150), biofilms alone were evaluated. Therefore, 60 mL of the liquid of each vial was carefully removed with a sterile syringe and replaced by the same volume of mineral medium (table S1) in order to selectively leave the biofilm attached on the carrier material and remove the major part of suspended microorganisms. Similarly to part 1, the acetate and TAN levels were adjusted (1.4 gAcetate L<sup>-1</sup> and 3.5 gTAN L<sup>-1</sup>) (Table 7.2), adding 1.5 mL per vial of the previously concentrated acetic and TAN solutions. Two pulses were also performed (pulses 2a and 2b). The concentration of acetic acid, other VFA (propionic, butyric, valeric, caproic, hexanoic) and TAN in the liquid media per vial was determined just after each pulse of acetate.

**Table 6. 1** Mineral medium composition

Micronutrients sol – 80 µL·L <sup>-1</sup>	
NiCl <sub>2</sub> ·6H <sub>2</sub> O	0.125g·L <sup>-1</sup>
FeCl <sub>2</sub> ·6H <sub>2</sub> O	25 g·L <sup>-1</sup>
(NH <sub>4</sub> ) <sub>6</sub> MO <sub>7</sub> O <sub>2</sub> ·4H <sub>2</sub> O	1.25 g·L <sup>-1</sup>
CoCl ·12H <sub>2</sub> O	0.075 g·L <sup>-1</sup>
Macronutrients sol 1 – 1mL·L <sup>-1</sup>	
NH <sub>4</sub> Cl·12H <sub>2</sub> O	17 g·L <sup>-1</sup>
Macronutrients sol 2 – 1mL·L <sup>-1</sup>	
KHPO <sub>4</sub>	3.7 g·L <sup>-1</sup>
Macronutrients sol 3 – 1 mL·L <sup>-1</sup>	
MgSO <sub>4</sub>	0.56 g·L <sup>-1</sup>
Macronutrients sol 4 – 1 mL·L <sup>-1</sup>	
Ca <sub>2</sub> Cl <sub>2</sub> ·2H <sub>2</sub> O	0.8 g·L <sup>-1</sup>

Headspace biogas volume and composition (CH<sub>4</sub>, CO<sub>2</sub>) were determined along the assay (day 0-150). The whole cumulative methane (parts 1 and 2 of the experiment) was fitted to a modified Gompertz equation (Eq.1).

Eq. (1)

$$B = B_0 \cdot \{x \cdot \exp(-\exp[(\mu_1 \cdot e/B_0) \cdot (\lambda_1 - t) + 1]) + (1-x) \cdot \exp(-\exp[(\mu_2 \cdot e/B_0) \cdot (\lambda_2 - t) + 1])\}$$

Where, B is cumulative methane yield (LCH<sub>4</sub> kgCOD-*t*) at time t (days); B<sub>0</sub> is the ultimate methane yield (LCH<sub>4</sub> kgCOD-*t*); μ<sub>1</sub> and μ<sub>2</sub> are the methane production rate

( $LCH_4$  kgCOD- $^{-1}$  d. $^{-1}$ ) of each acetate pulse;  $e$  is the Euler's number (2.7182);  $\lambda_1$  and  $\lambda_2$  is the lag phase period (days) or the minimum time required to produce methane after each acetate addition. The  $B_0$ ,  $x$ ,  $\mu_1$ ,  $\lambda_1$ ,  $\mu_2$  and  $\lambda_2$  were determined using the non-linear regression with the aid of Solver function of the Microsoft Excel Tool Pack. The squared correlation coefficient ( $R^2$ ) was used to evaluate the precision of the model fit.

**Table 6.2** Main characteristics of the different support media added to each batch analysis

Support	Supplier	Granulometry	Composition
Zeolite	Horticola Pedralbes	1 – 3 mm	Clinoptilolite: 85%; cristobalite:8%; clay:4%; plagioclase:3%; TiO $_2$ :0,1-0,3%; quartz traces
Magnetite	LKAB	3 – 6 mm	Fe $^{2+}$ Fe $^{23+}$ O $_4^{2-}$ 100%
Nylon	Dejay distributions	3 mm	Du Pont nylon resin zytel 100%
LDPE	Sigma Aldrich	4 mm	Low density polyethylene 100%
Steel	Schulpen Schum	filament 1 mm thickness	C:0,02%; Mn:0,09%; P:0,007%; S:0,0078%; Si:1,08%; Cu:0,029; Ni:10%; Cr:18,5%; V:0,041%; Mo:0,004%; Co:0,09%; Fe:71,1%
Graphite	Enviro-cell	2 – 4 mm	Carbon 100%
PTFE	Dejay distributions	3 mm	Tetrafluoroethylene

In parallel, both total eubacteria (16S rRNA gene) and methanogenic archaea (*mcrA* gene) of both support-attached and planktonic cells were quantified, by means of qPCR and RT-qPCR, from samples taken in the methane exponential production phase (day 70). The presence of biofilms on each support was qualitatively evaluated by confocal scanning laser microscopy (CSLM). The active population in the developed biofilms was assessed with high throughput sequencing of 16S rRNA-based cDNA (MiSeq Illumina platform) (see Chapter 3 for more details).

### 6.3.2 Confocal scanning laser microscopy (CSLM)

The standard operating procedure of the CSLM was applied, in which a sterile coverglass was mounted in a metal ring that was stuck to the material with double-sided tape. The metal ring was then attached to the microscope and could be moved laterally with a xy-translation stage. In this way, a target of interest could be positioned in the

focused laser beam. The sample was previously stained with Hoechst 33342 (Life technologies), the confocal measurements were performed at room temperature using confocal Leica TCS SP5. Laser stabilized at 405 nm was used for excitation, and confocal laser scanning signals were collected between 425 and 485 nm, always working at 10x objective.

## **6.4 Results and discussion**

### **6.4.1 Part 1 – CH<sub>4</sub> production with suspended and attached biomass**

In the first part of the activity test, two acetate pulses (1a and 1b in Table 7.2) were done to boost the activity and the biofilm formation through the TAN level. The evolution of methane was monitored along the whole experiment, while acetate and total VFA were measured just before each acetate addition (Figure 7.1). The inoculum contained a high level of total VFA, which was also methanised. The activation of the inoculum after the addition of the materials was demonstrated with a general increased rate and a reduced lag phase for all vials (Table 7.2). Some exception to this behaviour was revealed: those nylon, LDPE and PTFE amended vials showed a longer lag phase for the depletion of the second acetate addition. Opposite, the introduction of zeolite and magnetite improved 3 times the rate of the control, and reduced the lag phase from 12 days (control) to 0-4 days (amended vials) after the second acetate pulse of the activation step. The methane yield attained was between the 63% and 95% of the maximum yield at the end of the activation (part 1), finding the lowest yield in the control vials (164 NLCH<sub>4</sub> kgCOD<sup>-1</sup>). The effect of the support introduction was especially evident with magnetite (333 NLCH<sub>4</sub> kgCOD<sup>-1</sup>), zeolite (304 NLCH<sub>4</sub> kgCOD<sup>-1</sup>), LDPE (275 NLCH<sub>4</sub> kgCOD<sup>-1</sup>) and nylon (260 NLCH<sub>4</sub> kgCOD<sup>-1</sup>), reaching a near 2-fold yield increase regarding the control, mainly due to a positive effect favoured with the addition of these materials on the production rate under inhibitory conditions. A second level of methane yield increment was attained in those vials with steel, graphite and PTFE (242, 222 and 230 NLCH<sub>4</sub> kgCOD<sup>-1</sup>, respectively) that showed lower increase compared with the control in the part 1. This different methane yield could be due to the high energy expenditure required in the formation of new biomass to develop biofilm colonies.

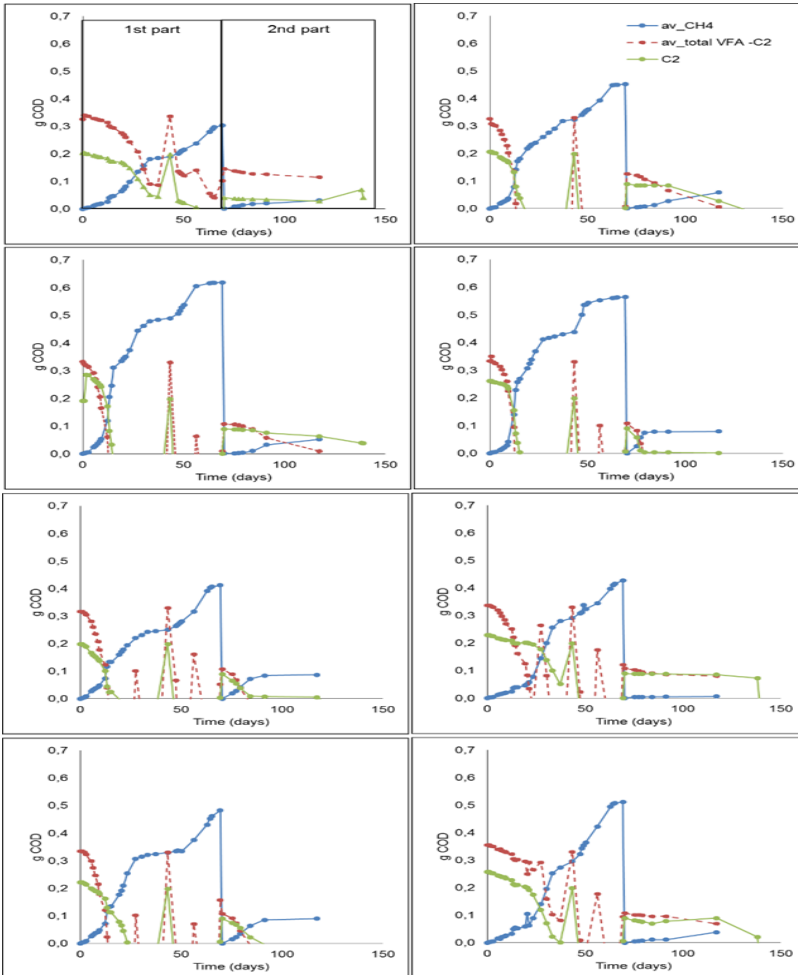


**Figure 6. 1** Evolution of mean cumulative methane, acetic and VFA, expressed as COD-equivalents. Left top to bottom: control, magnetite, graphite, nylon. Right, top to bottom: steel, zeolite, PTFE, LDPE. Blue-methane part 1 & 2. Green- cetic. Red – total VFA minus a



At the end of this activation part, the C isotope fractionation pattern in the biogas was determined. The CH<sub>4</sub> generated by CO<sub>2</sub> reduction tended to be more depleted in <sup>13</sup>C than that formed directly from acetate (Conrad et al., 2005; Conrad et al., 2009). An exclusively or predominant hydrogenotrophic path, including the control vials, was found. Only zeolite amended vials showed a clear and exclusively acetoclastic methanogenic pathway, which agreed with the significant decrement of the TAN content in these vials (0.67 - 0.85 and 2.4 gN L<sup>-1</sup> in parts 1 and 2 of the experiment, respectively; Table 7.2) due to the ion-exchange capability of zeolite (cv, 2014) and the described high affinity with acetate of AMA in low N and rich acetate environments (Jetten et al., 1992). Opposite, the TAN level was constant throughout the experiment in 3.5 gN L<sup>-1</sup> (equivalent to FAN 450 mgN L<sup>-1</sup> at pH 7 and 35°C) in the other cases.

The inoculum had a bacterial community with *Firmicutes* (86%), *Bacteroidetes* (4%) and *Synergistetes* (7%) as the most abundant phyla (Figure 7.1). This relative high abundance of Synergistetes indicate that this phylum could have a major importance in N and VFA rich anaerobic environments. In fact, this phylum is considered heterotrophic amino acid-degrading anaerobic microbes (Godon et al., 2005) and they are involved in the turnover of aminoacids (Milton et al., 2015).

Among all materials, the introduction of zeolite and magnetite aroused a greater shift in the profile of lesser abundant bacterial phyla. Chloroflexi (relative abundance of 6%) was clearly activated with both materials, while active Planctomycetes (relative abundance of 3%) and Proteobacteria (relative abundance of 4%) were more abundant with zeolite and magnetite supports respectively.

The isotopic fractionation pointed out the activity of exclusively HMA in the control vials, also confirmed within the characterization of the methanogens at the end of the activation part 1. The relative abundance of active *Methanosarcina* and *Methanosaeta* in the inoculum almost disappeared in the control batches, but it was improved in the LDPE and zeolite after the acetate pulses under the initial TAN level of 3.5 gN L<sup>-1</sup> (Figure 7.1b). Contrary, HMA *Methanomassiliicoccus* improved its abundance with all supports, except PTFE and nylon, at the end of the activation.

The biogas production enhancement in the magnetite batches suggests that the mineral could facilitate the bioelectrochemical syntrophy in the direct electron transfer between microorganisms (Cruz Viggì et al., 2014). A similar effect was found in rice paddy sediments where magnetite stimulated methane production and the enrichment of *Geobacter* species, which could donate electrons more efficiently to methanogens, which were also enriched (Liu et al., 2014).

**Table 6. 3** Set-up and results of the batch tests with different supports: acetate and TAN concentration at the end of different pulses, methane yield, rate and lag phase, isotopic fractionation ( $\alpha_c$  values of each material at exponential phase of second pulse)

Material	Pulse	Initial	Final	Fitting	$\mu$ (NLCH <sub>4</sub> kgCOD <sup>-1</sup> d <sup>-1</sup> )	B <sub>0</sub> (NLCH <sub>4</sub> kgCOD <sup>-1</sup> )	EXP	Isotopic	Fractionation
		Acetate (g L <sup>-1</sup> )	TAN (gN L <sup>-1</sup> )	$\lambda$ (days)			% max yield	$\alpha_c$ values*	Methanogenic pathway
Zeolite	1a	3.5	0.67	8	15.7				Exclusively acetoclastic
	1b	3.5	0.85	0	27.6	304 ±14	87	0.69 ± 0.01	
	2a	1.4	2.4	4	14.0	214 ±24	61		
Magnetite	1a	3.5	3.5	7	13.2				Exclusively
	1b	3.5	3.5	4	22.7	333 ±27	95	1.11 ± 0.00	hydrogenotrophic
	2	1.4	3.5	9	2.5	175 ±8	50		
Nylon	1a	3.5	3.5	7	8.0				Exclusively
	1b	3.5	3.5	14	14.2	260 ±55	74	1.11 ± 0.00	hydrogenotrophic
	2	1.4	3.5	3	5.0	243 ±49	43		
LDPE	1a	3.5	3.5	15	7.9				Exclusively
	1b	3.5	3.5	12	21.3	275 ±49	79	1.10 ± 0.01	hydrogenotrophic
	2	1.4	3.5	4	0.5	152 ±33	69		
Steel	1a	3.5	3.5	7	10.3				Predominance
	1b	3.5	3.5	0	8.3	242 ±18	69	1.07 ± 0.03	Hydrogenotrophic
	2	1.4	3.5	5	0.9	236 ±29	44		
Graphite	1a	3.5	3.5	5	7.2				Predominance
	1b	3.5	3.5	7	7.7	222 ±36	63	1.07 ± 0.03	Hydrogenotrophic
	2	1.4	3.5	3	5.0	236 ±29	27		
PTFE	1a	3.5	3.5	16	5.7				Exclusively
	1b	3.5	3.5	15	17.0	230 ±75	66	1.08 ± 0.02	hydrogenotrophic
	2	1.4	3.5	0	0.1	95 ±59	67		
Control	1a	3.5	3.5	9	3.5				Exclusively
	1b	3.5	3.5	12	8.6	164 ±13	47	1.09 ± 0.00	hydrogenotrophic
	2	1.4	3.5	1	1.5	84 ±7	24		

**Table 6. 4** Compilation of data for the support assessment

media	A*S	A*S	A*S	A	A	A	A
Support	Yield increment	Rate improvement	Isotopic fr.	Yield increment	Rate improvement	Known SAO	CLSM
Zeolite	85%	3	ama	162%	9		
<b>Magnetite</b>	<b>103%</b>	<b>3</b>	<b>hama</b>	<b>112%</b>	<b>2</b>		
<b>Nylon</b>	<b>59%</b>	<b>2</b>	<b>hama</b>	<b>197%</b>	<b>3</b>		
LDPE	68%	2	hama	83%	0		no biofilm
Steel	48%	1	sobre todo hama	85%	1		aggregates
Graphite	35%	1	sobre todo hama	189%	3		
PTFE	40%	2	hama	16%	0		

A-attached; S- planktonik

#### 6.4.2 Part 2 – CH<sub>4</sub> production with attached biomass

In the second part, the activity of the biofilm was assessed after removing the planktonic cells and, therefore a lower acetate addition was done in this experimental part to avoid the substrate inhibition of the remaining cells. In fact, a reduced rate and CH<sub>4</sub> yield reflected the decrement of active biomass.

The best yields were attained with nylon (251 NLCH<sub>4</sub> kgCOD<sup>-1</sup>), graphite (244 NLCH<sub>4</sub> kgCOD<sup>-1</sup>) and zeolite (221 NLCH<sub>4</sub> kgCOD<sup>-1</sup>), followed by vials with steel (156 NLCH<sub>4</sub> kgCOD<sup>-1</sup>), magnetite (179 NLCH<sub>4</sub> kgCOD<sup>-1</sup>) and LDPE (154 and 84 NLCH<sub>4</sub> kgCOD<sup>-1</sup>). The PTFE amended vials and controls reached the lowest but similar yield (98 and 84 NLCH<sub>4</sub> kgCOD<sup>-1</sup>).

With zeolite supports, a mitigated TAN effect again improved the methane yield and rate: an increment of 162% for the methane yield, compared to control vials, and the highest rate (9 times greater than the control) was attained with this biofilm. The zeolite was not renewed at the beginning of part 2 of the experiment and therefore, it might be partially saturated leading to a lower soluble TAN decrement in part 2 than in part 1. As it has been described, zeolite is widely used as cation adsorbent, including ammonia (Zhou and Boyd, 2014) and is a well-known support material to enhanced anaerobic digestion, as described Fotidis et al (2014). Furthermore, this improvement could also be related with the micro and macronutrients that were introduced in the zeolite before the incubation, as well as, provide microhabitats for microorganism immobilization (Weiß et al., 2013).

The reported beneficial effect of iron oxides in AD (Cruz Viggi et al., 2014) fitted well with magnetite amended vials, that reached a high yield increment (112% regarding the control), but did not reduced the rate (1.6 times the rate in control vials), after the removal of the suspended biomass. In contrast, with graphite support, all three, rate, lag phase and yield reached better results than magnetite vials. The highest yield, better than zeolite, and the second best production rate increment was found within graphite support. In the presence of graphite, the lag phase in part 1 was 5-6 days, but it decreased till 3 days without the planktonic cells, similarly to the rest of vials. This enhancement could be because graphite has the beneficial effect that facilitates the establishment of electrothrophic biofilm with an increment of active biomass (Pisciotta et al., 2012). Furthermore, graphite is also related to DIET stimulation, as described Zhao et al., (2015) who observed an improvement of CH<sub>4</sub> production introducing graphite electrodes in their system. This phenomenon is related with the utilization of CO<sub>2</sub>, H<sub>2</sub> and electrons transports through graphite for microbial electrosynthesis, and

consequently CH<sub>4</sub> production. Therefore, this could be the reason because isotopic profile also evidenced the predominance of HMA.

Those vials with polymeric supports (nylon, PTFE and LDPE) evolved not the same, depending the polymer. Similarly, to graphite vials, the lag phase in nylon, PTFE and LDPE vials was clearly reduced ( $\leq 3$ -4 days) in the second part of the experiment. However, the methane yield reached the lowest values for PTFE (98 NLCH<sub>4</sub> kgCOD<sup>-1</sup>) while nylon vials attained the best yield (251 NLCH<sub>4</sub> kgCOD<sup>-1</sup>). Considering that polymers do not have the capability to limit the ammonia levels in the liquid media, it was suggested that the main factor was the biofilm formation mechanism.

With steel support, the lag phase was again reduced but the methane production rate was small, also as LDPE and PTFE vials. However, an +85% methane yield increment was shown, close to that observed with LDPE. These results suggested that steel, like graphite and magnetite, is susceptible to be a shuttle material for electron exchange that favours CH<sub>4</sub> production. However, the low roughness of steel diffculted the bacterial adhesion thus avoiding biofilm formation. It is hypothesized that biomass aggregates were formed instead of a proper biofilm, based on visual revision of these vials (Figure 6.6).

### 6.4.3 Microbial population

The microbial population, planktonic and attached biomass, was characterized at the end of part 1 based assessed by Miseq sequencing analysis of active bacteria and archaeal communities. Quantification of total (genes) and active (transcripts) bacterial and archaeal communities was based on qPCR analysis. In addition, CSLM images were taken to confirm the presence or absence of biofilms on the surface of the different materials (Figure 7.6). Samples were taken in the exponential phase of CH<sub>4</sub> production to identify active population dynamics or changes induced by the supports.

Based on DNA quantification (total populations) a similar presence of 16S rRNA and *mcrA* was revealed in the liquid media of all vials (Figure 6.4a and 6.4c). Regarding support material, bacterial activity showed a similar behaviour in the control, steel, magnetite and zeolite vials (Fig. 6.4b), but it was enhanced in graphite, PTFE, nylon and LDPE. That results complemented with Miseq analysis based on cDNA (active population) showed a common pattern with *Bacteroidetes* and *Firmicutes* as predominant active phyla in all liquid media (Figure 6.2), that became clearly dominated by *Firmicutes* in the biofilms. The profile of minority active phyla changed, standing out the increment of *Proteobacteria* possibly due to this group of microbes have bacterial lipopolysaccharides in their outer membrane facilitating the attachment on surface carrier (Atabek and Camesano, 2007). And it was also showed the decrement of

*Chloroflexi* in the supports, with the exception of zeolite vials where this last phylum maintained its activity. *Chloroflexi* was not detected, even as minority, in the inoculum nor in the control.

Regarding methanogens, the population was present in all liquid media and support materials, except zeolite (DNA neither cDNA were found), but active methanogens were only quantified on graphite (Fig. 6.4d). Concerning archaeal communities (Figure 1b), results revealed that profile changes were caused by TAN concentration, regarding the inoculum. The main archaea belonged to *Methanoculleus*, *Methanobacterium* and *Methanomassiliicoccus*, more resistant to ammonia inhibition (Wang et al., 2015). The abundance of *Methanoculleus* and *Methanobacterium* was in agreement with isotopic profile, which indicated the predominance or exclusively hydrogenotrophic methanogenesis (Table 6.2). This fact has been previously described by Wang et al., (2015) who found an increment of *Methanoculleus*, at the expenses of *Methanosaeta*, because their low tolerance to FAN. Furthermore, it is reported that *Methanoculleus* plays a major role in nitrogen-rich environments because its capability to perform a syntrophic relation with SAOB, usually described as homoacetogenic bacteria that mainly belong to *Firmicutes* phylum (Sun et al., 2014). This distributed profile between *Firmicutes* and *Bacteroidetes* in the amended vials matched with recent studies described a putative enrolment of *Bacteroidetes* as homoacetogenic bacteria (Ruiz-Sánchez et al., 2018).

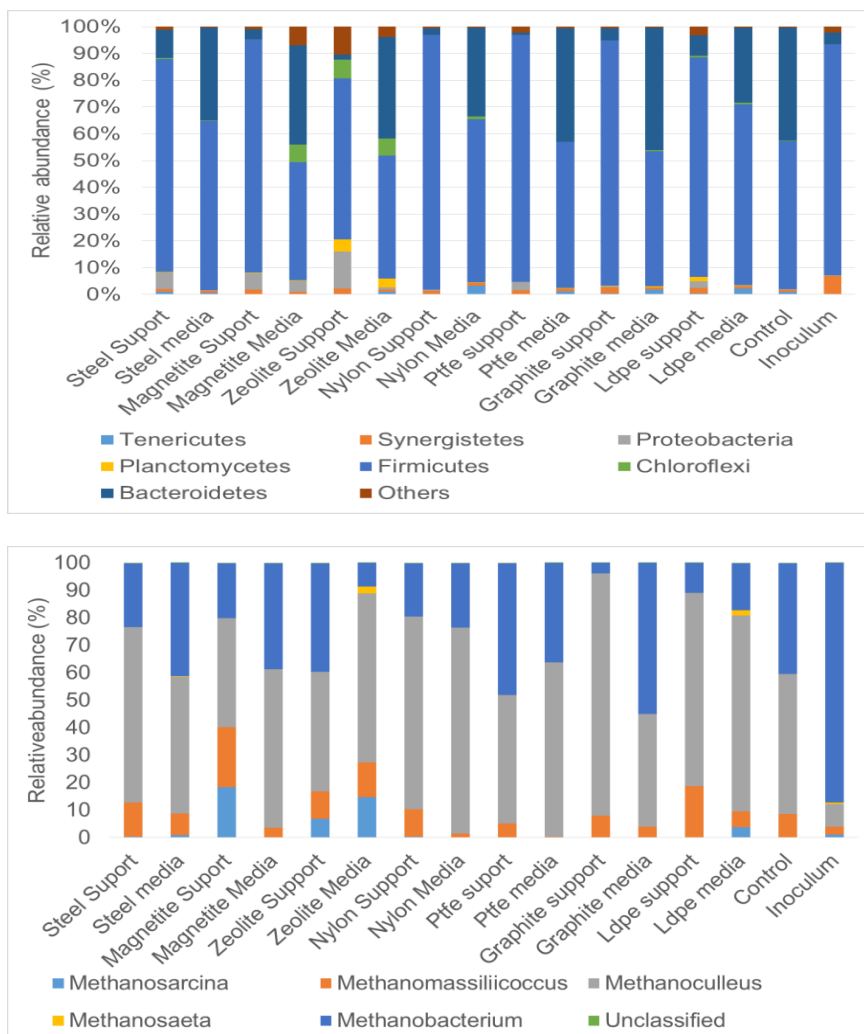


**Figure 6. 2** Taxonomy classification (a) at phylum level of bacteria community and (b) at genera level of archaeal community, based on 16S rRNA (cDNA).

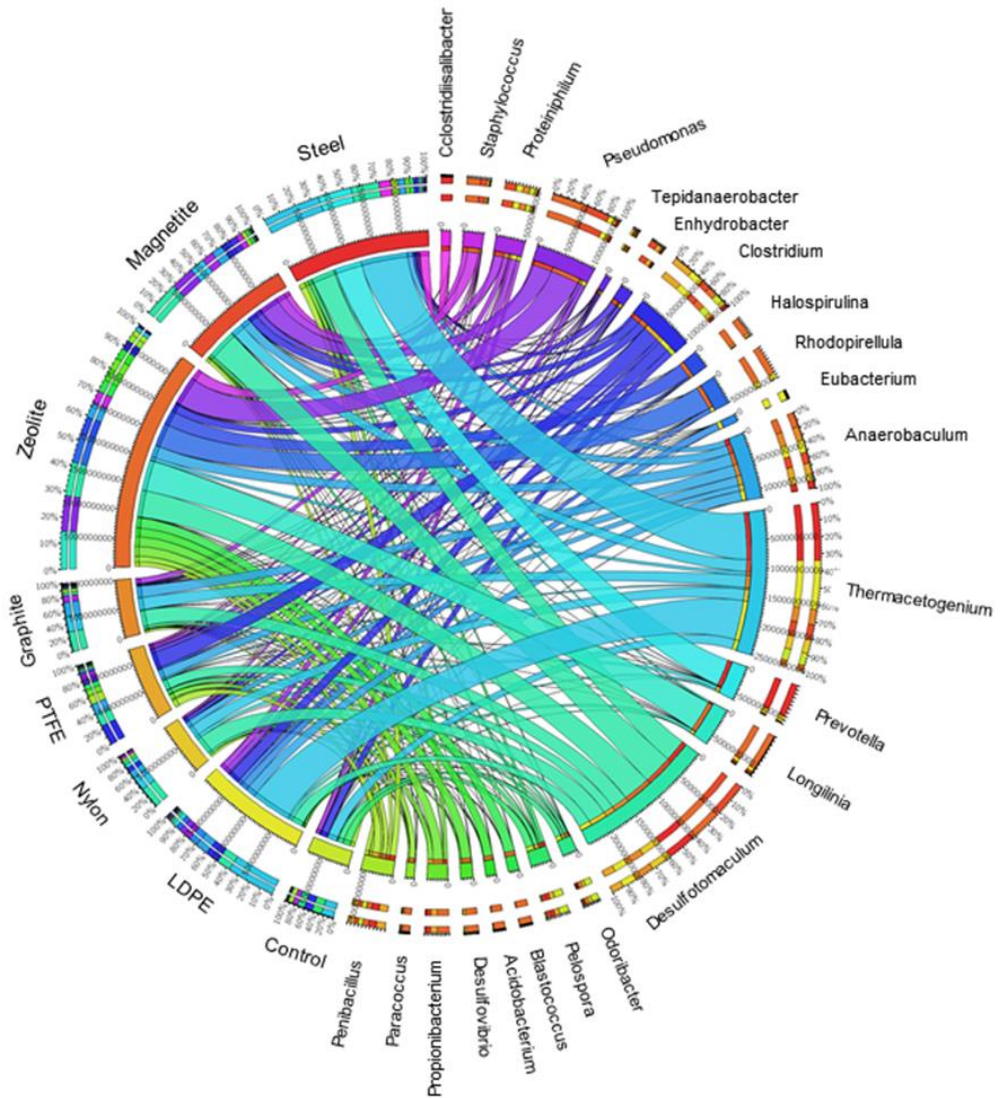


**Figure 6.3** Chord diagram showing those genus with a relative abundance > 1% in the planktonic biomass samples, using the open software CIRCOS (Krzyszowski, M., et al. 2009).



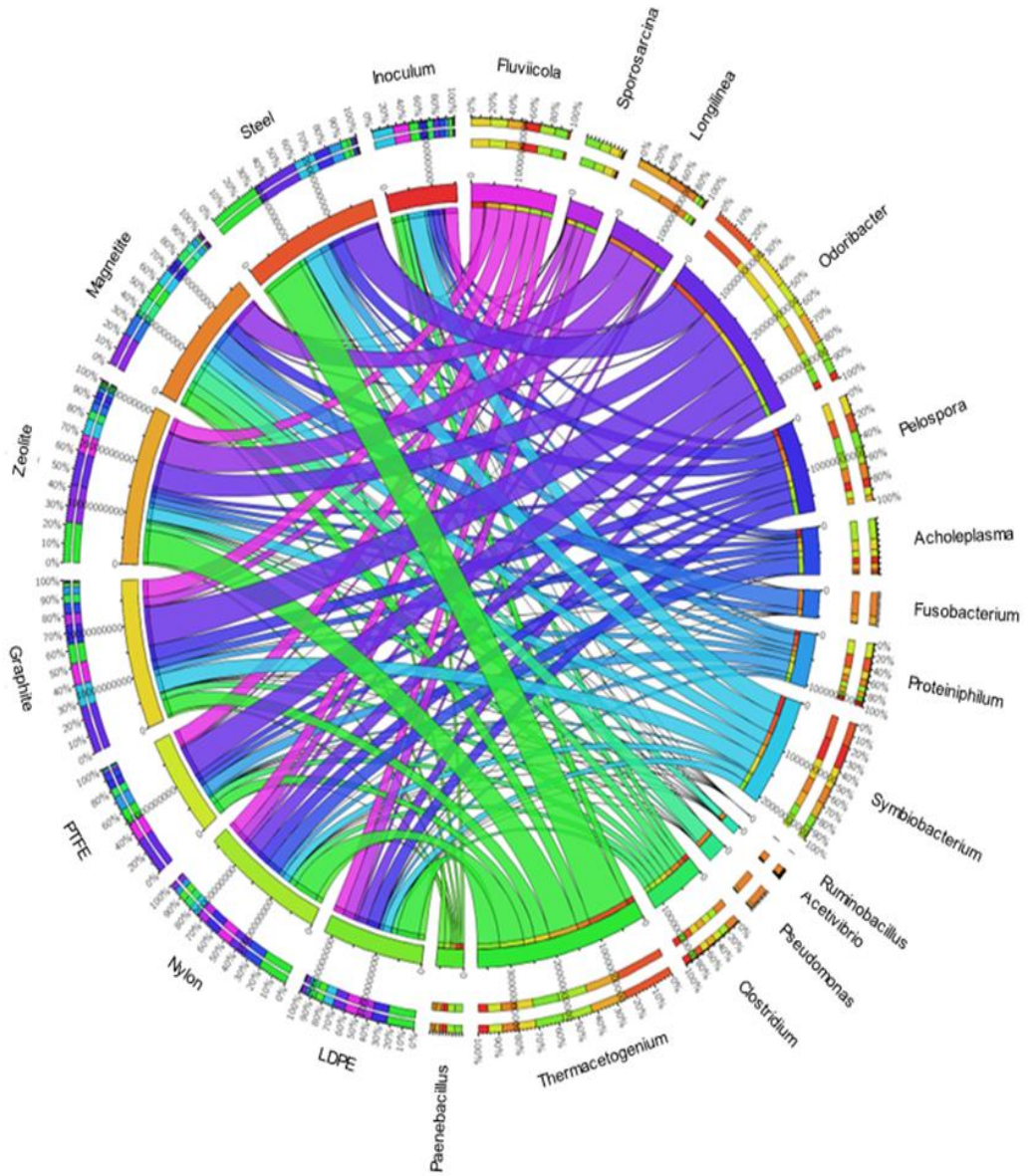


**Figure 6. 4**Chord diagram showing those genus with a relative abundance > 1% in the attached biomass samples, using the open software CIRCOS (Krzyszowski, M., et al. 2009).Microbial communities in the biofilms

Other active genera as *Methanosarcina* and *Methanosaeta* were minor (< 0.1%) in all the cases. The lonely exception was zeolite and LDPE vials that also had a 15% abundance of *Methanosarcina* in the liquid media, but only remained active on the zeolite support (relative abundance of 7%).

With zeolite material, through confocal analysis, it was confirmed the capacity of zeolite to retain biomass (Figure 6.6a). The lower FAN concentration prompted the proliferation of facultative acetoclastic methanogens, as *Methanosarcina* and *Methanosaeta* (15% and 2% of relative abundance, respectively), suspended in the liquid media, and keeping *Methanosarcina* active in the support (Figure 6.2b). In the bacterial domain, zeolite vials showed the most assorted community: *Firmicutes* (60%), *Proteobacteria* (14%) and *Chloroflexi* (7%) were the most abundant phyla in both the support surface and in the liquid media. Curiously, *Plancomycetes* and *Actinobacteria* (relative abundance < 5%) only appeared active in zeolite amended vials. Li et al., (2016) described that *Planctomycetes* showed high sensitivity to high FAN levels (> 30 mgN L<sup>-1</sup>). Moreover, as shown on Figures 6.2 and 6.3, vials amended with zeolite were the most biodiverse due to the lower ammonia concentration. This evidence is in accordance with previous studies (Dai et al., 2016; Gao et al., 2015) that describe similar trend. Interestingly, the most relevant genera in zeolite was *Longilinia* and *Thermoacetogenium*. The predominant OTU belonging to *Longilinia* was OTU\_11, with 89% of similarity to *Longilinea arvoryzae* isolated from from methanogenic propionate-degrading consortia (Yamada et al., 2007). Meanwhile, *Thermoacetogenium* genera was dominated by OTU\_7 that was assigned with 99% of similarity to *Syntrophaceticus schinkii*, a well-known SAO bacteria (Westerholm et al., 2010). This results are quiet expected because this bacteria is directly associated to anaerobic digesters, however, this contradictory results (*Thermoacetogenium* in qiime – *Syntrophaceticus* in Blast) evidenced the necessity to standardized bioinformatics and databases procedures.

With magnetite material, a rather uneven biofilm development was observed on the magnetite surface (Figure 6.6), but the relatively medium methane production rate of the attached biomass indicates that suspended archaeal biomass was largely responsible for the biogas of these vials. The isotopic fractionation indicated a hydrogenotrophic pathway and therefore, the active archaeal community (Figure 6.1b) revealed that HMA dominated: *Methanoculleus* and *Methanobacterium* in the liquid media; *Methanoculleus* (40%), *Methanomassilicoccus* (21%), *Methanobacterium* (20%) in the support. The presence of *Methanosarcina* (18%) attached to this support was explained because *Methanosarcinaceae* is a versatile population able to perform both hydrogenotrophic and acetoclastic methanogenesis, as well as, their enrolment in SAO function under high nitrogen stress conditions was evidenced before (De Vrieze et al., 2012; Hao et al., 2015). Regarding bacterial communities, dominant phyla in liquid were *Firmicutes* (44%), *Bacteroidetes*

(37%), *Chloroflexi* (6%) and *Proteobacteria* (4%), while *Firmicutes* (87%), *Proteobacteria* (6%) and *Bacteroidetes* (4%) were mainly attached on the support.

The DIET phenomenon prompted by magnetite might favoured syntrophic relationship between microbes. *Proteobacteria* (*gammaproteobacteria* class), that was found as an active bacteria in the liquid media of magnetite vials; include prominent families related with exoelectrogens bacteria as *Geobacteraceae* and *Desulfuromonadaceae* (Zhang et al. 2009). *Firmicutes* (mainly, *Desulfotomaculum* genus revealed in figures 6.2 and 6.3, as a dominant phylum in this vials, are described as able to perform syntrophic acetate and/or propionate oxidation process interacting with HMA in nitrogen-rich environment (Nordgård et al., 2017). Furthermore, by means of a blastn analysis of partial 16S rRNA sequences regarding already known SAOB *C.ultunense*, *T.acetatoxydans* and *S.schinkii* (similarity > 97%) (Figure 7.5) were found. For example, *S.schinkii* was a SAOB relatively abundant in both the support surface and the liquid media (23% and 3%, respectively).

With graphite support, due to the irregular and leaf surface of graphite granules, the biofilm observed through CLSM was discontinuous (Figure 6.6), finding biomass aggregates mainly in the clefts of the material. However, a significant activity was observed on the graphite (table 6.2) based on high methane yields. The archaeal population on the support was formed by *Methanoculleus* (88%), *Methanomassillicoccus* (8%) and *Methanobacterium* (4%). In parallel, the bacterial community was almost totally dominated by *Firmicutes* (92%), dominated by *Desulfotomaculum* and *Symbiobacterium* genus (Figure 6.2 and 6.3). That tendency was very similar to that observed in magnetite vials, possibly due to DIET phenomenon also improved by graphite material (Zhao et al., 2015); however, the comparison with known SAOB (Figure 6.5) found out a lower abundance than in magnetite support. Previous phylogenetic studies (Oshima et al., 2011) revealed high similarity between both genera (*Desulfotomaculum* and *Symbiobacterium*) and reports that are closely related to *Morella thermoacetica*, an acetogenic bacterium commonly used to study the Wood-Ljungdahl pathway. This evidence suggested the enrolment of both genera in acetate consumption supplying H<sub>2</sub> and CO<sub>2</sub> for H<sub>2</sub>-utilizers methanogens. Interestingly, Shimoyama et al., (2009) described the interaction between acetogenic bacteria and methanogenic archaea mediated by flagella, a similar syntrophic interactions that could occur between *Symbiobacterium* and HM.

With polymeric supports (nylon, PTFE and LDPE), the CLSM assessment showed a very different superficial distribution of the attached biomass and biomass retention. Nylon balls were extensively colonised (Figure 6.6e), while PTFE had an external thin film (Figure 6.6b) and LDPE was slightly colonised (Figure 6.6f). Differences in the

hydrophobic or hydrophilic nature of the different surfaces (Liu et al., 2004), together with other parameters (roughness, porosity, specific area, etc.) might influence the formation of biofilms. Some previous studies revealed that hydrophobic surfaces stimulate cell-to-cell and cell-surface interactions between bacterial consortia, thereby enhancing the formation of aggregates (Liu et al., 2002). Hydrophobic bacteria tend to attach better to hydrophobic (as polypropylene and PTFE) than to hydrophilic (as nylon and polysulfone) surfaces. Syntrophic bacteria and methanogens possess hydrophobic cell surfaces and are expected to adhere well to hydrophobic matrices (Chauhan et al., 2005). Contradictory, our results revealed different evidences. According to manufacturer description, the water absorption for nylon, PTFE and LDPE was 1.5%, 0.0005% and 0.001%, respectively, which suggested that hydrophilic behaviour of nylon could facilitate the microbial adhesion and hence increase CH<sub>4</sub> production.

Regarding microbial profile, the isotopic profile that showed a total predominance of HM was confirmed: *Methanoculleus* (70%, 47% and 70%) and *Methanobacterium* (19%, 48% and 11% on nylon, PTFE and LDPE, respectively) totally dominated. A subtle abundance of *Methanosarcina* (0.3%) was observed on the nylon support. The main OTU related to *Methanosarcina* in the present study was 98% similar, based on blastn alignment, to *Methanosarcina flavescens* sp. that showed the ability to perform both methanogenic pathway AMA and HMA, opposite to the generalised assumption that the activity of *Methanosarcina* is exclusively acetoclastic in rich-TAN environments (Hao et al., 2015). Regarding the bacterial community, the active population was also dominated by *Firmicutes* (95%, 92% and 82% on nylon, PTFE and LDPE, respectively), very similar to other supports. Interestingly the blastn analysis (Figure 6.5) revealed that up to 23% of OTUs from biofilm samples on nylon corresponded to well-known SAOB *S.schinkii*, suggesting that this could be favoured in the presence of magnetite and nylon.

With steel support, the CLSM images showed discontinuous but homogenous biofilm development, similar to biofilm on graphite or magnetite surface. The methane yield clearly decreased when planktonic biomass was removed suggesting that active archaea were located in liquid media. Curiously, the black layer was observed above steel support after incubation time, revealing that a corrosion process occurred. This evidence jointly with the intermediate yield of this biofilm suggested that biogas production might be enhanced by means of a DIET process, as recently described by Li et al. (2017). Mainly active archaea enrolled in that process were *Methanoculleus* (50%), *Methanobacterium* (41%) and *Methanomassillicoccus* (8%) (Figure 6.1b). Meanwhile, *Firmicutes* (80%) (dominated mainly by *Thermoacetogenium* genus, (Figures 6.2 and 6.3), *Bacteroidetes* (11%) and *Proteobacteria* (6%) were relevant to eubacterial community in the biofilm.

Again, similar to magnetite communities, *Proteobacteria* appeared as an active community, reinforcing the hypothesis of DIET phenomenon occurred.

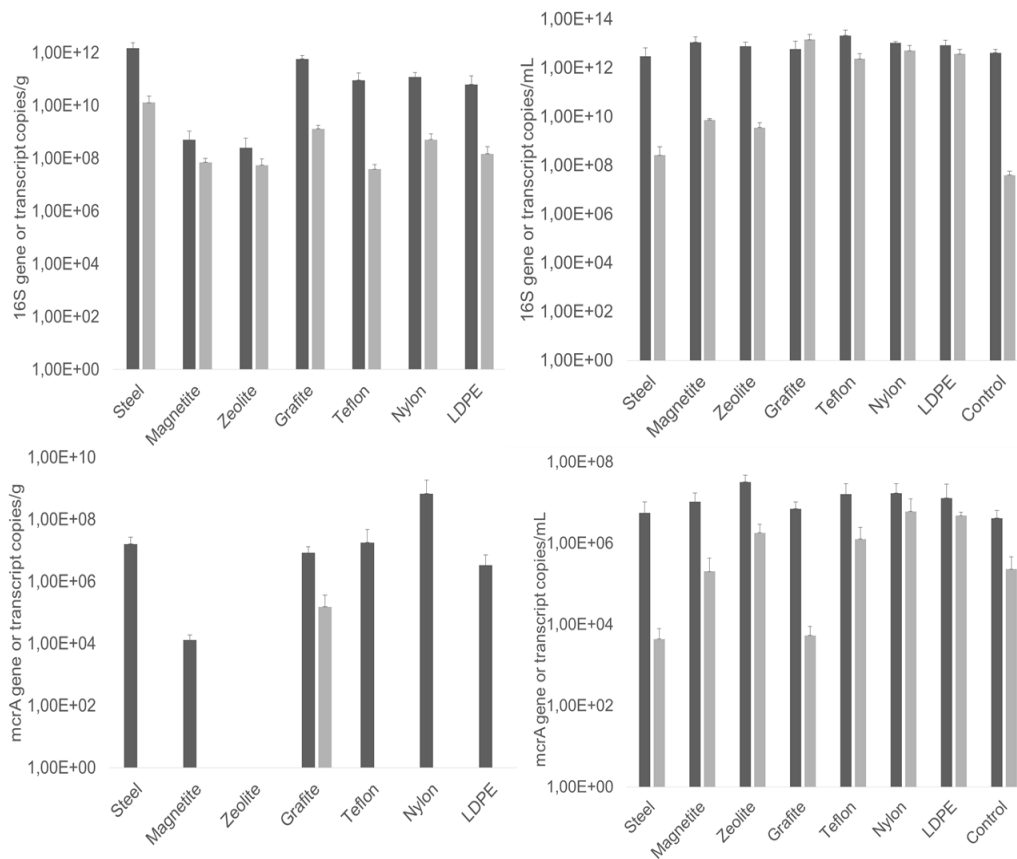


**Figure 6. 5** qPCR results of the planktonic and attached biomass samples. Dark grey bars are gene copies and light grey are transcript. Dark grey bars are gene copies and light grey are transcript. A.16SrRNA support B.16SrRNA liquid; C. mcrA support D.mcrA liquid

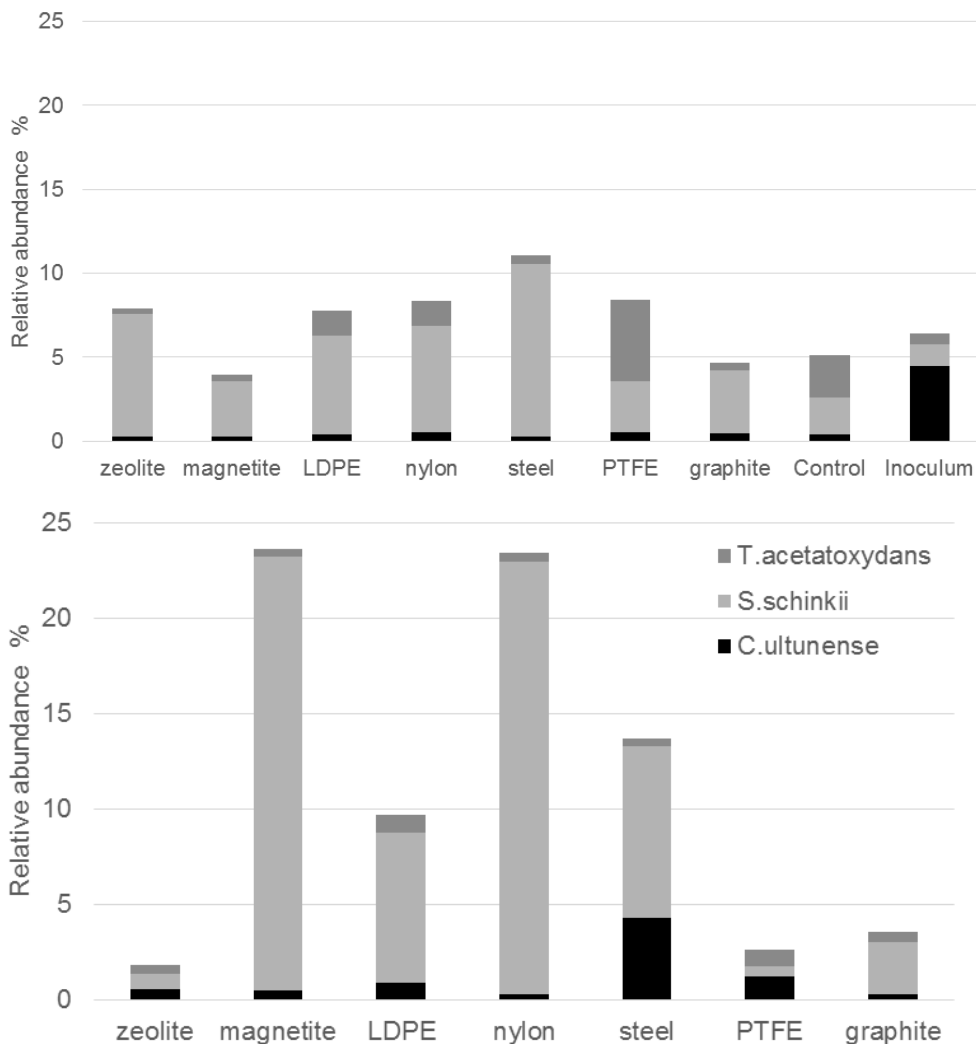


**Figure 6. 6** Figure 6.6 SAOB relative abundance (cDNA), based on 96% of similarity to SAOB literature-described species: (a) attached over the supports or (b) in suspension in the liquid media. Colours: *C. ultunense*, black; *S. schinkii*, light grey; *T. acetatoxydans*,

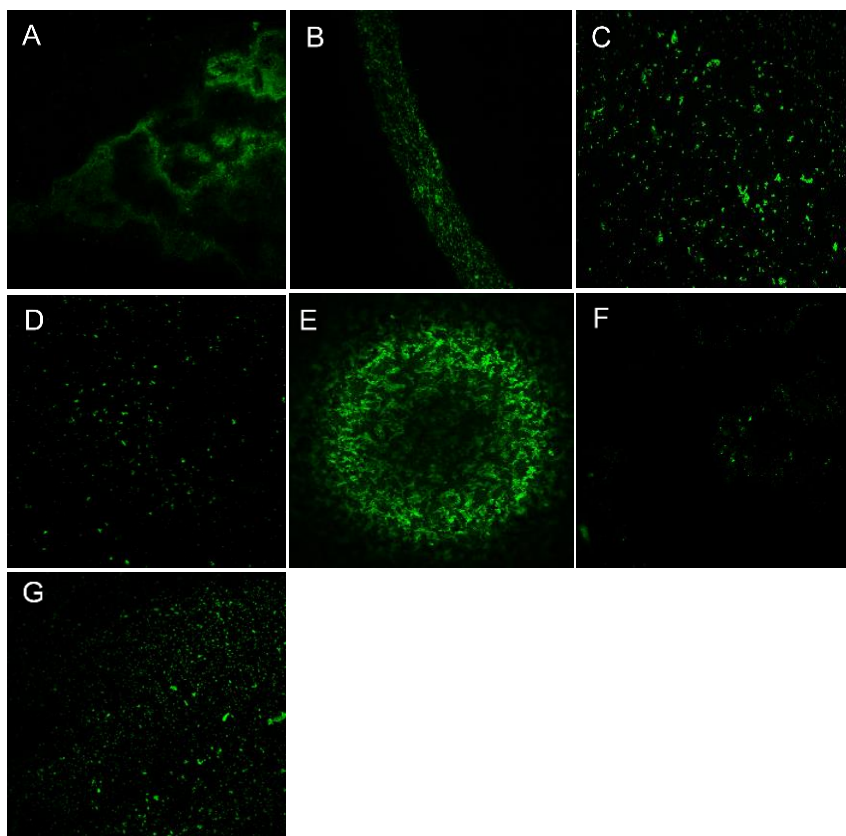


**Figure 6. 7** Confocal laser microscopy images of different support materials. Images: A zeolite; B PTFE; C graphite; D magnetite; E nylon; F LDPE; G steel.

#### **6.4.4 General outcomes**

It was demonstrated that the support material had a strong influence on all different biofilms development and its microbial community structure. These results suggested that different mechanisms were affecting the methane production, besides the predominant methanogenic pathways and prompted different effect depending on the material. table 6.3 compiles the main outputs of the assesment.

The biogas isotopic fractionation showed that the HMA activity was preserved, except in the zeolite amended vials with a clear shift towards the acetoclastic route. Zeolite is widely used as cation adsorbent, including ammonia; so, the lower free ammonia concentration in the liquid medium prompted the proliferation of AMA, but also retained active biomass forming a biofilm on its surface.

The addition of steel and graphite slightly decreased the HMA ascendency on methanogenesis, and intermediate methane yields and production rates were shown. In general, graphite amended vials had better response tha steel but nay known SAOB was identified in biofilms.

The best production rate and yields were shown in biofilms developed on magnetite and nylon, having the last a denser biofilm. Moreover, a clear enrichment of SAOB, when comparing to known SAOB, was clearly attained in both magnetite and nylon biofilms. In the case of magnetite, steel and graphite, syntrophy might be favoured by the direct electron transfer between microorganisms due to their exoelectrogenic nature, but it did not endorsed the formation of dense biofilms.

Finally, the polymeric materials LDPE and PTFE did not show SAOB-HMA biofilm formation, also showing the lowest methane production rates (part 2 of the experiment). The assessed polymers (nylon, PTFE and LDPE), usually used for biomass retention, showed the prevailing effect of the hydrophobicity of the support on the cells attatchment process, being the nylon support that one with a clear thick and even film.

#### **6.5 Conclusions**

It was demonstrated the strong influence of support material on biofilms development and its microbial community structure, as well as it was evidenced that it can get an overcoming of ammonia inhibition by following different mechanisms. Regardless of the phenomenon that was occurring in each material, it was noted that some of them have a greater efficiency in the retention and stimulation of SAOB proliferation, facilitating a major tolerance and resistance to nitrogen stress. Furthermore, research is



currently underway to confirm the beneficial effects of these materials in continuous anaerobic digesters in a view to overcome the inhibition caused by nitrogen-rich substrates.

## 6.6 References

- Ahammad, S.Z., Davenport, R.J., Read, L.F., Gomes, J., Sreekrishnan, T.R., Dolfing, J., Heidrich, E.S., Curtis, T.P., Dolfing, J., McCarty, P.L., Bae, J., Kim, J., McCarty, P.L., Smith, D.P., 2013. Rational immobilization of methanogens in high cell density bioreactors. *RSC Adv.* 3, 774–781.
- Angelidaki, I. & Ahring, B.K. 1993. Thermophilic anaerobic digestion of livestock waste: the effect of ammonia. *Appl Microbiol Biotechnol* 38: 560
- Atabek A, Camesano, T. 2007 Atomic Force Microscopy Study of the Effect of Lipopolysaccharides and Extracellular Polymers on Adhesion of *Pseudomonas aeruginosa*
- Balk, M., Weijma, J., Stams, A.J.M., 2002. *Thermotoga lettingae* sp. nov., a novel thermophilic, methanol-degrading bacterium isolated from a thermophilic anaerobic reactor. *Int. J. Syst. Evol. Microbiol.* 52, 1361–1368.
- Chauhan A., Ogram A. 2005. Evaluation of support matrices for immobilization of anaerobic consortia for efficient carbon cycling in waste regeneration. *Biochemical and Biophysical Research Communication* 327(3), 884–893.
- Chen, Y., Cheng, J.J., Creamer, K.S., 2008. Inhibition of anaerobic digestion process: A review. *Bioresour. Technol.* 99, 4044–4064.
- Conrad, R., 2005. Quantification of methanogenic pathways using stable carbon isotopic signatures: A review and a proposal. *Org. Geochem.* 36, 739–752.
- Conrad, R., Claus, P., Casper, P., 2009. Characterization of stable isotope fractionation during methane production in the sediment of a eutrophic lake, Lake Dagow, Germany. *Limnol. Oceanogr.* 54, 457–471.
- Cruz Viggì, C., Rossetti, S., Fazi, S., Paiano, P., Majone, M., Aulenta, F., 2014. Magnetite particles triggering a faster and more robust syntrophic pathway of methanogenic propionate degradation. *Environ. Sci. Technol.* 48, 7536–7543.
- Cuetos, M.J., Martínez, E.J., Moreno, R., Gonzalez, R., Otero, M., Gomez, X., 2017. Enhancing anaerobic digestion of poultry blood using activated carbon. *J. Adv. Res.* 8, 297–307.
- Dai, X., Yan, H., Li, N., He, J., Ding, Y., Dai, L., Dong, B., 2017. Metabolic adaptation of microbial communities to ammonium stress in a high solid anaerobic digester with dewatered sludge. *Sci. Rep.* 7.
- Dang, H., Lovell, C.R., 2017. Microbial Surface Colonization and Biofilm Development in Marine Environments. *Microbiol. Mol. Biol. Rev.* 80, 91–138.
- De Vrieze, J., Hennebel, T., Boon, N., Verstraete, W., 2012. Methanosarcina: The rediscovered methanogen for heavy duty biomethanation. *Bioresour. Technol.* 112, 1–9.
- Fotidis, I.A., Wang, H., Fiedel, N.R., Luo, G., Karakashev, D.B., Angelidaki, I., 2014. Bioaugmentation as a solution to increase methane production from an ammonia-rich substrate. *Environ. Sci. Technol.* 48, 7669–7677.
- Fuchslocher Hellemann, C., Grade, S., Heuer, W., Dittmer, M.P., Stiesch, M., Schwestka-Polly, R., Demling, A. P., 2013. Three-dimensional analysis of initial biofilm formation on polytetrafluoroethylene in the oral cavity. *J. Orofac. Orthop.* 1–10.

- Gao, S., Zhao, M., Chen, Y., Yu, M., Ruan, W., 2015. Tolerance response to in situ ammonia stress in a pilot-scale anaerobic digestion reactor for alleviating ammonia inhibition. *Bioresour. Technol.* 198, 372–379.
- Godon, J.J., Morinière, J., Moletta, M., Gaillac, M., Bru, V., Delgènes, J.P., 2005. Rarity associated with specific ecological niches in the bacterial world: The “Synergistes” example. *Environ. Microbiol.* 7, 213–224.
- Hao, L., Lü, F., Mazéas, L., Desmond-Le Quéméner, E., Madigou, C., Guenne, A., Shao, L., Bouchez, T., He, P., 2015. Stable isotope probing of acetate fed anaerobic batch incubations shows a partial resistance of acetoclastic methanogenesis catalyzed by *Methanosarcina* to sudden increase of ammonia level. *Water Res.* 69, 90–99.
- Hattori, S., Kamagata, Y., Hanada, S., Shoun, H., 2000. *Thermacetogenium phaeum* gen. nov., sp. nov., a strictly anaerobic, thermophilic, syntrophic acetate-oxidizing bacterium. *Int. J. Syst. Evol. Microbiol.* 50, 1601–1609.
- Henze, M., Harremoës, P., 1983. Anaerobic treatment of wastewater in fixed film reactors - A literature review. *Water Sci. Technol.* 15,1-101
- Karadag, D., Körollu, O.E., Ozkaya, B., Cakmakci, M., 2015. A review on anaerobic biofilm reactors for the treatment of dairy industry wastewater. *Process Biochem.* 50, 262–271.
- Kayhanian, M., 1994. Performance of a high-solids anaerobic digestion process under various ammonia concentrations. *J. Chem. Technol. Biotechnol.* 59, 349–352.
- Krzywinski, M.I., Schein, J.E., Birol, I., Connors, J., Gascoyne, R., Horsman, D., Jones, S.J., Marra, M.A. 2009. Circos: An information aesthetic for comparative genomics. *Genome Res.* Published in Advance June 18, 2009,
- Lee, M.J., Zinder, S.H., 1988. Hydrogen partial pressures in a thermophilic acetate-oxidizing methanogenic coculture. *Appl. Environ. Microbiol.* 54, 1457–61
- Li, T., Liu, J. 2017. Rapid formation of biofilm grown on gas-permeable membrane induced by famine incubation. *Biochem. Eng. J.* 121, 159-162.
- Li B., Logan B. E. 2004. Bacterial adhesion to glass and metal-oxide surfaces. *Colloids and surfaces B: Biointerfaces* 36(2), 81-90.
- Militon, C., Hamdi, O., Michotey, V., Fardeau, M.L., Ollivier, B., Bouallagui, H., Hamdi, M., Bonin, P., 2015. Ecological significance of Synergistetes in the biological treatment of tuna cooking wastewater by an anaerobic sequencing batch reactor. *Environ. Sci. Pollut. Res.* 22, 18230–18238.
- Montalvo, S., Guerrero, L., Borja, R., Sánchez, E., Milán, Z., Cortés, I., Angeles de la la Rubia, M., 2012. Application of natural zeolites in anaerobic digestion processes: A review. *Appl. Clay Sci.*
- Mori, K., Iino, T., Suzuki, K.I., Yamaguchi, K., Kamagata, Y., 2012. Aceticlastic and NaCl-requiring methanogen “*Methanosaeta pelagica*” sp. Nov., isolated from marine tidal flat sediment. *Appl. Environ. Microbiol.* 78, 3416–3423.
- Nordgård, A.S.R., Bergland, W.H., Vadstein, O., Mironov, V., Bakke, R., Østgaard, K., Bakke, I., 2017. Anaerobic digestion of pig manure supernatant at high ammonia concentrations characterized by high abundances of *Methanosaeta* and non-euryarchaeotal archaea. *Sci. Rep.* 7.
- Ojha, N., Pradhan, N., Singh, S., Barla, A., Shrivastava, A., Khatua, P., Rai, V., Bose, S., 2017. Evaluation of HDPE and LDPE degradation by fungus, implemented by statistical optimization. *Sci. Rep.* 7.
- Oshima, K., Ueda, K., Beppu, T., & Nishida, H. (2011). Unique Evolution of *Symbiobacterium thermophilum* Suggested from Gene Content and Orthologous Protein Sequence Comparisons. *International Journal of Evolutionary Biology*, 376831.

- Pisciotta, J.M., Zaybak, Z., Call, D.F., Nam, J.Y., Logan, B.E., 2012. Enrichment of microbial electrolysis cell biocathodes from sediment microbial fuel cell bioanodes. *Appl. Environ. Microbiol.* 78, 5212–5219.
- Simon Poirier, Céline Madigou, Théodore Bouchez, Olivier Chapleur, 2017. Improving anaerobic digestion with support media: Mitigation of ammonia inhibition and effect on microbial communities. *Bioresour. Technol.* 235, 229–239
- Ramm, P., Jost, C., Neitman, E., Sohling, U., Menhorn, K., Mumme, J., Linke, B. 2014. Magnetic Biofilm Carriers: The Use of Novel Magnetic Foam Glass Particles in Anaerobic Digestion of Sugar Beet Silage. *J. Ren. Energy*, article ID 208718.
- Renner, L. D., & Weibel, D. B. (2011). Physicochemical regulation of biofilm formation. *MRS Bulletin / Materials Research Society*, 36(5), 347–355.
- Ruiz-Sánchez, J., Campanaro, S., Guivernau, M., Fernández, B., Prenafeta-Boldú, F.X., 2018. Effect of ammonia on the active microbiome and metagenome from stable full-scale digesters. *Bioresour. Technol.* 250, 513–522.
- Sanchez, J.M., Arijó, S., Muñoz, M.A., Morínigo, M.A., Borrego, J.J., 1994. Microbial colonization of different support materials used to enhance the methanogenic process. *Appl. Microbiol. Biotechnol.* 41, 480–487.
- Schnürer A, Schink B, Svensson B. *Clostridium ultunense* sp. nov., a Mesophilic Bacterium Oxidizing Acetate in Syntrophic Association with a Hydrogenotrophic Methanogenic Bacterium. *Int J Syst Evol Microbiol* 46(4):1145-1152
- Sheng X., Peng Ting Y., Pehkonen S. O. 2008. The influence of ionic strength, nutrients and pH on bacterial adhesion to metals. *Journal of Colloid and Interface Science* 321(2), 256–264.
- Sun, L., Müller, B., Westerholm, M., Schnürer, A., 2014. Syntrophic acetate oxidation in industrial CSTR biogas digesters. *J. Biotechnol.* 171, 39–44.
- Wang, H., Fotidis, I.A., Angelidaki, I., 2015. Ammonia effect on hydrogenotrophic methanogens and syntrophic acetate-oxidizing bacteria. *FEMS Microbiol. Ecol.* 91.
- Weiß, S., Leubhn, M., Andrade, D., Zankel, A., Cardinale, M., Birner-Gruenberger, R., Somitsch, W., Ueberbacher, B.J., Guebitz, G.M., 2013. Activated zeolite - Suitable carriers for microorganisms in anaerobic digestion processes. *Appl. Microbiol. Biotechnol.* 97, 3225–3238.
- Westerholm, M., Levén, L., Schnürer, A., 2012. Bioaugmentation of syntrophic acetate-oxidizing culture in biogas reactors exposed to increasing levels of ammonia. *Appl. Environ. Microbiol.* 78, 7619–7625.
- Westerholm, M., Roos, S., Schnürer, A.; 2010. *Syntrophaceticus schinkii* gen. nov., sp. nov., an anaerobic, syntrophic acetate-oxidizing bacterium isolated from a mesophilic anaerobic filter, *FEMS Microbiology Letters*, 309, 100–104
- Westerholm, M., Roos, S., Schnürer, A.; 2011. *Tepidanaerobacter acetatoydans* sp. nov., an anaerobic, syntrophic acetate-oxidizing bacterium isolated from two ammonium-enriched mesophilic methanogenic processes. *Syst Appl Microbio.* 34, 260–267.
- Yamada T, Imachi H, Ohashi A, Harada H, Hanada S, Kamagata Y, Sekiguchi Y. 2007. *Bellilinea caldifistulae* gen. nov., sp. nov. and *Longilinea arvoryzae* gen. nov., sp. nov., strictly anaerobic, filamentous bacteria of the phylum Chloroflexi isolated from methanogenic propionate-degrading consortia. *Int J Syst Evol Microbiol* 57(10):2299-2307.
- Yenigün, O., Demirel, B., 2013. Ammonia inhibition in anaerobic digestion: A review. *Process Biochem.* 48, 901–911.
- Zhao Q., Wang C., Liu Y., Wang S. 2007. Bacterial adhesion on metal-polymer composite coatings. *International Journal of Adhesion & Adhesives* 27(2), 85-91.

Zhou, L., Boyd, C.E., 2014. Total ammonia nitrogen removal from aqueous solutions by the natural zeolite, mordenite: A laboratory test and experimental study. *Aquaculture* 432, 252–257.

# **Chapter 7 Response of anaerobic methanogenic biomass to immobilized multi-walled C nanotubes exposure**

---

Nanotechnologies have been developing rapidly in the last years. The use of nanoparticles and nanocomposites formed by multiwalled carbon nanotubes (MWCNTs) have been described to prompt beneficial effects in biogas production. In this chapter, a novel and cost-effective methodology for the immobilization of MWCNTs onto low-density polyethylene pearls is presented. The obtained results show that immobilised MWCNTs had a relevant impact on the maximum CH<sub>4</sub> yield and on the acetate assimilation.

## 7.1 Introduction

The anaerobic digestion (AD) of organic materials is a well-consolidated process for valorising organic wastes into renewable energy (e.g. biogas). However, one of the major limitations of the AD process is the high nitrogen content of many organic wastes resulting in the accumulation of ammonia, which is a major inhibitor of the methanogenic biomass and, particularly, the acetotrophic methanogenic archaea (AMA; Demirel and Scherer, 2008). When the acetotrophic methanogenic pathway is inhibited by ammonia, the accumulated acetate can be metabolized via an alternative pathway, known as syntrophic acetate oxidation (SAO), carried out by the homonymous bacteria (SAOB) (Sun et al., 2014). SAOB are able to reverse the Wood–Ljungdahl pathway, so that acetate is converted to  $H_2$  and  $CO_2$ , which are then consumed by hydrogenotrophic methanogenic archaea (HMA). Under such conditions, formate-consuming methanogenic archaea seem to play a relevant role as well. Hence, a syntrophic interaction involves interspecies hydrogen and/or formate transfer between SAOB and HMA (Schink et al., 2017; Stams and Plugge, 2009). This process is known as interspecies electron/hydrogen transfer (IET/IHT), which is a key step of the process that determines a systematic energy flow and ensures the efficiency of AD system, because HMA maintain the concentration of  $H_2$  low enough for the SAO process to be thermodynamically favourable (Lee and Zinder, 1988).

However, the exchange of  $H_2$  between syntrophs and methanogens is a vulnerable link that often becomes a bottleneck in the anaerobic digestion process (Min et al., 2017). Direct interspecies electron transfer (DIET) has been proposed as a successful alternative to promote and accelerate the IET/IHT process (Zhao et al., 2015). Rotaru et al. (2014) described the DIET mechanism between *Geobacter metallireducens* and *Methanosarcina barkeri* (aceticlastic and hydrogenotrophic). Similarly, Liu et al., (2014) demonstrated that *Geobacter metallireducens* interacted with *Methanosaeta barundinacea*, an obligate aceticlastic methanogen.

Recently, some studies have proposed the utilization of nanomaterials as a means to modulate the IET/IHT process and improve methanogenic efficiency (Salvador et al., 2017). The addition of different support materials to AD process has led to significant increases of biogas production and of organic matter degradation. The electrical conductivity of the used materials is a particularly interesting property because it contributes to the electron transfer. The explanation for the improvement of the AD has been related to the existence of electrical connections forged by microorganisms via

biological mechanisms (structures that provide cell-to-cell electron channels) or via non-biological mechanisms, including conductive materials in the medium as biochar, activated carbon, magnetite particles or carbon nanotubes (CNT) (Li et al., 2015; Capson-Tojo et al., 2018). A specific examples of this phenomenon is the increased methane production in cultures of *Methanospirillum hungatei* and *Methanobacterium formicium* in the presence of CNT (Li et al., 2015). The use of CNT has previously been described as a promising option for enhanced electrode surface modification because its optimal electrical conductivity (Hirsch, 2002). In fact, glucose oxidase-based microbial fuel cells have been improved by adding DNA-wrapped single-walled CNT as an electron mediator (Wang and Musameh, 2005; Ivnitiski et al. 2006) developed an enhanced DIET strategy based on CNT combined with various enzymes and biomolecules (such as cytochromes or NADH).

However, the potential environmental and health risks of nanotechnologies, including those based on CNT, must be assessed and accounted (Savolainen et al., 2010). Currently, the limited use of nanomaterials is unlikely to pose any significant risk to the public health. Nevertheless, as the number and types of new nanomaterials used in several industrial processes increase, the toxicological risks associated to these materials will also increase as they are released into the environment in greater amounts (Renn and Roco, 2006). Therefore, in order to retain CNT inside the bioreactor and avoid its environmental discharge, a novel and cost-effective immobilization method has been applied in this study to enhance the AD process. The immobilization method is extensively used in enzymatic catalysis, and refers to enzymes that are physically localized in a certain region of space with the objective to retain their catalytic activities, and which can be used continuously (Chen et al., 2003; Hirsch, 2002; Nakashima et al., 2002). This immobilization process also allows an efficient recovery and reuse of immobilised enzymes, and here this strategy has been extended to the rather expensive CNT for its application in continuous fixed-bed AD bioreactors.

This work is aimed at evaluating the effectiveness of using immobilised MWCNT for the enhancement of IET phenomena, in order to mitigate ammonia inhibition during the AD process. The impact of the electrical conductive MWCNT material on the active bacterial and archaeal populations was analysed through the NGS profiling of 16S rRNA transcripts.

## 7.2 Materials and methods

### 7.2.1 Carbon nanotubes immobilization

Carbon nanotubes (CNT) with 50-85 nm of diameter and 10-15  $\mu\text{m}$  of length, with >94% of carbon content (Graphene Supermarket, Calverton, NY, EEUU), were used.

Low-density polyethylene (LDPE) spheres (Sigma Aldrich – Merck, Madrid, Spain) with a uniform diameter ranging 3-5 mm, a density of  $0.918 \text{ g}\cdot\text{mL}^{-1}$  (at  $25^\circ\text{C}$ ) and melting point of  $110^\circ\text{C}$  were selected as immobilization agent.

The immobilization process consisted in placing the LDPE spheres into a thermal/protective glass tray as a monolayer. The tray was then heated up to  $110^\circ\text{C}$ , under atmospheric pressure, for 15 minutes. Once the surface of LDPE spheres melted, a uniform layer of CNTs was distributed through constant shaking. Then, CNT-coated LDPE (I-CNT) spheres were held for 5 min and cooled at  $25^\circ\text{C}$  before their collection. Excess CNT were removed by placing I-CNT spheres in plastic containers filled with ethanol. These containers were mechanically agitated and the ethanol was regularly changed until no more CNT staining was apparent in the ethanol. The I-CNT spheres obtained at the end of this process had a particle size ranging from 2 to 5 mm (Table 7.1).

### 7.2.2 Experimental set-up

The methanogenic activity was evaluated in triplicate batch assays at  $35^\circ\text{C}$  in two different experiments. Freshly collected methanogenic biomass (characterised by  $25.8 \text{ gVSS L}^{-1}$  and  $3 \text{ gN-TAN L}^{-1}$ ) was distributed into vials (60 mL of inoculum per vial; total volume 120 mL per vial). This biomass was taken from a mesophilic full-scale CSTR anaerobic digester (hydraulic retention time of 65 days; the influent was composed by nitrogen-rich agricultural wastes from Vilasana, Lleida, and is operated under stable conditions).

For the Experiment 1, one treatment was prepared with the addition of I-CNT spheres and an initial TAN content of  $7.0 \text{ gN-TAN L}^{-1}$  (labelled as NT+TAN), and two controls without CNT with an initial TAN content of 3.5 and  $7.0 \text{ gN-TAN L}^{-1}$ , respectively (labelled as B-TAN and B+TAN, respectively). These initial TAN values were adjusted through addition of  $\text{NH}_4\text{Cl}$  (Merck, Madrid, Spain). For the amended batches, I-CNT spheres were added up to 30% of the apparent volume (18 mL). All vials were then purged with  $\text{N}_2$  gas to create anaerobic conditions, sealed tight, and incubated under identical conditions, constant shaken at  $37^\circ\text{C}$ . Three pulses of sodium acetate were added of  $3.0 \text{ g L}^{-1}$  of acetic acid each. The first two pulses were applied in days 0 and 25. Before the third pulse (day 40), the liquid fraction (60 mL) was carefully removed and replaced by fresh mineral medium. That medium was composed by  $1 \text{ mL}\cdot\text{L}^{-1}$  of ( $0.125 \text{ gNiCl}_2\cdot 6\text{H}_2\text{O}\cdot\text{L}^{-1}$ ;  $25 \text{ g FeCl}_2\cdot 6\text{H}_2\text{O L}^{-1}$ ;  $1.25 \text{ g}(\text{NH}_4)_6\text{MO}_7\text{O}_2\cdot 4\text{H}_2\text{O L}^{-1}$ ;  $0.075 \text{ g CoCl}_2\cdot 6\text{H}_2\text{O L}^{-1}$ ) and  $1 \text{ mL}\cdot\text{L}^{-1}$  ( $17 \text{ g NH}_4\text{Cl}\cdot 12\text{H}_2\text{O L}^{-1}$ ;  $3.7 \text{ g KHPO}_4 \text{ L}^{-1}$ ;  $0.56 \text{ g MgSO}_4 \text{ L}^{-1}$ ;  $0.8 \text{ g CaCl}_2\cdot 2\text{H}_2\text{O L}^{-1}$ ) and  $\text{NH}_4\text{Cl}$  solution (to ensure 3.5 or  $7.0 \text{ gN-TAN L}^{-1}$ , depending on the batch), without altering the developed biofilm on I-CNT spheres and the headspace of the vials.



For the Experiment 2, five different treatments were prepared by varying the amount of the CNT (3.00, 0.50, 0.25 and 0.02 g L<sup>-1</sup>), and one control without CNT. An initial TAN concentration of 7 gN-TAN L<sup>-1</sup> was ensured by the addition of NH<sub>4</sub>Cl (Merck, Madrid, Spain). As with the Experiment 1, all vials were tight sealed and purged with N<sub>2</sub> gas. Only one pulse of sodium acetate was given in this case, ensuring an initial concentration to 3.0 Acetate g·L<sup>-1</sup>.

The evolution of the composition and cumulative volume of biogas, as well as the concentration of individual volatile fatty acids (VFA) in the liquid media, including acetic (Ac), propionic, butyric, valeric and caproic acids, were measured in both experiments and used to calculate the methane yield and production rate ( $rCH_4$ ). The data set from Experiment 2 was fitted to the modified Gompertz equation (1):

Eq. (1)

$$B = B_o \cdot \{x \cdot \exp(-\exp[(\mu_1 \cdot e/B_o) \cdot (\lambda_1 - t) + 1]) + (1-x) \cdot \exp(-\exp[(\mu_2 \cdot e/B_o) \cdot (\lambda_2 - t) + 1])\}$$

The settled fraction (pellets obtained after centrifuging 1,5 mL sample at 4000 g for 30' at 4°C) was used for total DNA and RNA extraction (in triplicate) (see Chapter 3 for more details on the Materials and Methods).

### 7.2.3 Scanning electron microscopy (SEM)

Scanning electron microscopy (SEM) was used to analyse the surface of I-CNT spheres, before and after the nanoparticle immobilization procedure. I-CNT spheres were also analysed at the end of the Experiment 1, once they had been exposed to the methanogenic biomass. For that purpose, I-CNT spheres and their attached biofilms were air-dried (2–4 nm thickness) and analyzed at nanometer image resolution by SEM (MERLIN Carl Zeiss, Germany) at 2–5 kV range accelerating voltage. No sputter coating was needed because the surface of the primary substrate had a large carbon component.

## 7.3 Results and discussion

### 7.3.1 The feasibility of the immobilisation method

The implementation of nanotechnology in the field of anaerobic digestion is currently being hindered because of the high costs and technical difficulties of nanoparticle production, handling, and immobilization (Li et al., 2007; Wang and Musameh, 2005). Hence, this approach is being implemented in high added-value applications (e.g. medical, sensing, monitoring, etc.), in which nanoelectronic devices with functionalized polymers and CNT composites improve electronic transport. An alternative option is to use MWCNT, but this methodology does not allow the retention of CNT inside of the

AD-system and, consequently, it also results in increased operational costs (Li et al., 2015; Salvador et al., 2017).

In this study, we have used an inexpensive polymeric material (LDPE) and a novel and simple strategy for MWCNT immobilization. LDPE pellets were chosen because of their relatively low melting point (190°C/2.56kg) reduces the energy and costs that are necessary its handling. A continuous and homogenous MWCNT coating on LDPE spheres is shown in Figure 7.2, in relation to the surface of LDPE spheres before the immobilization treatment. These SEM images also demonstrated that there were many one-dimensional nanostructures over the surface, which had a uniform size and retained their functionality without being dipped in the LDPE material.

SEM images of LDPE pearl coated with nanotubes at the end of the biological incubation Experiment 1 (73 days) are also shown in Figure 7.2. A homogeneous and uniform nanostructure cover was still observed on the spheres' surface, even after being in contact with the liquid medium and microbial communities under constant shaking conditions. The formation of exopolymeric matrix facilitated the attachment of microorganisms: when bacteria growth on biofilm structure, they develop a polymeric substance matrix that confer higher resistance to stressed-environments (Lembre et al., 2012; Donlan, 2002).

### **7.3.2 Methane production and microbial community analysis after CNT exposure**

#### **7.3.2.1 Experiment 1**

The evolution of CH<sub>4</sub> in the headspaces was monitored after every acetate pulse, along the whole incubation process (Figure 7.1). The biological activation of the inoculum was faster in batches that contained a low ammonia concentration, and in batches that were supplemented with I-CNT spheres. The CH<sub>4</sub> yield in batches with a high TAN (7.0 gN-TAN L<sup>-1</sup>) but without I-CNT spheres (B+TAN) was significantly lower than in those with a low TAN (3.5 gN-TAN L<sup>-1</sup>; B-TAN). These results were expected because it has extensively been described that AD-systems are very sensitive to TAN concentration, and unbalanced operation has been described above 3.0 gN-TAN L<sup>-1</sup> (Yenigün and Demirel, 2013). However, a progressive adaptation of the biomass was observed in that the CH<sub>4</sub> yield reduction of B+TAN, in relation to B-TAN, was of 73.3% and 17.3% in the first and second pulse. No differences were observed after the third pulse, which highlights the phenomenon of biological acclimation. Concerning the

methanogenic activity, it varied by a 89%, 15% and 11% in B-TAN and a -12%, 29% and 24% for NT+TAN, for the three successive acetate pulses and in relation to the B+TAN values. The progressive acclimation of methanogenic biomass has been proposed as a strategy for the anaerobic digestion of nitrogen-rich substrates such as food waste, slaughterhouse waste etc. (Tian et al., 2018).

CNTs have been reported to be cytotoxic because they damage the cell membrane and increase the expression levels of stress-related genes (Kang et al., 2008). Interestingly, in the results of the present study, however, evidenced that the addition of immobilized carbon nanotubes was beneficial for the methanogenic activity. These is in agreement with previous studies that explained this phenomenon by the capacity of C-nanomaterials to facilitate electron transfer through IET mechanisms. The addition of carbon conductive material would stimulate the CH<sub>4</sub> production because fermentative bacteria can transfer the electrons to methanogens directly, which is faster mechanism than than from the H<sub>2</sub> released from acetate degradation (Dang et al., 2016; Li et al., 2015; Salvador et al., 2017).

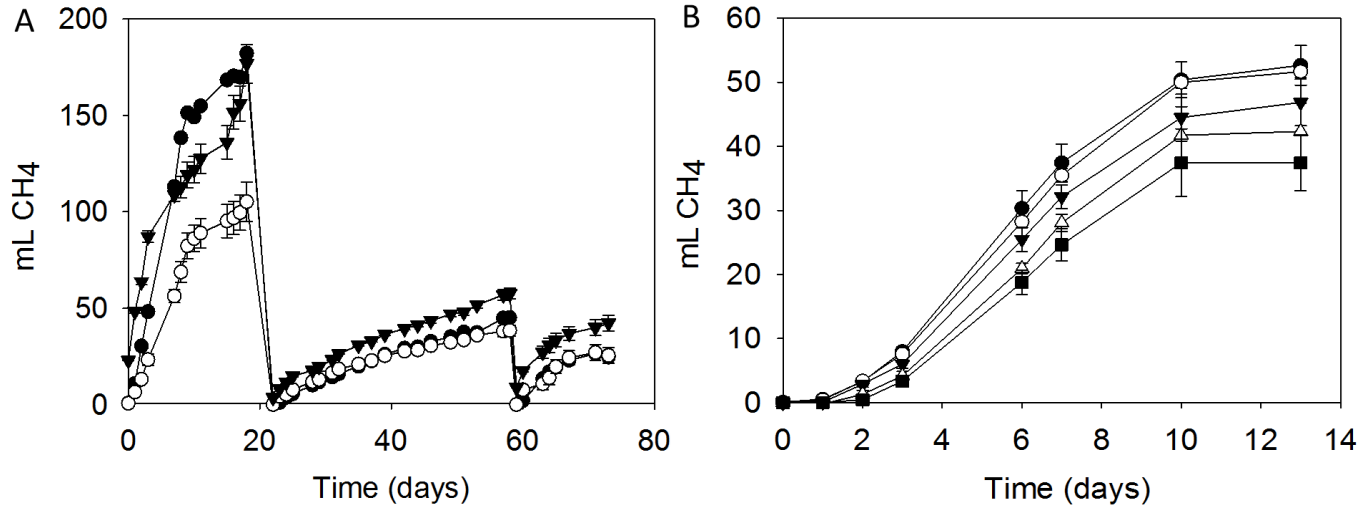


**Figure 7.1** Time-course CH<sub>4</sub> production in batch incubations. (a) Experiment 1. Symbols: (▼) treatment with I-CNT spheres and 7.0 gN-TAN L<sup>-1</sup>; (●) control with 3.5 gN-TAN L<sup>-1</sup>; (○) control with 7.0 gN-TAN L<sup>-1</sup>. (b) Experiment 2. Symbols: (●) 3 g CNT L<sup>-1</sup>; (○) 0.5 g CNT L<sup>-1</sup>; (▼) 0.25 gCNT L<sup>-1</sup>; (Δ) 0.02 gCNT L<sup>-1</sup>; (■) without CNT.

**Table 7.1** Set up results of experiment 1 with differnt TAN concentrations

	Acetate pulse 1			Acetate pulse 2			Acetate pulse 3			pulse 1	pulse 2	pulse 3	
Batch	Slope*	gVSS**	MA***	Slope*	gVSS**	MA***	Slope*	gVSS**	MA***	Batch	Methanogenic activity increment		
<b>B-TAN</b>	17,5	1,76	9,95	1,45	0,59	2,47	3,06	0,39	7,82	<b>B-TAN</b>	89%	15%	11%
<b>B+TAN</b>	9,25	1,76	5,25	1,27	0,59	2,16	2,77	0,39	7,08	<b>B+TAN</b>	0%	0%	0%
<b>NT+TAN</b>	8,18	1,76	4,65	1,63	0,59	2,78	3,43	0,39	8,77	<b>NT</b>	-12%	29%	24%

\*Slope from regression curve of mLCH<sub>4</sub>·d<sup>-1</sup>

\*\*g Volatile suspended solids

\*\*Methanogenic activity (mgDQO-CH<sub>4</sub>·gSSV<sup>-1</sup>·d<sup>-1</sup>)

**Table 7. 2** Set-up and fitting results of experiment 2, with different CNT concentration. Note: \* Fresh inoculum at 3.5 gN-TAN L<sup>-1</sup> and without CNT. \*\* Fresh inoculum at 7.0 gN-TAN L<sup>-1</sup> and without CNT.

CNT (g L <sup>-1</sup> ) (experiment)	TAN (gN L <sup>-1</sup> )	Initial Acetic Acid (g L <sup>-1</sup> )	Lag phase (days)	Mathematical fitting	
				CH <sub>4</sub> production rate (NLCH <sub>4</sub> kgCOD <sup>-1</sup> d <sup>-1</sup> )	Max. Yield (NLCH <sub>4</sub> kgCOD <sup>-1</sup> )
0.00 (E2)*	3.5	0	0.69	14.2	127
0.00 (E2)**	7.0	3.5	2.18	37.6	367
3.00 (E2)	7.0	3.5	1.69	47.7	387
0.50 (E2)	7.0	3.5	1.72	45.4	399
0.25 (E2)	7.0	3.5	1.78	42.3	381
0.02 (E2)	7.0	3.5	2.00	40.4	351

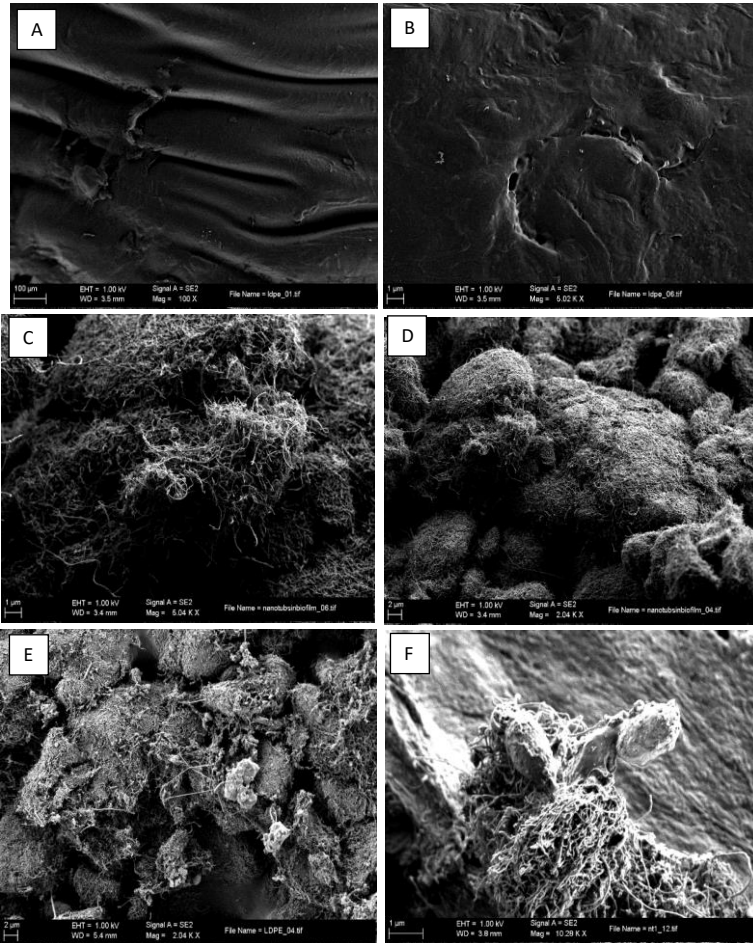


**Figure 7. 2** SEM images from Experiment 1. (a-b) LDPE pellets without CNTs. (c-d) I-CNT spheres. (e-f) I-CNT spheres with attached bacterial after 73 days of incubation.

### 7.3.3 Microbial community analysis

Microbial populations from the Experiment 1 were characterized by NGS on both genetic presence and expression of selected genes. A total of 605,184 and 312,719 high quality 16S rRNA cDNA reads (151,296 and 78,179 per sample, in average) were obtained for the *Bacteria* and the *Archaea* domains, respectively. The bacterial community structured based on expression profiles remained rather stable in batches without nanotubes (B-TAN and B+TAN), regardless on the TAN concentration (Figure 7.3). Representatives of the order *Anaerolineales* and *Bacteroidales* were predominant in terms of 16S rRNA transcript counts with an average relative abundance of more than 20%. In addition, the high abundance of the *Clostridiales* (12-14%) was particularly relevant in the present study, as the well-known SAOB belong to this taxon, and has extensively been described for its hydrolytic and fermentative activity. Other important groups included the *Plancomycetales* (12-11%) and *Spirochaetales* (8%). The incidence of both groups was quit expected results as there are frequently detected in AD systems under different substrates, e.g. municipal sludge, industrial waste, manure, and synthetic organic media (Lee et al., 2015; St-Pierre and Wright, 2014).

The most active species in terms of gene expression in the absence of nanotubes, was associated to the genus *Leptolinia* (OTU 2, 10% in abundance; order *Anaerolineales*). Other important OTUs in these batches were related to the genera *Levillinia* and *Bellilinea*, also in the *Anaerolineales*. Members of this order have displayed enhanced growth when co-cultivated with HMA (Hug et al., 2013; Yamada et al., 2006), which is the predominant archaeal group found in the present study (see section 7.3.3.1).

The *Bacteroidales* order was dominated predominantly by OTU 3, which had a 88% in homology sequence with *Alkalitalea saponilacus*, and might therefore correspond to a yet underscribed species. The related *A. saponilacus* has been reported to have a high hydrolytic activity, with an ability to metabolize a variety of organic compounds including protein, sugars and lipids, which explained its high abundance in waste activated sludge digesters (Cardinali-Rezende et al., 2012). A number of unidentified *Clostridiales* (OTU 5, 21 and 26) with a lower yet significant presence in the active biomass (>1%) in batches incubated without carbon nanotubes had a high sequence similarity with phylotypes previously reported in other ammonia-rich anaerobic digesters. It could thus well be that some of the those ribotypes correspond to yet to be described SAOB.



Despite of the TAN inhibitory effect in the AD process, no relevant differences were observed on the active populations between B-TAN and B+TAN batches. This absence of bacterial profile changes should be due because the inoculum used in the present study came from industrial reactor that normally operate around 3.0 gN-TAN L<sup>-1</sup>, and it could therefore be adapted to relatively high TAN levels. The similarities between the active bacterial community structure of B-TAN and B+TAN has been highlighted by a Correspondance Analysis (CA; Figure 7.4).

The introduction of carbon nanotubes on the AD batches had a clear impact on active microbial communities. Little is known about the microbial community interactions in relation to CNT, and it has been described that CNT have a notorious impact on phospholipidic membrane (Liu et al 2013). However, such deleterious interactions might be highly dependent on the cell membranes of specific microorganisms, and on the physicochemical properties of the used CNT (SWCNT versus MWCNT, associated impurities, etc). The active microbial community found in the liquid media of batches amended with CNT presented some similarities with the rest of batches: the most active bacteria belonged to the *Anaerolineales* (22%), *Bacteroidales* (13%) and *Planctomycetales* (15%). However, NT-batches were characterized by the specific appearance of the orders *Desulfuromonadales* (14%) and *Bacillales* (7%), which increased in terms of expression levels at the expense of the *Clostridiales* order (7%) and other minor groups.

**Table 7.3** Estimators of microbial species diversity/richness based on NGS of 16S rRNA genes and transcripts from the Bacteria and Archaea domains, obtained from the initial inoculum and after its incubation during 11 and 17 days under increasing TAN content. Predominant assigned genera (abundance > 5%) are also listed.

Parameter	Microbial group	B-TAN	B+TAN	NT Support	NT media
No. of reads	Bacteria	201930	189534	71783	141587
	Archaea	90267	93465	40113	88874
No. of OTU	Bacteria	1423	1409	739	1494
	Archaea	215	234	151	183
Coverage (%)	Bacteria	99.0	98.9	98.9	99.4
	Archaea	99.9	99.9	99.9	99.9
Shannon( diversity)	Bacteria	4.0 ± 0.0	4.1 ± 0.0	3.98 ± 0,01	3.7 ± 0.0
	Archaea	1.6 ± 0.0	1,52 ± 0,0	1,18 ± 0	1.7 ± 0.0
Chao1 (richness)	Bacteria	1447 ± 46.9	1426 ± 43.1	973 ± 59.3	1581 ± 62,8
	Archaea	235 ± 13.7	215 ± 16.0	196 ± 15.0	200 ± 16.0

**Table 7.4** Best match in BLAST searches (GenBank, NCBI, USA) on TAN-responding OTUs (Figure 3). Only OTUs with a relative abundance in the original methanogenic biomass higher than 1% are listed.

OTU	Identification	Abundance (%)				Accession nr	H (%)	Source
		B-TAN	B+TAN	NTs	NTm			
2	<i>Uncultured leptolinea sp</i>	12,0	11,3	1,9	14,9	KM597168	89	Methanogenic sludge
3	<i>Alkalitalea spp.</i>	10,5	7,9	0,3	3,2	NR117932	89	Environmental sample
5	<i>Alkaliphilus spp.</i>	6,5	8,9	0,9	3,2	NR116395	95	Environmental sample
7	<i>Desulfuromonas thiophila</i>	0,1	0,1	14,4	12,1	NR026407	93	Anoxic water sediment
16	<i>Chondromyces spp.</i>	0.0	0.0	19.5	0.9	Diverse	85	Environmental samples
21	<i>Uncultured clostridiales</i>	1,2	0,7	0.4	0.7	Diverse	99	Environmental samples
26	<i>Uncultured clostridia</i>	0.8	0.7	0.3	0.6	Diverse	99	Environmental sample
31	<i>Bacillus sp.</i>	0.0	0.0	3.4	0.0	AJ536432	99	Environmental sample
33	<i>Uncultured Bacillus sp</i>	0.0	0.0	3.3	0.0	LC315993.1	99	High-temperature compost

Interestingly, a very different active bacterial community was found on the surface of the introduced I-CNT coated spheres. The most abundant gene transcripts belonged to the order *Myxococcales* (mainly dominated by *Chondromyces* genus) with a 21% of relative abundance (mainly belongs to OTU 16). Berleman et al. (2016) described that *Myxococcus xanthus* and *Chondromyces crocatus* have the capability to organize the secretion of EPS in a high level of complexity. For these microbes, EPS are a highly systematized structural biofilm component, for the formation of microchannels that align cells and promote directed cells migration assuring an efficient surface colonization. Other mechanisms that confer optimal characteristics to biofilm formation on carbon nanotubes have also been reported for the *Myxococcales*. Sun et al.

(2000) described the presence of conductive pili (e-pili) in representatives of the *Myxococcales*. Those structures are essential for extracellular electron transport in long-range electron transport through the conductive biofilms form on conductive materials, such as biochar, microbial fuel cells, and, like in the present study, in contact with CNT. In fact, Walker et al. (2016) demonstrated that e-pili play an important role in AD-systems because they prompted electron exchange between bacteria and methanogenic archaea, thus increasing the conversion rate of waste into biogas.

A similar behavior has been observed in others groups of microbes, such as in *Desulfuromonas* spp., because of their physiology encompasses the capacity to develop e-pili (Walker et al., 2016). In the present study, the second most active species (OTU 7) belonged to the *Desulfuromonadales* order and presented the highest similarity with *Desulfuromonas thiophila* (OTU 7, 93% homology). This species drastically increased its activity on NT+TAN batches (15% on the support and 14% in liquid media, in relation to B+TAN). This result is coherent with previous works that reported *Desulfuromonas* spp. as an effective acetate oxidizing bacterium, with the subsequent transfer of electrons (Walker et al., 2016). It has also been reported that *Desulfuromonas* spp. are often the most abundant microbes colonizing anodic surfaces of AD-bioelectrochemical systems (Hirano et al., 2013). *Desulfuromonas* is known to grow anaerobically by coupling the oxidation of acetate to the reduction of elemental sulfur to sulfide, while being unable to reduce sulfate, thus evidencing the necessity of an organic electron acceptor to use acetate as a carbon source (Dutta et al., 2009). In the present study, *Desulfuromonas* were not significantly active in the absence of CNT, but with the introduction of carbon nanoparticles the abundance of 16S rRNA transcripts peaked up to 15% of the total bacterial community. With no available sulfur-compounds in the media, the acetate oxidation by *Desulfuromonas* might be, in principle, not possible. However, with the introduction of CNT, an alternative strategy was made possible for transferring electrons through extracellular connections on an external electron acceptor.

A ribotype closely related to the *Bacillus* genus (OTUs 31 and 33; order *Bacillales*), might also play a relevant role in AD batches amended with CNT, given its relatively high abundance of ribosomal transcripts (18%) on the attached biomass. However, we hypothesize that the high abundance of this taxon on the biofilm of CNT was caused by the specialization and capacity of *Bacillus* species to develop biofilms (Cairns et al., 2014).

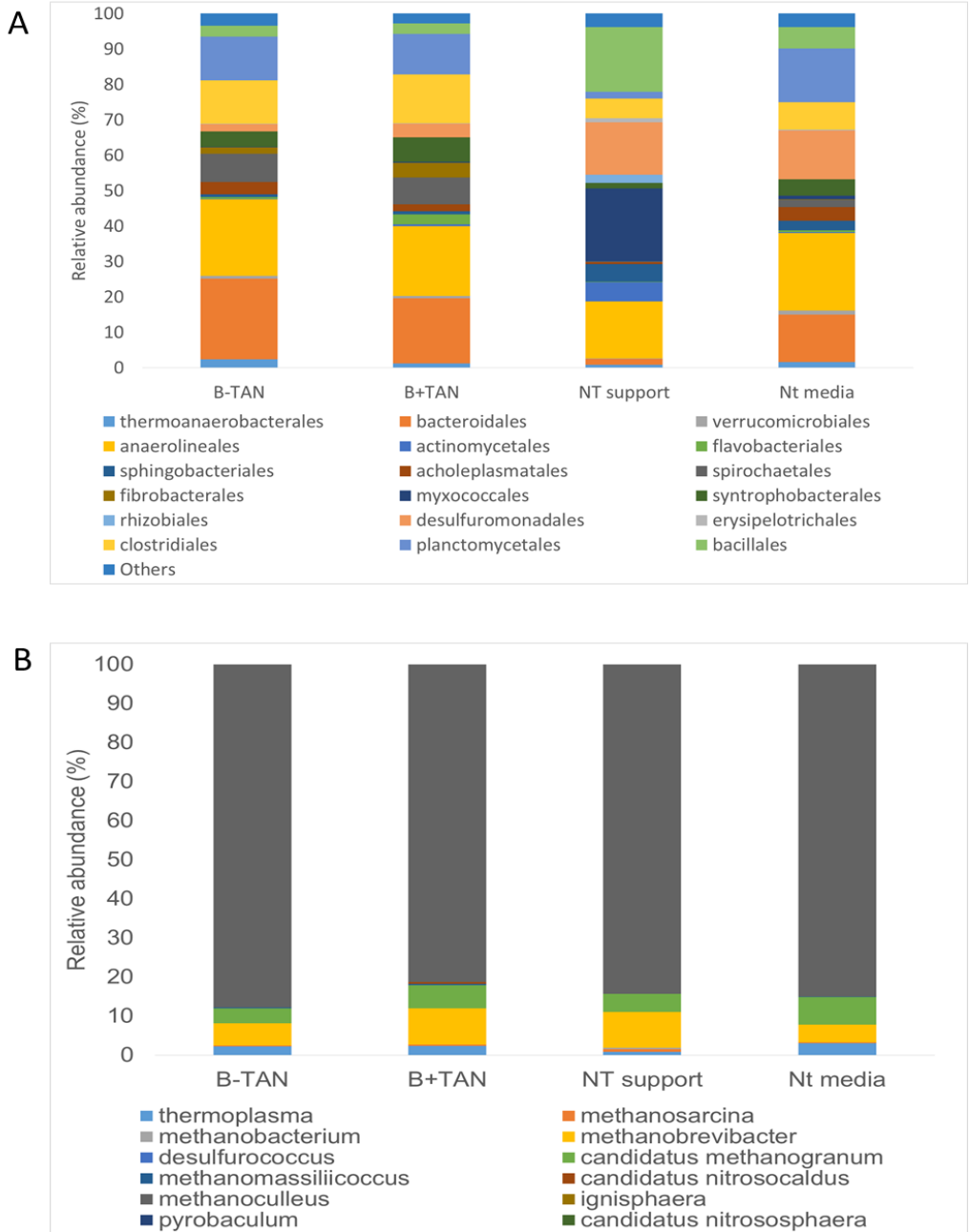


**Figure 7. 3** Relative abundance of bacterial (order) (A) and archaeal (genus) (B) ribotypes, in terms of 16S rRNA transcripts counts in methanogenic batch assays, experiment 1.

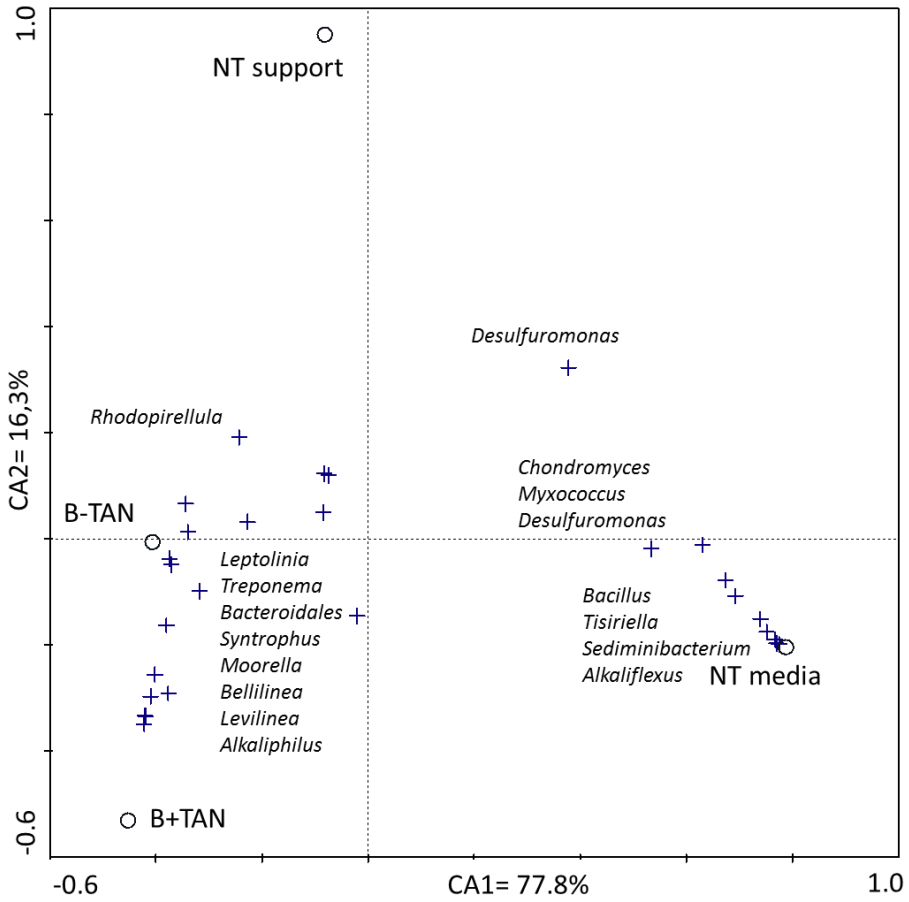


**Figure 7.4** Correspondence Analysis biplot on sample scores (circles) and operational taxonomic units (crosses) from the unpacked controls (B-TAN and B+TAN), and batches amended with CNTs (Nt Support and NT Media), concerning the abundance of 16S rRNA transcripts bacteria. Only OTUs with a sample relative abundance higher than 3% have been represented.

### 7.3.3.1 Response of methanogenic archaeal communities to MWCNTs and ammonia

The methanogenic archaeal communities, particularly the AMA, have long been recognized to be particularly sensitive to ammonia inhibition. However, HMA are able to remain active even under the relatively high ammonia levels that are inhibitory for other microbial groups. Nevertheless, despite changes in ammonia exposure and on the use of materials between the different AD batches, the microbial community structure of the active archaea remained relatively constant. The predominant methanogen belonged to the genus *Methanoculleus*, with a relative abundance of ribosomal transcripts higher than the 81% in all cases. The predominant OTU1 affiliated to *Methanoculleus* had a 98% sequence homology with *Methanoculleus bourgenis*. This methanogen has been identified as HMA syntrophic partner in mesophilic anaerobic reactors running under high TAN concentrations ( $>3 \text{ gN L}^{-1}$ ) (Wang et al., 2015). Due to the capacity of this archaeon to consume hydrogen for  $\text{CO}_2$  reduction, a thermodynamic equilibrium can be maintained, so that a syntrophic relation with acetate-oxidising bacteria is established (Manzoor et al., 2016). Other strict and facultative hydrogenotrophic methanogens were found to be active in minor amounts in all batches, which belonged to the genera *Methanobrevibacter* ( $>6\%$ ), Candidatus *Methanogranum* ( $>4\%$ ), and *Methanomasiliicoccus* ( $>1\%$ ).

Although those results were expected at high TAN level, the same tendency was observed in batches incubated with a low nitrogen concentration. These results contradict what we found in previous results (Chapter 4) in that methanogenic biomass from an industrial AD subjected to a variable nitrogen load was able to modulate acetotrophic versus hydrogenotrophic metabolism in response to ammonia exposure. This outcome might be due because the inoculum used in the present study comes from a very stable industrial reactor with a well-established syntrophic bacterial-archaeal interaction. Consequently, due to the short period of time that the experiment was running is not enough to break down those microbial interactions.

### 7.3.2 I-CNT dose assessment (Experiment 2)

Once the beneficial effects of supplementation with CNT on the methanogenic activity at high TAN levels (Experiment 1), the objective of the Experiment 2 was to optimize the amount of CNT in order to attain the maximum effect with the minimum dose.

The lag phase preceding the onset of CH<sub>4</sub> production were slightly longer (2 days) in the assay without or with the lowest amount of CNT, but it decreased with increasing amounts of CNT, from 2.18 to 1.69 days, for 0.00 to 3.00 g L<sup>-1</sup> of CNT (Table 7.2). A coherent tendency was observed for the CH<sub>4</sub> production rate, in that it increased along with the content of CNT from 37.6 NLCH<sub>4</sub> kgCOD<sup>-1</sup> d<sup>-1</sup> without CNT, to 47.7 NLCH<sub>4</sub> kgCOD<sup>-1</sup> d<sup>-1</sup> with 3.00 g L<sup>-1</sup> of CNT. Although the rate and lag phase were more favorable in batches with 3 g L<sup>-1</sup>, the maximum CH<sub>4</sub> yield was found with 0.5 g L<sup>-1</sup> of nanotubes-coated spheres (399 NLCH<sub>4</sub> kgCOD<sup>-1</sup>). These results are in accordance with experimental results that shown the highest increment of methanogenic activity (mgDQO-CH<sub>4</sub> gVSS<sup>-1</sup> d<sup>-1</sup>) and yield in 0.5 g L<sup>-1</sup> experiment.

Regarding the methanogenic activity, the increment of this parameter in relation to the assay without nanotubes was 7%, 20%, 35% and 21% for 0.02, 0.25, 3 and 0.5g L<sup>-1</sup>, respectively. In terms of yield, the increment was 60%, 80%, 99% and 91% and for 0.02, 0.25, 0.5 and 3g L<sup>-1</sup>, respectively. As in the Experiment 1, the introduction of carbon nanotubes gave positive results in terms of both methane yield and activity rate. This observations might be explained because of the stimulation of the DIET phenomena, but also because the increase of the redox potential due to the addition of CNT. The increases of methanogenic activity and yield have been described to be proportional to the amount of carbon nanotubes (Salvador et al., 2017), but this parameter has not been measured in the current study. Variations in the redox potential have a high impact on CH<sub>4</sub> production in anaerobic digesters because methanogenic archaea increase their activity along with the redox potential (Hirano et al., 2013).

However, it is important to mention that carbon nanotubes might have a toxic impact on microbes above certain concentrations. This compounds are considered to be xenobiotics may affect the diversity and metabolism of microbial communities, including those involved in biological process such as fermentation and methanogenesis taking place in AD systems (Pasquini et al., 2012). In the present study, the increment of CNT was beneficial for the enhancement of microbial activity and, consequently, to the improvement of methanogenesis. Nevertheless, when CNT were added at the highest amount of 3.00 g L<sup>-1</sup>, the methanogenic activity and CH<sub>4</sub> production was lower than in batches amended only with 0.50 g L<sup>-1</sup> of CNT. This fact suggests that above that content, the added CNT might display an inhibitory effect. Previous studies hace reported biological activity might be compromised at more than 5 gCNT L<sup>-1</sup> (Salvador et al., 2017).

Once the increment CH<sub>4</sub> yield and methanogenic activity was demonstrated in Experiment 1, the objective of the Experiment 2 was the evaluation of different doses



of CNT to define the minimum dose that improve the methanogenic activity under a clearly TAN inhibitory level.

## 7.4 Conclusions

In this work, a novel methodology for carbon nanotubes immobilization and the effect of this novel material on methanogenic microbial communities was studied. Immobilization process have provided successful results, reducing economic costs and equipment requirements, as well as, develop a great strategy to retain CNT inside of different AD systems. In addition, it has been demonstrated that the conductive materials such as CNT have a direct impact on methanogenic biomass and accelerate the methane production. Methanogenic sludge under CNTs exposure is greatly affected by direct effect of conductive material that prompted interspecies electron transfer mechanisms, as well as, enhanced the EPS excretion allowing the well-stablish biofilms. For that reason, outcomes obtained in the ongoing study boost the utilization of carbon nanotubes in producing methanogenic environments to enhanced and increase AD-stability and production.

## 7.4 References

- APHA/AWWA/WEF, 2012. Standard Methods for the Examination of Water and Wastewater. Stand. Methods 541.
- Berleman, J.E., Zemla, M., Remis, J.P., Liu, H., Davis, A.E., Worth, A.N., West, Z., Zhang, A., Park, H., Bosneaga, E., Van Leer, B., Tsai, W., Zusman, D.R., Auer, M., 2017. Exopolysaccharide microchannels direct bacterial motility and organize multicellular behavior. *ISME J.* 10, 2620–2632.
- Cairns, L.S., Hobley, L., Stanley-Wall, N.R., 2014. Biofilm formation by *Bacillus subtilis*: New insights into regulatory strategies and assembly mechanisms. *Mol. Microbiol.*
- Capson-Tojo, G., Moscoviz, R., Ruiz, D., Santa-Catalina, G., Trably, E., Rouez, M., Crest, M., Steyer, J.P., Bernet, N., Delgenès, J.P., Escudí, R., 2018. Addition of granular activated carbon and trace elements to favor volatile fatty acid consumption during anaerobic digestion of food waste. *Bioresour. Technol.* 260,157-168.
- Cardinali-Rezende, J., Colturato, L.F.D.B., Colturato, T.D.B., Chartone-Souza, E., Nascimento, A.M.A., Sanz, J.L., 2012. Prokaryotic diversity and dynamics in a full-scale municipal solid waste anaerobic reactor from start-up to steady-state conditions. *Bioresour. Technol.* 119, 373–383.
- Chen, R.J., Bangsaruntip, S., Drouvalakis, K.A., Kam, N.W.S., Shim, M., Li, Y., Kim, W., Utz, P.J., Dai, H., 2003. Noncovalent functionalization of carbon nanotubes for highly specific electronic biosensors. *Proc. Natl. Acad. Sci. U. S. A.* 100, 4984–9.
- Dang, Y., Holmes, D.E., Zhao, Z., Woodard, T.L., Zhang, Y., Sun, D., Wang, L.Y., Nevin, K.P., Lovley, D.R., 2017. Enhancing anaerobic digestion of complex organic waste with carbon-based conductive materials. *Bioresour. Technol.* 220, 516–522.

- Demirel, B., Scherer, P., 2008. The roles of acetotrophic and hydrogenotrophic methanogens during anaerobic conversion of biomass to methane: A review. *Rev. Environ. Sci. Biotechnol.* 7, 173–190.
- Donlan, R.M., 2002. Biofilms: Microbial life on surfaces. *Emerg. Infect. Dis.*
- Dutta, P.K., Keller, J., Yuan, Z., Rozendal, R.A., Rabaey, K., 2009. Role of sulfur during acetate oxidation in biological anodes. *Environ. Sci. Technol.* 43, 3839–3845.
- Hirano, S., Matsumoto, N., Morita, M., Sasaki, K., Ohmura, N., 2013. Electrochemical control of redox potential affects methanogenesis of the hydrogenotrophic methanogen *Methanothermobacter thermoautotrophicus*. *Lett. Appl. Microbiol.* 56, 315–321.
- Hirsch, A., 2002. Functionalization of single-walled carbon nanotubes. *Angew. Chemie - Int. Ed.*
- Ivnitski, D., Branch, B., Atanassov, P., Apblett, C., 2007. Glucose oxidase anode for biofuel cell based on direct electron transfer. *Electrochem. commun.* 8, 1204–1210. doi:10.1016/j.elecom.2007.05.024
- Kang, S., Herzberg, M., Rodrigues, D.F., Elimelech, M., 2008. Antibacterial effects of carbon nanotubes: size does matter! *Langmuir* 24, 6409–13. doi:10.1021/la800951v
- Kovács, E., Wirth, R., Maróti, G., Bagi, Z., Rákhely, G., Kovács, K.L., 2013. Biogas Production from Protein-Rich Biomass: Fed-Batch Anaerobic Fermentation of Casein and of Pig Blood and Associated Changes in Microbial Community Composition. *PLoS One* 8. doi:10.1371/journal.pone.0077265
- Lee, M.J., Zinder, S.H., 1988. Hydrogen partial pressures in a thermophilic acetate-oxidizing methanogenic coculture. *Appl. Environ. Microbiol.* 54, 1457–61. doi:10.1002/cphc.200900055
- Lee, S.H., Park, J.H., Kim, S.H., Yu, B.J., Yoon, J.J., Park, H.D., 2015. Evidence of syntrophic acetate oxidation by Spirochaetes during anaerobic methane production. *Bioresour. Technol.* 190, 543–549. doi:10.1016/j.biortech.2015.02.066
- Lembre, P., Lorentz, C., Di, P., 2012. Exopolysaccharides of the Biofilm Matrix: A Complex Biophysical World, in: *The Complex World of Polysaccharides*.
- Li, L.-L., Tong, Z.-H., Fang, C.-Y., Chu, J., Yu, H.-Q., 2015. Response of anaerobic granular sludge to single-wall carbon nanotube exposure. *Water Res.* 70, 1–8.
- Li, Y., Wang, P., Wang, L., Lin, X., 2007. Overoxidized polypyrrole film directed single-walled carbon nanotubes immobilization on glassy carbon electrode and its sensing applications. *Biosens. Bioelectron.* 22, 3120–3125.
- Liu L., Yang C., Li J., Wu, H., 2016. Ultrashort single-walled carbon nanotubes in a lipid bilayer as a new nanopore sensor. *Nature communications* 4, 2989.
- Liu, F., Rotaru, A.-E., Shrestha, P.M., Malvankar, N.S., Nevin, K.P., Lovley, D.R., 2014. Magnetite compensates for the lack of a pilin-associated c-type cytochrome in extracellular electron exchange. *Environ. Microbiol.* 17, 648–55.
- Manzoor, S., Schnürer, A., Bongcam-Rudloff, E., Müller, B., 2017. Complete genome sequence of *Methanoculleus bourgensis* strain MAB1, the syntrophic partner of mesophilic acetate-oxidising bacteria (SAOB). *Stand. Genomic Sci.* 11.
- Nakashima, N., Tomonari, Y., Murakami, H., 2002. Water-Soluble Single-Walled Carbon Nanotubes via Noncovalent Sidewall-Functionalization with a Pyrene-Carrying Ammonium Ion. *Chem. Lett.* 638–638.
- Pasquini, L.M., Hashmi, S.M., Sommer, T.J., Elimelech, M., Zimmerman, J.B., 2012. Impact of surface functionalization on bacterial cytotoxicity of single-walled carbon nanotubes. *Environ. Sci. Technol.* 46, 6297–305.
- Pelissari, C., Guivernau, M., Viñas, M., de Souza, S.S., García, J., Sezerino, P.H., Ávila, C., 2017. Unraveling the active microbial populations involved in nitrogen utilization in a

- vertical subsurface flow constructed wetland treating urban wastewater. *Sci. Total Environ.* 584–585, 642–650.
- Renn, O., Roco, M.C., 2007. Nanotechnology and the need for risk governance. *J. Nanoparticle Res.* 8, 153–191.
- Rotaru, A.E., Shrestha, P.M., Liu, F., Markovaite, B., Chen, S., Nevin, K.P., Lovley, D.R., 2014. Direct interspecies electron transfer between *Geobacter metallireducens* and *Methanosarcina barkeri*. *Appl. Environ. Microbiol.* 80, 4599–4605.
- Ruiz-Sánchez, J., Campanaro, S., Guivernau, M., Fernández, B., Prenafeta-Boldú, F.X., 2018. Effect of ammonia on the active microbiome and metagenome from stable full-scale digesters. *Bioresour. Technol.* 250, 513–522. doi:10.1016/j.biortech.2017.11.068
- Salvador, A.F., Martins, G., Melle-Franco, M., Serpa, R., Stams, A.J.M., Cavaleiro, A.J., Pereira, M.A., Alves, M.M., 2017. Carbon nanotubes accelerate methane production in pure cultures of methanogens and in a syntrophic coculture. *Environ. Microbiol.* 19, 2727–2739.
- Savolainen, K., Alenius, H., Norppa, H., Pylkkänen, L., Tuomi, T., Kasper, G., 2010. Risk assessment of engineered nanomaterials and nanotechnologies-A review. *Toxicology.*
- St-Pierre, B., Wright, A.D.G., 2014. Comparative metagenomic analysis of bacterial populations in three full-scale mesophilic anaerobic manure digesters. *Appl. Microbiol. Biotechnol.* 98, 2709–2717.
- Sun, H., Zusman, D.R., Shi, W., 2000. Type IV pilus of *Myxococcus Xanthus* is a motility apparatus controlled by the frz chemosensory system. *Curr. Biol.* 10, 1143–1147.
- Sun, L., Müller, B., Westerholm, M., Schnürer, A., 2014. Syntrophic acetate oxidation in industrial CSTR biogas digesters. *J. Biotechnol.* 171, 39–44. d
- Tian, H., Fotidis, I.A., Mancini, E., Treu, L., Mahdy, A., Ballesteros, M., González-Fernández, C., Angelidaki, I., 2018. Acclimation to extremely high ammonia levels in continuous biomethanation process and the associated microbial community dynamics. *Bioresour. Technol.* 247, 616–623.
- Walker, D.J.F., Dang, Y., Holmes, D.E., Lovley, D.R., 2017. The electrically conductive pili of *Geobacter* species are a recently evolved feature for extracellular electron transfer. *Microb. Genomics* 2.
- Wang, J., Musameh, M., 2005. Carbon-nanotubes doped polypyrrole glucose biosensor. *Anal. Chim. Acta* 539, 209–213.
- Yenigün, O., Demirel, B., 2013. Ammonia inhibition in anaerobic digestion: A review. *Process Biochem.* 48, 901–911.
- Zhao, Z., Zhang, Y., Wang, L., Quan, X., 2015. Potential for direct interspecies electron transfer in an electric-anaerobic system to increase methane production from sludge digestion. *Sci. Rep.* 5.

## **Chapter 8 Identification of syntrophic acetate oxidation and electron transfer mechanisms in methanogenic biomass by DNA-stable isotope probing and metagenomics**

---

An interdisciplinary approach based on stable isotope probes combined with metagenomic analysis and characterization of the ribosomal transcriptome, was implemented for characterizing the biomass of three batch assays amended with two different support materials: magnetite and nylon. These batches were incubated with  $^{13}\text{C}$ -acetate under a relatively high ammonia concentration and their performance compared against a control (without support). About 10 Gbp of metagenomics sequence data was obtained through Illumina sequencing. More than 0.5M of protein-encoding genes and 56 population genomes (PG) were extracted from  $^{13}\text{C}$ -DNA by applying a combination of two binning processes. The inclusion of the tested supports was beneficial for methanogenesis but the results also evidenced our limited knowledge about the core biogas microbiome and metabolic pathways. This particularly true for the syntrophic acetate oxidation (SAO), since the majority of 56 PG have not previously been described.

## 8.1 Introduction

Anaerobic digestion (AD) is a well-established technology for the valorisation of organic waste into renewable energy and contributes significantly to the sustainability of several industrial processes. The main environmental parameters that determine the AD efficiency are organic loading rate, pH, temperature and concentration of ammonia (Watson-Craik and Stams, 1995). High levels of ammonia have usually been reported as the main factor causing AD process imbalance due to the inhibition of acetotrophic methanogenic archaea (AMA) (Poggi-Varaldo et al., 1997). This microbial group is responsible for about 70% of methane production under normal conditions, while the remaining 30% is synthesised from hydrogen and carbon dioxide by hydrogenotrophic methanogenic archaea (HMA) (Angelidaki and Ahring, 1993). While all AMA belong to the order Methanosarcinales, HMA is a more ancient phylogenetic group of organisms that diversified in the orders *Methanomicrobiales*, *Methanobacteriales* and *Methanococcales* (Baptiste et al., 2005). Both methanogenic pathways have evolved in *Methanosarcina* spp. (*Methanosarcinales*), which might be considered as facultative AMA or HMA depending on the environmental conditions (Vavilin et al., 2008).

Different strategies have been applied to prevent ammonia inhibition in AD systems: substrate dilution, changes in the operational temperature, the use of additives or materials that favour electron transfer or bioaugmentation (Fotidis et al., 2014). The enrichment of microbial communities that are tolerant to total ammonia nitrogen (TAN) values in the inhibitory range ( $> 2.5 \text{ gTAN L}^{-1}$ ) has been reported as the key process behind the stable operation of anaerobic digesters treating nitrogen-rich substrates (Kayhanian, 1994). One possible explanation for this phenomenon is the selection of ammonia-tolerant microorganisms (Westerholm et al., 2012). The presence of materials that facilitate biofilm formation and/or enhance interspecies electron transfer mechanisms also increment the capacity of AD to overcome ammonia inhibition (Li et al., 2017).

Besides serving as a direct growth substrate for AMA, acetate can also be oxidized to hydrogen and carbon dioxide by the so-called syntrophic acetate oxidizing bacteria (SAOB). These two products can in turn be used by HMA to generate methane. Recent works have demonstrated that the microbes involved in SAOB/HMA syntrophic associations are more tolerant towards ammonia toxicity than the AMA (Fotidis et al., 2013). Little is still known about the biodiversity of SAOB, though it appears that they are a polyphyletic group of microorganisms distributed among distinct clusters of mesophilic and thermophilic species. Known SAOB in the mesophilic range include the species *Clostridium ultunense* (Schnurer et al., 1996), *Syntrophaceticus schinkii* (Westerholm et al., 2010) and *Tepidanaerobacter acetatoxydans* (Westerholm et al.,

2011). The yet to be cultured strain AOR (Lee and Zinder, 1988), and members of *Thermacetogenium phaeum* (Hattori et al., 2000) and *Thermotoga lettingae* (Balk et al., 2002) are adapted to SAO in thermophilic conditions. A recent metagenomic study has shown that the biodiversity of SAOB might be wider than the aforementioned species (Ruiz-Sánchez et al., 2018). DNA stable-isotope probing (DNA-SIP) can specifically identify the members of complex microbial communities actively involved in labelled-tracer ( $^{13}\text{C}$  or  $^{15}\text{N}$ ) turnover. However the identification of syntrophic partnerships, such as the SAOB-HMA, in complex communities is still challenging.

The aim of this work was to characterize the microbial community structure from a mesophilic methanogenic biomass previously adapted to high TAN concentration, stressing on the identification of bacterial species that play an active role in the SAO process, along with their HMA syntrophic partners. Two support materials with very different physicochemical characteristics, magnetite and nylon, were evaluated concerning their effect on methanogenesis. Under those conditions, communities actively assimilating  $^{13}\text{C}$ -acetate were characterized from the analysis of  $^{13}\text{C}$ -enriched DNA (DNA-SIP) by high throughput sequencing of the microbiome (16S rRNA amplicon sequencing) and shotgun metagenomic screens.

## 8.2 Materials and methods

### 8.2.1 Experimental setup

Methanogenic activity on acetate was evaluated in triplicate batch assays (35°C; total volume 120 mL). A fresh inoculum (25.8 gVSS L<sup>-1</sup>, 60 mL of inoculum per vial) was immediately added to all vials after its collection from a mesophilic full-scale CSTR anaerobic digester ( $V = 1,500 \text{ m}^3$ ; HRT = 65 days; Vila-sana, Lleida) fed with nitrogen-rich agricultural wastes (4.5-3.2 gN-TAN L<sup>-1</sup>). Two treatments were prepared with the addition of support materials: magnetite pebbles (LKBA minerals, Luleå, Sweden) and nylon spheres (Dejay distribution, Cornwall, UK), plus a control without support. The particle size range of both support materials was 2-5 mm (Table 8.1). These materials were added to each vial up to 30 % of the apparent volume (18 mL).

All vials were incubated under identical conditions. Three subsequent pulses of acetate and TAN were added to the vials: the first two pulses (days 0 and 25; Figure 8.1) ensured an initial concentration of 3 gAcetate L<sup>-1</sup> of unlabelled sodium acetate and 7 gN L<sup>-1</sup> of TAN. The liquid fraction (60 mL) was carefully removed and replaced by fresh mineral medium. That medium was composed by 1ml/L of (0.125 gNiCl<sub>2</sub>·6H<sub>2</sub>O/L ; 25 g FeCl<sub>2</sub>·6H<sub>2</sub>O/L; 1.25 g(NH<sub>4</sub>)<sub>6</sub>MO<sub>7</sub>O<sub>2</sub>·4H<sub>2</sub>O/L; 0.075 g CoCl<sub>2</sub>·6H<sub>2</sub>O/L) and 1ml/L

(17 g  $\text{NH}_4\text{Cl}\cdot 12\text{H}_2\text{O}/\text{L}$ ; 3.7 g  $\text{KHPO}_4/\text{L}$ ; 0.56 g  $\text{MgSO}_4/\text{L}$  ; 0.8 g  $\text{CaCl}_2\cdot 2\text{H}_2\text{O} /\text{L}$ ) and  $\text{NH}_4\text{Cl}$  solution (to ensure 3.5 or 7.0 gN-TAN  $\text{L}^{-1}$ , depending on the vial),(day 40; Figure 8.1). The replacement was done without altering the attached biofilm on the carrier material and the headspace inside the vials, in order to minimize the presence of phosphate and carbonate that might hinder the subsequent DNA-SIP experiments. A final pulse of 1 gacetate  $\text{L}^{-1}$  of uniformly  $^{13}\text{C}$ -labelled sodium acetate and 7 gN  $\text{L}^{-1}$  of TAN was given at day 40 (Figure 8.1).

Samples for total DNA extraction and separation of  $^{13}\text{C}$ -enriched DNA were taken from each vial at days 40 and 45, respectively. The supernatant was derived to VFA quantification (see Chapter 3 for details) throughout time. The composition of biogas was determined and, once normalised at 273 K and 1 atm, then used to determine the net methane yield and specific production rate ( $r\text{CH}_4$ ; see Chapter 3 for details).

## 8.2.2 DNA extraction and separation of $^{13}\text{C}$ -enriched DNA

Total DNA was extracted from samples (approx. 0.25 g) of the liquid phase and the support materials collected in the course of the third feeding pulse, during the exponential phase of biogas production, using the PowerSoil® DNA Isolation Kit (MoBio Laboratories Inc., Carlsbad, USA). DNA extracts were then mixed with a cesium chloride solution (final density 1.72 g  $\text{mL}^{-1}$ ) in a 6 mL polyallomer ultracrimp tube (Kendro Laboratory Products, Newtown, USA). The tubes were crimp-sealed and ultracentrifuged in a Sorvall RC70 ultracentrifuge using a TV-1665 rotor (Sorvall, Newtown, USA) at 145,200 g for 48 h at 20°C. Fractions of 250  $\mu\text{L}$  each were collected from the bottom of each tube. The density of each fraction was directly determined based on its refractometry index on a Reichert AR200 digital refractometer (Reichert Technologies, Buffalo, NY). Total DNA in each fraction was quantified using a NanoDrop 3300 fluorospectrometer (NanoDrop Products, Wilmington, USA) with the Quant-iT PicoGreen double-stranded DNA (dsDNA) assay kit (Invitrogen, Eugene, USA). To identify shifts in the community DNA resulting from isotopic enrichment, a denaturing gradient gel electrophoresis (DGGE) was performed on each fraction using the bacteria-specific primers 341FGC/517R, in 10% acrylamide gels with a linear denaturing gradient of 35 to 65%. Electrophoresis was performed at a constant voltage of 60V for 16 hours on a DCode universal mutation detection system (Bio-Rad Laboratories, Hercules, USA). Fractions that corresponded to heavy DNA in extracts from each flask containing  $^{13}\text{C}$ -labeled acetate were identified based on total DNA concentration and DGGE analysis by comparison with unlabeled samples. Subsequently next generation sequencing was performed by following procedure describe in chapter 3.

### 8.2.3 Metagenome sequencing

DNA-SIP fractions containing  $^{13}\text{C}$ -enriched DNA from each treatment (magnetite and nylon packing) and from control incubations were pooled (from independent triplicates), and prepared for sequencing using Nextera DNA Library Preparation Kit (Illumina, San Diego, USA). All the samples were paired-end sequenced ( $2 \times 150$  bp) using Illumina HiSeq 2500 (Molecular Research DNA, Shallowater, USA).

Paired-end reads obtained from Illumina sequencing were quality-filtered and adaptors were removed using Trimmomatic software (v0.33) with the following parameters: Illumina clip (NexteraPE-PE:2:30:10), leading (10), trailing (10), sliding window (4:20, minlen (65) (Bolger et al., 2014). Filtered reads were assembled using metaSPAdes (3.9.0) with kmers 55, 77, 99 and a minimum scaffold length of 500 bp (Nurk et al., 2017). Metrics of the assembly were checked using QUAST software (Gurevich et al., 2013). Gene finding was performed on all the scaffolds with Prodigal (v2.7.2) run in metagenomic mode (Hyatt et al., 2012). All the protein-encoding genes identified in the assembly were annotated using reverse-position specific BLAST algorithm and using COG RPSBLAST data base (Galperin et al., 2015); only results with e-value lower than  $1e-5$  were considered. Genes were also annotated according to KEGG with GhostKOALA software (Kanehisa et al., 2016). The coverage of the genes identified in the assembly was determined by aligning back the reads to the scaffolds and calculating the number of reads per each gene defined in the “gff” annotation file by using HTSeq software. Scaffolds were binned into Population Genomes (PGs) using MetaBAT (v0.25.4) (parameters --specific, -m 1500) (Kang et al., 2015). 39 PGs were obtained using this method. The scaffolds assigned to the PGs were then visualized using MeV software (Saeed et al., 2003) and PGs that escaped the MetaBAT binning were captured with the “hierarchical clustering followed by canopy profile selection” strategy (Campanaro et al., 2016). Additional 17 PGs were collected with this method demonstrating that the combined use of multiple binning strategies markedly increase the number of PGs recovered. The PGs obtained from the two approaches were compared using the “bin-compare” module of checkM package to ensure that the PGs recovered with the “hierarchical clustering followed by canopy profile selection” were completely independent from those obtained using MetaBAT (Parks et al., 2015). After this verification, a small group of scaffolds assigned to more than one PG was removed and “completeness” and “contamination” was determined using checkM for the PGs included in the final selection.

Functional analysis of the PGs was based on KEGG annotation performed using Hidden Markov Models present in the FOAM software (Prestat et al., 2014). Taxonomical assignment for the PGs was obtained using Phylophlan (v0.99) (Segata et



al., 2013). The presence of genomes belonging to the same species in the NCBI microbial genome database and in PGs recovered in previous genome-centric studies was determined using Average Nucleotide Identity calculation (ANI) as previously described (Treu et al., 2016; Vanwonderghem et al., 2016; Campanaro et al., 2017; Campanaro et al., 2016). Genomes were considered as belonging to the same species when ANI value was higher than 95% and the number of common genes was more than 50% (Varghese et al., 2015).

Abundance of PGs in different reactors was derived from the scaffold coverage. This parameter was determined by aligning the reads on the assembly using Bowtie2 software (v2.2.4) and converting the results in the corresponding coverage value using BEDTools package (v2.17.0). Results were normalized considering the sample with the lower number of reads as a reference. Coverage values were visualized with MeV software (Saeed et al., 2003) in order to identify the behaviour of PGs in different samples. Data derived from 16S rRNA gene amplicon sequencing and metagenome raw data were deposited in the NCBI Sequence Read Archive (SRA) under accession number SRR6277370.

## **8.3 Results**

### **8.3.1 Effect of support materials on methanogenic activity**

Methane production was monitored during three acetate pulses in batch reactors subjected to a high ammonia concentration ( $7 \text{ gN L}^{-1}$ ) (Figure 8.1 and Table 8.1). The VFA content was determined upon decline of methane production and before a new acetate pulse, but VFA accumulation was never detected (data not shown). The cumulative  $\text{CH}_4$  production was consistently higher in reactors packed with nylon, with a 23% increase in the  $\text{CH}_4$  yield with respect to the controls. A similar yet more moderate increment in  $\text{CH}_4$  yield (17%) was also observed in batches amended with magnetite.

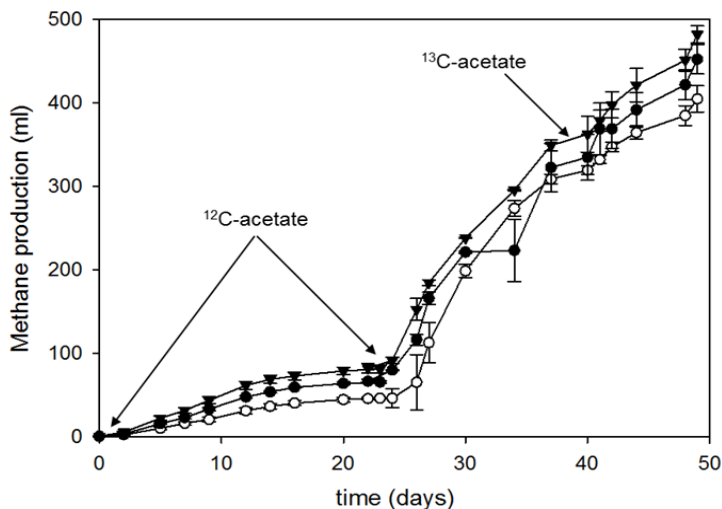


**Figure 8.1** Time-course methane production in batch incubations packed with ( $\blacktriangle$ ) Nylon, ( $\bullet$ ) Magnetite and ( $\circ$ ) unpacked control.

### 8.3.2 DNA stable-isotope probing of the $^{13}\text{C}$ -acetate metabolism

Total DNA extracts from the batch incubations subjected to acetate pulses with and without the  $^{13}\text{C}$ -label were subjected to isopycnic ultracentrifugation in a CsCl density gradient. Relatively well defined smear peaks in DNA concentration profiles appeared in  $^{13}\text{C}$ -labeled samples at buoyant densities above  $1.726\text{-}1.728\text{ g}\cdot\text{mL}^{-1}$ , which were absent in unlabeled samples. In addition, positive PCR amplification was achieved in those heavy  $^{13}\text{C}$ -DNA fractions, while such results were not observed in the corresponding fractions from unlabeled samples. DGGE banding profiles of heavy DNA fractions showed a reduced number of bands when compared with light DNA fractions (densities below  $1.726\text{ g}\cdot\text{mL}^{-1}$ ). As a result, DNA enriched with  $^{13}\text{C}$  derived from labeled acetate was successfully recovered from batch incubations of the three assayed incubation conditions by pooling together fractions with buoyant densities  $1.726\text{-}1.74\text{ g}\cdot\text{mL}^{-1}$  for control and magnetite samples, and  $1.728\text{-}1.746\text{ g}\cdot\text{mL}^{-1}$  for nylon samples.

### 8.3.3 Microbial community composition

The different DNA fractions obtained from the previously described methanogenic batch reactors were analysed by 16S rRNA gene amplicon sequencing. Both heavy ( $^{13}\text{C}$ -enriched) and light (natural abundance of  $^{12}\text{C}$ ) DNA fractions from biomass samples

exposed to  $^{13}\text{C}$ -acetate were used as templates. Total DNA extracts from batches supplemented with unlabelled-acetate were used as representatives of the total communities. More than 60,000 sequences per sample passed the quality filters.

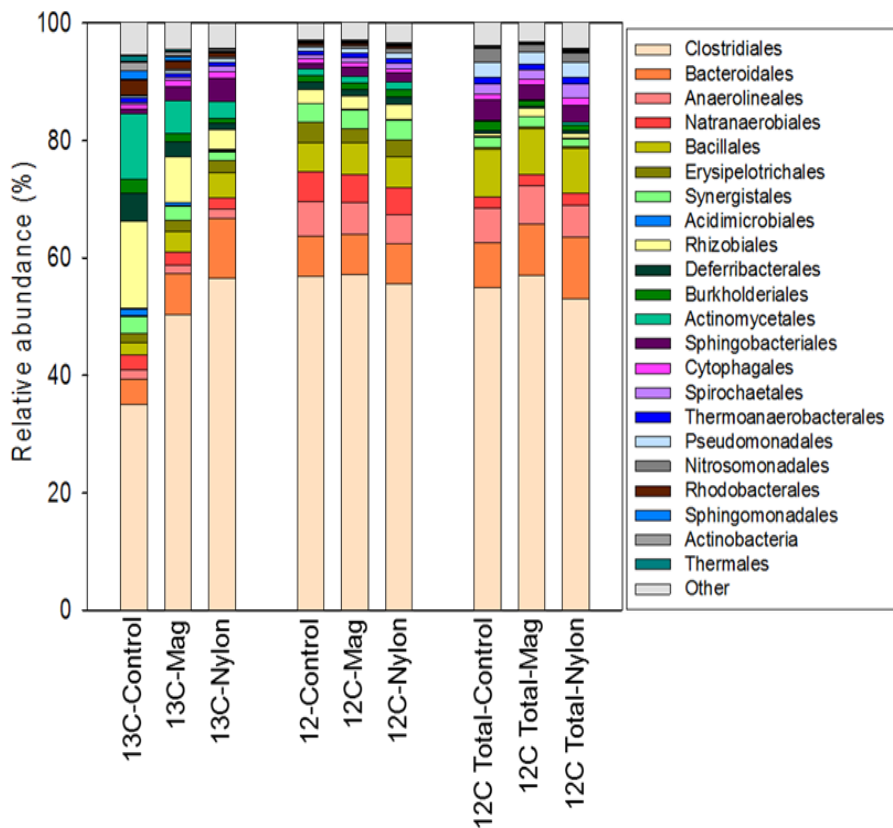


**Figure 8.2** Relative abundance of bacterial (order) (A) and archaeal (genus) (B) ribotypes, in terms of 16S rRNA gene counts in methanogenic batch assays, for the  $^{13}\text{C}$  (heavy fraction),  $^{12}\text{C}$  (light fraction) and  $^{12}\text{C}$ -Total (total DNA for batches without  $^{13}\text{C}$ -Acetate).

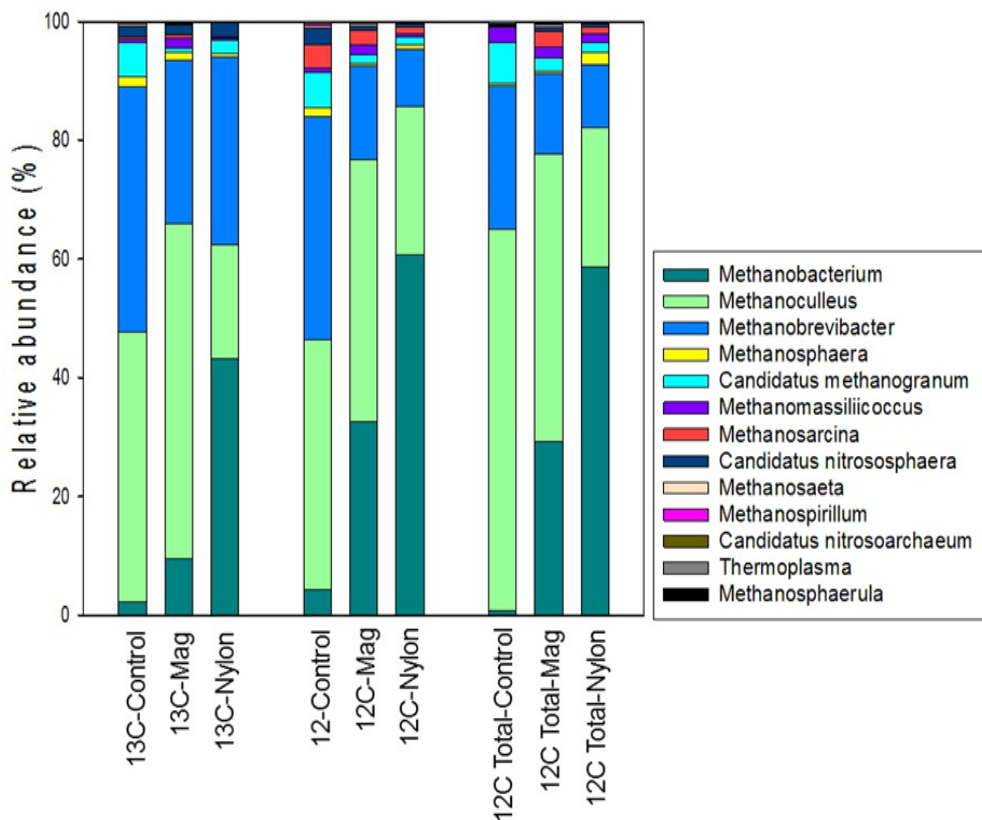


**Figure 8.3** Relative abundance of bacterial (order) (A) and archaeal (genus) (B) ribotypes, in terms of 16S rRNA gene counts in methanogenic batch assays, for the  $^{13}\text{C}$  (heavy fraction),  $^{12}\text{C}$  (light fraction) and  $^{12}\text{C}$ -Total (total DNA for batches without  $^{13}\text{C}$ -Acetate).

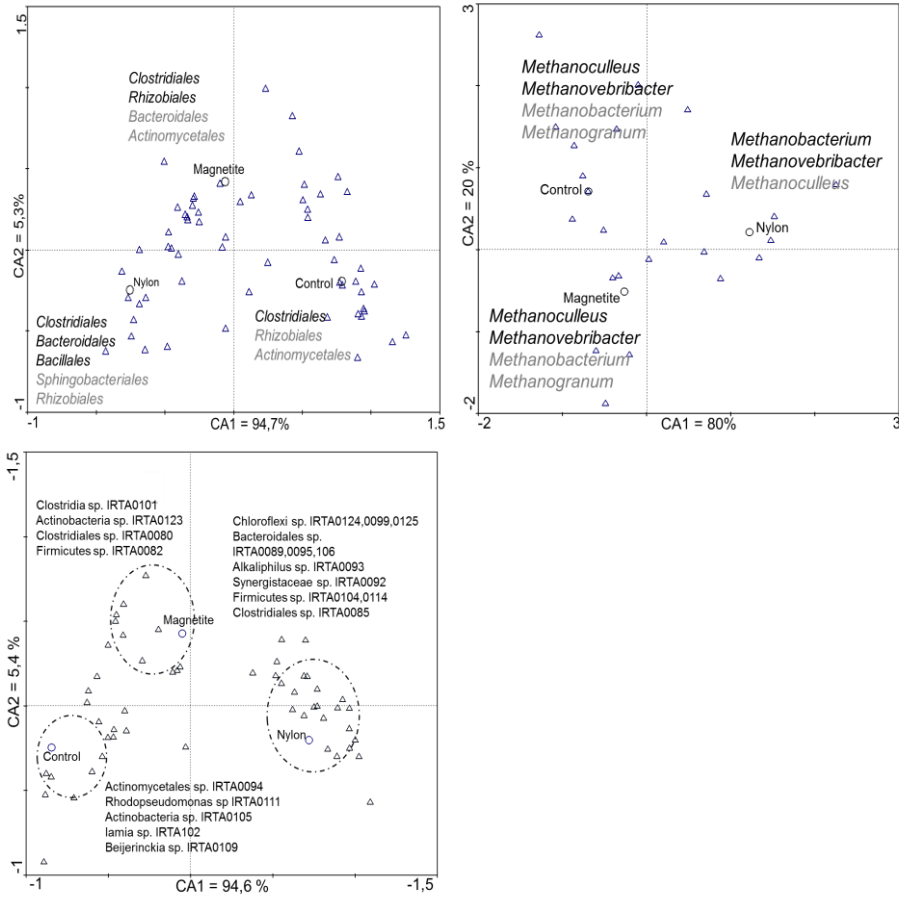


**Figure 8.4** Correspondence Analysis biplot on sample scores (circles) and operational taxonomic units (triangles) from the unpacked control, and batches amended with magnetite and nylon, concerning the abundance of 16S rRNA gene copies (based on  $^{13}\text{C}$ -DNA) for bacteria (a), archaea (b), and for bacterial metagenomes (c). In a and b only OTUs with a sample relative abundance higher than 3% have been represented; those with a relative abundance higher than 10% have been highlighted in bold

and for bacterial metagenomes (c). In a and b only OTUs with a sample relative abundance higher than 3% have been represented; those with a relative abundance higher than 10% have been highlighted in bold.

(CA) revealed differences between treatments based on  $^{13}\text{C}$ -DNA (Figure 8.3). Regarding the bacterial communities, the analysis of the total DNA extracts and the  $^{12}\text{C}$ -DNA fractions no differences were observed between samples. However, for every treatment, the populations observed in the heavier  $^{13}\text{C}$ -DNA fractions were meaningfully different from those in the lighter  $^{12}\text{C}$ -DNA fractions (figure 8.2). This result indicates that the  $^{13}\text{C}$ -DNA fractions were enriched with microbial species that were using acetate as a carbon source. In all cases, the relative abundance of OTUs assigned to the order *Clostridiales* (56%) predominated well above those identified in the *Bacteroidales* (7%), *Bacillales* (6%), and *Anaerolineales* (6%) (Figure 8.2).

Microbial populations in the  $^{13}\text{C}$ -DNA fractions were similar in all samples, with *Clostridiales* being the predominant order; however some differences were observed in the abundances of the other orders (Figure 9.2). Within the order *Clostridiales*, representatives of the genera *Clostridium* and *Acetivibrio* predominated. The relative abundance of *Clostridium* was 21%, 36% and 46% in the control, magnetite and nylon, respectively, while that of *Acetivibrio* was 10%, 9% and 5%. Such dominance of *Clostridium* was somehow expected, as members of this genus are commonly found in AD systems and play a fundamental role as hydrolytic/fermentative microorganisms. In fact, a well described SAO bacteria belongs to *Clostridium* genus (*Clostridium ultunense*). In contrast, reports on the occurrence of the genus *Acetivibrio* in acetate and ammonia-rich environments are scarce. However, this genus has extensively been reported that produces acetic acid, hydrogen, and carbon dioxide in cellulose-rich environments (Laube and Martin, 1981). *Acetivibrio* are also common hydrolytic bacteria in anaerobic bioreactors, and their presence in the heavy DNA fraction could be explained by co-metabolic acetate assimilation.

Individual BLAST searches on predominant OTUs sequences belonging to *Clostridiales* taxon (>1% of relative abundance) from the  $^{13}\text{C}$ -DNA fraction yielded uncultured bacteria. The relevant OTU1 (abundance 2.8-11.2%) and OTU22 (abundance 7.2-11.6%) were closely related to the genus *Clostridium* (99% and 100% sequence similarity). Other abundant OTU from the heavy DNA fraction (OTU5, abundance 2-4.5%), was highly similar (99% sequence similarity) to *Terrisporobacter petrolearius*, recently isolated from an oilfield petroleum reservoir with high hydrolytic capabilities (Deng et al., 2015). Additional OTUs ascribed to this genus (*Clostridium*) have also been found to be active upon ammonia exposure, but their abundance was considerably lower.

Representatives of the order *Rhizobiales* were enriched in the control (15% in relative abundance) in relation to the magnetite and nylon batches (8% and 3.3% in abundance). A similar trend was observed in the Actinomycetales order, where the relative abundance dropped from 11% in the control to 6% and 3% in the magnetite and nylon batches. Conversely, other microbial taxa, such as *Bacteroidales*, became more abundant in the packed batches (6% and 8% of relative abundance in magnetite and nylon, compared to 4% in the control). *Bacillales* order was also relevant in the presence of nylon and magnetite (4%) compared to the control (2%).

From the archaeal population, the most abundant genera were affiliated to the primarily hydrogenotrophic methanogen genera *Methanoculleus* (45%, 56% and 20%), *Methanobrevibacter* (41%, 28% and 32%), and *Methanobacterium* (2%, 9% and 43%) for control, magnetite and nylon, respectively. Yet, hydrogen-dependent methylotrophs as *Methanogranum* (6%, 1% and 2%) and *Methanomassillicoccus* (0.5%, 2% and 0.5%) were also detected. Furthermore, the CA from the heavy DNA fraction, revealed evident differences between treatments. While representatives of the genera *Methanoculleus* and *Methanobrevibacter* were more relevant in the unpacked control and on the magnetite support material, *Methanobacterium* was the main genus on nylon.

#### 8.3.4 Metagenome reconstruction

After quality filtering, the number of sequences per sample ranged from 9.4 to 10.5 million of single-end reads. The assembly included 213,170 scaffolds (~283 Mbp, after removing scaffolds shorter than 500 bp), and the gene-finding and annotation process resulted in the identification of 426,166 protein-encoding genes. A binning strategy was applied to the scaffolds and allowed the extraction of 56 population genomes (PG), 25 of them with completeness higher than 70% (table 8.2). Despite this extensive investigation, only 10 PGs could be affiliated to known genera: two were assigned to the genus *Clostridium*, while the other eight belonged to the genera *Sphaerochaeta*, *Illumatobacter*, *Alkaliphilus*, *Iamia*, *Beijerinckia*, and *Rhodopseudomonas* in the bacterial domain, and *Methanoculleus* and *Methanomicrobiales* in the archaeal domain. The remaining 44 PGs could only be assigned to higher taxonomic categories.

The relative abundance of PGs in the heavy DNA collected from vials treated with different support materials was investigated. Four PGs (i.e. *Illumatobacter* sp. IRTA0091, Synergistaceae sp. IRTA0092, Xanthobacteraceae sp. IRTA0097 and *Aciditerrimonas* sp. IRTA0096) presented similar abundances in the three different assayed conditions (unpacked control, packing with magnetite and nylon). Nevertheless, some PGs changed their abundance depending on the packing material, as shown by multivariate analysis (Figure 8.3c). Unpacked control batch reactors were dominated by Actinomycetales sp. IRTA0094, *Rhodopseudomonas* sp IRTA0111, Actinobacteria sp.

IRTA0105, *Iamia* sp. IRTA102 and *Beijerinckia* sp. IRTA0109. An increased abundance of *Clostridia* sp. IRTA0101, *Actinobacteria* sp. IRTA0123, *Clostridiales* sp. IRTA0080 and *Firmicutes* sp. IRTA0082 was observed with the magnetite packing. The most diverse community, though, was found with the nylon packing, which promoted the enrichment of *Chloroflexi* sp. IRTA0099, 0124 and 0125, *Bacteroidales* sp. IRTA0089, 0095 and 0106, *Alkaliphilus* sp. IRTA0093, *Synergistaceae* sp. IRTA0092, *Firmicutes* sp. IRTA0104 and 0114 and *Clostridiales* sp. IRTA0085. These results are in agreement with those obtained from the 16S rRNA sequencing of the heavy DNA fraction (Figure 8.2 and Figure 8.3a).

In an independent procedure, all the genes identified from the assembled metagenome were identified and annotated based on similarity to KEGG and COG databases. Additionally, the abundance of each gene in the different samples was examined and normalized depending on the total number of reads obtained for each sample. Since the Wood-Ljungdahl (WL) pathway is a key mechanism for acetate utilization (Drake, 1994; Ragsdale, 2008; Ragsdale and Pierce, 2008) the abundance of genes belonging to this pathway (i.e. *Acs*, *Pta*, *MTHFR*, *MTHFD1*, *MTHFD2*, *MTHFD1L* and *fdh*) was studied (Figure 8.4). However, no evident differences were observed between treatments. Furthermore, genes encoding for glycine cleavage system (GCS), an alternative pathway for acetate assimilation described by (Nobu et al., 2015) were also assembled and counted (figure 8.7)

From the reconstruction of genes associated to the WL and GCS pathways, it is concluded that only those PGs affiliated to the phyla *Firmicutes*, *Chloroflexi* and *Bacteroidetes* contained all the genes involved in those pathways, except for the methyltransferase gene, which no assignment could be obtained. It was remarkable the predominance in all samples of members of the phylum *Firmicutes*, which is the group encompassing most well-known SAO bacteria (Schnürer and Nordberg, 2008; Schnürer et al., 1996; Westerholm et al., 2011). For the remaining PGs belonging to the phyla *Proteobacteria*, *Actinobacteria* and *Synergistetes*, some genes of the WL pathway were missing. These results suggested that not all 56 PGs assembled in the present study from the heavy DNA fraction were strictly associated to SAO via the WL pathway, and they could have obtained the labelled carbon from cross-feeding.



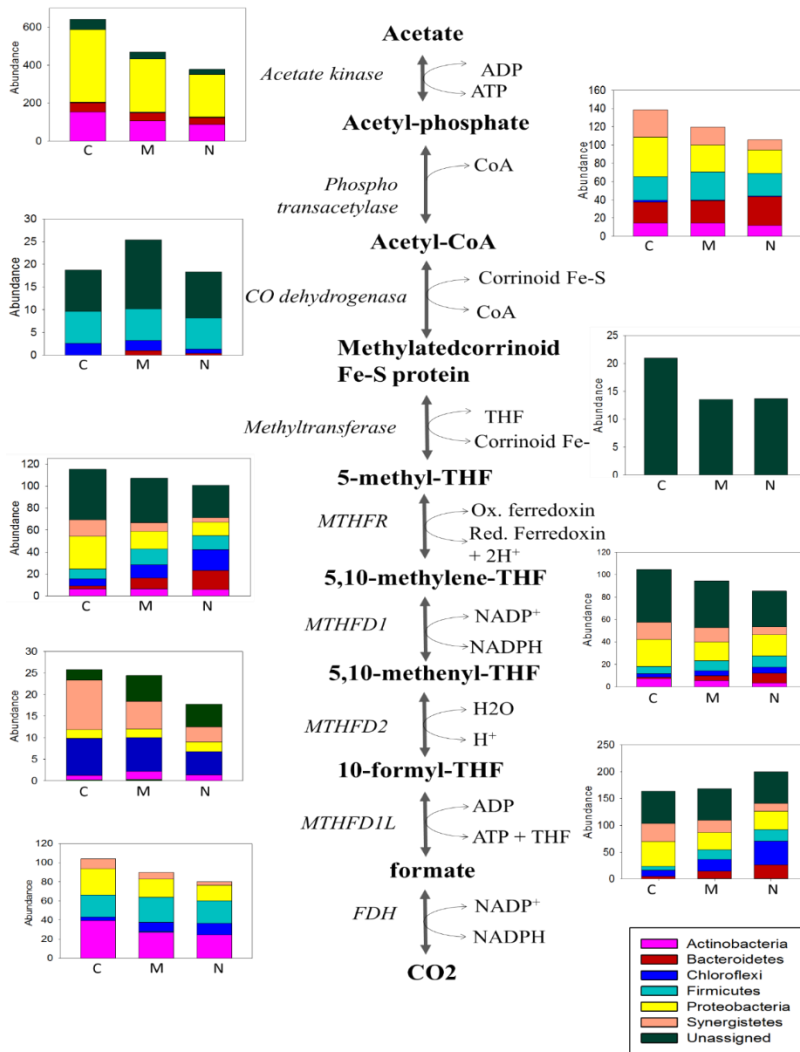


**Figure 8.5** Abundance of genes involved in the Wood-Ljungdahl pathway based on SEED annotation. c. Control m.Magnetite n. Nylon

Additionally, the abundance based on counted genes of WL pathway was quite similar in all conditions.

The mechanisms directly involved in acetate assimilation were assessed through metagenomic sequencing of the  $^{13}\text{C}$ -enriched DNA fractions. Bacterial communities in AD systems under nitrogen stress are known to be usually dominated by members of the order *Clostridiales* (*Firmicutes* phyla) (Westerholm et al., 2012). Here, despite the predominance of Firmicutes, PGs belonging to the phyla *Chloroflexi* and *Bacteroidetes* were also present in relatively high proportions. Based on COG and KEGG annotation, key genes involved in acetate assimilation were identified. Special attention was given to genes encoding for the formyltetrahydrofolate synthase, which has been proposed as a biomarker of SAO activity due to its relevance in the reductive acetogenesis (Matsui et al., 2008), and the acetyl-CoA synthase, which is exclusive of the WL pathway (Schauder et al., 1988). From this data, it was possible to reconstruct the full WL pathway in some PGs (figure 8.4), suggesting their implication in the SAO process and, thus, widening the biodiversity of bacteria that might be involved in the SAOB-HM syntrophy.

It is noteworthy to mention the effect of packing materials (magnetite and nylon) on genes that might be involved in interspecies electron transfer (IET). IET, which is strongly associated to syntrophism, which might be stimulated by conductive materials, such as magnetite. It has previously been described that electrons can be transferred through microbial membranes, in a process that involves a number of proteins induced by the external redox potential. In Figure 8.5, we show the relative abundance of the different IET-related genes (*cbc*-cluster, *omc*, *mtrABC* cluster and *c*-type genes) previously identified in the literature (Shi et al., 2016; Yang et al., 2012). Significant Apparent differences on their relative abundance were observed in relation to the packing material. Furthermore, phylogenetic analysis of all the detected IET-related genes detected revealed their predominant affiliation to members of *Proteobacteria*, suggesting that this phylum plays a major role in IET-processes.

Concerning the archaeal domain, 2 PGs belonging to the genus *Methanoculleus* (IRTA0126 and IRTA0119), with an estimated completeness of 45.7% and 95.5%, respectively, were assembled from the heavy DNA fraction. Despite the genus *Methanoculleus* has been described as hydrogenotrophic, recent evidences suggest that it could also assimilate acetate to a certain extent (Ruiz-Sánchez et al., 2018).

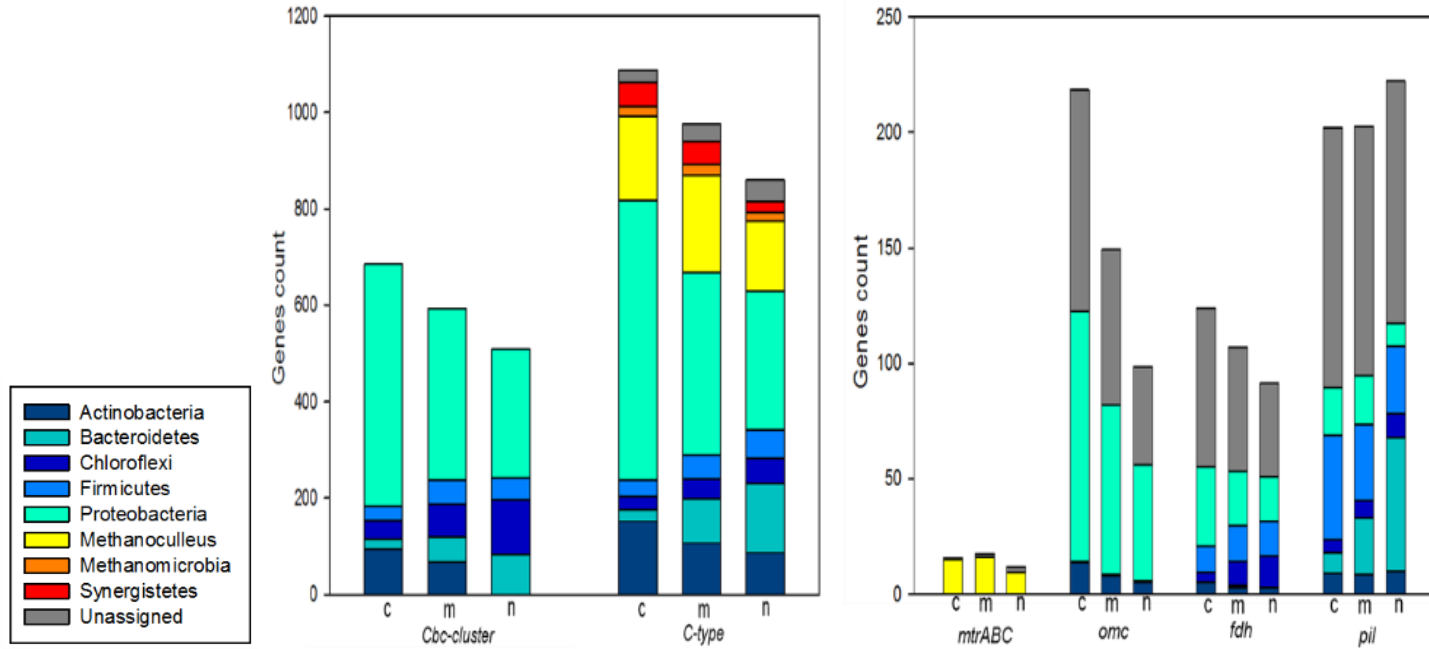


**Figure 8.6** Abundance of genes involved in electron transfer mechanisms based on SEED annotation (cbc cluster, omp, mtrABC, c-type, fdh and pil). c. Control; m. Magnetite; n. Nylon.

## 8.4 Discussion

The methanogenic biomass used as inoculum in the present study was taken from a full-scale AD treating nitrogen-rich waste, from which the SAOB-HMA syntrophism was described as the main pathway for acetate conversion into methane (Ruiz-Sánchez et al., 2018). The predominance of HMA as the major methanogenic pathway in that digester was confirmed from the  $^{13}\text{C}/^{12}\text{C}$  isotopic fractionation pattern for  $\text{CO}_2$  and  $\text{CH}_4$  (Ruiz-Sánchez et al., 2018). In our incubations, the TAN level was set at  $7 \text{ gTAN L}^{-1}$  to ensure HMA activity (Poirier et al., 2017).

The performance of all batches in terms of methane production showed significant differences between treatments during the three acetate pulses (SM). Supplementation with  $3 \text{ g }^{12}\text{C-acetate L}^{-1}$  (first and second pulses) and  $1 \text{ g }^{13}\text{C-acetate L}^{-1}$  (third pulse) resulted in similar lag phases and methane production rates (Figure 8.1), but differences were observed in methane yield (table 8.1), which was increased by 20% and 12% with nylon and magnetite, respectively, in relation to the control. Ahammad et al., 2013 reported that nylon-based packing materials promote the preferential immobilization of methanogens and, thus, results in an increased methane production. Batches packed with magnetite also increased methane production, but this enhancement has been attributed to the electrical conductivity of the material facilitating the direct electron transfer between microorganisms (Cruz Viggi et al., 2014).

Based on the relative abundance of 16S rRNA gene amplicon reads, the proportion of archaea was very low (1-2%) if compared to the bacterial community (98-99%). These results were consistent in all tested DNA fractions, and were in accordance with the phylogenetic information retrieved from the metagenome analysis. Most of the taxa affiliated within the archaeal domain corresponded to hydrogenotrophic methanogens (rang more than 90%), being *Methanoculleus*, *Methanobrevibacter* and *Methanobacterium* the most abundant genera, which is in agreement with previous findings obtained from similar ammonia-stressed environments (Zhuang et al., 2015; Ruiz-Sánchez et al. 2018). The archaeal community structure found in the three assayed conditions was quite similar (Figure 8.2), something expected considering that HMA primarily use  $\text{CO}_2$  and formate as C-source, but not acetate (Demirel and Scherer, 2008). However, the relative abundances of HMA were rather different in relation to the tested support materials (Figure 8.3b). *Methanobacterium* was the major group with nylon and *Methanoculleus* with magnetite, while *Methanobrevibacter* predominated in the unpacked control. These results suggest that members of *Methanobacterium* could be more efficient in biofilm formation than other HMA. This hypothesis has also been suggested in agreement with a previous study by (Siegert et al., 2014) based on experimental evidence from microbial electrolysis cells. Remarkably, the 2 assembled archaeal PGs (highest completeness

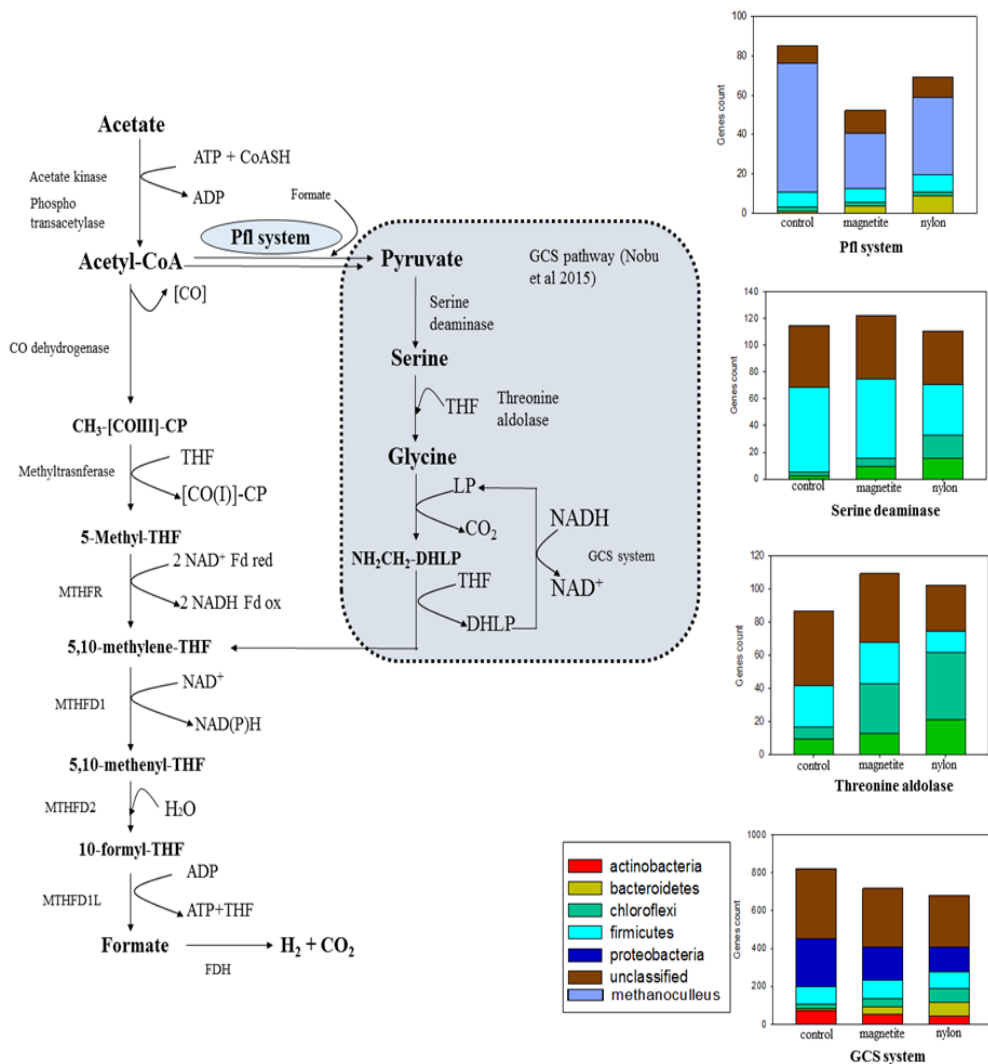
95.10%, table 8.2) were affiliated to the genus *Methanoculleus*, which has been described as an exclusively HMA (Maus et al., 2012). The dominance of *Methanoculleus* spp. in the  $^{13}\text{C}$ -DNA rich fraction upon relatively short  $^{13}\text{C}$ -acetate exposure supports recent studies on the presumed capability of this genus to assimilate acetate (Ruiz-Sanchez et al., 2018; Barret et al., 2015).

The two tested support materials, magnetite and nylon, are different in terms of conductivity, hydrophobicity, and rugosity, affecting their ability to favour biofilm formation and electron transfer mechanisms (Figure 8.6). Both processes have been reported to promote synergistic microbial interactions in methanogenic biomass, including the SAOB-HMA syntrophy that turns the AD process more resistant to ammonia inhibition. The bacterial community profile observed in samples from batches incubated with unlabelled acetate was very similar in all cases, thus pointing to the fact that no substantial microbial shifts occurred during the experiments (DGGGE Supp material?). In contrast, the analysis of the  $^{13}\text{C}$ -enriched DNA depicted some distinctive active microbial communities that were specific from acetate assimilation. The most abundant taxon present in all batches was affiliated to the *Clostridiales* (phylum *Firmicutes*). Members of this order are commonly related to different stages of the AD process, such as hydrolysis, acidogenesis, and acetate oxidation (Mosbæk et al., 2016), and species in the *Clostridiales* usually dominate ammonia-stressed AD systems.

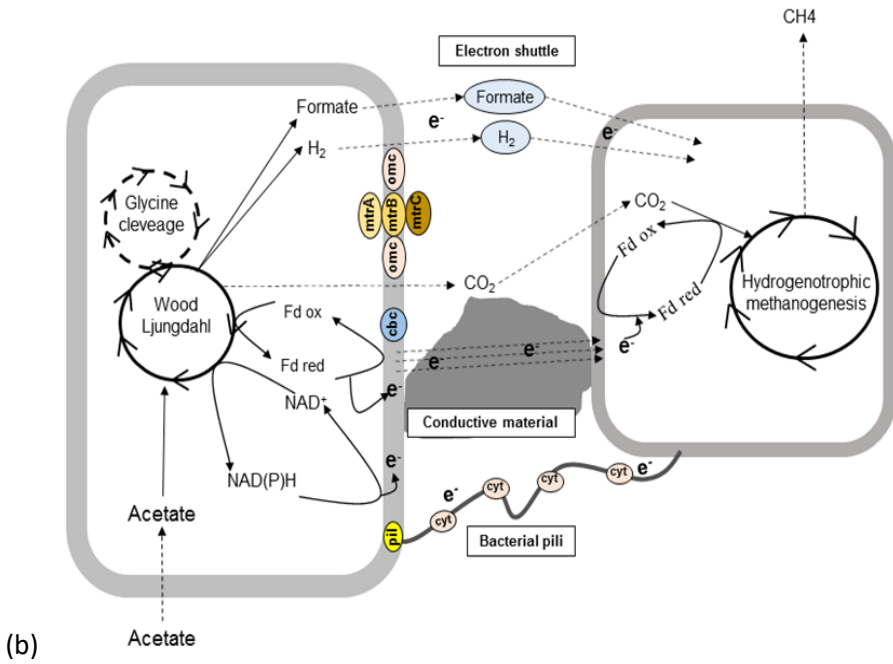
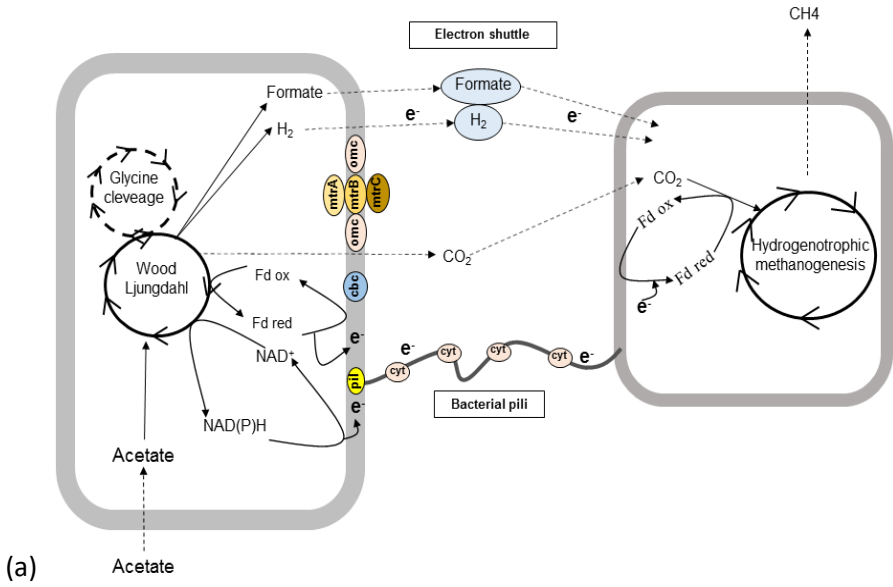
Along with the order *Clostridiales*, representatives of *Chloroflexi*, *Bacteroidales* and *Bacillales* were observed in relatively high proportion in the nylon packing (Figure 9.3c). This result is in agreement with the general tendency of species in *Bacteroidales* and *Bacillales* to produce biofilms under different environments (Bertin et al., 2006; Wang et al., 2017). Because of the polymeric and fibrous structure of nylon, this material has the optimum conditions to stimulate cell aggregation and biofilm formation (Ahammad et al., 2013). Biofilms cover microorganisms in an exopolymeric matrix that favours the exchange of electrons and biomolecules, which could favour methane production by increasing the direct contact between bacteria and methanogenic archaea (Kouzuma et al., 2017). In contrast, species in *Acetivibrio* (family Clostridiaceae) became more relevant with the magnetite packing and in the unpacked control batches. To our knowledge, this genus has not been found previously to be predominant in ammonia rich AD systems, but it has been described as an efficient cellulose-degrading taxon that can grow as well on acetate (Murray, 1986). Hence, *Acetivibrio* might very well be involved in the SAO process. In addition, the biodiversity of acetate assimilating microorganisms was higher with magnetite and in the unpacked control batches, with an increased relative abundance of species of the orders Rhizobiales, Actinomycetales and Bacteroidales in  $^{13}\text{C}$ -DNA fraction. Members of the order Rhizobiales (phylum Proteobacteria) have

recently been described as partners in extracellular electron transfer, being capable to generate electrical current in microbial fuel cells (Milner et al., 2016).

Biofilm formation was only promoted on nylon and, hence, other mechanisms might be responsible for interspecies electron transfer in the magnetite packing and the unpacked control. Syntrophic species involved in acetate metabolism can be driven by electrons from either a solid material (such as an electrode) or acetate oxidation, via interspecies electron transfer (IET), or by direct interspecies electron transfer (DIET) from a heterotrophic partner bacterium (Ha et al., 2017). IET can also occur via biotic mechanisms, such as pili, or via conductive materials, like Fe(III) and Fe(II) of magnetite (Smith et al., 2013). Such electron transfer mechanisms increase the microbial biodiversity and facilitate the energy gain from reactions that cannot be catalysed by a single microbe. The proteins directly involved in IET, cytochrome bc type (CBC-cluster), outer membrane cytochromes (OMC), and metal-reducing (MTR), were described previously (Schagger et al., 1994; De Bok, Plugge and Stams, 2004) and assessed in this study (Figure 6). All these proteins converge in a pathway that oxidizes quinol in the cytoplasmic membrane and transfers the released electrons through the external membrane (Shi et al., 2012). With respect to this, a higher abundance of the cbc-cluster protein was observed in the unpacked control, in relation to the magnetite and nylon packings (Figure 5), which decreased by a 13.5% and 14.2% in those packings in relation to the control. IET also plays a key role in the physiology of methanogens; the formate dehydrogenase (*fdh*) genes involved in the oxidation of formate are powerful electron donors/acceptor in anaerobic environments that can act as an electron carrier between syntrophic partners. Counts of this gene decreased by a 47% and 25% in the magnetite and nylon packed batches, with respect to the control (Figure 8.6).



**Figure 8.7** GCS system pathway (linked to Wood-Ljungdahl pathway) genes abundance based on SEED annotation.





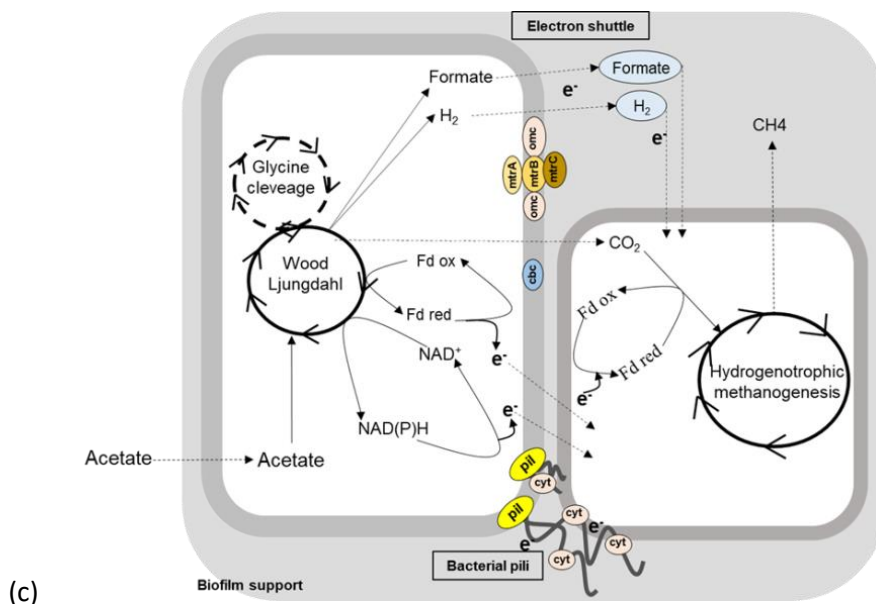


**Figure 8.8** Conceptual model of syntrophic interaction between acetate oxidizing bacteria and hydrogenotrophic methanogen. Genes directly involved in specific mechanisms have been indicated (cbc, omc, mtrABC, pil). 6A Mechanisms involved in unpacked batches. 6B Mechanisms involved when conductive materials are introduced in the environment. 6C Electron transfer processes in biofilm formation

DIET has been described recently as an effective syntrophic mechanism in methanogenic communities, and little is known about the biodiversity of the involved species. DIET might be promoted by adding conductive or semi-conductive materials, such as magnetite, thus bypassing biological electrical conduits (Cruz-Viggi et al., 2014). However, Rotaru et al., 2014 pointed out to the importance of proteins involved in pili formation (encoded by the pil gene) and in electron transport (encoded by omc and c-type genes) in DIET. Pili formation is not essential for IET, but the expression of genes involved in electron transfer (CBC-cluster, OMC, and MTR) are needed when a conductive material is added (Walker et al., 2016). Our results showed that pili genes were slightly more abundant in nylon-packed vials than in magnetite or control vials. These differences indicated that pili-forming microbes with an ability to form biofilms are favoured in nylon-packed batches. In contrast, genes involved uniquely in electron transfer pathways (cbc-cluster, mtrABC and fdh) were clearly more abundant in unpacked batches, suggesting that microbes with higher capacity to establish syntrophic interactions were favoured under planktonic conditions.

As mentioned previously, an increment of species in the Rhizobiales order (*Proteobacteria* phylum) was observed in the batches that did not promote biofilm formation, the unpacked control and the magnetite packing, which enhance IET and/or DIET. These results are in agreement with previous reports on the dominance of *Proteobacteria* when DIET and/or IET processes were favoured (de bok et al., 2004, Rotaru et al., 2014). It has been suggested that the phylum *Proteobacteria* is not directly related to the SAOB-HMA syntrophism, but could still participate in electronic exchange processes because of the high presence of genes encoding for exoelectrogenic proteins. In fact, previous studies reported that most of the exoelectrogenic bacteria belong to the phylum *Proteobacteria*, as *Geobacter sulfurreducens* (Reguera et al., 2006) or *Shewanella oneidensis* (Min et al., 2017). In summary, our results indicate that the physicochemical nature of packing materials has a very strong influence on the biodiversity and functionality of the active methanogenic biomass. The understanding of the bioprocesses prompted by the packing can be used advantageously when designing advanced full-scale anaerobic digesters for the treatment of nitrogen-rich wastes.

## 8.5 Conclusion

The combination of DNA-SIP with microbiome and metagenome analyses in batch incubations with  $^{12}\text{C}/^{13}\text{C}$ -acetate facilitated the identification of key acetate-assimilating microbial species in the AD process under ammonia-inhibitory conditions. The assembling of partial genomes from the metagenomic analysis of the  $^{13}\text{C}$ -enriched DNA, revealed the association of major phylotypes involved in acetate assimilation with relevant metabolic pathways and IET mechanisms. The physicochemical nature of different support materials strongly influenced the active microbial communities through biofilm formation and/or the enrichment of alternative electron transfer mechanisms. The identification of relevant genes from bacterial population genomes indicated that species in *Firmicutes*, *Chloroflexi* and *Bacteroidetes* might play an important role in the oxidation of acetate via Wood-Ljungdahl pathway. Hence, the biodiversity of SAOB in anaerobic digesters might be higher and more complex than what has been described until now. The assembled archaeal genome of *Methanoculleus* evidenced the relevance of this genus in the SAOB-HMA syntrophy and the presumed capability of this taxon to assimilate acetate has been highlighted.

## 8.6 References

- Ahammad, S.Z., Davenport, R.J., Read, L.F., Gomes, J., Sreekrishnan, T.R., Dolfing, J., 2013a. Rational immobilization of methanogens in high cell density bioreactors. *RSC Adv.* 3, 774–781.
- Ahammad, S.Z., Davenport, R.J., Read, L.F., Gomes, J., Sreekrishnan, T.R., Dolfing, J., Heidrich, E.S., Curtis, T.P., Dolfing, J., McCarty, P.L., Bae, J., Kim, J., McCarty, P.L., Smith, D.P. 2013b. Rational immobilization of methanogens in high cell density bioreactors. *RSC Adv.* 3, 774–781.
- Angelidaki, I., Ahring, B.K., 1993. Thermophilic anaerobic digestion of livestock waste: the effect of ammonia. *Appl. Microbiol. Biotechnol.* 38, 560–564.
- Balk, M., Weijma, J., Stams, A.J.M., 2002. *Thermotoga lettingae* sp. nov., a novel thermophilic, methanol-degrading bacterium isolated from a thermophilic anaerobic reactor. *Int. J. Syst. Evol. Microbiol.* 52, 1361–1368.
- Bapteste, E., Brochier, C., Boucher, Y., 2005. Higher-level classification of the Archaea: evolution of methanogenesis and methanogens. *Archaea* 1, 353–63.
- Barret, M., Gagnon, N., Morissette, B., Kalmokoff, M.L., Topp, E., Brooks, S.P.J., Matias, F., Neufeld, J.D., Talbot, G., 2015. Phylogenetic identification of methanogens assimilating acetate-derived carbon in dairy and swine manures. *Syst. Appl. Microbiol.* 38, 56–67.
- Bertin, L., Colao, M.C., Ruzzi, M., Marchetti, L., Fava, F., 2007. Performances and microbial features of an aerobic packed-bed biofilm reactor developed to post-treat an olive mill effluent from an anaerobic GAC reactor. *Microb. Cell Fact.* 5, 17.
- Bolger, A.M., Lohse, M., Usadel, B., 2014. Trimmomatic: A flexible trimmer for Illumina sequence data. *Bioinformatics* 30, 2114–2120.
- Campanaro, S., Treu, L., Cattani, M., Kougias, P.G., Vendramin, V., Schiavon, S., Tagliapietra, F., Giacomini, A., Corich, V., 2017. In vitro fermentation of key dietary compounds with rumen fluid: A genome-centric perspective. *Sci. Total Environ.* 584–585, 683–691.
- Campanaro, S., Treu, L., Kougias, P.G., De Francisci, D., Valle, G., Angelidaki, I., 2017. Metagenomic analysis and functional characterization of the biogas microbiome using high throughput shotgun sequencing and a novel binning strategy. *Biotechnol. Biofuels* 9, 26
- Cruz Viggì, C., Rossetti, S., Fazi, S., Paiano, P., Majone, M., Aulenta, F., 2014. Magnetite particles triggering a faster and more robust syntrophic pathway of methanogenic propionate degradation. *Environ. Sci. Technol.* 48, 7536–7543.
- De Bok, F.A.M., Plugge, C.M., Stams, A.J.M., 2004. Interspecies electron transfer in methanogenic propionate degrading consortia. *Water Res.*
- Demirel, B., Scherer, P., 2008. The roles of acetotrophic and hydrogenotrophic methanogens during anaerobic conversion of biomass to methane: A review. *Rev. Environ. Sci. Biotechnol.* 7, 173–190.
- Drake, H.L., 1994. Acetogenesis, acetogenic bacteria, and the acetyl-CoA “Wood/Ljungdahl” pathway: past and current perspectives, in: *Acetogenesis*. pp. 3–60.
- Fotidis, I.A., Karakashev, D., Angelidaki, I., 2014. The dominant acetate degradation pathway/methanogenic composition in full-scale anaerobic digesters operating under different ammonia levels. *Int. J. Environ. Sci. Technol.* 11, 2087–2094.
- Fotidis, I.A., Karakashev, D., Kotsopoulos, T.A., Martzopoulos, G.G., Angelidaki, I., 2013. Effect of ammonium and acetate on methanogenic pathway and methanogenic community composition. *FEMS Microbiol. Ecol.* 83, 38–48.
- Galperin, M.Y., Makarova, K.S., Wolf, Y.I., Koonin, E. V., 2015. Expanded Microbial genome coverage and improved protein family annotation in the COG database. *Nucleic Acids Res.* 43, D261–D269.

- Gurevich, A., Saveliev, V., Vyahhi, N., Tesler, G., 2013. QUASt: Quality assessment tool for genome assemblies. *Bioinformatics* 29, 1072–1075.
- Ha, P.T., Lindemann, S.R., Shi, L., Dohnalkova, A.C., Fredrickson, J.K., Madigan, M.T., Beyenal, H., 2017. Syntrophic anaerobic photosynthesis via direct interspecies electron transfer. *Nat. Commun.* 8.
- Hattori, S., Kamagata, Y., Hanada, S., Shoun, H., 2000. *Thermacetogenium phaeum* gen. nov., sp. nov., a strictly anaerobic, thermophilic, syntrophic acetate-oxidizing bacterium. *Int. J. Syst. Evol. Microbiol.* 50, 1601–1609.
- Hyatt, D., Locascio, P.F., Hauser, L.J., Uberbacher, E.C., 2012. Gene and translation initiation site prediction in metagenomic sequences. *Bioinformatics* 28, 2223–2230. doi:10.1093/bioinformatics/bts429
- Kanehisa, M., Sato, Y., Morishima, K., 2017. BlastKOALA and GhostKOALA: KEGG Tools for Functional Characterization of Genome and Metagenome Sequences. *J. Mol. Biol.* doi:10.1016/j.jmb.2015.11.006
- Kang, D.D., Froula, J., Egan, R., Wang, Z., 2015. MetaBAT, an efficient tool for accurately reconstructing single genomes from complex microbial communities. *PeerJ* 3, e1165. doi:10.7717/peerj.1165
- Kayhanian, M., 1994. Performance of a high-solids anaerobic digestion process under various ammonia concentrations. *J. Chem. Technol. Biotechnol.* 59, 349–352.
- Kouzuma, A., Tsutsumi, M., Ishii, S., Ueno, Y., Abe, T., Watanabe, K., 2017. Non-autotrophic methanogens dominate in anaerobic digesters. *Sci. Rep.* 7.
- Laube, V.M., Martin, S.M., 1981. Conversion of Cellulose to Methane and Carbon Dioxide by Triculture of *Acetivibrio cellulolyticus*, *Desulfovibrio* sp., and *Methanosarcina barkeri*. *Appl. Environ. Microbiol.* 42, 413–420.
- Lee, M.J., Zinder, S.H., 1988. Hydrogen partial pressures in a thermophilic acetate-oxidizing methanogenic coculture. *Appl. Environ. Microbiol.* 54, 1457–61.
- Li, Y., Zhang, Y., Yang, Y., Quan, X., Zhao, Z., 2017. Potentially direct interspecies electron transfer of methanogenesis for syntrophic metabolism under sulfate reducing conditions with stainless steel. *Bioresour. Technol.* 234, 303–309.
- Matsui, H., Kojima, N., Tajima, K., 2008. Diversity of the formyltetrahydrofolate synthetase gene (fhs), a key enzyme for reductive acetogenesis, in the bovine rumen. *Biosci. Biotechnol. Biochem.* 72, 3273–3277.
- Maus, I., Wibberg, D., Stantscheff, R., Eikmeyer, F.G., Seffner, A., Boelter, J., Szczepanowski, R., Blom, J., Jaenicke, S., König, H., Pühler, A., Schlüter, A., 2012. Complete genome sequence of the hydrogenotrophic, methanogenic archaeon *Methanoculleus bourgensis* strain MS2T, isolated from a sewage sludge digester. *J. Bacteriol.*
- Milner, E.M., Popescu, D., Curtis, T., Head, I.M., Scott, K., Yu, E.H., 2017. Microbial fuel cells with highly active aerobic biocathodes. *J. Power Sources* 324, 8–17.
- Min, D., Cheng, L., Zhang, F., Huang, X.N., Li, D.B., Liu, D.F., Lau, T.C., Mu, Y., Yu, H.Q., 2017. Enhancing Extracellular Electron Transfer of *Shewanella oneidensis* MR-1 through Coupling Improved Flavin Synthesis and Metal-Reducing Conduit for Pollutant Degradation. *Environ. Sci. Technol.* 51, 5082–5089.
- Mosbæk, F., Kjeldal, H., Mulat, D.G., Albertsen, M., Ward, A.J., Feilberg, A., Nielsen, J.L., 2017. Identification of syntrophic acetate-oxidizing bacteria in anaerobic digesters. *ISME J.* 2, 1–14.
- Murray, W.D., 1987. *Acetivibrio cellulosolvans* Is a synonym for *Acetivibrio cellulolyticus*: Emendation of the genus *Acetivibrio*. *Int. J. Syst. Bacteriol.* 36, 314–317.
- Nobu, M.K., Narihiro, T., Rinke, C., Kamagata, Y., Tringe, S.G., Woyke, T., Liu, W.-T., 2015. Microbial dark matter ecogenomics reveals complex synergistic networks in a methanogenic bioreactor. *ISME J.* 9, 1710–1722.

- Nurk, S., Meleshko, D., Korobeynikov, A., Pevzner, P.A., 2017. MetaSPAdes: A new versatile metagenomic assembler. *Genome Res.* 27, 824–834.
- Parks, D.H., Imelfort, M., Skennerton, C.T., Hugenholtz, P., Tyson, G.W., 2015. CheckM: assessing the quality of microbial genomes recovered from isolates, single cells, and metagenomes. *Genome Res.* 25, 1043–55.
- Poggi-Varaldo, H.M., Rodríguez-Vázquez, R., Fernández-Villagómez, G., Esparza-García, F., 1997. Inhibition of mesophilic solid-substrate anaerobic digestion by ammonia nitrogen. *Appl. Microbiol. Biotechnol.* 47, 284–291.
- Poirier, S., Madigou, C., Bouchez, T., Chapleur, O., 2017. Improving anaerobic digestion with support media: Mitigation of ammonia inhibition and effect on microbial communities. *Bioresour. Technol.* 235, 229–239.
- Prestat, E., David, M.M., Hultman, J., Taş, N., Lamendella, R., Dvornik, J., Mackelprang, R., Myrold, D.D., Jumpponen, A., Tringe, S.G., Holman, E., Mavromatis, K., Jansson, J.K., 2014. FOAM (Functional Ontology Assignments for Metagenomes): A Hidden Markov Model (HMM) database with environmental focus. *Nucleic Acids Res.* 42.
- Ragsdale, S.W., 2008. Enzymology of the Wood-Ljungdahl pathway of acetogenesis, in: *Annals of the New York Academy of Sciences.* pp. 129–137.
- Ragsdale, S.W., Pierce, E., 2008. Acetogenesis and the Wood-Ljungdahl pathway of CO<sub>2</sub> fixation. *Biochim. Biophys. Acta - Proteins Proteomics.*
- Reguera, G., Nevin, K.P., Nicoll, J.S., Covalla, S.F., Woodard, T.L., Lovley, D.R., 2007. Biofilm and nanowire production leads to increased current in *Geobacter sulfurreducens* fuel cells. *Appl. Environ. Microbiol.* 72, 7345–7348.
- Rotaru, A.E., Shrestha, P.M., Liu, F., Markovaite, B., Chen, S., Nevin, K.P., Lovley, D.R., 2014. Direct interspecies electron transfer between *Geobacter metallireducens* and *Methanosarcina barkeri*. *Appl. Environ. Microbiol.* 80, 4599–4605. doi:10.1128/AEM.00895-14
- Ruiz-Sánchez, J., Campanaro, S., Guivernau, M., Fernández, B., Prenafeta-Boldú, F.X., 2018. Effect of ammonia on the active microbiome and metagenome from stable full-scale digesters. *Bioresour. Technol.* 250, 513–522.
- Saeed, A.I., Sharov, V., White, J., Li, J., Liang, W., Bhagabati, N., Braisted, J., Klapa, M., Currier, T., Thiagarajan, M., Sturn, A., Snuffin, M., Rezantsev, A., Popov, D., Ryltsov, A., Kostukovich, E., Borisovsky, I., Liu, Z., Vinsavich, A., Trush, V., Quackenbush, J., 2003. TM4: A free, open-source system for microarray data management and analysis. *Biotechniques* 34, 374–378.
- Schagger, H., Cramer, W.A., Vonjagow, G., 1994. Cytochrome bc<sub>1</sub> complexes of microorganisms. *Anal. Biochem.* 217, 220–230.
- Schauder, R., Preuß, A., Jetten, M., Fuchs, G., 1988. Oxidative and reductive acetyl CoA/carbon monoxide dehydrogenase pathway in *Desulfobacterium autotrophicum* - 2. Demonstration of the enzymes of the pathway and comparison of CO dehydrogenase. *Arch. Microbiol.* 151, 84–89.
- Schnürer, A., Nordberg, A., 2008. Ammonia, a selective agent for methane production by syntrophic acetate oxidation at mesophilic temperature. *Water Sci. Technol.* 57, 735–740.
- Schnürer, A., Schink, B., Svensson, B.H., 1997. *Clostridium ultunense* sp. nov., a mesophilic bacterium oxidizing acetate in syntrophic association with a hydrogenotrophic methanogenic bacterium. *Int. J. Syst. Bacteriol.* 46, 1145–1152.
- Segata, N., Börnigen, D., Morgan, X.C., Huttenhower, C., 2013. PhyloPhlAn is a new method for improved phylogenetic and taxonomic placement of microbes. *Nat. Commun.* 4, 2304.

- Shi, L., Dong, H., Reguera, G., Beyenal, H., Lu, A., Liu, J., Yu, H.Q., Fredrickson, J.K., 2017. Extracellular electron transfer mechanisms between microorganisms and minerals. *Nat Rev Microbiol* 14, 651–662.
- Shi, L., Rosso, K.M., Clarke, T.A., Richardson, D.J., Zachara, J.M., Fredrickson, J.K., 2012. Molecular underpinnings of Fe(III) oxide reduction by *Shewanella oneidensis* MR-1. *Front. Microbiol.* 3.
- Siegert, M., Li, X.F., Yates, M.D., Logan, B.E., 2014. The presence of hydrogenotrophic methanogens in the inoculum improves methane gas production in microbial electrolysis cells. *Front. Microbiol.* 5.
- Smith, J.A., Lovley, D.R., Tremblay, P.L., 2013. Outer cell surface components essential for Fe(III) oxide reduction by *Geobacter metallireducens*. *Appl. Environ. Microbiol.* 79, 901–907.
- Treu, L., Kougias, P.G., Campanaro, S., Bassani, I., Angelidaki, I., 2017. Deeper insight into the structure of the anaerobic digestion microbial community; The biogas microbiome database is expanded with 157 new genomes. *Bioresour. Technol.* 216, 260–267.
- Vanwonterghem, I., Jensen, P.D., Rabaey, K., Tyson, G.W., 2017. Genome-centric resolution of microbial diversity, metabolism and interactions in anaerobic digestion. *Environ. Microbiol.* 18, 3144–3158.
- Varghese, N.J., Mukherjee, S., Ivanova, N., Konstantinidis, K.T., Mavrommatis, K., Kyrpides, N.C., Pati, A., 2015. Microbial species delineation using whole genome sequences. *Nucleic Acids Res.* 43, 6761–6771.
- Vavilin, V.A., Qu, X., Mazéas, L., Lemunier, M., Duquenois, C., He, P., Bouchez, T., 2008. *Methanosarcina* as the dominant acetate-oxidizing methanogens during mesophilic anaerobic digestion of putrescible waste. *Antonie van Leeuwenhoek, Int. J. Gen. Mol. Microbiol.* 94, 593–605.
- Walker, D.J.F., Dang, Y., Holmes, D.E., Lovley, D.R., 2017. The electrically conductive pili of *Geobacter* species are a recently evolved feature for extracellular electron transfer. *Microb. Genomics* 2.
- Wang, X., Meng, S., Han, J., 2017. Morphologies and phenotypes in *Bacillus subtilis* biofilms. *J. Microbiol.* 55, 619–627.
- Watson-Craik, I. a, Stams, a J., 1995. Anaerobic digestion. *Antonie Van Leeuwenhoek* 67, 1–2.
- Westerholm, M., Levén, L., Schnürer, A., 2012. Bioaugmentation of syntrophic acetate-oxidizing culture in biogas reactors exposed to increasing levels of ammonia. *Appl. Environ. Microbiol.* 78, 7619–7625.
- Westerholm, M., Roos, S., Schnürer, A., 2011. *Tepidanaerobacter acetatoxydans* sp. nov., an anaerobic, syntrophic acetate-oxidizing bacterium isolated from two ammonium-enriched mesophilic methanogenic processes. *Syst. Appl. Microbiol.* 34, 260–267.
- Westerholm, M., Roos, S., Schnürer, A., 2010. *Syntrophaceticus schinkii* sp. nov., an anaerobic, syntrophic acetate-oxidizing bacterium isolated from a mesophilic anaerobic filter. *FEMS Microbiol. Lett.* 309, 100–104.
- Yang, Y., Xu, M., Guo, J., Sun, G., 2012. Bacterial extracellular electron transfer in bioelectrochemical systems. *Process Biochem.*



# Part IV

---

Biogas production from protein/sulphate rich wastes



## Chapter 9 Strategies for recovering from inhibition caused by ammonia and sulphate in mesophilic biogas fixed-bed reactors

---

The recovery of four mesophilic biogas reactors, previously inhibited by relatively high concentrations of ammonia and sulphate, was assessed upon the increment of the hydraulic retention time and the COD/sulphate ratio. Inhibition indicators such as total volatile fatty acids (VFA) and biogas composition were monitored, and the dynamics of methanogenic archaea (MA) and sulphate reducing bacteria (SRB) were quantified by qPCR. Two different support materials (magnetite, zeolite) were assayed with different compositional combinations, in terms of their capacity to prevent microbial inhibition. The digester packed with a mixture of magnetite and zeolite showed the best recovery, based on a decrement of 50% and 35% of the content of total VFA and sulphide in biogas, respectively, in relation to the non-packed reactor.

*Part of this chapter was presented as a poster AD15 Beijing conference*

## 9.1 Introduction

Anaerobic digestion (AD) is defined as the biological conversion of organic matter into a variety of value products, as biogas, composed by methane (65–70%) and carbon dioxide. The advantages of anaerobic digestion include low levels of biological sludge, low nutrient requirements and high efficiency in the production of methane, which can be used as an energy source for on-site heating and electricity (Zeeman et al., 2008). As part of the AD process, organic N (i.e. proteins, nucleic acids, etc.) is transformed into ammonia nitrogen (which can be as neutral (free ammonia  $\text{NH}_3$ ) or cationic forms depending on pH and temperature, in the fermentative and acidogenic steps (Braun et al., 1981). While organic S and sulphate-S are reduced by sulfate-reducing bacteria (SRB) to sulphide ( $\text{H}_2\text{S}$ ) (Karunakaran et al., 2016). These SRB have the ability to couple the oxidation of organic matter to the reduction of sulfate, depending on hydrolytic and fermentative bacteria that degrade complex organic matter. In parallel, SRB compete with methane producing archaea and homoacetogenic bacteria for common substrates in anaerobic bioreactors (Muyzer and Stams, 2008).

Furthermore,  $\text{H}_2\text{S}$  and  $\text{NH}_3$  have been reported as inhibitors since they are freely membrane-permeable.  $\text{H}_2\text{S}$  readily permeates cell membranes and denatures native proteins inside the cytoplasm producing sulphide cross-links between polypeptide chains (Annachatre and Suktrakoolvait, 2015). Sulphides are also involved in the precipitation of non-alkali metals, reducing their availability for methanogenic archaea (Isa et al., 1986).  $\text{NH}_3$  also diffuses into the cell due to the fact that it is uncharged and lipid soluble, causing proton imbalance with a consequent changes in the intracellular pH, potassium deficiency, increase in the maintenance energy requirement and inhibition of a specific enzymes (Siles et al., 2010; Antonenko et al., 1997). However, the literature on anaerobic digestion of sulphate-ammonium containing wastewaters is highly complex and often contradictory.

It is extensively described that ammonia levels play a key role in the good performance and stability of AD systems (Dai et al., 2016). A suitable ammonia levels ensures a satisfactory buffering capacity for methane-producing environment. However, high ammonia directly inhibits microbial activity and even leads to collapse of the AD process (Yenigün and Demirel, 2013). Some studies affirmed that ammonia inhibition starts at 4 gTAN  $\text{L}^{-1}$ , corresponding to 0.9 mgFAN  $\text{L}^{-1}$  (Rajagopal et al., 2013). Moreover, another studies defined that absolute AD system failure occurs above 10 gTAN  $\text{L}^{-1}$  (Wang et al., 2017). Regarding  $\text{H}_2\text{S}$ , it is reported by previous studies that methanogenic activity was negatively influenced by sulfidogenesis (Santegoeds et al., 1999), pathway favoured at low COD/ $\text{SO}_4^{2-}$  ratios ( $< 2 \text{ g g}^{-1}$ ) (O'Reilly and Colleran, 2006). At high  $\text{SO}_4^{2-}$  concentrations, combined with low ratio COD/  $\text{SO}_4^{2-}$ , SRB always dominated the organic matter consumption (Vela et al., 2002). Furthermore, SRB

activity normally entails a H<sub>2</sub>S increment, which is inhibitory compound for AD systems: 50–400 and 100–800 mg L<sup>-1</sup> for undissociated and dissociated sulfide, respectively (Parkin et al., 1990).

The H<sub>2</sub>S, produced by SRB while decomposing sulphates, combined with FAN, released from protein degradation, are highly toxic to both communities MPA, particularly the acetate degradation of AM (Maillacheruvu and Parkin, 1996), and SBR (Jing et al., 2013). Recent studies described that high ammonia and sulphate contents can modify the microbial community structure (Joshi et al., 2017; Smith et al., 2017). Other studies showed that high ammonia levels can alter the community structure of MPA, but this effect is quite different when sulphate is combined with high ammonia levels (Moestedt et al., 2013). However, remains unclear how that the combination of both inhibitory compounds could affect activity variation of MPA and SRB.

Instability caused by inhibitory compounds during the operation of the anaerobic degradation process can be challenging due to the low specific growth rate of the methanogenic communities involved. Under unstable conditions, intermediates such as volatile fatty acids (VFA) accumulate at different rates, depending on the cause of the instability (Zitomer et al., 2016). Industrial wastewaters are characterised by high concentrations of chemical oxygen demand (COD) but also high total nitrogen (TN) or sulphate (SO<sub>4</sub><sup>2-</sup>), being treated by biological and physicochemical processes. Even though physicochemical methods are effective, their limitations restrict their usage mainly the need for separation and appropriate disposal of the solid phase that increase energy and economical costs (Zhao et al., 2006). On the other hand, the biological treatments are encouraged because anaerobic technologies are achieving promising results (Joshi et al., 2017) (Sarti and Zaiat, 2011). Wasterwater from paper mill , chemical industries, beverage industries or pharmaceutical companies are usually treated in high load anaerobic digesters as packed and granular AD reactors (Karadag et al., 2015). Their high treatment capacity lays in high cellular retention times, thanks to a great microbial concentration as granules or biofilms attached to support materials. These configurations prevent bacterial washout and also provide a larger surface area for faster biofilm development and improved methanogenesis (Qureshi et al., 2005).

The biofilm formation on carrier materials improves the conversion rates by reducing its sensitivity toward inhibitory compounds or conditions. For example, previous studies have shown that biofilm based-processes, as well as the supporting material composition and structure, can improve the acetoclastic methanogenesis (AM) resilience towards inhibitors (Habouzit et al., 2014). Also Barana et al., (2013) evidenced that the efficiency of removing organic matter in fixed-bed reactors is directly related to the characteristics of the support material used for immobilization of anaerobes.

Within this framework, four similarly operated lab-scale anaerobic digesters were fed with an identical organic wastewater from a pharmaceutical industry (heparin production), in order to optimize the biogas production by incorporating different support materials. This work was aimed at examining the effect of two different packing materials, zeolite and magnetite, on the recovery of methanogenic activity previously inhibited by high concentrations of ammonia and sulphate. These materials have been reported to be beneficial because of their absorptive (Montalvo et al., 2012) and/or electrochemical properties (Cruz Viggì et al., 2014) but this study is, to our knowledge, the first time they are implemented for the recovery of ammonia and sulphur inhibited reactors.

## 9.2 Materials and methods

### 9.2.1 Experimental set-up and operational conditions

An inoculum from a full scale mesophilic digester, running at 5 gTAN L<sup>-1</sup> and 20 days of hydraulic retention time (HRT), was used to start-up three fixed bed (RZ, RM, RMZ) and one stirred tank (RC) mesophilic lab-scale reactors. The working volume was 0.6 L. Two different support materials were used, zeolite and magnetite, taking up the 30% working volume. Zeolite (LKAB) was added in reactor RZ. Magnetite (Horticolas Pedralbes) was added in reactor RM. A blend 1:1 of zeolite: magnetite was prepared for reactor RMZ. The stirred reactor worked without any support material and was used as control (RC).

All four digesters had identical influent, composed by the raw wastewater diluted with deionised water: 4.2 gTAN L<sup>-1</sup>; 8 gSO<sub>4</sub><sup>2-</sup> L<sup>-1</sup>; 7 ratio COD/SO<sub>4</sub><sup>2-</sup>. The raw wastewater was characterised by a high organic matter, total ammonia nitrogen (TAN) and sulphur contents (120 gO<sub>2</sub> L<sup>-1</sup>, 5 gTAN L<sup>-1</sup> and 16 gSO<sub>4</sub><sup>2-</sup>L<sup>-1</sup>, respectively).

After the inoculation, all four reactors were fed with the same wastewater and operational conditions (a HRT of 20 days and an organic loading rate (OLR) of 2.5 kgCOD m<sup>-3</sup> d<sup>-1</sup>). After 50 days, the recovery strategy was applied and consisted in the increment of the HRT up to 30 days, the OLR was decreased to 1.5 kgCOD m<sup>-3</sup>d<sup>-1</sup> and on the adjustment of the COD/ SO<sub>4</sub><sup>2-</sup> ratio of the influent from 7.5 to 15 gO<sub>2</sub> gSO<sub>4</sub><sup>2-</sup> (Table 10.1).

Influent and effluent flows, as well as biogas composition (CH<sub>4</sub>, CO<sub>2</sub> and H<sub>2</sub>S) and the concentration of total and partial alkalinity, total volatile fatty acids (VFA), TAN and sulphates of effluents, were monitored (see section Chapter 3). The concentrations of VFA was expressed as meq of acetic acid per litre. In the present study, free ammonia nitrogen (FAN) levels were calculated based on TAN concentrations and pH (eq 1).

$$[\text{NH}_3] = [\text{TAN}] / (1 + [\text{H}^+]/K_a) \quad (\text{Eq 1})$$

A biogas isotopic fractionation of  $^{13}\text{C}/^{12}\text{C}$  from methane and carbon dioxide was also determined (see Chapter 3). Microbial communities were monitored by qPCR technique, from supernatants from the centrifuged samples of effluents and from the biofilm attached to support materials. Each sample was analysed in triplicate by means of three independent DNA extracts. Total bacteria and methanogenic archaea were quantified by 16S rRNA and *mcrA* genes (see Chapter 3). Target genes for sulphate-reducing microorganisms (*aprA*) have been widely used as functional markers of these organisms and their quantitative variations of abundance.

The operation of the digesters was evaluated in terms of methane production rate and yield (normalised at 273 K and 1 atm), organic matter (COD) removal efficiency, gas composition and VFA accumulation (acidification degree, calculated as equivalent COD of VFA as percentage of the influent COD). Mean values of these parameters were calculated with values from the whole period (inhibition and recovery)

## 9.3 Results and discussion

### 9.3.1 Failure and recovery periods

Average values of TAN, FAN and pH during the whole process, before and after recovery, are shown in Table 10.1. For RZ and RMZ the maximum value for TAN concentration was obtained after day 15 (Figure 10.1), which can be explained by the well-known absorption capacity of zeolite (Zheng et al., 2015). Even though ammonia concentration did not reach the reported failure level ( $10 \text{ gTAN L}^{-1}$ ), the reactors were totally inhibited at day 45, because the high sulphate content of influent.

To study the operational performance and stability of the four reactors, the biogas production, methane content, VFA content,  $\text{H}_2\text{S}$  production (Figure 9.1 and figure 9.2) and COD removal were determined before and after recovery strategy application. The biogas production before the recovery was very low in all reactors, below  $0.11 \text{ Nm}_3\text{CH}_4\text{m}^{-3}\text{d}^{-1}$ , suggesting that a FAN and  $\text{H}_2\text{S}$  combined effect were adversely affecting the microbial communities, especially to methanogens. Complementary, the  $\text{CH}_4$  biogas content during failure period keeps low in all the reactors: reactors amended with magnetite and magnetite-zeolite showed a constant value around 43%; meanwhile control and zeolite reactors presented 10% and 16%, respectively, even accounting the advantage for methanogenic archaea due to the ammonia absorption availability of zeolite (Wang et al., 2011).

Magnetite packed reactors showed major stability and resistance during failure period, in agreement with recent studies that affirm that reactors with magnetite were more

resistant and resilient to inhibitory conditions (Baek et al., 2017). Process instability due to the presence of ammonia,  $\text{SO}_4^{2-}$  and  $\text{H}_2\text{S}$  led to VFA accumulation, up to the inhibitory range (Franke-Whittle et al., 2014), so that methanogenic activity stopped leading to AD failure. The total VFA during starting period (Figure 9.1b) tended to increase achieving the maximum value at day 40, with values between 28 and 32 eq acetic  $\text{L}^{-1}$  in all reactors, as a consequence of incomplete organic matter oxidation. Furthermore,  $\text{H}_2\text{S}$  quantification showed their maximum values synchronized with the rest of parameters (Table 9.1), indicating an imbalance of the methanisation process in all reactors, indistinctly of support material added.

From day 50, the recovery strategy was applied (incrementing HRT from 20 to 30 days combined with the increment ratio  $\text{COD}/\text{SO}_4^{2-}$  from 7 to 15  $\text{g g}^{-1}$ ). Packed reactors RM, RZ and RMZ showed a more quickly response than RC, although this last reactor without biomass retention recovery strategy showed an improvement in biogas production and methane content (Figure 9.1). The reactor performance parameters denoted a clearly improvement after 12 days once the recovery strategy began. The COD removal, the biogas production and methane content incrementes in all the reactors (Table 9.1 and Figure 9.1), meanwhile VFA concentrations were keep constant.

Another clear indicator of recovery was that total VFA and  $\text{H}_2\text{S}$  decreased drastically, represented in Figure 10.2. For both parameters, RM, RZ and RMZ showed values in the same magnitude order, however RC showed highest values at the end of operation time. The results were consistent with the observation (Sabumon, 2008), in which high alkalinity was generated at low  $\text{COD}/\text{SO}_4^{2-}$  ratio (7.5 in the present study), caused by the enhanced sulfidogenesis process. Opposite, when  $\text{COD}/\text{SO}_4^{2-}$  ratio was high (15 in the present study), the partial alkalinity of effluents slowly decreased (Figure 9.1c).

These evidences agree with previous studies that report major stability performance when complex substrates are treated in biomass attached AD-systems. As demonstrated Loukidou and Zouboulis, 2001, a suspended carrier biofilm treatment method with granular activated carbon it is an interesting alternative option to the conventional activate sludge process for the effective biological removal of carbon and nitrogen. In the present study this effect was prompted by zeolite and magnetite particles. It is reported that magnetite enhances the establishment of a direct interspecies electron transfer (DIET), as an electron shuttle particle between acetogens and HMA (Cruz Viggli et al., 2014), meanwhile zeolite is a cation adsorbent which diminished the available ammonia in the medium, as well as, its porous structure facilitate the biomass attachment.

**Table 9.1** Physic-chemical and operational parameters before and after recovery strategy application

	Temperature (°C)	HRT (days)	VFA (mg/l)	pH	NH <sub>4</sub> <sup>+</sup> - N (g/l)	NH <sub>3</sub> -N (g/l)	H <sub>2</sub> S
Inoculum	37	65	165	8,05	5	0,67089462	0
<b>Failure period</b>							
Operational parameters	Digester Temperature (°C)	RC		RM		RZ	RMZ
		35		35		35	35
	DQO/ SO <sub>4</sub> <sup>2-</sup>	7,5		7,5		7,5	7,5
	OLR(kgDQOt/d)	2,5		2,5		2,5	2,5
	HRT (days)	20		20		20	20
	VFA (mg/l)	27958		28507		27324	31622
	pH	7,40		7,73		7,75	7,30
	NH <sub>4</sub> <sup>+</sup> -N (g/l)	5,015		5,444		4,023	4,849
	NH <sub>3</sub> -N (g/l)	0,154		0,345		0,266	0,119
	COD (g/kg)	50		50		50	50
	SO <sub>4</sub> <sup>2-</sup> (ppm)	6500		6500		6500	6500
Experimental results	Nm <sup>3</sup> CH <sub>4</sub> / m <sub>3</sub> d	0,02		0,06		0,05	0,11
	NLCH <sub>4</sub> / kgCODin	8,98		28,35		23,45	41,27
	H <sub>2</sub> S(ppm)	147,60		95,68		162,41	65,88
	CH <sub>4</sub> %	8,91		31,49		11,77	36,95
	COD removal %	3		8		7	13
<b>Recovering period</b>							
Operational parameters	Digester Temperature (°C)	RC		RM		RZ	RMZ
		35		35		35	35
	DQO/ SO <sub>4</sub> <sup>2-</sup>	15		15		15	15
	OLR(kgDQOt/d)	1,5		1,5		1,5	1,5
	HRT (days)	30		30		30	30
	VFA (mg/l)	25096		16882		20057	15555
	pH	7,17		7,58		7,59	7,79
	NH <sub>4</sub> <sup>+</sup> -N (g/l)	4,359		4,257		4,294	4,252
	NH <sub>3</sub> -N (g/l)	0,080		0,194		0,200	0,306
	COD (g/kg)	60		60		60	60
	SO <sub>4</sub> <sup>2-</sup> (ppm)	2800		2800		2800	2800
Experimental results	Nm <sup>3</sup> CH <sub>4</sub> / m <sub>3</sub> d	0,08		0,21		0,22	0,23
	NLCH <sub>4</sub> / kgCODin	46,20		68,50		72,28	80,38
	H <sub>2</sub> S(ppm)	81,75		30,46		42,43	42,54
	CH <sub>4</sub> %	33,66		44,33		47,95	49,87
	COD removal %	13		16		18	23
	α-value	1,0588		1,0582		1,0649	1,0662

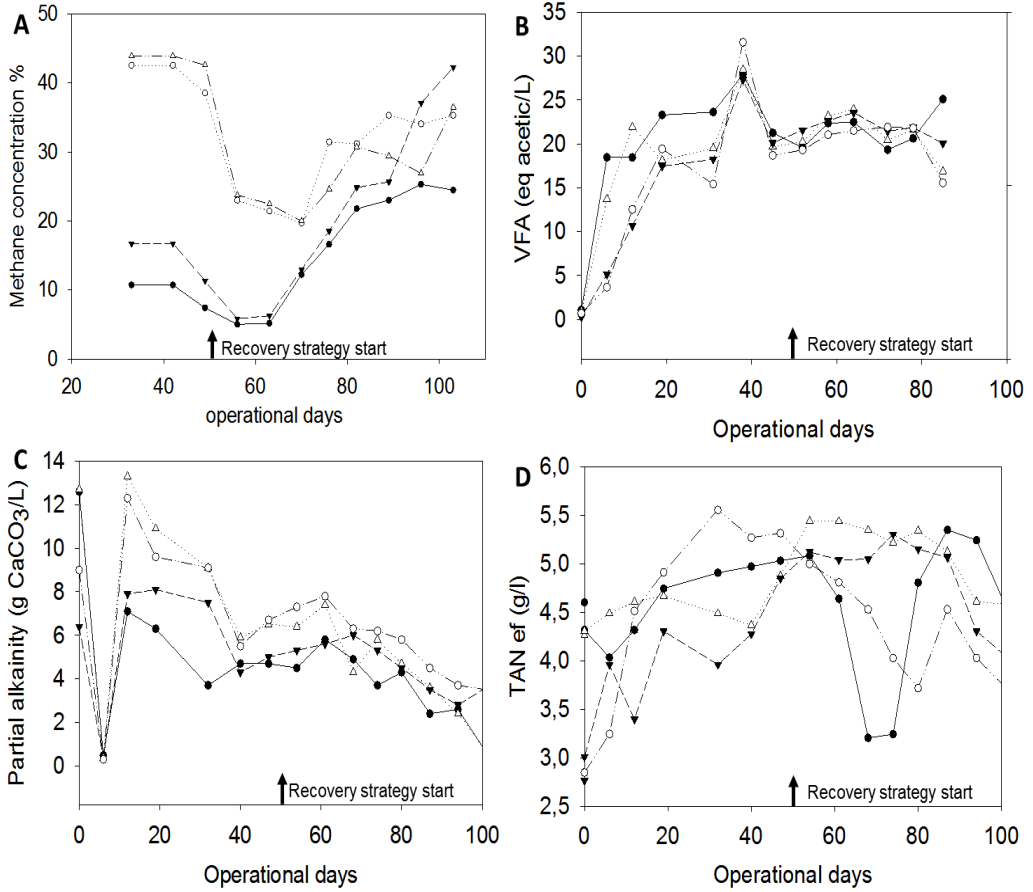


**Figure 9.1** H<sub>2</sub>S concentration before (dark) and after(grey) recovery. b VFA (meq ac) before (dark) and after(grey) recovery. c Evolution of methane content (●) RC (▼) RZ, (Δ) RM and (○) RMZ; d. VFA evolution (●) RC (▼) RZ, (Δ) RM and (○)RMZ and partial alkalinity evolution (◇) RC (□) RZ, (◆) RM and (■) RMZ



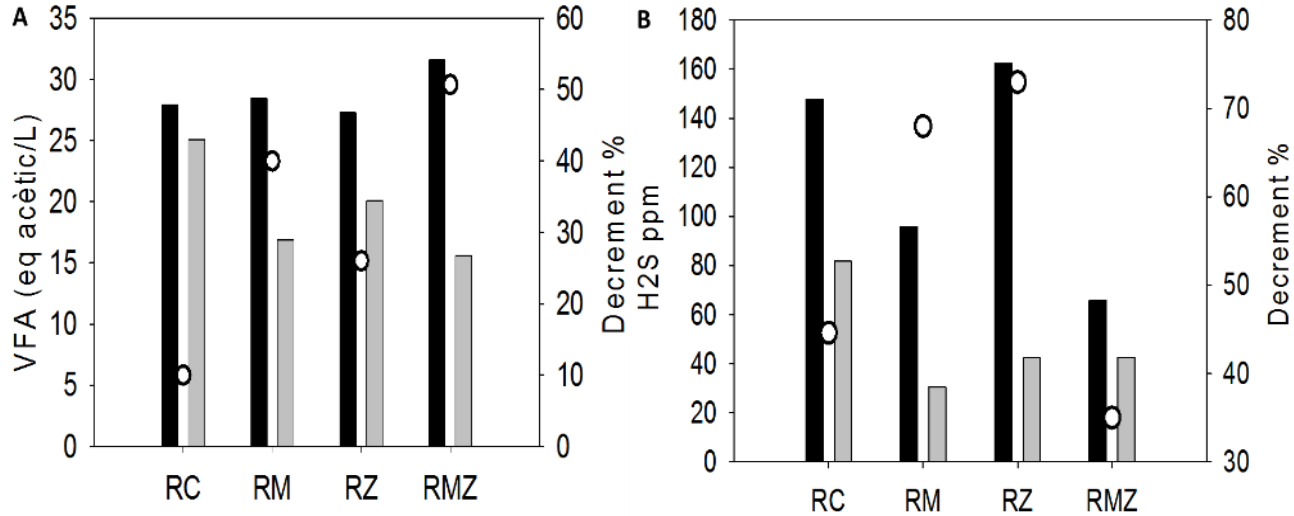


**Figure 9.2** a) VFA (meq ac) before (dark) and after (grey) recovery. b) H<sub>2</sub>S concentration before (dark) and after (grey) recovery.

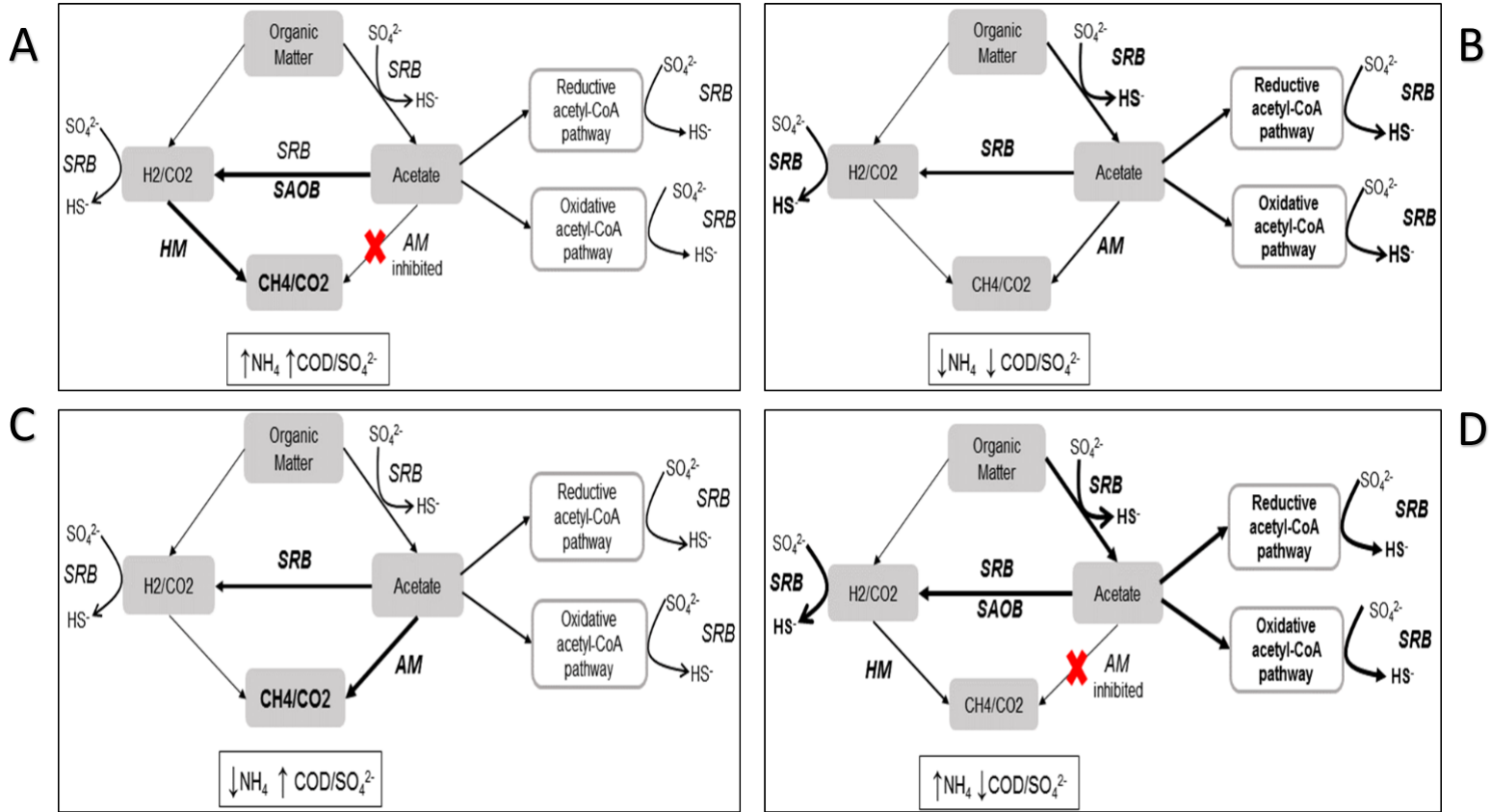


Figure 9.3 Main active pathways at different TAN concentrations and ratio COD/SO<sub>4</sub><sup>2-</sup>

### 9.3.2 Effect of COD/SO<sub>4</sub><sup>2-</sup> ratio on electron flow and the impact on methanogenic pathway

Isa et al., (1986), described that is possible to quantify the electron utilization by MPA and SRB and it is relatively important and useful to evaluate the competition between methanogens and SRB. The proportions of electrons utilized (%) by SRB and methanogens were calculated applying the following equations:

- [1] Electron flow to Methanogenesis =  $\text{CH}_4\text{-COD} / (\text{CH}_4\text{-COD} + \text{H}_2\text{S-COD})$
- [2] Electron flow to Sulfidogenesis =  $\text{H}_2\text{S-COD} / (\text{CH}_4\text{-COD} + \text{H}_2\text{S-COD})$

The results from electron flow calculation were in agreement with physico-chemical parameters. Indicating the main reaction under low COD/SO<sub>4</sub><sup>2-</sup> ratio (7.5) was SO<sub>4</sub><sup>2-</sup> reducing process, meanwhile after recovery application (15 ratio COD/SO<sub>4</sub><sup>2-</sup> methanogenesis prevail in all the reactors. O'Reilly and Colleran, 2006 described similar results, reporting that over 8 COD/ SO<sub>4</sub><sup>2-</sup> ratio MA became the main active community. However, other studies reported a clear drop from MA to SRB electron flow dominance after the COD/ SO<sub>4</sub><sup>2-</sup> ratio was under 5 in AD systems treating sludge material (Hu et al., 2015). Evidencing that substrate has a significant influence in the MPA and SRB competition. Weijma et al., (2002), described that at low COD/ SO<sub>4</sub><sup>2-</sup> ratio SRB utilized less efficiently acetate and H<sub>2</sub>/CO<sub>2</sub> than MPA. This evolution is shown on figure 9.4, where is possible to observed that when COD/ SO<sub>4</sub><sup>2-</sup> ratio increase the electron flow used by methanogenic communities, meanwhile the electron flow used by SRB decrease drastically.

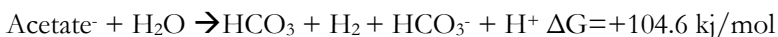
It is worth mentioning other operational parameters (HRT, OLR, substrate composition, etc.), not only COD/SO<sub>4</sub><sup>2-</sup> ratio, that directly affect to electron flow through sulfidogenesis or methanogenesis in AD-systems. In the present study, the high TAN concentration of the raw wastewater must be considered, because the synergistic inhibitory effect of TAN and SO<sub>4</sub><sup>2-</sup> described in the literature (Siles et al., 2010). As described Sürmeli et al., (2017), in anaerobic reactors treating chicken manure with microbial communities acclimatized to high TAN concentrations, the unexpected introduction of high sulphur concentrations motivated a drastically decrement of the CH<sub>4</sub> yield.

The MPA community cannot be considered as a whole, since the tolerance to TAN toxicity of the microbial communities involved in the methanogenic pathways is different (Fotidis et al., 2013). The isotopic fractionation of biogas components of the reactors provided a deeper insight on the predominance of acetotrophic and

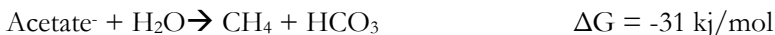
hydrogenotrophic methanogenesis. During recovery period,  $\alpha$ -values for revealed that hydrogenotrophic methanogenesis (HM) was the dominant pathway for methane production in all reactors indistinctly of added material (Table 9.1). Results indicated that totally HM dominance is mainly because high content of TAN and FAN, as reported by Wang et al., (2015).

Instead, sulphate seems a parameter less influenced by  $\alpha$ -value. In AD-systems with total or partial inhibited AM, syntrophic methanisation (the cooperation of HM and acetate oxidizers bacteria (SAOB)) is crucial for methane production (Westerholm et al., 2011). Nevertheless, when  $\text{SO}_4^{2-}$  is introduced (and the ratio  $\text{COD}/\text{SO}_4^{2-}$  decreases) in AD-systems with inhibited AM, the  $\text{H}_2\text{S}$  production increments. This is because SBR communities are favoured at low  $\text{COD}/\text{SO}_4^{2-}$  ratios and still outcompete with SAOB and  $\text{CH}_4$ -producer communities because the conversion of  $\text{H}_2$  and acetate are more thermodynamically favourable via sulphate reduction, as expressed the following equations (Dar et al., 2008). Figure 9.3 shows how the TAN content and  $\text{COD}/\text{SO}_4^{2-}$  ratio could favoure or inhibit the metabolic pathways involved in biogas production. So, in that figure is it possible to observed for each situations (TAN concentrations and  $\text{COD}/\text{SO}_4^{2-}$  ratio conditions) what is the predominant pathway and consequently the main microbial community. As an overview, when  $\text{COD}/\text{SO}_4^{2-}$  is low, predominated the acetate consumption via sulfidogenesis, however when that ratio increase,  $\text{CH}_4$  production is enhanced. Then, when  $\text{COD}/\text{SO}_4^{2-}$  ratio is over 8, the main path is determined by TAN concentration. Therefore, when TAN concentration is kept low, AMA dominates the predominant methanogenic production, meanwhile when TAN concentrations increase the  $\text{CH}_4$ -producers are mainly HMA.

SAOB reaction:



Aceticlastic methanogenesis (AM):



Hydrogenotrophic methanogenesis (HM):



Sulfate reduction reactions:



### 9.3.3 Effect of ammonia and sulfate stress on the abundance of methane-producing archaea and sulfate-reducing bacteria

In AD systems, SRB compete with MA for substrates such as H<sub>2</sub> and acetate, as is described above. The H<sub>2</sub>S produced by SRB while decomposing sulphates combined with NH<sub>3</sub> nitrogen released from protein degradation are highly toxic to both CH<sub>4</sub>-producing archaea and SRB (Jing et al., 2013). Recent studies showed that high NH<sub>3</sub> levels can alter the community structure of CH<sub>4</sub>-producing archaea, but this effect is quite different when SO<sub>4</sub><sup>2-</sup> is combined with high NH<sub>3</sub> levels (Moestedt et al., 2013). However, little is known how affect the combination of both compounds will affect the abundance and activity variation of SRB and MA communities.

To quantify activity and abundance variation of CH<sub>4</sub> producing and SO<sub>4</sub><sup>2-</sup> producing microorganisms in the four different reactors RC, RM, RZ and RMZ before and after recovery strategy application and linked to electron flow calculation, qPCR assays used to determine the magnitude of changes. Target genes for CH<sub>4</sub> producing archaea and sulphate-reducing microorganisms (were *mcrA* and *aprA* respectively) have been widely used as functional markers of these organisms and their quantitative variations of presence can be evaluated by measuring the copy numbers of the target genes.

#### 9.3.3.1 Sulfate reducing bacteria monitorization

Sulfide reduction was identified as an active process in all reactors during both periods (before and after recovery) where *aprA* were actively detected (figure 9.5). The gene copy numbers were analysed after and before of recovery applications. In general trends, the activity of SRB decreased during recovery period, when COD/ SO<sub>4</sub><sup>2-</sup> was incremented until 15 (2.9g SO<sub>4</sub><sup>2-</sup>-L<sup>-1</sup>) which is in agreement with physical-chemical parameter results. Results obtained in the present study are in accordance with much of the literature, where there is consensus that, acetate and H<sub>2</sub> is almost catalysed by sulphate reducer communities at low COD/SO<sub>4</sub><sup>2-</sup> ratios (Ren et al., 2007). Moreover, (Moon et al., 2015), analysing the microbial communities through 16S rDNA gene cloning showed a high increment of those genera involved sulphate reducers process when ratio COD/ SO<sub>4</sub><sup>2-</sup> decrease. At the same time it was evaluated effect of the different reactors configuration and support material in the sulphate reducer communities. It was observed a clearly decrement of these communities in fixed bed reactors (RM, RZ and RMC). However, the decrement was more evident in reactors supplied with magnetite. This effect could be due because magnetite increment the interspecies electron transfer effect. Consequently increment the growth of those communities that were inhibited during inhibitory period, such as acetogens or methanogens.

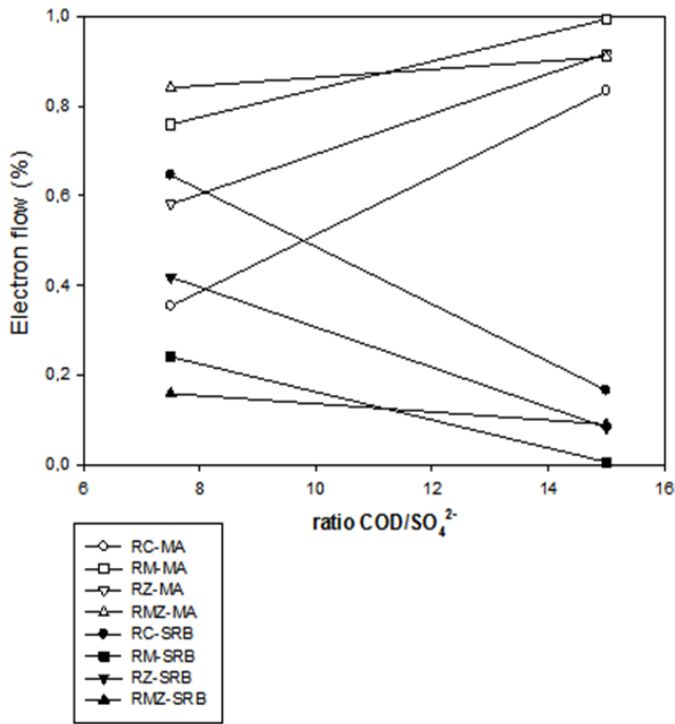
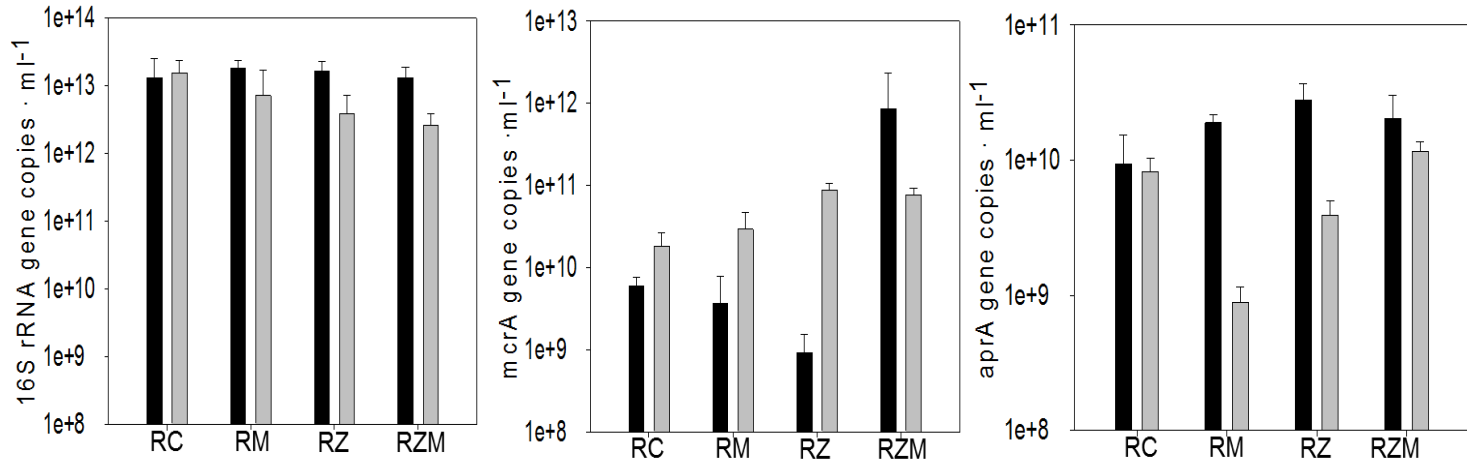


Figure 9.4 Electron flow (%) changes along increment of ratio COD/SO<sub>4</sub><sup>2-</sup>



**Figure 9.5** Quantitative analysis based on qPCR expressed as *16S* rRNA gene copies/ml, *mcrA* gene copies/ml and *aprA* gene copies/ml

### 9.3.3.2 Methane-producing archaea monitorization

Methanogenesis was checked before and after recovery strategy application and was identified more active in the final stage (after recovery). Figure 9.5 shows the tendency of the 16S rRNA, *mcrA* and *aprA* genes copies abundance.

The results of real-time PCR analysis indicated that the methanogenic activity increased 1-2 order of magnitude from the before stage to after stage in fix bed reactors. However, methanogenic activity slightly decreased in CSTR reactor (RC). That decrement could be linked to solid retention time, interval that particulate substrate and microorganisms are retained in the process vessel. This parameter is important in AD systems because determines the time available for microbial growth. For that, when SRT is under the duplication time of key member of microbial community (methanogenic populations in the present study) biomass washout could occur reducing those communities, and promoting process failure (Kaksonen et al., 2004). As it is previously described, methanogenic communities have long a duplication time and are highly impacted at low SRT (Jabłoński et al., 2015). In contrast, packed-bed reactors (RM,RZ and RMZ) has been observed as a great configuration to retain high density of methanogenic biomass inside the reactor by immobilizing microbes in a biofilm developed around of support materials, avoiding washout effect. Similar results were described by (Tatara et al., 2005), that incrementing SRT and reducing HRT with packed bed reactors, facilitate the conversion of propionate and acetate to methane formation.

## 9.4 Conclusions

The effect of two different packing materials, magnetite and zeolite, was evaluated successfully during the implementation of a recovery strategy for anaerobic digesters exposed previously to inhibitory concentration of ammonia and sulphate. Recovery of the methanogenic activity was prompted by increasing the HRT and the COD/  $\text{SO}_4^{2-}$  ratio, but the more significant improvement of the methanogenic activity was found with the mixed magnetite/zeolite packing (RMZ). This reactor was the only one that displayed an increase in the methanogenic population (*mcrA* gene copies). In summary, monitoring the *mcrA* and *aprA* genes during transitional periods is a novel tool for monitoring the direct effect on the biomass of operational strategies to overcome sulphate and nitrogen inhibition.



## 9.5 References

- Ali Shah, F., Mahmood, Q., Maroof Shah, M., Pervez, A., Ahmad Asad, S., 2014. Microbial ecology of anaerobic digesters: The key players of anaerobiosis. *Sci. World J.* doi:10.1155/2014/183752
- Annachatre, A.P., Suktrakoolvait, S., 2015. Biological Sulfate Reduction Using Molasses as a Carbon Source. *Water Environ. Res.* 73, 118–127. doi:10.2175/106143001X138778
- Antonenko, Y.N., Pohl, P., Denisov, G.A., 1997. Permeation of ammonia across bilayer lipid membranes studied by ammonium ion selective microelectrodes. *Biophys. J.* 72, 2187–95. doi:10.1016/S0006-3495(97)78862-3
- Baek, G., Jung, H., Kim, J., Lee, C., 2017. A long-term study on the effect of magnetite supplementation in continuous anaerobic digestion of dairy effluent – Magnetic separation and recycling of magnetite. *Bioresour. Technol.* 241, 830–840. doi:10.1016/j.biortech.2017.07.018
- Barana, A.C., Lopes, D.D., Martins, T.H., Pozzi, E., Damianovic, M.H.R.Z., Del Nery, V., Foresti, E., 2013. Nitrogen and organic matter removal in an intermittently aerated fixed-bed reactor for post-treatment of anaerobic effluent from a slaughterhouse wastewater treatment plant. *J. Environ. Chem. Eng.* 1, 453–459. doi:10.1016/j.jece.2013.07.015
- Braun, R., Huber, P., Meyrath, J., 1981. Ammonia toxicity in liquid piggy manure digestion. *Biotechnol. Lett.* 3, 159–164. doi:10.1007/BF00239655
- Conrad, R., 2005. Quantification of methanogenic pathways using stable carbon isotopic signatures: A review and a proposal. *Org. Geochem.* 36, 739–752. doi:10.1016/j.orggeochem.2004.09.006
- Conrad, R., Claus, P., Casper, P., 2010. Stable isotope fractionation during the methanogenic degradation of organic matter in the sediment of an acidic bog lake, Lake Grosse Fuchskuhle. *Limnol. Oceanogr.* 55, 1932–1942. doi:10.4319/lo.2010.55.5.1932
- Cruz Vigg, C., Rossetti, S., Fazi, S., Paiano, P., Majone, M., Aulenta, F., 2014. Magnetite particles triggering a faster and more robust syntrophic pathway of methanogenic propionate degradation. *Environ. Sci. Technol.* 48, 7536–7543. doi:10.1021/es5016789
- Dai, X., Yan, H., Li, N., He, J., Ding, Y., Dai, L., Dong, B., 2017. Metabolic adaptation of microbial communities to ammonium stress in a high solid anaerobic digester with dewatered sludge. *Sci. Rep.* 7. doi:10.1038/srep28193
- Dar, S.A., Kleerebezem, R., Stams, A.J.M., Kuenen, J.G., Muyzer, G., 2008. Competition and coexistence of sulfate-reducing bacteria, acetogens and methanogens in a lab-scale anaerobic bioreactor as affected by changing substrate to sulfate ratio. *Appl. Microbiol. Biotechnol.* 78, 1045–1055. doi:10.1007/s00253-008-1391-8
- Fotidis, I.A., Karakashev, D., Kotsopoulos, T.A., Martzopoulos, G.G., Angelidaki, I., 2013. Effect of ammonium and acetate on methanogenic pathway and methanogenic community composition. *FEMS Microbiol. Ecol.* 83, 38–48. doi:10.1111/j.1574-6941.2012.01457.x
- Franke-Whittle, I.H., Walter, A., Ebner, C., Insam, H., 2014. Investigation into the effect of high concentrations of volatile fatty acids in anaerobic digestion on methanogenic communities. *Waste Manag.* 34, 2080–2089. doi:10.1016/j.wasman.2014.07.020
- Habouzit, F., Hamelin, J., Santa-Catalina, G., Steyer, J.P., Bernet, N., 2014. Biofilm development during the start-up period of anaerobic biofilm reactors: The biofilm Archaea community is highly dependent on the support material. *Microb. Biotechnol.* 7, 257–264. doi:10.1111/1751-7915.12115

- Hu, Y., Jing, Z., Sudo, Y., Niu, Q., Du, J., Wu, J., Li, Y.Y., 2015. Effect of influent COD/SO<sub>4</sub><sup>2-</sup> ratios on UASB treatment of a synthetic sulfate-containing wastewater. *Chemosphere* 130, 24–33. doi:10.1016/j.chemosphere.2015.02.019
- Isa, Z., Grusenmeyer, S., Vestraete, W., 1987. Sulfate reduction relative to methane production in high-rate anaerobic digestion: Technical aspects. *Appl. Environ. Microbiol.*
- Jabłoński, S., Rodowicz, P., Łukaszewicz, M., 2015. Methanogenic archaea database containing physiological and biochemical characteristics. *Int. J. Syst. Evol. Microbiol.* 65, 1360–1368. doi:10.1099/ijs.0.000065
- Jing, Z., Hu, Y., Niu, Q., Liu, Y., Li, Y.Y., Wang, X.C., 2013. UASB performance and electron competition between methane-producing archaea and sulfate-reducing bacteria in treating sulfate-rich wastewater containing ethanol and acetate. *Bioresour. Technol.* 137, 349–357. doi:10.1016/j.biortech.2013.03.137
- Joshi, D.R., Zhang, Y., Gao, Y., Liu, Y., Yang, M., 2017. Biotransformation of nitrogen- and sulfur-containing pollutants during coking wastewater treatment: Correspondence of performance to microbial community functional structure. *Water Res.* 121, 338–348. doi:10.1016/j.watres.2017.05.045
- Kaksonen, A.H., Franzmann, P.D., Puhakka, J.A., 2004. Effects of Hydraulic Retention Time and Sulfide Toxicity on Ethanol and Acetate Oxidation in Sulfate-Reducing Metal-Precipitating Fluidized-Bed Reactor. *Biotechnol. Bioeng.* 86, 332–343. doi:10.1002/bit.20061
- Karunakaran, E., Vernon, D., Biggs, C.A., Saul, A., Crawford, D., Jensen, H., 2017. Enumeration of sulphate-reducing bacteria for assessing potential for hydrogen sulphide production in urban drainage systems. *Water Sci. Technol.* 73, 3087–3094. doi:10.2166/wst.2017.026
- Loukidou, M.X., Zouboulis, A.I., 2001. Comparison of two biological treatment processes using attached-growth biomass for sanitary landfill leachate treatment. *Environ. Pollut.* 111, 273–281. doi:10.1016/S0269-7491(00)00069-5
- Lv, Z., Hu, M., Harms, H., Richnow, H.H., Liebetrau, J., Nikolauz, M., 2014. Stable isotope composition of biogas allows early warning of complete process failure as a result of ammonia inhibition in anaerobic digesters. *Bioresour. Technol.* 167, 251–259. doi:10.1016/j.biortech.2014.07.029
- Maillacheruvu, K.Y., Parkin, G.F., 1997. Kinetics of growth, substrate utilization and sulfide toxicity for propionate, acetate and hydrogen utilizers in anaerobic systems. *Water Environ. Res.* 68, 1099–1107. doi:10.2175/106143096X128126
- Moestedt, J., Nilsson Pålédal, S., Schnürer, A., 2013. The effect of substrate and operational parameters on the abundance of sulphate-reducing bacteria in industrial anaerobic biogas digesters. *Bioresour. Technol.* 132, 327–332. doi:10.1016/j.biortech.2013.01.043
- Montalvo, S., Guerrero, L., Borja, R., Sánchez, E., Milán, Z., Cortés, I., Angeles de la la Rubia, M., 2012. Application of natural zeolites in anaerobic digestion processes: A review. *Appl. Clay Sci.* doi:10.1016/j.clay.2012.01.013
- Moon, C., Singh, R., Veeravalli, S.S., Shanmugam, S.R., Chaganti, S.R., Lalman, J.A., Heath, D.D., 2015. Effect of COD: SO<sub>4</sub><sup>2-</sup> ratio, HRT and linoleic acid concentration on mesophilic sulfate reduction: Reactor performance and microbial population dynamics. *Water (Switzerland)* 7, 2275–2292. doi:10.3390/w7052275
- Muyzer, G., Stams, A.J.M., 2008. The ecology and biotechnology of sulphate-reducing bacteria. *Nat. Rev. Microbiol.* doi:10.1038/nrmicro1892
- O'Reilly, C., Collieran, E., 2007. Effect of influent COD/SO<sub>4</sub><sup>2-</sup> ratios on mesophilic anaerobic reactor biomass populations: Physico-chemical and microbiological properties. *FEMS Microbiol. Ecol.* 56, 141–153. doi:10.1111/j.1574-6941.2007.00067.x

- Parkin, G.F., Lynch, N.A., Kuo, W.C., Vankeuren, E.L., Bhattacharya, S.K., 1990. Interaction between Sulfate Reducers and Methanogens Fed Acetate and Propionate. *Res. J. Water Pollut. Control Fed.* 62, 780–788. doi:10.2307/25043913
- Pelissari, C., Guivernau, M., Viñas, M., de Souza, S.S., García, J., Sezerino, P.H., Ávila, C., 2017. Unraveling the active microbial populations involved in nitrogen utilization in a vertical subsurface flow constructed wetland treating urban wastewater. *Sci. Total Environ.* 584–585, 642–650. doi:10.1016/j.scitotenv.2017.01.091
- Prenafeta-Boldú, F.X., Fernández, B., Viñas, M., Lizardo, R., Brufau, J., Owusu-Asiedu, A., Walsh, M.C., Awati, A., 2017. Effect of *Bacillus* spp. direct-fed microbial on slurry characteristics and gaseous emissions in growing pigs fed with high fibre-based diets. *Animal* 1–10. doi:10.1017/S1751731116001415
- Qureshi, N., Annous, B.A., Ezeji, T.C., Karcher, P., Maddox, I.S., 2005. Biofilm reactors for industrial bioconversion process: Employing potential of enhanced reaction rates. *Microb. Cell Fact.* doi:10.1186/1475-2859-4-24
- Rajagopal, R., Mass??, D.I., Singh, G., 2013. A critical review on inhibition of anaerobic digestion process by excess ammonia. *Bioresour. Technol.* doi:10.1016/j.biortech.2013.07.030
- Ren, N.Q., Chua, H., Chan, S.Y., Tsang, Y.F., Sin, N., 2007. Effects of COD/SO<sub>4</sub><sup>2-</sup> ratios on an acidogenic sulfate-reducing reactor. *Ind. Eng. Chem. Res.* 46, 1661–1667. doi:10.1021/ie060589w
- Ruiz-Sánchez, J., Campanaro, S., Guivernau, M., Fernández, B., Prenafeta-Boldú, F.X., 2018. Effect of ammonia on the active microbiome and metagenome from stable full-scale digesters. *Bioresour. Technol.* 250, 513–522. doi:10.1016/j.biortech.2017.11.068
- Rummel, C.D., Jahnke, A., Gorokhova, E., Kühnel, D., Schmitt-Jansen, M., 2017. Impacts of biofilm formation on the fate and potential effects of microplastic in the aquatic environment. *Environ. Sci. Technol. Lett.* doi:10.1021/acs.estlett.7b00164
- Sabumon, P.C., 2008. Development of enhanced sulphidogenesis process for the treatment of wastewater having low COD/SO<sub>4</sub><sup>2-</sup> ratio. *J. Hazard. Mater.* 159, 616–625. doi:10.1016/j.jhazmat.2008.02.097
- Santegoeds, C.M., Damgaard, L.R., Hesselink, G., Zopfi, J., Lens, P., Muyzer, G., De Beer, D., 1999. Distribution of sulfate-reducing and methanogenic bacteria in anaerobic aggregates determined by microsensor and molecular analyses. *Appl. Environ. Microbiol.* 65, 4618–4629. doi:10.1128/aem.65.12.4618-4629.1999
- Sarti, A., Zaiat, M., 2011. Anaerobic treatment of sulfate-rich wastewater in an anaerobic sequential batch reactor (AnSBR) using butanol as the carbon source. *J. Environ. Manage.* 92, 1537–1541. doi:10.1016/j.jenvman.2011.01.009
- Siles, J.A., Brekelmans, J., Martín, M.A., Chica, A.F., Martín, A., 2010. Impact of ammonia and sulphate concentration on thermophilic anaerobic digestion. *Bioresour. Technol.* 101, 9040–9048. doi:10.1016/j.biortech.2010.07.163
- Smith, A.L., Shimada, T., Raskin, L., 2017. A comparative evaluation of community structure in full-scale digesters indicates that two-phase digesters exhibit greater microbial diversity than single-phase digesters. *Environ. Sci. Water Res. Technol.* 3, 304–311. doi:10.1039/C6EW00320F
- Sürmeli, R.Ö., Bayrakdar, A., Molaey, R., Çalli, B., 2017. Synergistic Effect of Sulfide and Ammonia on Anaerobic Digestion of Chicken Manure. *Waste and Biomass Valorization* 1–7. doi:10.1007/s12649-017-0090-z
- Tatara, M., Yamazawa, A., Ueno, Y., Fukui, H., Goto, M., Sode, K., 2005. High-rate thermophilic methane fermentation on short-chain fatty acids in a down-flow anaerobic packed-bed reactor. *Bioprocess Biosyst. Eng.* 27, 105–113. doi:10.1007/s00449-004-0387-8

- Vela, F.J., Zaiat, M., Foresti, E., 2002. Influence of the COD to sulphate ratio on the anaerobic organic matter degradation kinetics. *Water SA* 28, 213–217. doi:10.4314/wsa.v28i2.4887
- Wang, H., Fotidis, I.A., Angelidaki, I., 2015. Ammonia effect on hydrogenotrophic methanogens and syntrophic acetate-oxidizing bacteria. *FEMS Microbiol. Ecol.* 91. doi:10.1093/femsec/fiv130
- Wang, Q., Yang, Y., Yu, C., Huang, H., Kim, M., Feng, C., Zhang, Z., 2011. Study on a fixed zeolite bioreactor for anaerobic digestion of ammonium-rich swine wastes. *Bioresour. Technol.* 102, 7064–7068. doi:10.1016/j.biortech.2011.04.085
- Wang, W., Ren, X., Yang, K., Hu, Z., Yuan, S., 2017. Inhibition of ammonia on anaerobic digestion of synthetic coal gasification wastewater and recovery using struvite precipitation. *J. Hazard. Mater.* 340, 152–159. doi:10.1016/j.jhazmat.2017.07.002
- Weijma, J., Bots, E.A.A., Tandler, G., Stams, A.J.M., Pol, L.W.H., Lettinga, G., 2002. Optimisation of sulphate reduction in a methanol-fed thermophilic bioreactor. *Water Res.* 36, 1825–1833. doi:10.1016/S0043-1354(01)00390-6
- Westerholm, M., Dolfing, J., Sherry, A., Gray, N.D., Head, I.M., Schnürer, A., 2011. Quantification of syntrophic acetate-oxidizing microbial communities in biogas processes. *Environ. Microbiol. Rep.* 3, 500–505. doi:10.1111/j.1758-2229.2011.00249.x
- Yenigün, O., Demirel, B., 2013. Ammonia inhibition in anaerobic digestion: A review. *Process Biochem.* 48, 901–911. doi:10.1016/j.procbio.2013.04.012
- Zeeman, G., Kujawa, K., de Mes, T., Hernandez, L., de Graaff, M., Abu-Ghunmi, L., Mels, A., Meulman, B., Temmink, H., Buisman, C., van Lier, J., Lettinga, G., 2008. Anaerobic treatment as a core technology for energy, nutrients and water recovery from source-separated domestic waste(water). *Water Sci. Technol.* 57, 1207–1212. doi:10.2166/wst.2008.101
- Zhao, Q.I., Li, W., You, S.J., 2007. Simultaneous removal of ammonium-nitrogen and sulphate from wastewaters with an anaerobic attached-growth bioreactor, in: *Water Science and Technology*. pp. 27–35. doi:10.2166/wst.2007.762
- Zheng, H., Li, D., Stanislaus, M.S., Zhang, N., Zhu, Q., Hu, X., Yang, Y., 2015. Development of a bio-zeolite fixed-bed bioreactor for mitigating ammonia inhibition of anaerobic digestion with extremely high ammonium concentration livestock waste. *Chem. Eng. J.* 280, 106–114. doi:10.1016/j.cej.2015.07.024
- Zitomer, D., Maki, J., Venkiteshwaran, K., Bocher, B., 2017. Relating Anaerobic Digestion Microbial Community and Process Function. *Microbiol. Insights* 37. doi:10.4137/MBIS33593

# Chapter 10 Impact of recuperative thickening on syntrophic microbial interactions and biogas production in anaerobic digestion

---

The recuperative thickening, which increases the solids retention time (SRT; in this work 32 and 61 days in two independent reactors), was evaluated as a method to mitigate ammonia inhibition in anaerobic digesters (AD). A stepwise increment of the total ammonia nitrogen (TAN), above inhibitory reported conditions ( $3 \text{ gN L}^{-1}$ ), was obtained by a progressive increase of both the organic loading rate and the total nitrogen content of the influent. Recuperative thickening did not change main performance parameters of AD but it revealed the resilience of the microbial community. A clear bacterial activity shift, based on microbial community analysis, was found while the TAN acclimatization of methanogens was proved through activity tests. The methanogenesis proceeded via hydrogenotrophic archaea when reactors were operated at high organic loading rates. The lack of volatile fatty acids accumulation and stable operation further indicated the occurrence of the syntrophic acetate oxidation process. However, recuperative thickening stimulated a very specific syntrophism, which was based upon the predominance of *Pseudomonas* and *Methanoculleus*.

*Part of this chapter was presented as a poster communication in FEMS 2017 conference.*

*This chapter was submitted to New biotechnology journal*

## 10.1 Introduction

Anaerobic degradation of protein-rich materials (e.g. poultry manure, slaughterhouse waste) is characterized by high methane yields and nutrient-rich digestates, but requires strategies to overcome ammonia inhibition (Affes et al., 2013; Rajagopal et al., 2013). Different factors influencing ammonia inhibition and a wide range of total ammonium nitrogen (TAN) inhibitory levels has been reported in literature (at pH 7-8 and 35°C): 3-4 gN L<sup>-1</sup> (Kayhanian, 1999); 5-7 gN L<sup>-1</sup> (Wang et al., 2016); 7-9 gN L<sup>-1</sup> (Sun et al., 2016); 16 gN L<sup>-1</sup> (Niu et al., 2015).

Acclimation is usually used as explanation of such wide range of inhibitory levels and for several types of N-rich wastes, but also being proved as an economic option to improve microbial resilience under high TAN concentrations (Niu et al., 2015). Acclimation of microorganism is an evidence of process functional resilience, which keeps steady performance towards perturbations. For example, Gao et al., (2015) acclimatized in 160 days the anaerobic biomass in a mesophilic digester from 2 to 4.5 gN L<sup>-1</sup> while treating food waste, or Abouelenien et al. (2009) adapted the anaerobic biomass to treat chicken manure from 2 up to 8 gN kg<sup>-1</sup>, in a series of sequential batch experiments lasting over 400 days, without decreasing the process performance. Niu et al., (2014) recovered a mesophilic stirred digester, fed with chicken manure, reaching a stable operation after diluting the TAN content from 16 to 4 gN L<sup>-1</sup>.

Under high TAN concentration, microbial acclimation is prompted by a shift of acetogenesis and methanogenic pathways dominated by TAN tolerant species. This is the case of syntrophic acetate oxidation (SAO), followed by hydrogenotrophic methanogenesis (the so-called SAO process), demonstrated in AD operated with high TAN concentration using isotope labelling or molecular tools (Ho et al., 2013; Regueiro et al., 2016; Sun et al., 2014; Westerholm et al., 2016). Methanogens, primarily belonging to the genera *Methanothermobacter* (Kato et al., 2014), *Methanosarcina* and *Methanoculleus* (Mosbæk et al., 2016), have been described able to perform the SAO process in association with bacteria as the strain AOR (Lee and Zinder, 1988), or species *Thermacetogenium phaeum* (Hattori et al., 2000) and *Thermotoga lettingae* (Balk et al., 2002) at thermophilic conditions. Under mesophilic conditions, *Clostridium ultunense* (Schnurer et al., 1996), *Syntrophaceticus schinkii* (Westerholm et al., 2010) and *Tepidanaerobacter acetatoxydans* (Westerholm et al., 2011) have been described as able to perform the SAO process.

The microbial shift at high TAN concentration is affected by operational parameters, such as temperature, reactor configuration, organic loading rate (OLR) or the profile and concentration of volatile fatty acids (VFA) (Westerholm et al., 2012). Past works on acclimatization over ammonia focused mainly on choosing an adequate control of operational parameters such as temperature, OLR, hydraulic retention time (HRT) for

ammonia dilution, or co-digestion to optimize the C/N ratio (Abouelenien et al., 2009; Rajagopal et al., 2013; Mata-Alvarez et al., 2014; Niu et al. 2014). More recently, ammonia stripping, struvite precipitation, addition of inorganic and/or conductive materials, bioaugmentation, or the addition of trace metals have been tested (Romero-Güiza et al., 2015; Romero-Güiza et al., 2016; Fotidis et al., 2014; Capson-Tojo et al., 2018), but these approaches are sometimes not feasible or not cost-effective enough to be applied at full-scale (Tampio et al., 2015).

The solids retention time (SRT) is a crucial parameter to prevent the wash-out of the microbes involved in the SAO process and, ultimately, to promote a higher resilience of the reactor towards ammonia inhibition. The doubling time for a SAO culture at 37°C is 28 days (Demirel and Scherer, 2008; Schnurer et al., 1994), whereas the cellular duplication time of methanogens as *Methanosaeta* and *Methanosarcina* ranges 1 to 9 days and 8 to 6 hours, respectively, at mesophilic optimal conditions and depending on the acetate concentration (Demirel and Scherer, 2008; Smith and Mah, 1978). A prolonged SRT can be reached by increasing the HRT or biomass immobilization, but recuperative thickening (RT) is a simpler option for digesters that allows an increment of the treatment capacity with minor additional space or capital investment (Yang et al., 2017). RT increases the microbial population concentration, retaining micronutrients linked to the solid phase (Zhang et al., 2013) and improving the C/N ratio by removing the soluble TAN from the liquid phase (Nagao et al., 2012).

Therefore, this work aims to investigate if recuperative thickening enhances AD performance during the acclimation over ammonia. A stepwise increment of the OLR, with a subsequent increase in TAN concentration, was applied during the continuous operation of two AD, with similar HRT but different SRTs (37 and 86 days), at lab-scale for 310 days. Microbial dynamics based on diversity and density indexes were studied to evaluate the effect of SRT on ammonia resilience and resistance, linking them to conventional AD performance parameters and inhibition assessment (toxicity assays).

## 10.2 Materials and methods

### 10.2.1 Substrate and inoculum origin

A blend of slaughterhouse waste (SW), microalgae biomass (MA), chicken and pig manures (CM, PM) were used as feedstock of the digesters. The SW included blood, fat, stomach, solid dung, and whole intestines, that were shredded (till a particle size < 8 mm) and sterilized at 133 °C for 20 min as sterilization procedure established for animal byproducts of Category 2 (90/667/EEC, 2002). SW was collected from a pig slaughterhouse (Soria, Spain). Both manures PM and CM were collected at two intensively rearing farms (Barcelona and Soria, Spain). The MA was obtained, after

being settled, from a pilot-scale raceway treating municipal wastewater (Cádiz, Spain). The digestate of a mesophilic lab-scale AD, treating a mixture of slaughterhouse waste and pig manure (HRT 28 d; OLR 2 kgVS m<sup>-3</sup> d<sup>-1</sup>; effluent TAN 2.2 gN L<sup>-1</sup>) was used as inoculum. Table 1 summarizes the physicochemical characterization of all materials and the weight percentage composition of the feedstock per operational period.

### 10.2.2 Anaerobic digesters set-up

Two continuous stirred tank reactors of 5 L (working volume) were operated in semi-continuous mode, with daily feeding, at 37 ±1 °C. One reactor was operated under recuperative thickening (recirculation of the settled fraction of digestate), labeled as R1-RT. Thickening was done by (i) collecting digestate before feeding; (ii) settling the digestate for 24 hours at ambient temperature; and (iii) returning a mean flow 60.2 mL d<sup>-1</sup> of settled fraction (see supplementary material). The second reactor was operated as a conventional stirred reactor without recirculation; this one was referenced as R2-C. HRT (mean values were 31 ±14 and 34 ±9 days in R1-RT and R2-C, respectively) and SRT (mean values were 86 ±22 and 37 ±14 days in R1-RT and R2-C, respectively) were calculated similarly to Nagao et al., (2012).

The operation of both reactors was divided in four different periods (P0-P4). Both reactors were equally fed with the blend SW: PM = 50:50 in P0 and SW alone in P1. Then a blend SW: CM: PM: MA was used in P2 and P3 periods: 9:1:90:0 in P2; and 5:20:70:5 in P3 (percentages in wet weight basis; Table 1). These mixtures were diluted with deionized water to reach the desired inlet-TKN. No further corrections were applied to the physic-chemical parameters after dilution. Each reactor was fed 4 times per day, using a temporized feeding system that ensured the addition of a homogenized influent.

The start-up period (P0) lasted 50 days with an OLR of 0.9-1.4 kgVS m<sup>-3</sup> d<sup>-1</sup>, using an influent with a total Kjeldhal nitrogen (TKN) of 2.4 gN L<sup>-1</sup>. The following three periods (P1, P2, P3) lasted 95-100 days each and comprised a stepwise increased of the TKN inflow content (2.9, 4.6 and 9.0 gN L<sup>-1</sup> in P1, P2 and P3, respectively) and of the OLR (1.5-1.8, 3.0-3.1 and 2.6-3.3 kgVS m<sup>-3</sup> d<sup>-1</sup> in P1, P2 and P3, respectively; see supplementary material). The produced digestates had a mean TAN content of 3.9, 5.5 and 4.6 gN L<sup>-1</sup> in P1, P2 and P3, respectively (Figure 10.1).



**Table 10. 1** Raw materials characterization. Nomenclature: COD, chemical oxygen demand; TS, VS, total and volatile solids; TKN, TAN, total Kjeldhal and ammonia nitrogen; nm, not measured.

Parameter	Slaugh. Waste (SHW)	Chicken manure (CM)	Pig manure (PM)	Microalgal biomass (MA)	Inoculum
COD (g kg <sup>-1</sup> )	653.4	369.9	32.3	60.9	38.9
TS (g kg <sup>-1</sup> )	355.7	327.0	27.2	59.8	2.8
VS (g kg <sup>-1</sup> )	280.4	221.6	18.6	37.4	2.1
TKN (gN kg <sup>-1</sup> )	29.3	29.7	2.6	5.3	3.0
TAN (gN kg <sup>-1</sup> )	8.6	5.8	1.9	3.7	2.3
Grease (g kg <sup>-1</sup> )	81.7	10.8	0.6	nm	nm
Fibres (g kg <sup>-1</sup> )	35.9	61.6	13.6	nm	nm
C/N	15.9	4.0	5.0	5.6	nm

Feed composition per period (ratio in wet weight)

Period	SHW	CM	PM	MA	Deionized H2O
P0	25	0	24	0	51
P1	11	0	0	0	89
P2	9	1	90	0	0
P3	5	20	70	5	0

Flows (influent and effluent of both digesters, the clarified effluent of R1 and biogas), for mass and COD balance, and temperature were daily monitored. The volume of biogas was quantified by the water displacement method. Samples of those streams were collected once per week for determination of pH, total alkalinity (TA), total and volatile solids (TS, VS), total chemical oxygen demand (COD), N related compounds (i.e. TKN, TAN), total and individual volatile fatty acids (VFA) and biogas composition (CH<sub>4</sub>, CO<sub>2</sub>). Samples for microbial community analysis and inhibition tests were taken from the inside of each reactor at the end of each period.

### 10.2.3 Ammonia inhibition test

Ammonia inhibition tests were performed, in triplicate, in 120 mL glass serum bottles at mesophilic conditions following the procedure described in Astals et al. (2015). Serum bottles contained inoculum (diluted to 10 gVS L<sup>-1</sup>), sodium acetate (5 gCOD L<sup>-1</sup>), and ammonium chloride for each tested concentration (equivalent to TAN of 2, 4 and 6 gN L<sup>-1</sup>). All serum bottles were hermetically sealed and flushed with high-purity N<sub>2</sub> for two minutes, shaken and incubated at 35°C. Biogas production (normalized at 0°C and 1 bar) and biogas composition (CH<sub>4</sub> and CO<sub>2</sub>) was analyzed 2-3 times per day for 2 days, by gas chromatography (CO-300 Varian, USA) following Rodríguez-Abalde et al. (2011) methodology. The specific methanogenic activity (SMA) of the inoculum at each tested TAN concentration was determined as the slope of a linear regression fit (Analysis Toolpack in Microsoft Excel 2010) for subsets of data over which the rate of methane production was approximately constant. KI<sub>50</sub> was the free ammonia nitrogen (FAN) concentration at which SMA is reduced by 50% of the native SMA.

### 10.2.4 Analytical methods

The content of TS and VS were determined following the 2540G method by Standard methods for examination of water and wastewater (Eaton et al., 2005). Total COD was determined as for Noguerol et al. (2012). Total alkalinity (TA) was measured by manual titration with 0.25 N H<sub>2</sub>SO<sub>4</sub> to the end-point at pH 4.3 as for the standard method 2320B (Eaton et al., 2005). TAN and TKN were determined according to the standard methods procedure 4500-NH<sub>3</sub>D and 2500-NorgB, respectively (Eaton et al., 2005). The FAN content of the liquid fraction of digestates was calculated according to the equilibrium, for the pH and temperature inside each digester (Hansen et al., 1998; Romero-Güiza et al., 2014). Both volatile fatty acids (i.e. acetic, propionic, butyric, and valeric acids) profile and concentration were determined with a CP-3800 gas chromatograph (Varian, USA), and expressed as acetic acid equivalents (Palatsi et al. 2010). Biogas composition was determined using a gas chromatograph CP-3800 (Varian, USA), equipped with a Hayesep Q 80/100 Mesh (2m x 1/8" x 2.0 mm SS) packed column and a TCD detector. Biogas production was corrected for standard temperature (273.15 K) and pressure (100 kPa) conditions (i.e., STP).

### 10.2.5 Microbial community analysis

Microbial populations were characterized by culture-independent molecular methods. Total DNA and RNA extraction, as well as, qPCR analysis and MiSeq studies were performed by following procedure describes in chapter 3. To evaluate the diversity of the samples, the number of OTUs, the inverted Simpson index, Shannon index and Goods coverage estimators were all calculated using the Mothur software v.1.38.1 (<http://www.mothur.org>). All the estimators were normalized to the lower number of

reads from the different samples. Subsequently, the relative abundance of 16S rRNA transcripts grouped as operational taxonomic units (OTU), at a 97% sequence homology cut-off, was analyzed by canonical correspondence analysis (CCA) using the Canoco software v 4.51.

## **10.3 Results**

### **10.3.1 Reactors performance**

The time-course evolution of TAN, FAN, total VFA, acetic to propionic concentration ratio, and performance parameters (VS removal; CH<sub>4</sub> yield and rate) during the reactor experiments is shown in Figure 11.1. Under a similar HRT, the SRT of the thickening reactor (R1-RT) averaged 86 days but fluctuated significantly due to changes of the digestate solids concentration. The evolution of TAN and FAN was similar along the whole experiment, leading to an alike performance during periods P0 and P1 in terms of methane yield and VS removal.

The introduction of chicken manure (a fiber&N-rich material) and settled microalgae in P2 and P3, respectively, together with the increased OLR produced a decrement of methane yield, although remaining slightly higher in R2-C than in R1-RT (Figure 10.1). The total VFA and the acetic to propionic ratio also differed from P2 period and further OLR increment (from 1.4 to 3.2 kgVS m<sup>-3</sup> d<sup>-1</sup>) in P3 resulted in a sharp increase of the total VFA concentration. The total VFA peak content of 5.7 and 2.5 g L<sup>-1</sup> was registered in R2-C and R1-RT, respectively. The operation under the recuperative thickening mode attained a lower total VFA content but a more distributed profile, as the acetic to propionic ratio shows. time for the solids) of R1-RT, that would explain the slightly better gas yields. Total VFA and acetic to propionic ratio decreased only after the reduction of the OLR from 3.2 to 2.0 kgVS m<sup>-3</sup> d<sup>-1</sup> in the second half of period P3.

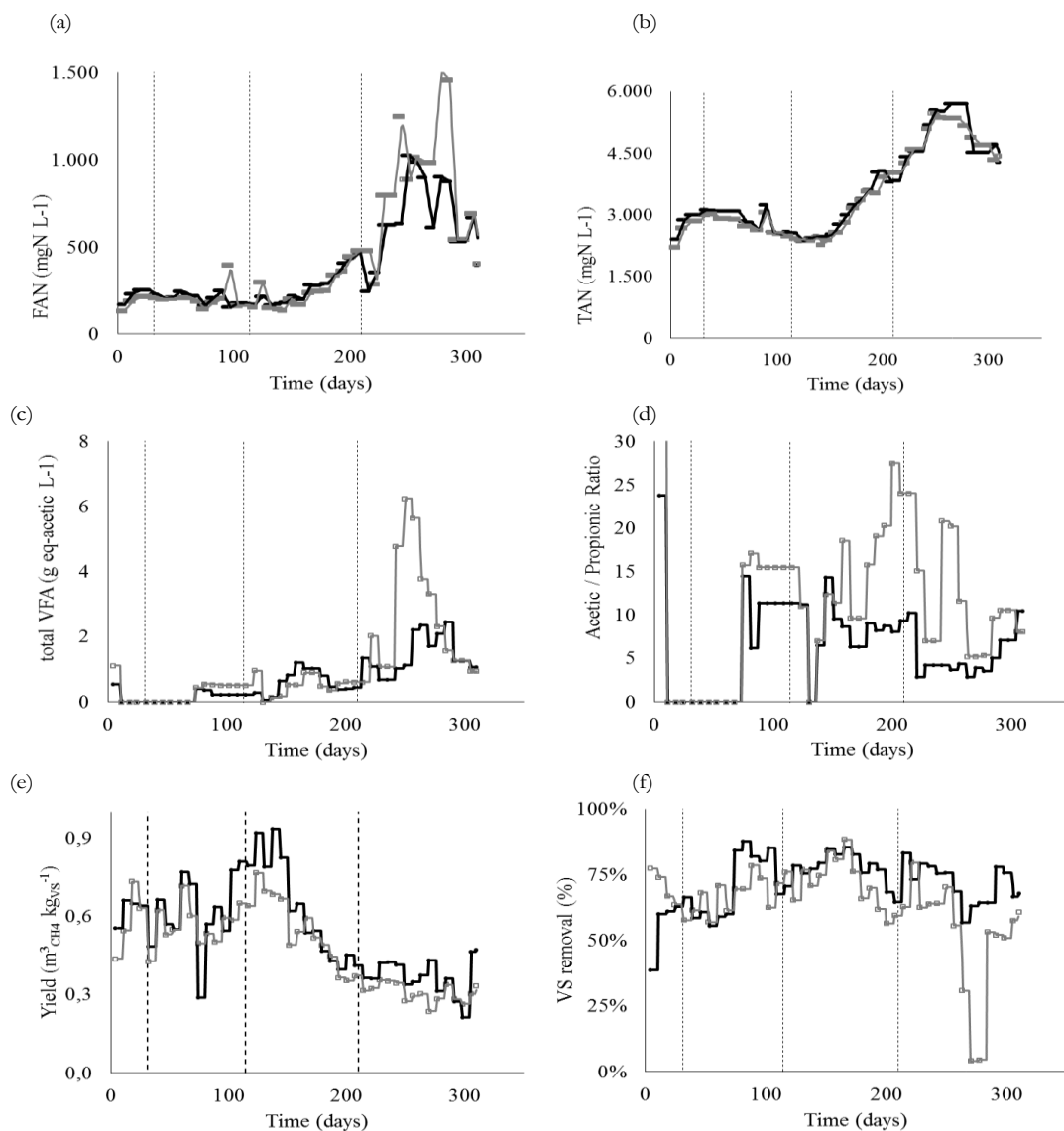


**Figure 10.1** Evolution of operational and control parameters in digesters R1-RT and R2-C. (a) Free ammonia nitrogen (FAN). (b) Total ammonia nitrogen (TAN). (c) Total volatile fatty acids (VFA). (d) Acetic to propionic acids ratio. (e) Methane yield. (f) Volatile (VS) removal efficiency. Note: vertical dotted lines denote performance periods. Colours: R1-RT, black; R2-C, grey.

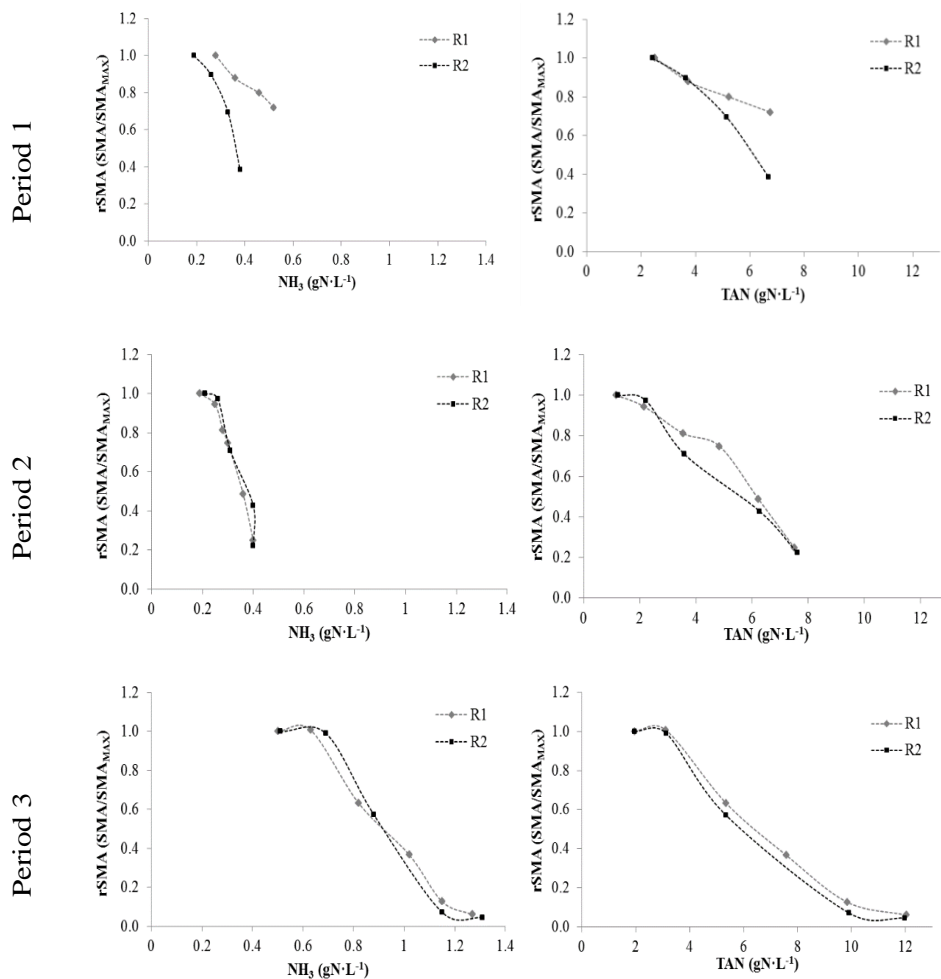


**Figure 10. 2** Specific methanogenic activity (SMA), expressed as percentage of the maximum SMA, as a function of the free ammonia (NH<sub>3</sub>; left) or total ammonia (TAN; right) contents in digesters R1-RT and R2-C. (a) Period 1. (b) Period 2. (c) Period 3.

In fact, this ratio increased with OLR rise, being more severe in R1-RT, but always below 1.4 or reported value for complete unbalance (Karthikeyan et al., 2016). This instability can be attributed to the degradation of the incoming feed (the VS removal trend did not change in P3), a subsequently increased the TAN and FAN concentration (1.0 and 1.6 gN-NH<sub>3</sub> L<sup>-1</sup> in R1-RT and R2-C, respectively) inside both digesters while the pH raised (see supplementary material). Nevertheless, a slightly better VS removal (mean) efficiencies in R2-C were registered, although the higher SRT (larger digestion

### 10.3.2 Ammonium inhibition tests

Ammonium inhibition assays were performed with biomass samples collected at the end of each operational period (days 143, 235 and 295 for P1, P2 and P3, respectively). Figure 11.2 shows the normalized curves of the inhibition tests for each period and reactor in terms of the FAN and TAN concentration. Inhibition profile plots were normalized to provide a more direct comparison since the SMA<sub>MAX</sub> (SMA of the non-inhibited test) is affected by the inoculum activity and background methane production (Figure S-II in supplementary material displays the non-normalized plots). The results show that during P1 the methanogenic biomass in R1-RT was more tolerant to ammonia than that in R2-C. However, the benefits of biomass thickening were neither observed in P2 nor in P3, as the microbial communities of both digesters showed similar resistance towards ammonia.

### 10.3.3 Microbial community dynamics

#### 10.3.3.1 Microbial population in R1-RT

The bacterial population dynamics was assessed upon cDNA libraries, finding at least 50,000 reads per sample. The phyla *Firmicutes* (30%), *Proteobacteria* (22%), *Bacteroidetes* (16%), *Cloacimonetes* (14%) and *Chloroflexi* (9%) composed most of the microbial community in P1 (Figure 3). However, there was a significant shift in the bacterial population during P2 and P3, with *Proteobacteria* (76% and 72%) becoming the most active phyla, followed by *Bacteroidetes* (14% and 15%) and *Firmicutes* (6% and 11%); the other phyla represented less than 1%.

The archaeal population (assessed using cDNA libraries with more than 90,000 reads per sample) also showed significant variations between periods but were characterized by a lower diversity in relation to the bacterial population (Figure 3b). Considering all periods together, only four archaeal genera accounted for 99% of the total active population. Hydrogenotrophic methanogenic archaea (HMA) were always the most abundant and active group, with *Methanobacterium* spp. dominating during P1 and P2, and *Methanoculleus* spp. becoming the most active HMA in P3. Specifically, the *Methanobacterium* spp. relative abundance of ribosomal transcripts decreased from 65% in P1, and 57% in P2, down to 8% in P3, whereas the *Methanoculleus* spp. followed the opposite trend and its relative abundance increased up to 61% in P3, from a 23% and 22% in P1 and P2. The relative abundance of ribosomal transcripts of acetotrophic methanogenic archaea (AMA; e.g. *Methanosaeta* spp.) remained constant in all periods, and only represented about 3% of the total for archaea.

### 10.3.3.2 Microbial population in R2-C

Bacterial community dynamics was assessed with at least 51,000 cDNA reads per sample. The evolution of the active bacterial community in R2-C followed the opposed trend in relation to that observed in R1-RT, since they tended to diversify over time (Figure 10.3). During P1 and P2, the active bacterial population was clearly dominated by species of the phylum *Proteobacteria*, which represented about 80% of the transcripts relative abundance. However, their abundance drastically decreased down to 15% in P3. Conversely, representatives of *Bacteroidetes* and *Firmicutes* increased from 2% and 15% in P1 up to 45% and 31% in P3.

In relation to the archaeal counterparts, with more than 88,000 reads per sample, the HMA *Methanoculleus* dominated the active archaeal population in P1 and P2 with a 42% and 64%, respectively, in terms of the relative abundance of ribosomal transcripts (Figure 3). In P3, *Methanoculleus* decreased down to 25%, which was concomitant to the increase of *Methanobacterium* (44 %) and *Methanomassilicoccus* (31 %), both genera belonging to the HMA. The expression level of AMA (i.e. *Methanosaeta* spp.) was noticeable in P1 with a 27% of relative abundance, but decreased down to 12% (P2) and 0.2% (P3), along with the increase of OLR and TAN concentration.

**Table 10.2** Indexes of performance and diversity of Bacteria and Archaea (H` and 1/Simpson).

Note: \* Mean values of the whole period

Sample	N° seqs	Sobs OTU	Shannon		Inverted Simpson		Coverage (%)
			Mean	c.i	Mean	c.i	
R1 - 100d	39531	726	3,8	3,7-3,8	14,1	13,8-14,4	99,6
R2 - 100d	24882	531	3,4	3,4-3,4	11,5	11,2-11,8	99,7
R1 - 200d	50666	797	3,7	3,7-3,8	15,8	15,6-16,1	99,5
R2 - 200d	87459	639	2,2	2,2-2,3	3,1	3,1-3,1	99,3
R1 - 300d	64578	859	2,5	2,5-2,5	2,9	2,9-3	99,6
R2 - 300d	46508	836	3,5	3,4-3,5	7,1	7-7,3	99,6

### 10.3.3.3 Microbial diversity indexes

The Shannon and inverted Simpson indexes indicate that the recuperative thickening applied in R1-RT, under non-stress conditions (P1), increased the diversity of active bacterial populations while it reduced that of the archaea in R1-RT for the same period (Table 11.2). However, this pattern was entirely reversed in P3 (period with the highest TAN concentration), when R1-RT had a lower bacterial diversity and a more diverse in archaeal population than R2-C. This diversity decrement could be due to recirculate the solid fraction, and therefore to constantly increase those majority populations adhered on the fibers. For this reason, a double selection could be carried out, on the one hand by increasing a type of complex substrate to degrade, and on the other hand, a constant recirculation of those predominant communities.

### 10.3.3.4 Quantitative analysis by qPCR

The content of bacterial 16S rRNA gene and transcripts remained fairly constant for both reactors over time, with values ranging  $10^{10}$ - $10^{11}$  copies  $\text{mL}^{-1}$  (Figure 10.4). These results indicate that the bacterial metabolic activity was maintained, regardless of the reactor configuration and operational conditions (e.g. OLR, SRT or TAN concentration). The content of *mcrA* gene copies was similar for both reactors and displayed a similarly stable trend as that of the bacteria, remaining constant over time ( $\sim 10^8$  copies  $\text{mL}^{-1}$ ). However, the evolution of *mcrA* transcripts revealed that there was a drop in the methanogenic expression level for both reactors as OLR and TAN increased (Figure 10.4), although the drop on *mcrA* transcripts was similar in both reactors, it occurred at different stages (in P2 for R2-C and in P3 for R1-RT).

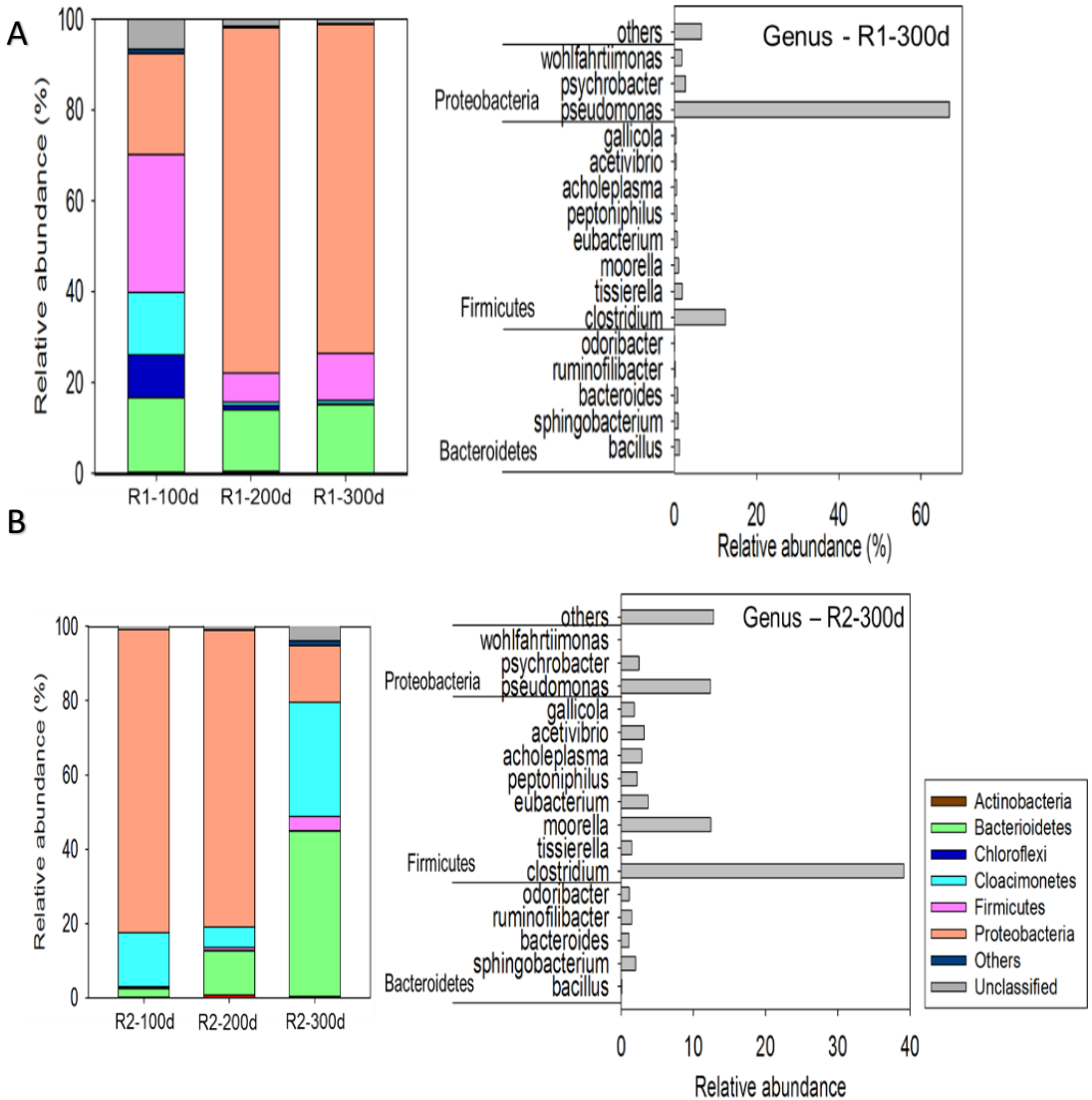


Table 10.3 Results of the Canonical Correspondence Analysis from Figure 5a (Bacteria). Note: \* Eigen values, weighted correlations between species and environmental axes, cumulative percentage of variance of species data and of species-environment relation, and weighted correlations between environmental and species-canonical axes.

CCA PARAMETERS	Canonical axes			
	1	2	3	4
Eigenvalues	0.386	0.167	0.149	0.079
Species-environment correlations	0.999	0.833	0.999	0.951
Cumulative percentage variance of species data	44.2	63.4	80.4	89.5
Cumulative percentage variance of species- environment relation	49.4	70.8	89.8	100.0
Variables:				
Total ammonia nitrogen (TAN)	-0.9094	-0.2126	0.2675	0.1780
Free ammonia nitrogen (FAN)	-0.7938	-0.0682	0.1179	-0.5611
Volatile fatty acids (VFA)	-0.6574	0.0501	0.7421	-0.1020

**Table 10.4** Results of the canonical correspondence analysis of Figure 5b (Archaea). Note: \* Eigen values, weighted correlations between species and environmental axes, cumulative percentage of variance of species data and of species-environment relation, and weighted correlations between environmental and species-canonical axes.

CCA PARAMETERS	Canonical axes			
	1	2	3	4
Eigenvalues	0.105	0.054	0.029	0.006
Species- environment correlations	0.993	0.998	0.999	0.887
Cumulative percentage variance of species data	52.1	79.0	93.4	97.4
Cumulative percentage variance of species- environment relation	54.1	81.9	97.8	100.0
Variables:				
Total ammonia nitrogen (TAN)	-0.8540	0.4359	0.2349	0.1034
Free ammonia nitrogen (FAN)	-0.4682	0.0408	0.6615	0.5153
Volatile fatty acids (VFA)	-0.8335	-0.0291	-0.1461	0.4629



**Figure 10.3** Relative abundance of bacterial (a, c) and archaeal (b, d) populations, obtained by MiSeq analysis based on 16S rRNA (a, b) and mcrA cDNA (c, d), respectively, in digesters R1-RT and R2-C.

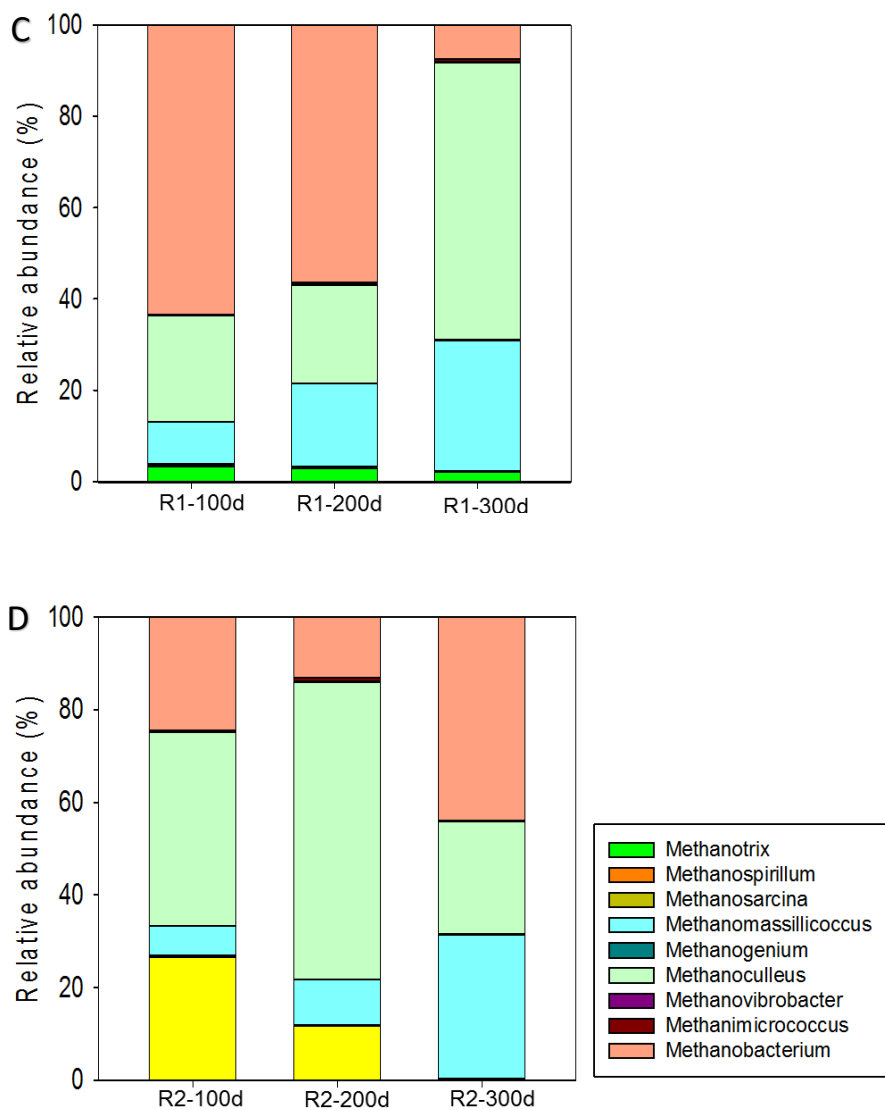


**Figure 10.3** Relative abundance of bacterial (a, b) and archaeal (c, d) populations, obtained by MiSeq analysis based on 16S rRNA (a, b) and *mcrA* cDNA (c, d), respectively, in digesters R1-RT and R2-C. (Continuation from previous page)

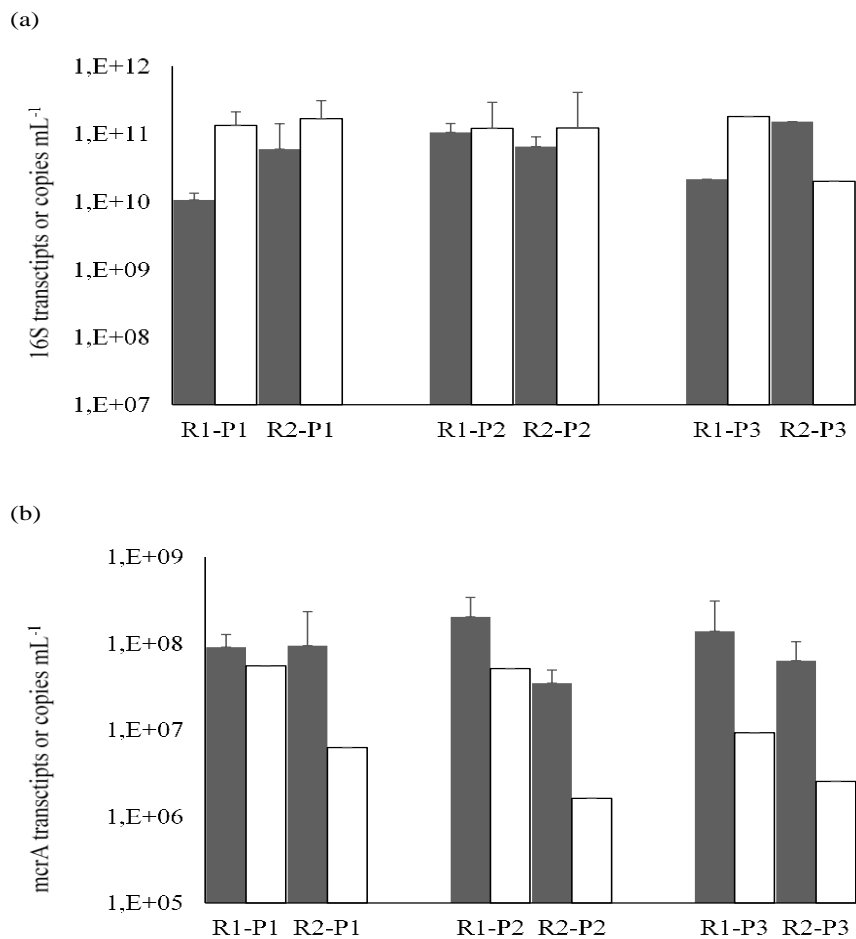


**Figure 10.4** Quantification of present and active microorganisms in both digesters R1-RT and R2-C along the performance periods (P1, P2, P3). (a) Bacteria 16S DNA and 16S RNA gene transcripts. (b) Archaeal *mcrA* and *mcrA* gene transcripts. Nomenclature: dark grey, 16S rRNA and *mcrA* transcripts copies in (a) and (b), respectively.



## 10.4 Discussion

### 10.4.1 Impact of recuperative thickening on process performance

The performance of R1-RT and R2-C was very similar during the start-up (P0) and P1, when reactors were operated at low OLR (0.9-1.4 kgVS m<sup>-3</sup> d<sup>-1</sup>), even though each reactor had a different active microbial community (Figure 10.3). Thereafter, the recuperative thickening reactor R1-RT reached a worse performance after the increment of the inlet-TKN content and OLR during P2 and P3, although the lower VFA accumulation (Figure 10.1). The methane yield decreased at higher OLR because of the accumulation of inhibitors in the digester liquor (e.g. NH<sub>4</sub><sup>+</sup>/NH<sub>3</sub> and VFA) and the decreased methanogenic activity (Figures 10.2 and 10.4). The inhibition phenomenon was attenuated to a certain extent in R1-RT, thanks to the prolonged degradation time and the higher retention of microbial communities. The lower methanogenic expression levels in R2-C, when compared to R1-RT (Figure 10.4), are apparently not in agreement with the SMA<sub>MAX</sub> results (Figure 10.2). Nonetheless, the SMA<sub>MAX</sub> only reflects the activity of a fraction of the methanogenic population since it was determined using acetate as model substrate.

The performance benefit of recuperative thickening over conventional CSTR operation was evidenced further during P3, when the OLR of both reactors was increased up to 3.2 kgVS m<sup>-3</sup> d<sup>-1</sup>. This final OLR led to a sharp increase of the total VFA concentration in R2-C (7.2 g L<sup>-1</sup>), while in R1-RT the total VFA concentration remained at a significantly lower level (2 g L<sup>-1</sup>). Considering that an OLR of 3.2 kgVS m<sup>-3</sup> d<sup>-1</sup> can be considered moderate for a CSTR, it is evident that the reduced reactor performance was caused by the higher concentration of inhibitory compounds induced by the feedstock composition rather than overloading itself. During P3, the TAN concentration increased from 4.1 to 5.7 gN L<sup>-1</sup> in both reactors, but the pH in R1-RT remained slightly lower than in R2 (see supplementary material). The maximum pH was 8.3 and 8.5 in R1-RT and R2-C, respectively (the pK<sub>a</sub> of the NH<sub>4</sub><sup>+</sup>-NH<sub>3</sub> equilibrium is 8.9 at 37 °C); this small difference on pH between reactors (~0.2 pH points) was responsible for a large difference on FAN concentration. The development of a more active microbial community linked to a higher CO<sub>2</sub> content in the biogas of R1-RT (thus lowering the pH in the liquor) is a plausible explanation for its performance. Other phenomena like the volatilization of VFA and NH<sub>3</sub>-N during the settling process cannot account for such differences.

## 10.4.2 Impact of biomass recuperative thickening on microbial composition

### 10.4.2.1 Bacterial community

Species belonging to the phyla *Firmicutes*, *Proteobacteria*, *Bacteroidetes*, *Cloacimonetes* and *Chloroflexi* were the main bacterial groups (phylum level) in R1-RT during P1. However, the change in feed composition and the increase in OLR during P2, and especially P3, resulted in a significant metabolic activity for the *Proteobacteria* (Figure 10.3). The bacterial population of R2-C showed a completely different trend in relative abundance and diversity of gene transcripts in that *Proteobacteria* were the predominantly active bacteria during P1 and P2, but its expression level decreased in P3 (Figure 10.3). This drop of *Proteobacteria* led to a more diverse bacterial community with *Bacteroidetes*, *Firmicutes*, and *Proteobacteria* as the main active phyla. The present results, especially those obtained in P1 and P2 periods, indicate that the OLR and the subsequent increase of TAN and VFA, as well as, SRT seems to be a relevant drivers of the bacterial population, as it is shown in canonical correspondence analysis of the active bacterial community (Figure 10.5 and Table 10.3). The performance of R1-RT, observed during P3, might be related to the genus *Pseudomonas* (phylum *Proteobacteria*), which represented about 60% of the active bacteria. *Pseudomonas* spp. are known to contain genes that encode for enzymes, such as the Dyp-peroxidase (de Gonzalo et al., 2016; Prabhakaran et al., 2015), that are able to degrade lignin and aromatic compounds among other recalcitrant compounds. It is plausible that the higher OLR in P2 and P3 and the change in feedstock composition (that contained more CM than the P1 influent) led to a higher fiber concentration in both reactors. Furthermore, visual observation clearly showed that fibers were the principal solid element of the recirculated settled fraction, which could be translated to a higher fiber content in R1-RT. The higher activity of *Pseudomonas* agrees with Rincón et al. (2008), who observed the raise of *Pseudomonas* along with OLR when treating olive mill waste.

There is not a univocal explanation on the drastic decrease of *Proteobacteria* in R2-C during P3, while this phylum was the most active in R1-RT along the period P3. However, there are two potential reasons that could explain this phenomenon: (i) the higher peak values of FAN and VFA concentration in R2-C compared to R1-RT (Figure 11.1), which are well-known inhibitors for several microbial communities, could have affected *Proteobacteria* more than other resistant phyla; and (ii) the formation of SAO-HMA syntrophic associations that facilitate the conversion of acetate into methane at high TAN concentration. To this date, the main SAO bacteria have been described within the *Firmicutes* phylum, which increased its activity in R2-C during period P3. Nevertheless, the significant activity increment observed in *Bacteroidetes* suggests that this phylum might also be involved in the SAO process, particularly when



considering its acetogenic potential (Ruiz-Sánchez et al., 2018) and, thus, might eventually outcompete the *Proteobacteria*.

#### 10.4.2.2 Archaeal community

The archaeal community of both reactors was dominated by hydrogenotrophic methanogens (i.e. *Methanoculleus*, *Methanobacterium* and/or *Methanomassillicoccus*) regardless of the operational conditions that, along with the non-accumulation of VFA in the first periods, suggests the existence of syntrophic interrelations with bacteria. Therefore the dominance of HMA appears to be related to the feedstock composition, since neither the SRT nor TAN concentration in P1 (Figure 10.5) favored hydrogenotrophic methanogens over acetotrophic methanogens, as also Regueiro et al., (2016) found. *Methanobacterium* was the most active methanogen in R1-RT during P1 and P2, while *Methanoculleus* became predominant in P3.

The reactor R2-C showed a completely different trend than R1-RT, with *Methanoculleus* being the main active methanogen in P1 and P2, and *Methanobacterium* playing a more significant role in P3. These results indicate that the OLR, and the subsequent increase of TAN and fatty acids, did not fully determine the archaeal population dynamics, likewise the observed bacterial population changes. Multivariate canonical correspondence analysis of archaeal community (Figure 10.5 and Table 10.4) suggests that FAN and VFA concentrations had a major effect in R2-C. These observations agree with the archaeal behavior reported by Wang et al., (2015), who suggested that *Methanobacterium congolense* are more vulnerable to high TAN concentrations than *Methanoculleus bourgenis*. Yet, the higher expression level of *Methanobacterium* in R2-C during period P3 (with the highest FAN) could be also related to the higher VFA concentration, taking into account the conclusion of Munk et al., (2017) that pointed out that HMA of this genus are comparatively tolerant to high VFA concentrations.

The presence of *Methanomassillicoccus* species in both reactors is quite interesting. This methylotrophic and methylamine hydrogen-dependent genus is very common in animal gut and manure (St-Pierre et al., 2015) but it also played an important role in a full-scale agricultural digester operated under high TAN content, presumed to encompass a SAO methanogenic biomass (Ruiz-Sánchez et al., submitted).

The major changes in the biodiversity of active archaea occurred during P3 in both reactors. In R2-C, the relative abundance of this archaeal population suddenly improved in period P3, also linked to an important change in the active bacteria, while it raised progressively in R1-RT from P1 to P2 (Figure 10.3c and 10.3d).

It is worth to mention that the strict acetotrophic methanogen (AMA) *Methanosaeta* was present in both reactors. The expression level of this genus remained relatively constant in R1-RT during the three operational periods, with relative abundances of ribosomal

transcripts below 3%. In R2-C, however, *Methanosaeta* reached a 27% of the expressed transcripts during P1, then decreased till 12% in P2, and finally till 0.2% in P3. These results agree with the fact that AMA are more susceptible to inhibition by TAN and VFA, as the influent strength increases (Fotidis et al. 2014).

The present results show that it is clear that the community structure of active methanogenic archaea is driven by an array of complex environmental parameters, rather than a single factor. The results showed that the used methanogenic inoculum had a metabolically diverse community that was capable of modulating specialized syntrophy in response to different environmental stress conditions. Such adaptability confers methanogenic biomass with a high resilience in front of environmental disturbance. In this study, when recuperative thickening was applied, an apparent syntrophy between *Pseudomonas* spp. and HMA was driven along the performance of R1-RT, while SAOB-HMA was enhanced in the R2-C without recirculation. For that reason, it was possible to assume that in this case resilience capability of the inoculum was relatively more important than its resistance (Allison et al., 2008). In other words, we can assume the resistance in both reactors based on physic-chemical parameters but, analyzing in detail microbial communities, it was observed a high impact resilience in this microbial communities.

## 10.5 Conclusions

At the experimental conditions studied, recuperative thickening did not change main performance parameters of AD fed with slaughterhouse blends, at high OLR and TAN content, but the resilience of the microbial community was shown. The recuperative thickening prompted a clear bacterial activity shift regarding the abundance of *Pseudomonas* and *Clostridium*. Both genera are known to encompass a number of species associated to the interspecies electron transfer and SAO processes that were confirmed through the predominance of HMA in both AD. However, recuperative thickening stimulated a very specific syntrophism, which was based upon the predominance of *Pseudomonas* and *Methanoculleus*. In parallel, the significant activity increment observed in *Bacteroidetes* (in the AD without RT) suggested that this phylum might also be involved in the SAO process, and might eventually outcompete the *Proteobacteria*. The abundance of active HMA was related to the feedstock composition, based on CCA, instead of the SRT or the TAN concentration and its resistance toward ammonia was proven under the applied OLR increment pattern.

## 10.6 References

- 90/667/EEC. 2002. Regulation (EC) No 1774/2002 of the European Parliament and of the Council, 3 October 2002, laying down health rules concerning animal by-products not intended for human consumption. Official Journal of the European Community.
- Abouelenien, F., Nakashimada, Y., Nishio, N., 2009. Dry mesophilic fermentation of chicken manure for production of methane by repeated batch culture. *J. Biosci. Bioeng.* 107, 293–295.
- Affes, R., Palatsi, J., Flotats, X., Carrère, H., Steyer, J.P., Battimelli, A., 2013. Saponification pretreatment and solids recirculation as a new anaerobic process for the treatment of slaughterhouse waste. *Bioresour. Technol.* 131, 460–7.
- Allison, S.D., Martiny, J.B.H., 2008. Resistance, resilience, and redundancy in microbial communities. *Proc. Natl. Acad. Sci.* 105, 11512–11519
- Angenent, L.T., Sung, S., Raskin, L., 2002. Methanogenic population dynamics during startup of a full-scale anaerobic sequencing batch reactor treating swine waste. *Water Res.* 36, 4648–4654.
- Astals, S., Batstone, D.J., Tait, S., Jensen, P.D., 2015. Development and validation of a rapid test for anaerobic inhibition and toxicity. *Water Res.* 81, 208–215.
- Balk, M.M., Weijma, J., Stams, A.J.M., 2002. *Thermotoga lettingae* sp. nov., a novel thermophilic, methanol-degrading bacterium isolated from a thermophilic anaerobic reactor. *Int. J. Syst. Evol. Microbiol.* 52, 1361–1368.
- Capson-Tojo, G., Moscoviz, R., Ruiz, D., Santa-Catalina, G., Trably, E., Rouez, M., Crest, M., Steyer, J.P., Bernet, N., Delgenès, J.P., Escudicé, R., 2018. Addition of granular activated carbon and trace elements to favor volatile fatty acid consumption during anaerobic digestion of food waste. *Bioresour. Technol.* 260, 157–168.
- de Gonzalo, G., Colpa, D.I., Habib, M.H.M., Fraaije, M.W., 2017. Bacterial enzymes involved in lignin degradation. *J. Biotechnol.* 236, 110–119.
- Demirel, B., Scherer, P., 2008. The roles of acetotrophic and hydrogenotrophic methanogens during anaerobic conversion of biomass to methane: a review. *Rev. Environ. Sci. Bio/Technology* 7, 173–190.
- Eaton, A., Franson, M., Association, A., Association, A., Federation, W., 2005. Standard Methods for the Examination of Water and Wastewater, in: Association, A.P.H. (Ed.), American Public Health Association, Washington.
- Fotidis, I. a, Wang, H., Fiedel, N., Gang, L., Karakashev, D., Angelidaki, I., 2014. Bioaugmentation as a solution to increase methane production from an Ammonia-Rich substrate. *Environ. Sci. Technol.* 48, 7669–7677.
- Gao, S., Zhao, M., Chen, Y., Yu, M., Ruan, W., 2015. Tolerance response to in situ ammonia stress in a pilot-scale anaerobic digestion reactor for alleviating ammonia inhibition. *Bioresour. Technol.* 198, 372–379.
- Hansen, K.H., Angelidaki, I., Ahring, B.K., 1998. Anaerobic digestion of swine manure: inhibition by ammonia. *Water Res.* 32, 5–12.
- Hattori, S., Kamagata, Y., Hanada, S., Shoun, H., 2000. *Thermacetogenium phaeum* gen. nov., sp. nov., a strictly anaerobic, thermophilic, syntrophic acetate-oxidizing bacterium. *Int. J. Syst. Evol. Microbiol.* 50, 1601–1609.
- Ho, D.P., Jensen, P.D., Batstone, D.J., 2013. Methanosarcinaceae and acetate-oxidizing pathways dominate in high-rate thermophilic anaerobic digestion of waste-activated sludge. *Appl. Environ. Microbiol.* 79, 6491–6500.
- Karthikeyan, O, P, Selvam, A, Wong, J, W, C, 2017. Hydrolysis–acidogenesis of food waste in solid–liquid–separating continuous stirred tank reactor (SLS-CSTR) for volatile organic acid production. *Bioresour. Technol.* 200, 366–373.

- Kato, S., Yoshida, R., Yamaguchi, T., Sato, T., Yumoto, I., Kamagata, Y., 2014. The effects of elevated CO<sub>2</sub> concentration on competitive interaction between acetoclastic and syntrophic methanogenesis in a model microbial consortium. *Front. Microbiol.* 5, 1–8.
- Kayhanian, 1999. Ammonia inhibition in high-solids biogasification: an overview and practical solution. *Environ. Technol.* 20, 355–365.
- Lee, M.J., Zinder, S.H., 1988. Carbon monoxide pathway enzyme activities in a thermophilic anaerobic bacterium grown acetogenically and in a syntrophic acetate-oxidizing coculture. *Arch. Microbiol.* 150, 513–518.
- Mata-Alvarez, J., Dosta, J., Romero-Güiza, M.S., Fonoll, X., Peces, M., Astals, S., Romero-Güiza, M.S., Fonoll, X., Peces, M., Astals, S., 2014. A critical review on anaerobic co-digestion achievements between 2010 and 2013. *Renew. Sustain. Energy Rev.* 36, 412–427.
- Mosbæk, F., Kjeldal, H., Mulat, D.G., Albertsen, M., Ward, A.J., Feilberg, A., Nielsen, J.L., 2017. Identification of syntrophic acetate-oxidizing bacteria in anaerobic digesters. *ISME J.* 2, 1–14.
- Munk, B., Guebitz, G.M., Leubhn, M., 2017. Influence of nitrogen-rich substrates on biogas production and on the methanogenic community under mesophilic and thermophilic conditions. *Anaerobe.* 46,146-154.
- Nagao, N., Tajima, N., Kawai, M., Niwa, C., Kurosawa, N., Matsuyama, T., Yusoff, F.M., Toda, T., 2012. Maximum organic loading rate for the single-stage wet anaerobic digestion of food waste. *Bioresour. Technol.* 118, 210-218
- Niu, Q., Takemura, Y., Kubota, K., Li, Y.-Y., 2015. Comparing mesophilic and thermophilic anaerobic digestion of chicken manure: Microbial community dynamics and process resilience. *Waste Manag.* 43, 114-122.
- Palatsi, J., Illa, J., Prenafeta-Boldú, F.X., Laureni, M., Fernandez, B., Angelidaki, I., Flotats, X., 2010. Long-chain fatty acids inhibition and adaptation process in anaerobic thermophilic digestion: Batch tests, microbial community structure and mathematical modelling. *Bioresour. Technol.* 101, 2243–2251.
- Pelissari, C., Guivernau, M., Viñas, M., de Souza, S.S., García, J., Sezerino, P.H., Ávila, C., 2017. Unraveling the active microbial populations involved in nitrogen utilization in a vertical subsurface flow constructed wetland treating urban wastewater. *Sci. Total Environ.* 584–585, 642–650.
- Prabhakaran, M., Couger, M.B., Jackson, C.A., Weirick, T., Fathepure, B.Z., 2015. Genome Sequences of the Lignin-Degrading *Pseudomonas* sp. Strain YS-1p and *Rhizobium* sp. Strain YS-1r Isolated from Decaying Wood. *Genome Announc.* 3, e00019-15
- Prenafeta-Boldú, F.X., Fernández, B., Viñas, M., Lizardo, R., Brufau, J., Owusu-Asiedu, A., Walsh, M.C., Awati, A., 2017. Effect of *Bacillus* spp. direct-fed microbial on slurry characteristics and gaseous emissions in growing pigs fed with high fibre-based diets. *Animal* 11, 209–218.
- Rajagopal, R., Massé, D.I., Singh, G., 2013. A critical review on inhibition of anaerobic digestion process by excess ammonia. *Bioresour. Technol.* 143, 632–41.
- Regueiro, L., Carballa, M., Lema, J.M., 2017. Microbiome response to controlled shifts in ammonium and LCFA levels in co-digestion systems. *J. Biotechnol.* 220, 35–44.
- Rincón, B., Borja, R., González, J.M., Portillo, M.C., Saiz-Jiménez, C., 2008. Influence of organic loading rate and hydraulic retention time on the performance, stability and microbial communities of one-stage anaerobic digestion of two-phase olive mill solid residue. *Biochem. Eng. J.* 40, 253–261.
- Romero-Güiza MS, Astals S, Chimenos JM, Martínez M, Mata-Alvarez J. 2014. Improving anaerobic digestion of pig manure by adding in the same reactor a stabilizing agent formulated with low-grade magnesium oxide. *Biomass Bioenergy* 67, 243–251.

- Romero-Güiza, M.S., Astals, S., Mata-Alvarez, J., Chimenos, J.M., 2015. Feasibility of coupling anaerobic digestion and struvite precipitation in the same reactor: evaluation of different magnesium sources. *Chem. Eng. J.* 270, 542–548.
- Romero-Güiza, M.S., Vila, J., Mata-Alvarez, J., Chimenos, J.M., Astals, S., 2017. The role of additives on anaerobic digestion: A review. *Renew. Sustain. Energy Rev.* 58, 1486–1499.
- Ruiz-Sánchez, J., Campanaro, S., Guivernau, M., Fernández, B., Prenafeta-Boldú, F.X., 2018. Effect of ammonia on the active microbiome and metagenome from stable full-scale digesters. *Bioresour. Technol.* 250, 513–522.
- Schnurer, A., Houwen, F.P., Svensson, B.H., 1994. Mesophilic syntrophic acetate oxidation during methane formation by a triculture at high ammonium concentration. *Arch. Microbiol.* 162, 70–74.
- Schnurer, a, Schink, B., Svensson, B.H., 1997. *Clostridium ultunense* sp. nov., a mesophilic bacterium oxidizing acetate in syntrophic association with a hydrogenotrophic methanogenic bacterium. *Int. J. Syst. Bacteriol.* 46, 1145–1152.
- Smith, M.R., Mah, R.A., 1978. Growth and methanogenesis by *Methanosarcina* strain 227 on acetate and methanol. *Appl. Environ. Microbiol.* 36, 870–9.
- St-Pierre, B., Cersosimo, L.M., Ishaq, S.L., Wright, A.D.G., 2015. Toward the identification of methanogenic archaeal groups as targets of methane mitigation in livestock animals. *Front. Microbiol.* 6, 1–10.
- Sun, L., Müller, B., Westerholm, M., Schnürer, A., 2014. Syntrophic acetate oxidation in industrial CSTR biogas digesters. *J. Biotechnol.* 171, 39–44.
- Tampio, E., Ervasti, S., Rintala, J., 2015. Characteristics and agronomic usability of digestates from laboratory digesters treating food waste and autoclaved food waste. *J. Clean. Prod.* 94, 86–92.
- Wang, H., Fotidis, I.A., Angelidaki, I., 2015. Ammonia effect on hydrogenotrophic methanogens and syntrophic acetate-oxidizing bacteria. *FFEMS Microbiol. Ecol.* 91.
- Wang, H., Zhang, Y., Angelidaki, I., 2017. Ammonia inhibition on hydrogen enriched anaerobic digestion of manure under mesophilic and thermophilic conditions. *Water Research*, 105, 314-319.
- Westerholm, M., Levén, L., Schnürer, A., 2012. Bioaugmentation of syntrophic acetate-oxidizing culture in biogas reactors exposed to increasing levels of ammonia. *Appl. Environ. Microbiol.* 78, 7619–7625.
- Westerholm, M., Moestedt, J., Schnürer, A., 2017. Biogas production through syntrophic acetate oxidation and deliberate operating strategies for improved digester performance. *Appl. Energy* 179, 124–135.
- Westerholm, M., Roos, S., Schnürer, A., 2011. *Tepidanaerobacter acetatoxydans* sp. nov., an anaerobic, syntrophic acetate-oxidizing bacterium isolated from two ammonium-enriched mesophilic methanogenic processes. *Syst. Appl. Microbiol.* 34, 260–267.
- Westerholm, M., Roos, S., Schnürer, A., 2010. *Syntrophacetivus schinkii* gen. nov., sp. nov., an anaerobic, syntrophic acetate-oxidizing bacterium isolated from a mesophilic anaerobic filter. *FEMS Microbiol. Lett.* 309, 100–104
- Yang, S., Phan, H.V., Bustamante, H., Guo, W., Ngo, H., Nghiem, L. 2017. Effects of shearing on biogas production and microbial community structure during anaerobic digestion with recuperative thickening. *Bioresour. Technol.* 234, 439-447.



# **Chapter 11 Assessment of support assisted vs support-free anaerobic digestion system operation under high ammonia level**

---

In this chapter, the knowledge that has been acquired thanks to this thesis has been put into practice in lab-scale anaerobic digesters. These experiments were carried out in three continuously operated reactors: the first was a CSTR used as a control (R4), and the other two had a hybrid-CSTR configuration (R5 and R10). Different packing materials were used to favor the formation of biofilm in order to retain more viable biomass inside the reactor. R5 was packed with zeolite because of its cationic adsorption capability, which might mitigate ammonia/ammonium inhibition. R10 was packed with a mixture of magnetite and nylon. Magnetite might favour the interspecies electron transfer between syntrophic communities, while nylon displays a great capability to promote biofilm formation.

## 11.1 Introduction

In the recent years, a major attitudinal shift has occurred in the consideration of wastes as resources rather than just materials requiring disposal. Waste as a resource is envisioned both as a means of reducing energy consumption, and even generation in the case of biogas, and by the recovery of raw materials (Angelidaki and Ahring, 1994). Organic wastes from the agricultural sector, such as animal manure, energy crops, and residues from the food processing industry (e.g. glycerine, beet tails, animal wastes, fruit pulp wastes). These wastes are often characterize by high values of chemical oxygen demand (COD) and total ammonia nitrogen (TAN)(Jarrell et al., 1987). The anaerobic digestion (AD) is a suitable treatment technology for converting these materials into biogas and a nitrogen-rich digestate. However, the AD technology is susceptible to the accumulation of TAN in that it can inhibit the methanogenic archaea (MA). For this reason, it is necessary to design and optimize new technological solutions to improve the AD treatment of nitrogen-rich wastes (Hunik et al., 1990).

This chapter is focused to the investigation of different reactor configurations with the objective to increment the efficiency and robustness of biogas production from nitrogen-rich wastes. Three continuously-operated digesters have been fed with synthetic media (glycerine and gelatine) simulating a real nitrogen-rich waste. The methane yield and the organic matter removal efficiency were monitored in order to evaluate the reactor stability and performance. The knowledge acquired from previous chapters in relation to the potential use of different packing materials (mainly from Chapters 6 and 8) have been applied in this work.

From the previous works from this thesis and from other authors, it has been concluded that zeolite is a very suitable material to mitigate ammonia inhibition in AD systems because of its capacity to adsorb ammonia cations and, because of its porous structure also enables the immobilization of microorganisms (Montalvo et al., 2012). Magnetite has also been described as a similarly suitable material, though the underlying mechanisms concerning the mitigation of ammonia inhibition are quite different. The electrical conductivity of this material has been reported to have a beneficial effect on the complete VFA degradation into methane (Cruz Viggì et al., 2014). This positive impact is exerted on the microbial syntrophic interactions by means of interspecies electron transfer (IET) or by direct interspecies electron transfer (DIET) (Rotaru et al., 2014; Zhao et al., 2016). Previous findings indicated that nylon was easily colonized by microorganisms and stimulate cell-to-cell and cell-surface interactions between bacterial consortia, thereby enhancing the formation of aggregates (Habouzit et al. 2011; Chapters 6 - 8).

The objective of this chapter was to assay the the effect of the above mentioned packing materials in anaerobic digesters fed with nitrogen-rich substrates. Zeolite and a



mixture of magnetite and nylon balls were tested in two hybrid reactors, configured as the so-called “Assisted Basket Anaerobic Digester” (ABAD) that includes packed support materials to enhance biomass attachment. A control un-packed CSTR was also included in the study.

## 11.2 Digesters experimental set-up

### 11.2.1 Set-up

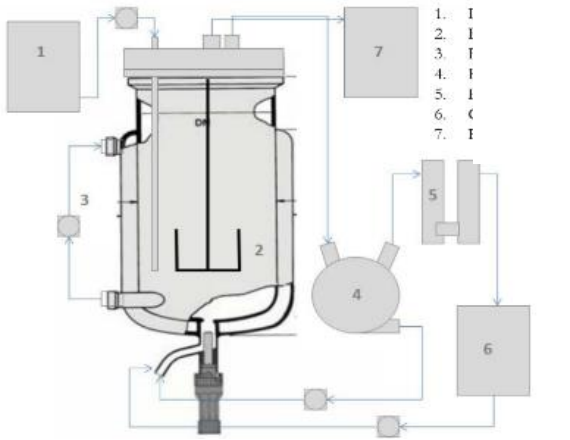
Three reactors were operated at mesophilic temperature ( $37\pm 4^\circ\text{C}$ ) maintained by the recirculation of water through the double glass jacket of the tank. All reactors were fed twice per day using a peristaltic pump and a temporized control system. The constant volume inside the digester was maintained using an overflow system. The biogas flow was measured by a displacement flow-meter (Ritter, Germany), after passage through a silica bed to retain water vapour and a filter to avoid particles in the gas. Digester inlet and outlet flows, biogas production and temperature were monitored daily, while pH, AR, concentration of COD, VS, N related compounds (TKN and TAN), VFA, and biogas composition were measured twice a week and expressed as a weekly average.

The unpacked control digester (R4) had a working volume of 1.8 L and was configured as a CSTR. The ABAD digester (R5) had a working volume of 2.0 L and was also stirred, but it was packed with zeolite as support material (20%v/v). This material was retained inside a methacrylate basket located in the top of the reactor. To avoid the ion exchange effect described for the zeolite (Weiß et al., 2013; Zheng et al., 2015), the support was introduced during the experimental set-up of R5 and was not replaced. In this way, the saturation of the zeolite was ensured with the TAN available in the medium. Finally, the mix-ABAD digester (R10), with a working volume of 4.5 L and also stirred, was partially filled with a mixture of magnetite:nylon at 1:1 (dry weight). In this case, the support mixture was introduced in a stainless steel system instead of a the basket, and located at the bottom of the reactor to avoid the blockage of the stirrer. As in the case of R5, the support mixture was introduced during the set-up of R10 and was maintained throughout the whole experiment.

The hydraulic retention time (HRT) and the organic loading rate (OLR) were chosen according to operational values of full-scale anaerobic digesters in individual and centralized manure treatment facilities (Flotats et al., 2009). In a first experiment, reactors R4 and R5 were operated in parallel with a HRT of 60 days and an OLR between 1-2 kgCOD  $\text{m}^{-3}\cdot\text{d}^{-1}$ . A similar synthetic medium was used as influent for both reactors, thus keeping the nitrogen content in the digesters at 3.0-4.5 gN-TAN  $\text{L}^{-1}$

(Table 12.1). Both digesters were inoculated with the SAO inoculum enriched previously a CSTR fed with a synthetic medium (see Section 3.4.4, Chapter 3).

(a)



(b)

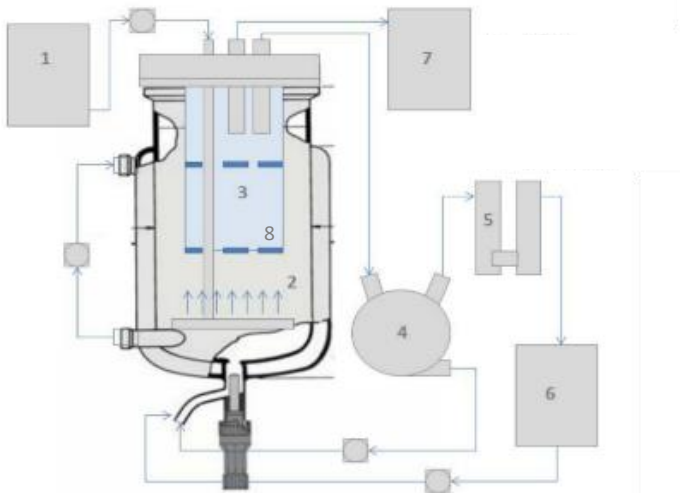


**Figure 11.1** Scheme of lab-scale digesters: (a) R4\_control; (b) R5\_abad; (c) R6\_mix abad. Numbers: 1- Influent. 2- Reactor. 3- Heater. 4- Effluent. 5- Gas flowmeter. 6- Gas counter. 7- Effluent tank. 8- Support material

(c)

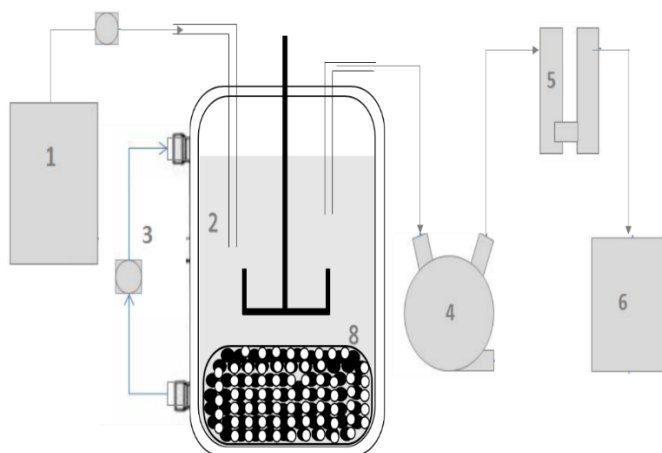


**Figure 11.2** Scheme of lab-scale digesters: (a) R4\_control; (b) R5\_abad; (c) R6\_mix abad. Numbers: 1- Influent. 2- Reactor. 3- Heater. 4- Effluent. 5- Gas flowmeter. 6- Gas counter. 7- Effluent tank. 8- Support material (Continuation from previous page).

In a second experiment, reactors R4 and R10 were operated in parallel, starting with the In a second experiment, reactors R4 and R10 were operated in parallel, both inoculated with the SAO biomass enriched in the same CSTR as before, fed with a synthetic medium, and keeping the nitrogen content in the digesters at 3.0-4.5 gN L<sup>-1</sup>. In this case, the HRT was 40-60 and 20 days for R4 and R10, respectively. The OLR was initially set at 1.0-1.5 kgCOD m<sup>-3</sup>·d<sup>-1</sup>, and was subsequently increased (day 240) to 1.7-2.0 kgCOD m<sup>-3</sup>·d<sup>-1</sup>.

Mass balances (kgCOD d<sup>-1</sup>) were routinely performed as a tool to assess the performance during the experiments, and to determine some control parameters like methane yield (Nm<sup>3</sup>CH<sub>4</sub>·kgCOD<sup>-1</sup>) and productivity (Nm<sup>3</sup>CH<sub>4</sub>·m<sup>-3</sup>·d<sup>-1</sup>), and COD removal efficiency (%in-COD). Other control parameters included the biogas composition, the alkalinity ratio, and the propionic to acetic acid ratio.

### 11.2.2 Synthetic medium

The medium contained 20 g·L<sup>-1</sup> of gelatine (CAT number 1704, Conda), as source of organic nitrogen, and 20 g·L<sup>-1</sup> of glycerine (CAS number 56-81-5, Scharlau), plus 160 µl/L of micronutrients (0.12g·L<sup>-1</sup> 5NiCl<sub>2</sub>·6H<sub>2</sub>O; 25 g·L<sup>-1</sup>FeCl<sub>2</sub>·6H<sub>2</sub>O; 1.25 g·L<sup>-1</sup>(NH<sub>4</sub>)<sub>6</sub>MO<sub>7</sub>O<sub>2</sub>·4H<sub>2</sub>O; 0.075 g·L<sup>-1</sup>CoCl<sub>2</sub>·6H<sub>2</sub>O) and macronutrients 1ml·L<sup>-1</sup> (17 g·L<sup>-1</sup> NH<sub>4</sub>Cl·12H<sub>2</sub>O; 3.7g·L<sup>-1</sup> KHPO<sub>4</sub>; 0.56g·L<sup>-1</sup>MgSO<sub>4</sub> ; 0.8g·L<sup>-1</sup> CaCl<sub>2</sub>·2H<sub>2</sub>O). The concentration of gelatine and glycerine was increased to 30 g·L<sup>-1</sup> when the OLR was increased in the second continuous experiment.

### 11.2.2 Analytical methods

Volatile fatty acids (VFA), total ammonia nitrogen (TAN) and sulphates ( $\text{SO}_4^{2-}$ ) were determined according to the Standard Methods for Wastewater from the American Public Health Association, the American Water Works Association, and the Water Pollution Control Federation (APHA, AWA, WEF, 2005). Biogas components ( $\text{CH}_4$ ,  $\text{CO}_2$  and  $\text{H}_2\text{S}$ ) were elucidated with a Varian CP-3800 gas chromatograph (GC; Varian, Walnut Creek, CA, USA) fitted with Hayesep Q 80/100 Mesh ( $2\text{m} \times 1/800 \times 2.0$  mSS) packed column (Varian) and thermal conductivity detector. Chemical oxygen demand (COD) was analysed according to an optimised Standard methodology (Noguerol et al., 2012). Biogas isotopic profile was analysed following the procedure described in chapter 3.

**Table 11. 1** Characterisation of synthetic medium used as inflow in the continuous systems

Component	COD g kg <sup>-1</sup>	TKN g kg <sup>-1</sup>	TAN g kg <sup>-1</sup>	VS g kg <sup>-1</sup>	pH
Gelatine	1198	155.5	-	98.50	-
Glycerine	1205	-	-	970	-
Medium	50	3000	-	25	7.8

## 11. 3 Results and discussion

### 11.3.1 Performance

The reactors were fed with mixtures of glycerine and gelatine during all performed experiments. The values obtained from the unpacked control reactor (R4) were used as reference in terms of increment/decrement of methane yield and organic matter removal efficiency in relation to the packed ones (R5 and R10). The average values of operational and control parameter per period and experiment, as well as, the methane potential of each period are shown in Table 12.2. The evolution of operational parameters (HRT, OLR, acetate and TAN) are shown in Figure 12.2. During the first experiment, R4 with R5 were operated under similar conditions, but relevant differences were observed in their performance. The  $\text{CH}_4$  production rate, methane yield and methane richness for R4 were  $0.2 \text{ Nm}^3\text{CH}_4 \text{ m}^{-3} \text{ d}^{-1}$ ,  $0.23 \text{ Nm}^3\text{CH}_4 \text{ kgCOD}^{-1}$  and 52%v/v respectively, while this parameter values were  $0.30 \text{ Nm}^3\text{CH}_4 \text{ kgCOD}^{-1}$ ,  $0.25 \text{ Nm}^3\text{CH}_4 \text{ kgCOD}^{-1}$  and 71%v/v for R5. In both cases the TAN concentrations were slightly higher than the values assumed as inhibitory for anaerobic digestion

(Yenigün and Demirel, 2013). Volatile fatty acids (VFA) were also used as indicator to monitor the reactor state. Some studies indicated different indexes to determine the imbalance between microbial communities involved in anaerobic digestion, as ratios propionic/acetic or the VFA to total alkalinity ratio (Gao et al., 2015). The alkalinity ratio in R4 was 0.60, compared to 0.27 in R5. Acetic acid was the main VFA in both reactors, but the propionic to acetic ratio indicated an unbalanced state in R4 (0.48) in relation to R5 (0.15).

In the second experiment, the operational and experimental parameters of the control reactor were compared with a third mix-ABAD reactor that contain a mixed support material of magnetite and nylon particles. The differences between control and packed reactor in this second experiment were more marked. Table 12.2 shows the operahere HRT was reduced down to 48 days in R4, along with an increment of the OLR up to  $1.26 \text{ kgCOD m}^{-3} \text{ d}^{-1}$ , while the HRT and the OLR in R10 was 45 days and  $1.62 \text{ kgCOD m}^{-3} \text{ d}^{-1}$ , respectively. In both cases the TAN concentrations were kept slightly higher than the values assumed to be inhibitory. Despite the increase in the OLR and the decrease in the HRT, R10 was able to cope with this situation significantly beter than the control R4. An improvement of COD removal efficiency, up to the 93%, was reached. The methane richness, methane yield and methane production rate also improved, with values of 63%,  $0.32 \text{ Nm}^3\text{CH}_4 \text{ kgCOD}^{-1}$  and  $0.51 \text{ Nm}^3\text{CH}_4 \text{ m}^{-3} \text{ d}^{-1}$ , respectively. Conversely, under similar operational conditions, R4 ended up in a failure state.

**Table 11.2** Average values of operational and control parameters per continuous system

Parameter	R4	R5	R4	R10
	Control	Abad	Control	Mix abad
Support material	None	Zeolite	None	Nylon & Magnetite
Experiment	1	1	2	2
Operational days	0-198		198-420	
HRT d	57±22	55±23	48±17	45±13
OLR kgCOD m <sup>-3</sup> d <sup>-1</sup>	0.61±0.03	0.62±0.35	1.26±0.58	1.62±0.60
TAN gN L <sup>-1</sup>	3493±14	3210±11	3189±43	3256 ±
	4	25	3	526
Total VFA g eq-C <sub>2</sub> L <sup>-1</sup>	7.67±5.33	2.81±2.50	12.04±2.0	2.61±1.76
			7	
Acetic acid g L <sup>-1</sup>	3.23±2.18	3.27±5.14	5.2±2.92	2.52±1.55
pH	7.40±0.58	8.31±0.25	7.97±0.59	7.85±0.30
Alk Ratio	0.60±0.29	0.27±0.14	0.73±0.16	0.29±0.11
Propionic to acetic ratio	0.48±0.27	0.15±0.02	0.57±0.29	0.57±0.42
COD removal (%in-COD)	60±9	62±35	34±14	93±5
Methane richness (%vol)	52±8	71±8	47±2.5	63±8
Yield (Nm <sup>3</sup> CH <sub>4</sub> kgCOD <sup>-1</sup> )	0.23±0.03	0.25±0.14	0.12±0.08	0.32±0.02
Production rate (Nm <sup>3</sup> CH <sub>4</sub> m <sup>-3</sup> d <sup>-1</sup> )	0.20±0.07	0.30±0.17	0.15±0.07	0.51±0.20
αc values*	1.07	1.06	1.07	1.09

\* These values were only taken once, at the end of the reactor operation. For this reason, they do not present standard deviation.

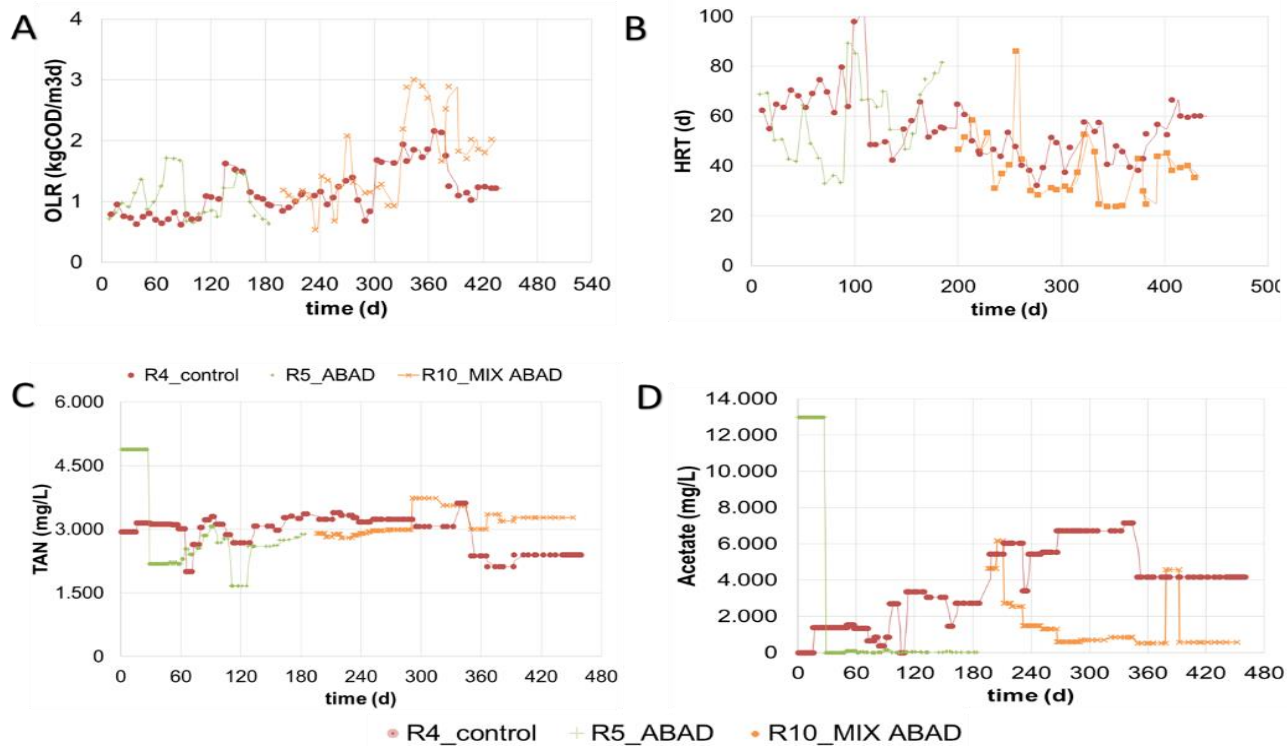


**Figure 11.3** Operational parameters of the three continuous systems. (a) OLR. (b) HRT. (c) TAN inside the reactor. (d) Concentration of acetic acid.

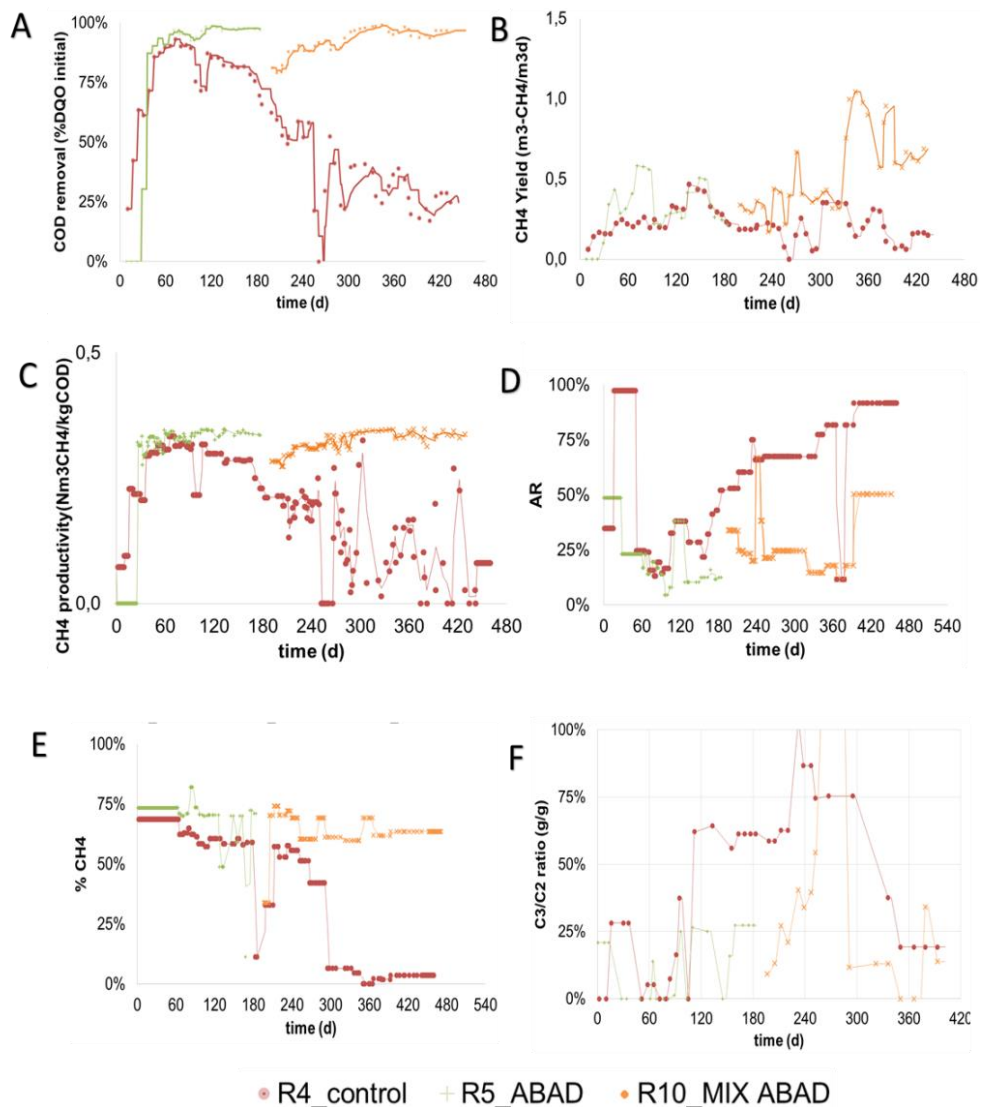


**Figure 11.** 4 Control parameters of the three continuous systems. (a) COD removal efficiency (%in-COD). (b) Methane productivity ( $\text{Nm}^3\text{CH}_4 \text{ m}^{-3} \text{ d}^{-1}$ ). (c) Methane yield ( $\text{Nm}^3\text{CH}_4/\text{kgCOD}$ ). (d) Alkalinity ratio. (e) Methane content of biogas (%v/v). (f) Propionic to acetic



### 11.3.2 Comparison between continuous systems

A comparison between the three reactors in terms of operational and control parameters is shown in Figures 11.2 and 11.3. The control reactor (R4) displayed the lowest CH<sub>4</sub> productivity for the applied operating conditions. In terms of degradation, the R4 had the worst: the evolution of the CH<sub>4</sub> richness and alkalinity ratio (RA), which indicated an imbalance between the stages of AD (Figure 11.2). The reactors with supports (R5 and R10) reached the best values of COD degradation and CH<sub>4</sub> yield, biogas CH<sub>4</sub> content, and ratio of alkalinities (Figure 11.3), indicating that the AD process was stable. It is noteworthy that R5 (packed with zeolite as support) maintained degradation and performance profile slightly better than the control reactor R4 (CSTR without support). This phenomenon might be explained due to the ion exchange effect of the zeolite (ammonium adsorbent). As it has previously been reported, zeolite is very useful in anaerobic digestion for enhancing biogas production from nitrogen-rich wastes because of its ammonia adsorption and cation exchange capacity. Zeolite has also a porous surface that confers a high immobilization capacity for microorganisms. It is also a resistant material under high temperature and acidic environments, and it is cheap to produce. Hence, the use of zeolite might well be economically feasible in industrial environmental applications.

The isotopic analysis of the biogas produced from these reactors indicated that the methanogenesis was dominated by the acetotrophic pathway. For this reason, considering the vulnerability of AMA to ammonia, the collapse of R4 is not surprising as it was directly exposed to ammonia. Instead, due to ammonia mitigation through adsorption on zeolite in R5, acetotrophic methanogenesis was unhalted. In relation to R10, packed with a mixed support of nylon and magnetite, showed a predominance of HMA. In general in R10 it was observed an improvement in all control parameters was observed in relation to the control R4, particularly during the period of OLR increment (from day 240 onwards).

We suggest that the high efficiency and resistance of this reactor is related to the retention of biomass, which increases the number of active populations in the reactor, but the used packing materials also play a very important role. Previous studies (Ahammad et al., 2013) reported that nylon is a suitable support material for the formation of anaerobic biofilms, in comparison with other materials, because of the preferential immobilization of methanogens. In one side, studies on the surface characteristics (zeta-potential) described that it should be possible to immobilize methanogens when the carrier material is negatively enough redox potential (around -24 mV). On the other side, the addition of conductive materials, as magnetite, can help the

microbial communities to establish strong syntrophic relationship incrementing the conversion of complex organic matter. It has also been reported that these materials promote the direct interspecies electron transfer (DIET) between bacteria and methanogenic archaea, which is more favourable in energetic terms than the indirect interspecies electron transfer (IET). Magnetite has shown that could stimulate the complete oxidation of propionate and butyrate to methane via DIET (Liu et al., 2014; Zhao et al., 2015).

## 11.4 Conclusions

This chapter describes the effect of different packing materials on the biomethanation potential and performance of anaerobic digesters fed with nitrogen-rich substrates. Two different ABAD reactors, packed with zeolite (R5) and a mix of magnetite-nylon (R10) were tested, and compared with a conventional CSTR (R4). The reactors with packaging material showed greater stability and efficiency in terms of an increased methane yield, COD degradation, CH<sub>4</sub> production, and biogas purity, when subjected at increased ammonia-exposure conditions. Our results confirm the feasibility of the addition of packing materials with specific functionalities, such as the adsorption of ammonia (zeolite), enhanced biofilm formation (zeolite and nylon), and direct interspecies electron transfer (magnetite). Further research is needed into the scalability of these packed configurations into pilot and full-scale anaerobic digesters fed with real wastes.

## 11.5 References

- Ahammad, S.Z., Davenport, R.J., Read, L.F., Gomes, J., Sreekrishnan, T.R., Dolfing, J., 2013. Rational immobilization of methanogens in high cell density bioreactors. *RSC Adv.* doi:10.1039/c2ra21901h
- Ahring, B.K., Angelidaki, I., Johansen, K., 1992. Anaerobic treatment of manure together with industrial waste. *Water Sci. Technol.*
- Ali Shah, F., Mahmood, Q., Maroof Shah, M., Pervez, A., Ahmad Asad, S., 2014. Microbial ecology of anaerobic digesters: The key players of anaerobiosis. *Sci. World J.* doi:10.1155/2014/183752
- Angelidaki, I., Ahring, B.K., 1992. Effects of free long-chain fatty acids on thermophilic anaerobic digestion. *Appl. Microbiol. Biotechnol.* 37, 808–812. doi:10.1007/BF00174850
- Annachhatre, A.P., Suktrakoolvait, S., 2015. Biological Sulfate Reduction Using Molasses as a Carbon Source. *Water Environ. Res.* 73, 118–127. doi:10.2175/106143001X138778
- Balk, M., Weijma, J., Stams, A.J.M., 2002. *Thermotoga lettingae* sp. nov., a novel thermophilic, methanol-degrading bacterium isolated from a thermophilic anaerobic reactor. *Int. J. Syst. Evol. Microbiol.* 52, 1361–1368. doi:10.1099/ijs.0.02165-0
- Calli, B., Mertoglu, B., Inanc, B., Yenigun, O., 2005. Effects of high free ammonia concentrations on the performances of anaerobic bioreactors. *Process Biochem.* doi:10.1016/j.procbio.2004.05.008
- Capson-Tojo, G., Moscoviz, R., Ruiz, D., Santa-Catalina, G., Trably, E., Rouez, M., Crest, M.,

- Steyer, J.P., Bernet, N., Delgenès, J.P., Escudicé, R., 2018. Addition of granular activated carbon and trace elements to favor volatile fatty acid consumption during anaerobic digestion of food waste. *Bioresour. Technol.* doi:10.1016/j.biortech.2018.03.097
- Coates, J.D., Coughlan, M.F., Colleran, E., 1997. Simple method for the measurement of the hydrogenotrophic methanogenic activity of anaerobic sludges. *J. Microbiol. Methods.* doi:10.1016/0167-7012(96)00915-3
- Conrad, R., 1999. Contribution of hydrogen to methane production and control of hydrogen concentrations in methanogenic soils and sediments. *FEMS Microbiol. Ecol.* doi:10.1016/S0168-6496(98)00086-5
- Conrad, R., Claus, P., Casper, P., 2009. Characterization of stable isotope fractionation during methane production in the sediment of a eutrophic lake, Lake Dagow, Germany. *Limnol. Oceanogr.* 54, 457–471. doi:10.4319/lo.2009.54.2.0457
- Cruz Vigg, C., Rossetti, S., Fazi, S., Paiano, P., Majone, M., Aulenta, F., 2014. Magnetite particles triggering a faster and more robust syntrophic pathway of methanogenic propionate degradation. *Environ. Sci. Technol.* 48, 7536–7543. doi:10.1021/es5016789
- Cuetos, M.J., Martínez, E.J., Moreno, R., Gonzalez, R., Otero, M., Gomez, X., 2017. Enhancing anaerobic digestion of poultry blood using activated carbon. *J. Adv. Res.* 8, 297–307. doi:10.1016/j.jare.2017.12.004
- Daniels, L., Sparling, R., Sprott, G.D., 1984. The bioenergetics of methanogenesis. *BBA Rev. Bioenerg.* doi:10.1016/0304-4173(84)90002-8
- Demirel, B., Scherer, P., 2008. The roles of acetotrophic and hydrogenotrophic methanogens during anaerobic conversion of biomass to methane: A review. *Rev. Environ. Sci. Biotechnol.* 7, 173–190. doi:10.1007/s11157-008-9131-1
- Donoso-Bravo, A., Retamal, C., Carballa, M., Ruiz-Filippi, G., Chamy, R., 2009. Influence of temperature on the hydrolysis, acidogenesis and methanogenesis in mesophilic anaerobic digestion: Parameter identification and modeling application. *Water Sci. Technol.* doi:10.2166/wst.2009.316
- Flotats, X., Bonmatí, A., Fernández, B., Magrí, A., 2009. Manure treatment technologies: On-farm versus centralized strategies. NE Spain as case study. *Bioresour. Technol.* doi:10.1016/j.biortech.2008.12.050
- Fotidis, I.A., Karakashev, D., Angelidaki, I., 2013. Bioaugmentation with an acetate-oxidising consortium as a tool to tackle ammonia inhibition of anaerobic digestion. *Bioresour. Technol.* 146, 57–62. doi:10.1016/j.biortech.2013.07.041
- Ganidi, N., Tyrrel, S., Cartmell, E., 2009. Anaerobic digestion foaming causes - A review. *Bioresour. Technol.* 100, 5546–5554. doi:10.1016/j.biortech.2009.07.024
- Gao, S., Zhao, M., Chen, Y., Yu, M., Ruan, W., 2015. Tolerance response to in situ ammonia stress in a pilot-scale anaerobic digestion reactor for alleviating ammonia inhibition. *Bioresour. Technol.* 198, 372–379. doi:10.1016/j.biortech.2015.09.044
- Gao, W.J., Lin, H.J., Leung, K.T., Schraft, H., Liao, B.Q., 2011. Structure of cake layer in a submerged anaerobic membrane bioreactor. *J. Memb. Sci.* doi:10.1016/j.memsci.2011.03.019
- Habouzit, F., Gévaudan, G., Hamelin, J., Steyer, J.P., Bernet, N., 2011. Influence of support material properties on the potential selection of Archaea during initial adhesion of a methanogenic consortium. *Bioresour. Technol.* 102, 4054–4060. doi:10.1016/j.biortech.2010.12.023
- Hansen, K.H., Angelidaki, I., Ahring, B.K., 1998. Anaerobic Digestion of Swine Manure: Inhibition By Ammonia. *Water Res.* 32, 5–12. doi:10.1016/S0043-1354(97)00201-7
- Hirano, S., Matsumoto, N., Morita, M., Sasaki, K., Ohmura, N., 2013. Electrochemical control of redox potential affects methanogenesis of the hydrogenotrophic methanogen *Methanothermobacter thermautotrophicus*. *Lett. Appl. Microbiol.* 56, 315–321.

- doi:10.1111/lam.12059
- Hirsch, A., 2002. Functionalization of single-walled carbon nanotubes. *Angew. Chemie - Int. Ed.* doi:10.1002/1521-3773(20020603)41:11<1853::AID-ANIE1853>3.0.CO;2-N
- Hug, L. a, Castelle, C.J., Wrighton, K.C., Thomas, B.C., Sharon, I., Frischkorn, K.R., Williams, K.H., Tringe, S.G., Banfield, J.F., 2013. Community genomic analyses constrain the distribution of metabolic traits across the Chloroflexi phylum and indicate roles in sediment carbon cycling. *Microbiome* 1, 22. doi:10.1186/2049-2618-1-22
- Hunik, J.H., Hamelers, H.V.M., Koster, I.W., 1990. Growth-rate inhibition of acetoclastic methanogens by ammonia and pH in poultry manure digestion. *Biol. Wastes* 32, 285–297. doi:10.1016/0269-7483(90)90060-6
- Isa, Z., Grusenmeyer, S., Vestraete, W., 1987. Sulfate reduction relative to methane production in high-rate anaerobic digestion: Technical aspects. *Appl. Environ. Microbiol.*
- Jabłoński, S., Rodowicz, P., Łukaszewicz, M., 2015. Methanogenic archaea database containing physiological and biochemical characteristics. *Int. J. Syst. Evol. Microbiol.* 65, 1360–1368. doi:10.1099/ijs.0.000065
- Joshi, D.R., Zhang, Y., Gao, Y., Liu, Y., Yang, M., 2017. Biotransformation of nitrogen- and sulfur-containing pollutants during coking wastewater treatment: Correspondence of performance to microbial community functional structure. *Water Res.* 121, 338–348. doi:10.1016/j.watres.2017.05.045
- Karadag, D., Köroğlu, O.E., Ozkaya, B., Cakmakci, M., 2015. A review on anaerobic biofilm reactors for the treatment of dairy industry wastewater. *Process Biochem.* 50, 262–271. doi:10.1016/j.procbio.2014.11.005
- Karunakaran, E., Vernon, D., Biggs, C.A., Saul, A., Crawford, D., Jensen, H., 2017. Enumeration of sulphate-reducing bacteria for assessing potential for hydrogen sulphide production in urban drainage systems. *Water Sci. Technol.* 73, 3087–3094. doi:10.2166/wst.2017.026
- Kayhanian, M., 1994. Performance of a high-solids anaerobic digestion process under various ammonia concentrations. *J. Chem. Technol. Biotechnol.* 59, 349–352. doi:10.1002/jctb.280590406
- Kim, J., Kim, K., Ye, H., Lee, E., Shin, C., McCarty, P.L., Bae, J., 2011. Anaerobic fluidized bed membrane bioreactor for wastewater treatment. *Environ. Sci. Technol.* doi:10.1021/es1027103
- Lee, M.J., Zinder, S.H., 1988. Hydrogen partial pressures in a thermophilic acetate-oxidizing methanogenic coculture. *Appl. Environ. Microbiol.* 54, 1457–61. doi:10.1002/cphc.200900055
- Li, L.-L., Tong, Z.-H., Fang, C.-Y., Chu, J., Yu, H.-Q., 2015. Response of anaerobic granular sludge to single-wall carbon nanotube exposure. *Water Res.* 70, 1–8. doi:10.1016/j.watres.2014.11.042
- Liu, F., Rotaru, A.-E., Shrestha, P.M., Malvankar, N.S., Nevin, K.P., Lovley, D.R., 2014. Magnetite compensates for the lack of a pilin-associated c-type cytochrome in extracellular electron exchange. *Environ. Microbiol.* 17, 648–55. doi:10.1111/1462-2920.12485
- Liu, Y., Whitman, W.B., 2008. Metabolic, phylogenetic, and ecological diversity of the methanogenic archaea, in: *Annals of the New York Academy of Sciences.* doi:10.1196/annals.1419.019
- Mata-Alvarez, J., Macé, S., Llabrés, P., 2000. Anaerobic digestion of organic solid wastes. An overview of research achievements and perspectives. *Bioresour. Technol.* 74, 3–17. doi:10.1016/S0960-8524(00)00023-7
- McInerney, M.J., Sieber, J.R., Gunsalus, R.P., 2009. Syntrophy in anaerobic global carbon cycles. *Curr. Opin. Biotechnol.* doi:10.1016/j.copbio.2009.10.001
- Min, D., Cheng, L., Zhang, F., Huang, X.N., Li, D.B., Liu, D.F., Lau, T.C., Mu, Y., Yu, H.Q., 2017. Enhancing Extracellular Electron Transfer of *Shewanella oneidensis* MR-1 through

- Coupling Improved Flavin Synthesis and Metal-Reducing Conduit for Pollutant Degradation. *Environ. Sci. Technol.* 51, 5082–5089. doi:10.1021/acs.est.6b04640
- Montalvo, S., Guerrero, L., Borja, R., Sánchez, E., Milán, Z., Cortés, I., Angeles de la la Rubia, M., 2012. Application of natural zeolites in anaerobic digestion processes: A review. *Appl. Clay Sci.* doi:10.1016/j.clay.2012.01.013
- Morgenroth, E., Kommedal, R., Harremoës, P., 2002. Processes and modelling of hydrolysis of particulate organic matter in aerobic wastewater treatment - a review. *Water Sci. Technol.*
- Morris, B.E.L., Henneberger, R., Huber, H., Moissl-Eichinger, C., 2013. Microbial syntrophy: Interaction for the common good. *FEMS Microbiol. Rev.* doi:10.1111/1574-6977.12019
- Müller, V., 2003. Energy Conservation in Acetogenic Bacteria. *Appl. Environ. Microbiol.* doi:10.1128/AEM.69.11.6345-6353.2003
- Muyzer, G., Stams, A.J.M., 2008. The ecology and biotechnology of sulphate-reducing bacteria. *Nat. Rev. Microbiol.* doi:10.1038/nrmicro1892
- Myint, M., Nirmalakhandan, N., Speece, R.E., 2007. Anaerobic fermentation of cattle manure: Modeling of hydrolysis and acidogenesis. *Water Res.* doi:10.1016/j.watres.2007.10.026
- Nagao, N., Tajima, N., Kawai, M., Niwa, C., Kurosawa, N., Matsuyama, T., Yusoff, F.M., Toda, T., 2012. Maximum organic loading rate for the single-stage wet anaerobic digestion of food waste. *Bioresour. Technol.* doi:10.1016/j.biortech.2012.05.045
- Niu, Q., Takemura, Y., Kubota, K., Li, Y.-Y., 2015. Comparing mesophilic and thermophilic anaerobic digestion of chicken manure: Microbial community dynamics and process resilience. *Waste Manag.* doi:10.1016/j.wasman.2015.05.012
- Nobu, M.K., Narihiro, T., Rinke, C., Kamagata, Y., Tringe, S.G., Woyke, T., Liu, W.-T., 2015. Microbial dark matter ecogenomics reveals complex synergistic networks in a methanogenic bioreactor. *ISME J.* 9, 1710–1722. doi:10.1038/ismej.2014.256
- O'Reilly, C., Collier, E., 2007. Effect of influent COD/SO<sub>4</sub> ratios on mesophilic anaerobic reactor biomass populations: Physico-chemical and microbiological properties. *FEMS Microbiol. Ecol.* 56, 141–153. doi:10.1111/j.1574-6941.2007.00067.x
- Ragsdale, S.W., 2008. Enzymology of the Wood-Ljungdahl pathway of acetogenesis, in: *Annals of the New York Academy of Sciences.* pp. 129–137. doi:10.1196/annals.1419.015
- Rajagopal, R., Mass, D.I., Singh, G., 2013. A critical review on inhibition of anaerobic digestion process by excess ammonia. *Bioresour. Technol.* doi:10.1016/j.biortech.2013.07.030
- Romero-Güiza, M.S., Astals, S., Chimenos, J.M., Martínez, M., Mata-Alvarez, J., 2014. Improving anaerobic digestion of pig manure by adding in the same reactor a stabilizing agent formulated with low-grade magnesium oxide. *Biomass and Bioenergy.* doi:10.1016/j.biombioe.2014.04.034
- Rotaru, A.E., Shrestha, P.M., Liu, F., Markovaite, B., Chen, S., Nevin, K.P., Lovley, D.R., 2014. Direct interspecies electron transfer between *Geobacter metallireducens* and *Methanosarcina barkeri*. *Appl. Environ. Microbiol.* 80, 4599–4605. doi:10.1128/AEM.00895-14
- Salvador, A.F., Martins, G., Melle-Franco, M., Serpa, R., Stams, A.J.M., Cavaleiro, A.J., Pereira, M.A., Alves, M.M., 2017. Carbon nanotubes accelerate methane production in pure cultures of methanogens and in a syntrophic coculture. *Environ. Microbiol.* 19, 2727–2739. doi:10.1111/1462-2920.13774
- Sarti, A., Zaiat, M., 2011. Anaerobic treatment of sulfate-rich wastewater in an anaerobic sequential batch reactor (AnSBR) using butanol as the carbon source. *J. Environ. Manage.* 92, 1537–1541. doi:10.1016/j.jenvman.2011.01.009
- Schink, B., Montag, D., Keller, A., Müller, N., 2017. Hydrogen or formate: Alternative key players in methanogenic degradation. *Environ. Microbiol. Rep.* doi:10.1111/1758-2229.12524
- Schnürer, A., Zellner, G., Svensson, B.H., 1999. Mesophilic syntrophic acetate oxidation during

- methane formation in biogas reactors. *FEMS Microbiol. Ecol.* 29, 249–261. doi:10.1016/S0168-6496(99)00016-1
- Shima, S., Thauer, R.K., 2005. Methyl-coenzyme M reductase and the anaerobic oxidation of methane in methanotrophic Archaea. *Curr. Opin. Microbiol.* 8, 643–648. doi:10.1016/j.mib.2005.10.002
- Shumkov, S., Terehova, S., 1995. Biological treatment of coals for their conversion to methan. *Coal Sci. Technol.* doi:10.1016/S0167-9449(06)80155-2
- Siles, J.A., Brekelmans, J., Martín, M.A., Chica, A.F., Martín, A., 2010. Impact of ammonia and sulphate concentration on thermophilic anaerobic digestion. *Bioresour. Technol.* 101, 9040–9048. doi:10.1016/j.biortech.2010.07.163
- St-Pierre, B., Wright, A.D.G., 2014. Comparative metagenomic analysis of bacterial populations in three full-scale mesophilic anaerobic manure digesters. *Appl. Microbiol. Biotechnol.* 98, 2709–2717. doi:10.1007/s00253-013-5220-3
- Stams, a. J.M., 1994. Metabolic interactions between anaerobic bacteria in methanogenic environments. *Antonie van Leeuwenhoek, Int. J. Gen. Mol. Microbiol.* 66, 271–294. doi:10.1007/BF00871644
- Stams, A.J.M., Plugge, C.M., 2009. Electron transfer in syntrophic communities of anaerobic bacteria and archaea. *Nat. Rev. Microbiol.* 7, 568–577. doi:10.1038/nrmicro2166
- Sung, S., Liu, T., 2003. Ammonia inhibition on thermophilic anaerobic digestion. *Chemosphere.* doi:10.1016/S0045-6535(03)00434-X
- Thauer, R.K., Hedderich, R., Fischer, R., 1993. Reactions and Enzymes Involved in Methanogenesis from CO<sub>2</sub> and H<sub>2</sub>, in: *Methanogenesis.* doi:10.1007/978-1-4615-2391-8\_5
- Vandevivere, P., Baere, L. De, Verstraete, W., 2003. Types of anaerobic digesters for solid wastes. *Biomethanization of OFMSW.*
- Veeken, A., Kalyuzhnyi, S., Scharff, H., Hamelers, B., 2000. Effect of pH and VFA on Hydrolysis of Organic Solid Waste. *J. Environ. Eng.* doi:10.1061/(ASCE)0733-9372(2000)126:12(1076)
- Walker, D.J.F., Dang, Y., Holmes, D.E., Lovley, D.R., 2017. The electrically conductive pili of *Geobacter* species are a recently evolved feature for extracellular electron transfer. *Microb. Genomics* 2. doi:10.1099/mgen.0.000072
- Wang, H., Fotidis, I.A., Angelidaki, I., 2015. Ammonia effect on hydrogenotrophic methanogens and syntrophic acetate-oxidizing bacteria. *FEMS Microbiol. Ecol.* 91. doi:10.1093/femsec/fiv130
- Wang, H., Zhang, Y., Angelidaki, I., 2017. Ammonia inhibition on hydrogen enriched anaerobic digestion of manure under mesophilic and thermophilic conditions. *Water Res.* 105, 314–319. doi:10.1016/j.watres.2017.09.006
- Wang, J., Musameh, M., 2005. Carbon-nanotubes doped polypyrrole glucose biosensor. *Anal. Chim. Acta* 539, 209–213. doi:10.1016/j.aca.2005.02.059
- Weiß, S., Leubhn, M., Andrade, D., Zankel, A., Cardinale, M., Birner-Gruenberger, R., Somitsch, W., Ueberbacher, B.J., Guebitz, G.M., 2013. Activated zeolite - Suitable carriers for microorganisms in anaerobic digestion processes? *Appl. Microbiol. Biotechnol.* 97, 3225–3238. doi:10.1007/s00253-013-4691-6
- Westerholm, M., Dolfing, J., Sherry, A., Gray, N.D., Head, I.M., Schnürer, A., 2011. Quantification of syntrophic acetate-oxidizing microbial communities in biogas processes. *Environ. Microbiol. Rep.* 3, 500–505. doi:10.1111/j.1758-2229.2011.00249.x
- Westerholm, M., Levén, L., Schnürer, A., 2012. Bioaugmentation of syntrophic acetate-oxidizing culture in biogas reactors exposed to increasing levels of ammonia. *Appl. Environ. Microbiol.* 78, 7619–7625. doi:10.1128/AEM.01637-12
- Yamada, T., Sekiguchi, Y., Hanada, S., Imachi, H., Ohashi, A., Harada, H., Kamagata, Y., 2007.

- Anaerolinea thermolimosa sp. nov., Levilinea saccharolytica gen. nov., sp. nov. and Leptolinea tardivitalis gen. nov., sp. nov., novel filamentous anaerobes, and description of the new classes Anaerolineae classis nov. and Caldilineae classis nov. in the . Int. J. Syst. Evol. Microbiol. 56, 1331–1340. doi:10.1099/ijs.0.64169-0
- Yenigün, O., Demirel, B., 2013. Ammonia inhibition in anaerobic digestion: A review. Process Biochem. 48, 901–911. doi:10.1016/j.procbio.2013.04.012
- Yuan, H., Zhu, N., 2017. Progress in inhibition mechanisms and process control of intermediates and by-products in sewage sludge anaerobic digestion. Renew. Sustain. Energy Rev. doi:10.1016/j.rser.2015.12.261
- Zeikus, J.G., Weimer, P.J., Nelson, D.R., Daniels, L., 1975. Bacterial methanogenesis: Acetate as a methane precursor in pure culture. Arch. Microbiol. doi:10.1007/BF00447312
- Zhao, Z., Zhang, Y., Holmes, D.E., Dang, Y., Woodard, T.L., Nevin, K.P., Lovley, D.R., 2017. Potential enhancement of direct interspecies electron transfer for syntrophic metabolism of propionate and butyrate with biochar in up-flow anaerobic sludge blanket reactors. Bioresour. Technol. 209, 148–157. doi:10.1016/j.biortech.2017.03.005
- Zhao, Z., Zhang, Y., Wang, L., Quan, X., 2015. Potential for direct interspecies electron transfer in an electric-anaerobic system to increase methane production from sludge digestion. Sci. Rep. 5. doi:10.1038/srep11094
- Zheng, H., Li, D., Stanislaus, M.S., Zhang, N., Zhu, Q., Hu, X., Yang, Y., 2015. Development of a bio-zeolite fixed-bed bioreactor for mitigating ammonia inhibition of anaerobic digestion with extremely high ammonium concentration livestock waste. Chem. Eng. J. 280, 106–114. doi:10.1016/j.cej.2015.07.024
- Zhuang, L., Tang, J., Wang, Y., Hu, M., Zhou, S., 2015. Conductive iron oxide minerals accelerate syntrophic cooperation in methanogenic benzoate degradation. J. Hazard. Mater. 293, 37–45. doi:10.1016/j.jhazmat.2015.03.039

# Part V

---

Final Remarks



# **Chapter 12 Conclusions & Future perspectives**

---

Based on the proposed objectives for this research (Chapter 2), the present chapter summarizes the main conclusions of this dissertation.

## **12.1 Part I**

Despite the long history of application of the anaerobic digestion, there are still some waste materials that might seriously affect the efficiency and stability of the process. This is the case of nitrogen-rich organic compounds, which release  $\text{NH}_3$  that might accumulate up to inhibitory levels. As discussed in Chapter 1, this phenomenon seriously hinders the valorization of agricultural wastes, such as animal manure, slaughterhouse wastes, and food waste. The underlying microbial communities in methanogenic biomass play a very significant role in the tolerance towards high ammonia exposure. Until recently, though, anaerobic digesters have primarily been contemplated as a “black box”, in which only macroscopic parameters have been considered, but the advancement of molecular biology tools allows the detailed study of the microbial communities. Thanks to this, the syntrophic acetate oxidation has been proposed as a key process for increasing the suitability of anaerobic digesters to treat nitrogen-rich wastes. Yet, despite these progresses, the functional biodiversity and microbial interactions under such conditions are still poorly understood. An interdisciplinary approach is therefore fundamental for gaining new knowledge, as that proposed in Chapter 3.

## **12.2 Part II**

This section of the thesis was aimed at the study of the microbial community structure and dynamics in response to increasing ammonia exposure, with a view on the occurrence and metabolism of the SAO process. For this purpose, an interdisciplinary approach that included qPCR quantification of functional genes, NGS of 16S rRNA genes and transcripts, metagenomics analysis, and isotopic fractionation of biogas components was undertaken.

- The characterization of the methanogenic biomass in full-scale anaerobic digesters subjected to high ammonia levels, demonstrated that stable operation is possible upon enrichment of SAOB/HMA (Chapters 4 and 5).
- Despite the strong evidence for the occurrence of the SAO process in anaerobic digesters operated at high ammonia concentrations, none of the SAOB that are currently known from the literature played a significant role in the studied biomass (Chapters 4 and 5).
- Microbial communities from the biomass of an adapted full-scale anaerobic digester displayed a functional plasticity in that they swiftly adapted their metabolic pathways for methanogenesis in response to the ammonia level, from

predominantly acetotrophic at  $<1 \text{ gN-TAN L}^{-1}$  to hydrogenotrophic  $>6 \text{ gN-TAN L}^{-1}$  (Chapter 4).

- Phylogenetic analysis on ammonia-adapted methanogenic biomass revealed that relevant bacterial ribotypes (Chapter 4) and assembled genomes (Chapter 5) could not be assigned to identified species, or were associated to taxa that play a poorly known role in the anaerobic digestion under high ammonia concentration.
- Combined metagenomic and RNA-based taxonomic analysis allowed the reconstruction of Wood–Ljungdahl and the glycine cleavage system pathways in *Bacteroidetes* and *Chloroflexi* genomes bin (Chapter 5). Hence, these taxa might encompass SAOB that are yet to be described.
- Concerning the archaea, the predominant and most active ribotypes under high ammonia exposure belonged to the known HMA genus *Methanoculleus* spp. (Chapters 4 and 5) and to representatives of the *Methanomassiliicoccales* (Chapter 4). These taxa have been associated to the capability of heterotrophic (non-methanogenic) growth on acetate.

### 12.3 Part III

This part of the thesis was focussed on the understanding and modulation of the microbial interactions taking place inside the anaerobic digester by introducing materials with specific physicochemical characteristics. Relevant phenomena concerned the adsorption of ammonia, the enhancement of biofilm formation, and the direct interspecies electron transfer.

- The physicochemical nature of the support material had a strong influence both on biofilm development and on the resulting microbial community structure (Chapters 6, 7 and 8).
- Under a high ammonia concentration ( $7 \text{ gN-TAN L}^{-1}$ ), zeolite displayed a positive effect in terms of biofilm formation, gene expression levels, and on methanogenic activity, in comparison to other support materials (Chapter 6). This effect was attributed to the ammonium adsorption on this material, due to its cation exchange capacity.
- Nylon also had a positive effect on biofilm formation and biological activity during anaerobic digestions (Chapter 6). A metagenomic and DNA-SIP study with this material (Chapter 8), combined with CLSM analysis (Chapter 6),

suggests that nylon promoted the expression of genes associated to biofilm formation.

- Magnetite demonstrated to be a suitable packing material for the anaerobic digestion under high ammonia concentration (via metagenomics and DNA-SIP; Chapter 8). No significant biofilm formation was observed but the biological stimulation mechanism was associated to the direct interspecies electron transfer (DIET).
- A novel methodology was developed for the cost-effective immobilization of carbon nanotubes (CNT) on LDPE spheres (Chapter 7). This new packing material was tested successfully in anaerobic digestion trials under high ammonia, as it combines the benefits of promoting biofilm formation and of DIET. An important impact in active microbiome was observed, in that known DIET-associated taxa were clearly stimulated (i.e. the bacterial orders *Desulfuromonadales* and *Myxococcales*).

## 12.4 Part IV

In this final section of the thesis, the generated knowledge from the previous chapters has been put into practice in lab-scale continuously operated anaerobic digesters, which were fed with real complex wastes in certain cases. Different reactor configurations designed to stimulate SAO activity (i.e. to increase of the cellular retention time, or the use of packing materials) were implemented and assayed.

- The reactor stability for the anaerobic digestion of a complex real waste (heparin production industry) characterized by high COD, ammonia, and sulphate content was severely compromised in relation to the ratio between COD and sulphate concentration inside the reactor (Chapter 9).
- The anaerobic digestion of the heparin production industry waste was enhanced in three independent reactors, packed with zeolite, magnetite, and a mixed 50:50 v/v zeolite/magnetite, in relation to a unpacked control (Chapter 9).
- The monitorization of the functional genes *mcrA* and *aprA* during transitional/unstability periods is proposed as a novel tool for monitoring the direct effect of certain operational strategies (e.g. organic loading rate, feed composition, HRT, etc.) on the activity of the methanogenic biomass (Chapter 9).

- The implementation of a recuperative thickening strategy, in comparison to a non-recirculating control reactor, for increasing the robustness of the anaerobic codigestion of chicken manure, pig slurries, and algi had a significant impact on the microbial communities. A slight increase on the overall reactor performance was also observed under the tested conditions (Chapter 10).
- A comparative operation of two ABAD reactors packed with zeolite and a 50:50 v/v mix of nylon and magnetite, respectively, in relation to a unpacked CSTR control, demonstrated that both packings promoted a higher operational stability and efficiency (Chapter 12).

**To finalize**, considering the importance of the circular economy concepts for resource recovery from wastes, the anaerobic digestion constitutes a fundamental technological choice in the agrifood sector. Despite the recent advances, reactor inhibition due to the excess of ammonia still poses serious threats to the economical and environmental sustainability of the process. The overcoming of this problem strongly relies on the understanding and engineering of the SAO process. As a first research priority, it is very important to increase the knowledge on the biodiversity, ecophysiology, and microbial interactions of the microorganisms that are involved in this process. In this thesis, we have demonstrated that there might be a wider diversity of SAOB than those that are currently known from the literature. It would be convenient to expand the interdisciplinary research approach from this work to new digesters, and complement these studies with attempts on the isolation and cultivation of new SAOB in the laboratory for their description and characterization.

In relation to the more applied aspects, our results illustrate the power of the implemented interdisciplinary approach for monitoring the process in industrial digesters (e.g. isotopic fractionation of biogas components for determining the predominant methanogenic pathway, the targeting of functional genes and of relevant microbial species for bioindication purposes, etc.). It is expected that the costs of these monitoring technologies will decrease in the near future, and so they might jump from the lab to full-scale digesters sooner than later. Such flow of data will need proper modelling and control algorithms, which will have to be developed as well. A final topic of research concerns the scaling-up of the use of nanotechnological materials for the modulation of the microbial interactions in the full-scale.

# **Annex – CV**

---



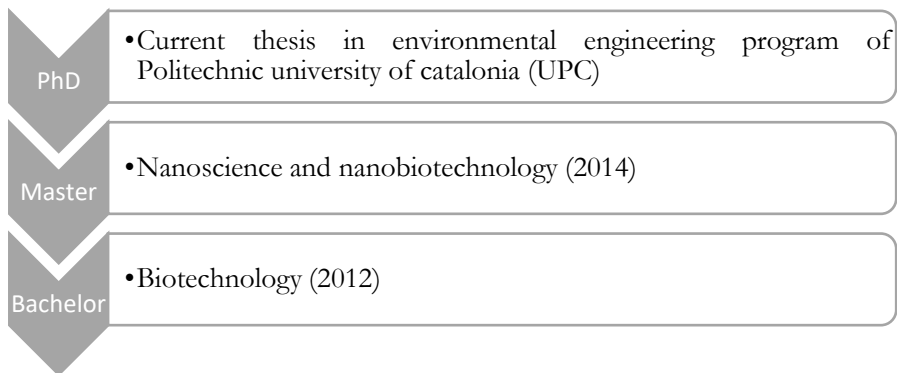
**Name:** Josep

**Surname:** Ruiz Sánchez

**Date of birth:** October 27th 1990

**Email:** josep2710@msn.com

## Education



## Complementary education

Basic Perl for bioinformatics at Universitat Autònoma de Barcelona (UAB) 20h.

Summer school Cost Action ES1302 (Anaerobic digestion and bioremediation of metal contaminated environments) at Paris Est Marne-le-valle. 30h

Bioinformatic and genomic conference at Institut d'Estudis Catalans, Barcelona. 16h

## Experience

Predoctoral research in INIA-RTA2012-00098-00-00: Optimization of anaerobic digestion and production of biogas from waste rich in proteins and gauzes, with ammonium recovery (PROGRAMO).

Predoctoral research in INIA-2017-0023 Integration of processes for the syntrophic oxidation of acetate and autotrophic ammonium in the anaerobic treatment of organic waste rich in nitrogen for its energy recovery (PIONER)

## Conference presentations

**Biomicroworld 2015 congress, Barcelona, Spain (2015). Oral presentation** Ruiz-Sánchez J., Fernández B., Viñas M., Riau V., Prenafeta-Boldú F.X. Are syntrophic acetate oxidizing (SAO) bacteria more common in high ammonia-loaded anaerobic digesters than we think?

**Cost action ES1302 Group 2, Galway, Ireland (2015). Oral presentation.** Ruiz-Sánchez J., Fernández B., Viñas M., Riau V., Prenafeta-Boldú F.X. Syntrophic acetate oxidation (SAO) in the anaerobic digestion of lipid/protein rich-wastes

**XII Latin American workshop and symposium on anaerobic digestion, Cusco, Perú. Poster presentation (2016).** Ruiz-Sánchez J., Fernández B., Viñas M., Guivernau M., Tey L., Riau V., Prenafeta-Boldú F.X. Influence of support materials on methanogenic biofilm formation in ammonia rich environments

**XII Latin American workshop and symposium on anaerobic digestion, Cusco, Perú. Poster presentation (2016).** Ruiz-Sánchez J., Fernández B., Viñas M., Guivernau M., Tey L., Riau V., Prenafeta-Boldú F.X. How much of microbial genetic expression profile, depending on ammonia stress, the anaerobic digesters change?

**7th Congress of European Microbiologists (FEMS 2017), Valencia, Spain. Poster presentation (2017)** Ruiz-Sánchez J., Romero-Güiza M., Astals S., Prenafeta-Boldúa F.X., Fernández B. Microbial community dynamics in nitrogen rich digesters: impact of effluent recirculation

**7th Congress of European Microbiologists (FEMS 2017), Valencia, Spain. Poster presentation (2017)** Ruiz-Sánchez J., Campanaro S., Guivernau M., Fernández B., and Prenafeta-Boldú F.X. Metagenome and active microbiome profiling in ammonia-rich anaerobic digestion

**7th Congress of European Microbiologists (FEMS 2017), Valencia, Spain. Engage your audience event – Speech your research (2017)**

**15<sup>th</sup> IWA World conference on anaerobic digestion, Beijing, China Poster presentation (2017).** Ruiz-Sánchez J., Campanaro S., Guivernau M., Fernández B., and Prenafeta-Boldú F.X. Metagenomic analysis and active microbiome profiling reveal novel microbial associations in ammonia-rich bioreactors

**15<sup>th</sup> IWA World conference on anaerobic digestion, Beijing, China Poster presentation (2017).** Ruiz-Sánchez J., Guivernau M., Prenafeta-Boldú F.X., Fernández B. Strategies for recovering from inhibition caused by ammonia and sulphate in mesophilic biogas fixed-bed reactors



## Scientific articles

Ruiz-Sánchez J, Campanaro S, Guivernau M, Fernández B, Prenafeta-Boldú FX. **Effect of ammonia on the active microbiome and metagenome from stable full-scale digesters.** *Bioresour Technol.* 2018 Feb;250:513-522. doi:10.1016/j.biortech.2017.11.068.

Ruiz-Sánchez J, Vila J, Guivernau M, Vinas M, Riau V, Fernández B, Prenafeta-Boldu FX. **Functional plasticity of methanogenic biomass from a full-scale mesophilic anaerobic digester treating nitrogen-rich agricultural wastes.** *Science of The Total Environment*, 2019. 649,760-769, doi:10.1016/j.scitotenv.2018.08.165.

Ruiz-Sánchez J, Romero-Guiza M, Astals S, Prenafeta-Boldu FX., Fernández B. **Impact of recuperative thickening on syntrophic microbial interactions and biogas production in anaerobic digestion.** Submitted to *Waste Management*.

Ruiz-Sánchez J, Vila J, Guivernau M, Vinas M, Riau V, Fernández B, Prenafeta-Boldu FX. **Functional plasticity of methanogenic biomass from a full-scale mesophilic anaerobic digester treating nitrogen-rich agricultural wastes.** Submitted to *Sci. Total Environ.*

Ruiz-Sánchez J, Vila J, Campanaro S, Fernández B, Prenafeta-Boldu. **Identification of syntrophic acetate oxidation and electron transfer mechanisms in methanogenic biomass by DNA-stable isotope probing and metagenomics.** In preparation

Ruiz-Sánchez J, Fernández B, Prenafeta-Boldu FX **Response of methanogenic biomass of anaerobic digester to immobilized multi-walled carbon nanotube exposition.** In preparation

Ruiz-Sánchez J, Guivernau M, Fernández B, Prenafeta-Boldu FX **Strategies for recovering from inhibition caused by ammonia and sulphate in mesophilic biogas fixed-bed reactors.** In preparation

## Book chapter

Magri A, Fernandez B., Prenafeta-Boldú F.X, Ruiz-Sánchez J. **Coupling syntrophic acetate oxidation and anaerobic ammonium oxidation when treating nitrogen-rich organic wastes for energy recovery and nitrogen removal: overview and prospects.** Submitted to Springer